UNIVERSIDADE DE LISBOA
INSTITUTO SUPERIOR TÉCNICO

Therapeutic contact lenses: layer-by-layer coatings and molecular imprinting as strategies for drug delivery control

Diana Cristina Morais da Silva Pereira

Supervisor:	Doctor Ana Paula Valagão Amadeu do Serro
	Doctor Hermínio José Cipriano de Sousa
Co-supervisor:	Doctor Benilde de Jesus Vieira Saramago

Thesis approved in public session to obtain the PhD Degree in Advanced Materials and Processing

Jury final classification: Pass with Distinction

Jury

Chairperson: Doctor Rogério Anacleto Cordeiro Colaço, Instituto Superior Técnico da Universidade de Lisboa

Members of the Committee:

Doctor Maria Helena Mendes Gil, Faculdade de Ciências e Tecnologia da Universidade de Coimbra

Doctor Carmen Isabel Alvarez Lorenzo, Facultade de Farmacia, Universidade de Santiago de Compostela, Espanha

Doctor Maria de Fátima Reis Vaz, Instituto Superior Técnico da Universidade de Lisboa

Doctor Benilde de Jesus Vieira Saramago, Instituto Superior Técnico da Universidade de Lisboa

Doctor Ana Isabel Henriques Dias Fernandes Pinto, Instituto Universitário Egas Moniz

Doctor Andreia Filipa Relvas Pimenta, Bioceramed

2020

To my grandmother Maria

ABSTRACT

The use of drug-loaded ophthalmic lenses has been regarded as an adequate solution to overcome the main disadvantages of conventional topical ocular treatments. In fact, therapeutic soft contact lenses (SCLs) may ensure a higher bioavailability of the drug in the eye, minimizing its wastage and side effects, and avoiding the frequent and regular instillation of eyedrops, which may be compromised by poor patients' compliance. However, to be efficient, the SCLs must ensure a sustained release of adequate amounts of drug. The present thesis focused on two strategies to control the release of ophthalmic drugs: surface modification through layer-by-layer (LbL) assembly and molecular imprinting.

Different LbL coatings, prepared using natural based polyelectrolytes (e.g. alginate (ALG), chitosan (CHI), poly-L-lysine (PLL) and hyaluronate (HA)), were deposited on a lab-made silicone-based hydrogel (TRIS/NVP/HEMA), a commercial silicone hydrogel for SCLs (Definitive 50), and two commercially available SCLs (SofLens and Purevision). The produced coatings were effective only in the control of the release of diclofenac (DCF), but had no effect on the releases of ketorolac (KETO), chlorhexidine (CHX) and moxifloxacin (MXF). The specificity of the barrier effect of these LbL coatings for DCF was attributed to the unique interactions between the polyelectrolytes and DCF (e.g. electrostatic interactions, H-bonds). Furthermore, some of the LbL coatings demonstrated antifouling and antibacterial properties, and were able to withstand high hydrostatic pressure (HHP) sterilization.

To overcome the inability of the LbL coatings to sustain the release of MXF, the TRIS/NVP/HEMA was submitted to molecular imprinting of the drug associated with the addition of a functional monomer (acrylic acid). The results showed a 6-fold increase in the amount of drug released.

The conjugation of the most promising LbL coating with the molecular imprinting technique allowed a sustained dual release of DCF+MXF from TRIS/NVP/HEMA. The release profiles obtained under hydrodynamic conditions demonstrated that DCF concentration remained above the IC_{50} values of COX-1 and COX-2 for 9 days and that MXF concentration remained above the MICs of *S. aureus* and *S. epidermidis* for more than 10 days. The samples were biocompatible, did not induce ocular irritancy,

demonstrated antifouling behaviour and kept suitable physical properties. Thus, they seem suitable for therapeutic SCLs application.

RESUMO

O uso de lentes oftálmicas carregadas com fármacos tem sido considerada uma solução adequada para superar as principais desvantages dos tratamentos oculares convencionais. De facto, as lentes de contacto (LCs) terapêuticas podem garantir uma maior biodisponibilidade do fármaco no olho, minimizando o seu desperdício e efeitos secundários, evitando a instilação frequente de colírios, que podem ser comprometidos pela baixa cooperação dos pacientes.No entanto, para alcançar esse desempenho, as LCs devem garantir uma libertação controlada do fármaco. A presente tese focou-se em duas estratégias para controlar a libertação de fármacos oftálmicos: modificação da superfície através da técnica de camada-sobre-camada (CsC) e impressão molecular.

Diferentes revestimentos CsC, preparados com polielectrólitos de base natural (e.g. alginato (ALG), quitosano (CHI), poli-L-lisina (PLL) e ácido hialurónico (HA)), foram depositados num hidrogel à base de silicone (TRIS/NVP/HEMA) preparado no laboratório, um hidrogel de silicone comercial para LCs (Definitive 50) e duas LCs comercialmente disponíveis (SofLens e Purevision). Os revestimentos produzidos foram eficazes apenas no controlo da libertação de diclofenac (DCF), mas não tiveram efeito nas libertações de ketorolac (KETO), clorexidina (CHX) e moxifloxacina (MXF). A especifidade do efeito de barreira desses revestimentos para o DCF foi atribuída às interacções específicas entre os polielectrólitos e o DCF (e.g. interacções electrostáticas, ligações de H). Além disso, alguns desses revestimentos CsC demonstraram propriedades antiaderentes e antibacterianas, tendo sido capazes de suportar condições de esterilização por alta pressão hidrostática (APH).

Para superar a incapacidade dos revestimentos CsC em controlar a libertação de MXF, o hidrogel TRIS/NVP/HEMA foi submetido à impressão molecular do fármaco e à adição de um monómero funcional (ácido acrílico). Os resultados mostraram um aumento de 6 vezes na quantidade de fármaco libertado.

A conjugação do revestimento CsC mais promissor com a técnica de impressão molecular, permitiu uma dupla libertação controlada de DCF+MXF do hidrogel TRIS/NVP/HEMA. Os perfis de libertação obtidos em condições hidrodinâmicas demonstraram que a concentração de DCF permaneceu acima dos valores de IC$_{50}$ de COX-1 e COX-2 por 9 dias e a concentração de MXF permaneceu acima das MICs de *S.*

aureus e *S. epidermidis* por mais de 10 dias. As amostras eram biocompatíveis, não induziram irritação ocular, demonstraram comportamento antiaderente e mantiveram as propriedades físicas adequadas. Assim, as amostras parecem ser adequadas para a aplicação em LCs terapêuticas.

KEYWORDS

Soft contact lenses

Layer-by-layer

Molecular imprinting

Ophthalmic drugs

Controlled drug release

PALAVRAS CHAVE

Lentes de contacto

Camada-sobre-camada

Impressão molecular

Fármacos oftálmicos

Libertação controlada de fármacos

ACKNOWLEDGEMENTS

To Doctor Helena Barroso, for allowing me to work in her laboratory, for all the meetings, explanations of concepts and transfer of knowledge regarding the sterilization assays.

A significant part of this thesis was carried out under the scope of collaborative projects as such a special thanks to Doctor Jorge Guiomar from University of Coimbra and to Doctor Dimitriya Bozukova from PhysIOL S.a.

To Doctor Jorge Saraiva, for his availability towards all the HHP sterilization experiments carried out at is laboratory in the University of Aveiro. Also, a special thanks to Carlos Pinto and Renata Amaral the PhD students responsible for the HHP equipment, for their good mood to forget the somewhat tiresome travels to Aveiro, and for making the HHP sterilization process a success.

To all my lab colleagues, Ana Catarina Branco, Andreia Pimenta, Diogo Silva, Marta Reis and Pedro Nolasco for their companionship, integration and good disposition. To my Greek friend Eleni Nydrioti, Ευχαριστώ. A special thanks to Ana Topete and Sofia Oliveira for their incredible patience, motivation, support, for understanding all the difficulties of a PhD work, and most important of all, for becoming my friends.

To my friend Andreia Dias, to whom I am truly grateful for all the chit-chat in my best and worst moments.

A special thanks to my small but incomparable family, for their infinite support, unconditional love, for having been there for me, and for knowing that they will always be, at all times, even in the most painful ones. To my grandmother Maria, to whom I dedicate this thesis, as this acknowledgement cannot be read, listen or understood, in hope you can understand in anyway what you meant to me, thank you.

To my husband Ricardo, for being my best friend, and the love of my life. Thank you for never letting go of my hand.

Finally, to Inês, for giving me a reason to be better.

INDEX

3 Antibacterial layer-by-layer coatings to control drug release from soft contact lenses material   **77**

5 Molecular imprinted silicone-based hydrogels as contact lenses materials for extended moxifloxacin release 158

LIST OF FIGURES

layers of HA/PLL(EDC)+DCF coating. The final steps correspond to the addition of DCF (6) and of the lachrymal protein solutions (7) of **(A)** lysozyme and **(B)** albumin, respectively. The successive additions are separated by rinsing with DD water (2) except after final EDC and of DCF addition where rinsing was done with 0.9% (w/v) NaCl (5) solution. EDC (4) and CHI (5), as a function of time, to form two double layers of HA(EDC)/CHI coating.

Figure 3.6 Normalized shift in the frequency, $\Delta f/n$ (blue line, left y-axis) and shift in the dissipation ΔD (red line, right y-axis) for the third harmonic of the resonant frequency of a quartz crystal sensor after being coated with a TRIS/NVP/HEMA hydrogel film, during successive additions of PEI (1), ALG (3), PLL (4), EDC (5) and HA (6), as a function of time, to form two double layers of ALG/PLL(EDC)//HA coating. The final steps correspond to the addition of DCF (8) and of the lachrymal protein solutions of (9) **(A)** lysozyme and **(B)** albumin, respectively. The successive additions are separated by rinsing with DD water (2) except after final EDC and of DCF addition where rinsing was done with NaCl (7) solution.

93

Figure 3.7 DCF release profiles from uncoated (●), ALG/PLL(EDC) (○), HA(EDC)/CHI (○) and HA/PLL(EDC)+Drug (○) coated TRIS/NVP/HEMA hydrogels. The DCF release profile obtained with ALG/PLL(EDC)//HA coated TRIS/NVP/HEMA hydrogels is also included (○). The inserts represent the first 24 h of the release data. The error bars are the ± standard deviations (n=8).

94

Figure 3.8 MXF release profiles from uncoated (▲), ALG/PLL(EDC) (△), HA(EDC)/CHI (△) and HA/PLL(EDC)+MXF (△) coated TRIS/NVP/HEMA hydrogels. The inserts represent the first 24 h of the release data. The error bars are the ± standard deviations (n=8).

95

Figure 3.9 CHX release profiles from uncoated (■), ALG/PLL(EDC) (□), and HA(EDC)/CHI (□) coated TRIS/NVP/HEMA hydrogels. The inserts represent the first 24 h of the release data. The error bars are the ± standard deviations (n=8).

95

represents the first 24 h of the release data. The error bars are the ± standard deviations (n=4).

LIST OF TABLES

errors are the ± standard deviations (in all cases n=3, except for Young's modulus and water contact angle where n=5 and n=10, respectively).

LIST OF ABBREVIATIONS

AA	Acrylic acid
AFM	Atomic Force Microscope
AIBN	2,2'-azobis(2-methylpropionitrile)
ALG	Alginate
AM	Acrylamide
CAM	Chorioallantoic membrane
CHI	Chitosan
CHX	Chlorhexidine monohydrate
COX	Cyclooxygenases
COX-1	Cyclooxygenase-1
COX-2	Cyclooxygenase-2
CS	Calf serum
DCF	Diclofenac sodium salt
DD	Distilled and deionized
DMA	N,N-dimethyl acrylamide
DMEM	Dulbecco's modified eagle's medium
DMSO	Dimethyl sulfoxide
DNA	Deoxyribonucleic acid
EDC	N-(3-dimethylaminopropyl)-N-ethylcarbodiimide hydrochloride

EGDMA	Ethylene glycol dimethacrylate
EMA	European Medicines Agency
FDA	Food and drug administration
GE	Genipin
GL	Glyoxal
GMA	Glyceryl methacrylate
HA	Hyaluronic acid
HEMA	Hydroxyethyl methacrylate
HET-CAM	Hen's egg test-chorioallantoic membrane
HHP	High hydrostatic pressure
IBM	Isobornyl methacrylate
IC_{50}	Half maximum inhibitory concentrations
ICCVAM	Interagency Coordinating Committee on the Validation of Alternative Methods
IGEPAL®	Oetylphenoxypolyethoxyethanol
IS	Irritation score
ISO	International Organization for Standardization
KETO	Ketorolac tromethamine
LbL	Layer-by-layer
MAA	Methacrylatic acid
MH	Mueller-Hinton agar
MHB	Mueller-Hinton broth
MIC	Minimum inhibitory concentration

NIH/3T3	Mouse embryonic fibroblasts
MMA	Methyl methacrylate
mPDMS	Monofunctional polydimethacrylate
MXF	Moxifloxacin hydrochloride
NSAID	Non-steroidal anti-inflammatory drug
NVA	N-vinyl aminobutynic acid
NVP	N-vinyl pyrrolidone
P. aeruginosa	*Pseudomonas aeruginosa*
PBS	Phosphate buffer solution
PBVC	Poly(dimethysiloxy)-di-(silylbutanol)-Bis-(vinyl carbonate)
PDMS	Poly dimethylsiloxane
PEI	Poly ethylenimide
pHEMA	Poly hydroxyethyl methacrylate
PLL	Poly-L-lysine
PLTF	Pre lens tear film
PMMA	Poly methyl methacrylate
POLTF	Post lens tear film
PS	Poly styrene
PVP	Poly vinyl pyrrolidone
QCM-D	Quartz crystal microbalance with dissipation
RH	Relative humidity
RPE	Retinal pigment epithelium

SAL	Sterility assurance level
S. aureus	*Staphylococcus aureus*
SCL	Soft contact lens
S. epidermidis	*Staphylococcus epidermidis*
SP	Steam and pressure
STF	Simulated tear fluid
TEGMA	Tetra-ethyleneglycol dimethacrylate
TPVC	Tris-trimethylsiloxysilyl
TRIS	Tris(trimethlylsiloxy)-methacryloxy-propylsilane
USA	United States of America
USAN	United States Adopted Names
UV	Ultraviolet light
UV-Vis	Ultraviolet and visible light
VMA	N-vinyl-N-methylacetamide

LIST OF SYMBOLS

A	Cross area
dC/dx	Initial saline solution concentration
D_{ion}	Ionic permeability
Dk/L	Oxygen transmissibility
F	Rate of ion transport
f	Resonance frequency
I	Intensity of the transmitted light
I_0	Intensity of the incident light
IS	Irritation score
k	Pseudokinetic constant
L	Thickness
L_g	Sample profile length
m_L	Mean line that divides the peaks and valleys of the sample's topography
m_t	Dry mass of the lens
M_d	Amount of drug delivered
M_t	Mass released at time t
M_∞	Mass released as time approaches infinity
n	Diffusional exponent
pKa	Acid dissociation constant at logarithmic scale

q	Drug release rate per unit mass of dry gel
r	Volume fraction of renovated fluid in each t (min)
R_a	Average roughness
rpm	Rotation per minute
T	Temperature
t	Time
T_C	Time of the first appearance of coagulation
T_H	Time of the first appearance of haemorrhage
T_L	Time of the first appearance of lysis
$T\%$	Transmittance
V_a	Volume of the receiver solution
V_{tear}	Average tear volume in the eye
W_D	Weight of the dry hydrogel
W_H	Weight of the hydrated hydrogel
z(x)	Surface height profile
$\Delta f/n$	Normalized frequency
ΔD	Dissipation
Δt	Time interval
γ^{LS}	Liquid/solid interfacial tension
γ^{LV}	Liquid/vapour interfacial tension
γ^{VS}	Vapour/solid interfacial tension
θ	Equilibrium contact angle

λ	Wavelenght
$[Drug]_t$	Drug concentration in the tear fluid at a given time t
$[Drug]_t$	Drug concentration in the tear fluid at a given time t-1

1 Introduction

Table of contents

1.1 State of the art

1.1.1 Eye anatomy and physiology

The human eye is the organ responsible for vision, which is achieved by photoreception. This mechanism consists in the activation of the nerve cells by light, inducing nerve potentials to travel through the optical nerve into the brain. Here, the information is processed and sequentially an image is created [1]. The human eye uses two different photoreceptors (rods and cones) that function in scarce light or at day light conditions. The rods do not possess colour perception, justifying the fact that humans do not identify colours in dark environments. Cones are mainly concentrated in the centre of the eye, conferring great detail in the central line of sight, in detriment of the peripheral vision which is unsuitable for high detail functions as reading [2].

The eye can be differentiated into two segments: the anterior and the posterior. The anterior or front segment is constituted by the cornea, conjunctiva, iris, lens and ciliary body. While the posterior segment includes the choroid, the retina, the optic nerve and the vitreous humour (**Figure 1.1**).
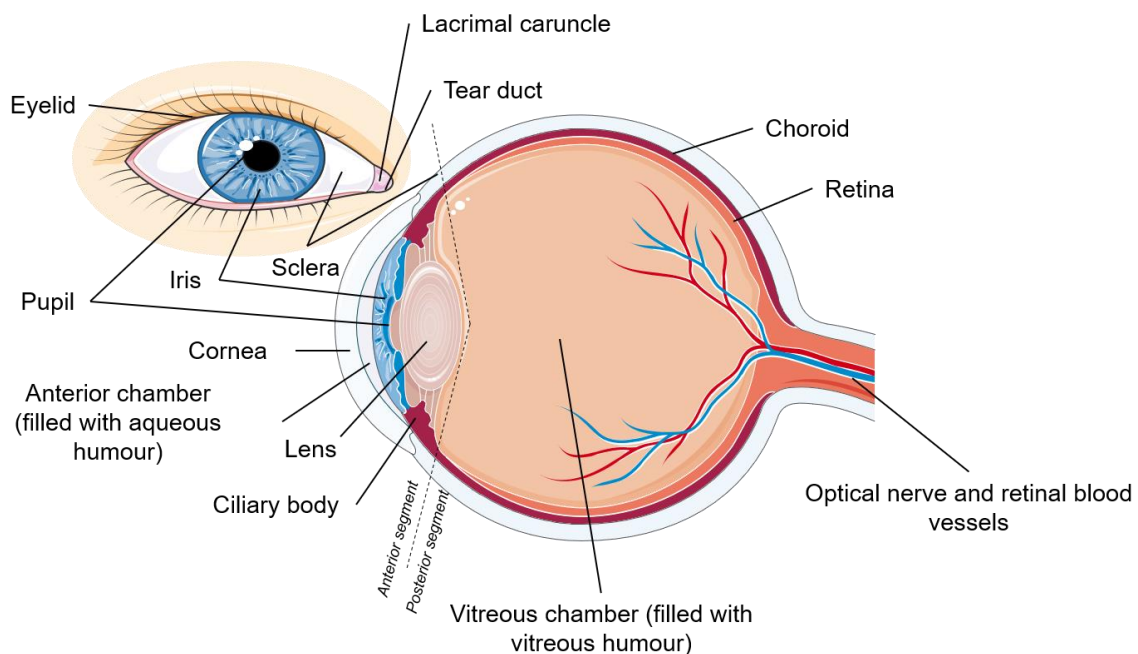
Figure 1.1 Schematic representation of the human eye with the major components. Adapted from [2].

The **cornea** is an avascular, thin (10 – 12 mm in diameter) and transparent tissue. Transparency is one of its most important properties, which results from the absence of blood vessels and the organization of its component's layers [1]. It is highly sensitive due to the presence of numerous nerves. The necessary nourishments and oxygen are provided to the cornea by two different paths, through lachrymal tears for the anterior part, and by the aqueous humour for the posterior part. The cornea is directly exposed to the environment and provides protection to the pupil, iris, and other eye components from foreign and harmful bodies. Also, in combination with the tear film, it provides 70% of the refractive power of the eye (40 – 44 diopters) [3,4]. The cornea is divided in five layers: the epithelium, bowman´s membrane, the stroma, Descemet's membrane and the endothelium. The stroma represents 90% of the cornea. The epithelium is composed of 6 layers of cells that are continuously being renewed, which is not the case for the Descemet's membrane. In case of disease or trauma of the Descemet's membrane, the patient will automatically require a cornea transplant. The endothelium shows a crucial role in avoiding the abnormal swelling of cornea from excess fluid [3].

The **sclera** is connected to the cornea by the limbus and extents until the *lamina cribosa* in the optical nerve. It maintains the shape and protects the eye from external chemical, physical and pathological action. It is white opaque due to the irregular arrangements of its collagen fibbers [1].

The **conjunctiva** is a semi-transparent thin layer, found in the inner lining of the upper and lower eyelids, and in the sclera extending until the cornea [4]. It facilitates the movement of the eyelids and the eyeball. It is highly vascularized and innervated, providing lubricant oils and mucous to the eye, thus offering extra protection [1].

The **ciliary body** is connected to the sclera and the iris. It is responsible for the aqueous humour secretion and its draining into the trabecular meshwork, it also provides focus adjustment through muscles that act on the crystalline lens, changing its shape [4].

The **iris** is suspended in aqueous humour between the cornea and the lens. It is a contractive and pigmented diaphragm with a small circular opening called **pupil**, that acts upon the regulation of light that is allowed to pass through. The colour of the iris is unique to each individual, depending on the level of pigmentation of its constituent's stroma cells [5].

The **aqueous humour** is a clear, neutral colourless fluid continuously secreted (average 2.5 μL/min) from epithelial cells in the ciliary body. It is usually completely renewed in 100 min.

It is constituted mainly by water (99%), but proteins, glucose, lactic acid, ascorbic acid and immunoglobulin G are also present. It favourably removes macrophages, debris and impurities from the posterior cornea while providing oxygen and nutrients. It is also crucial for the maintenance of the convex shape of the lens and of the intraocular pressure [4].

The **lens** maintains its position through the action of an arrangement of ligaments (i.e. zonules of Zinn) that are connected to the ciliary body. These zonules act on the lens, regulating the focus ability of the eye. The lens is a transparent, avascular and non-innervated structure, located behind the iris. The aqueous humour covers the anterior part of the lens, while the posterior is covered by the vitreous humour [1,4].

The **choroid** is located between the ciliary body and extends until the optical nerve. It is highly vascularized and innervated, and provides nutrients to the outer layers of the retina [6].

The **retina** is composed of two major layers, the inner neurosensory retina (i.e. neural retina) and the retinal pigment epithelium (RPE). The neural retina presents photoreceptors, and first and second order neurons (i.e. ganglion cells and the Müller´s cells (neuroglial elements)). It extends from the optical nerve till the ciliary body. It is responsible for the conversion of the light that crosses the pupil (more specifically the photons) into a nerve signal, which is sent through the optical nerve to the brain. The RPE consists of a single layer of non-dividing cells, that may proliferate. It is located above the neural retina and provides protection by preventing diffusion of toxic molecules originated in the choroid that could irreversibly damage the photoreceptors of the neural retina. Additionally, it secrets several growth factors, enzymes, and immunomodulatory cytokines.

The **optic nerve** is constituted by the axons of the retinal ganglion cells. It provides a pathway to safely transport the neural signals from the retina into the brain [7].

The **vitreous humour** is a clear viscoelastic gel-like fluid constituted mainly of water (~98%), and also of hyaluronic acid (HA), collagens type II and IX, fibronectin, fibrillin and opticin. Its function is to maintain the intraocular pressure to assure that the retina remains in place, and the eye keeps its shape [4].

1.1.2 Ophthalmic disorders of the anterior segment and respective treatment

The most common diseases that affect the structures of the anterior segment are: cataracts, dry eye, ocular keratitis, conjunctivitis and traumas [1,8].

Cataract is the opacification of the lens, whose origin can be congenital, traumatic or related to aging. It is treated by removal of the natural damaged lens and its substitution with an intraocular lens. This type of surgery is often ambulatory and does not require internment, however it can be preceded by topical antibiotic administration to prevent endophthalmitis in the post-operatory period [9]. Additionally, after surgery, both antibiotic and anti-inflammatory drugs can be prescribed.

Dry eye syndrome is a multifactorial disease of the ocular surface and lachrymal fluid. It may result from failure of the lachrymal glands to produce enough fluid or from improper functioning of the meibomian glands that do not produce or secrete enough oil (meibum), leading to a fast tear film evaporation. It is frequently related to aging, menopause, contact lens wear, medications, computer use and environmental factors. The development and aggravation of this disease can also be related with refractive and cataract surgeries [10]. Several ocular surface symptoms are associated to this condition, e.g. visual disturbance, tear film instability and discomfort [11]. In chronic dry eye cases frequent instillation of artificial tears is required to relief patients' discomfort, while in cases of inflammation the application of short-term steroids is necessary [12–14].

Ocular keratitis represents an infection and inflammation of the cornea. Karsten *et al.* (2012) reported 232 different microbiological agents which may be involved in the development of ocular keratitis. The severity of the keratitis depends on the infection agent. One of the most damaging keratitis is the *Acanthamoeba* keratitis caused by the parasite *Acanthamoeba* that is present in soil and fresh water [15]. This type of keratitis is often related to incorrect use of contact lenses, contact with contaminated water or eye trauma [16–18]. Bacterial keratitis is considered the most threatening form of keratitis; its rapid progression can result in cornea destruction in 24-48 h. Gram-positive bacteria are most commonly associated to keratitis formation, namely: *Staphylococcus aureus* (*S. aureus*), *Staphylococcus epidermidis* (*S. epidermidis*), *Streptococcus pneumonia* and *Bacillus* spp. While in the case of gram-negative bacteria, *Pseudomonas aeruginosa* (*P. aeruginosa*) represents the most common strain [19]. If

left untreated, it can result in blindness [20]. The treatment resides in the application of antiseptic and antibiotic drugs [17,21].

Conjunctivitis is the inflammation of the conjunctiva, manifesting through lachrymal excess production, red eyes and discomfort. Three types of conjunctivitis exist, bacterial, viral and allergic (caused by the immune system in response to an allergen or to an irritant extern agent). Treatment is carried out according to the conjunctivitis source. In severe cases, anti-inflammatory drugs must be prescribed to prevent further inflammations, and relieve pain, reduce redness and the patient's discomfort [22–24].

1.1.3 Drug delivery routes in ocular treatments

Vision impairment is regarded as major worldwide problem, affecting nearly 285 million people. As this number is anticipated to rise as age expectancy increases [25], the development of new and more efficient ocular treatments is regarded as a challenge for the pharmaceutical community [26]. Current pharmacological treatments are based on three major methods of delivery: topical; systemic and intraocular [27].

Topical administration through the instillation of eye drops represents the most common method of administration of drug in the treatment of ocular diseases/disorders [28]. It is a simple, non-invasive and self-administered method that is well accepted by patients. Both external (e.g. cornea, conjunctiva, sclera) and internal (e.g. aqueous humour, iris, ciliary body, vitreous humour, retina) structures can be targeted, according to the drug´s physiochemical properties [29]. However, several eye protecting barriers greatly affect eye drop instillation. Drug availability is reduced between 93% – 99%, through rapid tear turnover (0.5 – 2.2 µL/min), tear replacement (2 – 3 min), nasolacrimal drainage and flushed into the patient's cheek due to reflex eye blinking [30,31]. Additionally, the drug can diffuse into the highly permeable conjunctiva in detriment of other target structures. The reduced availability and low residence time of the ophthalmic drugs impose high concentrated doses and frequent applications. Increase in drug concentrations could result in undesirable side effects, as an estimated 80% of the drained drug can reach the blood circulation and subsequently major organs [32]. Extended eye drops instillation relies on patients' compliance, which is usually compromised due to the mandatory hourly application and can result in drug overdosing or underdosing [33].

Systemic drug delivery faces two major problems, the scarceness of blood vessels in the eye and the blood-retinal barrier of the RPE, ultimately reducing drug penetration. As such, high doses of drugs are needed to achieve an effective outcome, which inevitably leads to severe side effects [29,34].

Drug delivery into the posterior segment, relies mainly on intracameral injections of drug solutions. Although the drugs are directly injected in the vitreous chamber, the vitreous humour fast replacement and the dense network of fibbers present in the chamber, undermine the drugs efficiency. Inevitably, the reduction of drug availability and time of residence requires painful and uncomfortable frequent injections [35]. More, this is a very invasive method and may involve serious complications, such as endophthalmitis, retinal detachment, intravitreal haemorrhage and cataract.

Figure 1.2 resumes in a schematic representation of the referred drug delivery methods and of other also used, although in a lesser extent.

Considering the limitations stated above for current ophthalmic drug delivery systems, new and more efficient systems that follow ideal ocular delivery criteria are needed. Such systems should: (i) sustain drug release at the required therapeutic time and concentration; (ii) limit undesirable side effects; (iii) favour patient compliance; (iv) be cost-effective. Several attempts have been carried out to improve ocular therapeutics. Variations in eye drop formulations by increasing viscosity [36], application of nanoparticles [29], liposomes [37], micelles [38] and others, do not extensively improve drug availability, and therefore do not guarantee patients compliance. Innovative implantable devices have been studied to avoid conventional routes of drug delivery (**Figure 1.2**). All commercially available implantable devices are focussed on ocular delivery to the posterior segment, namely: Ozurdex® that provides a $60 - 90$ days release of dexamethasone; Surodex® for the release of dexamethasone for $7 - 10$ days, Iluvien® which provides a release of $18 - 36$ months of fluocinolone, and Retisert® that releases fluocinolone for 30 months. The anterior segment is a trickier structure, as implantable devices can more easily affect vision, comfort and can also move resulting in tissue damage [34].
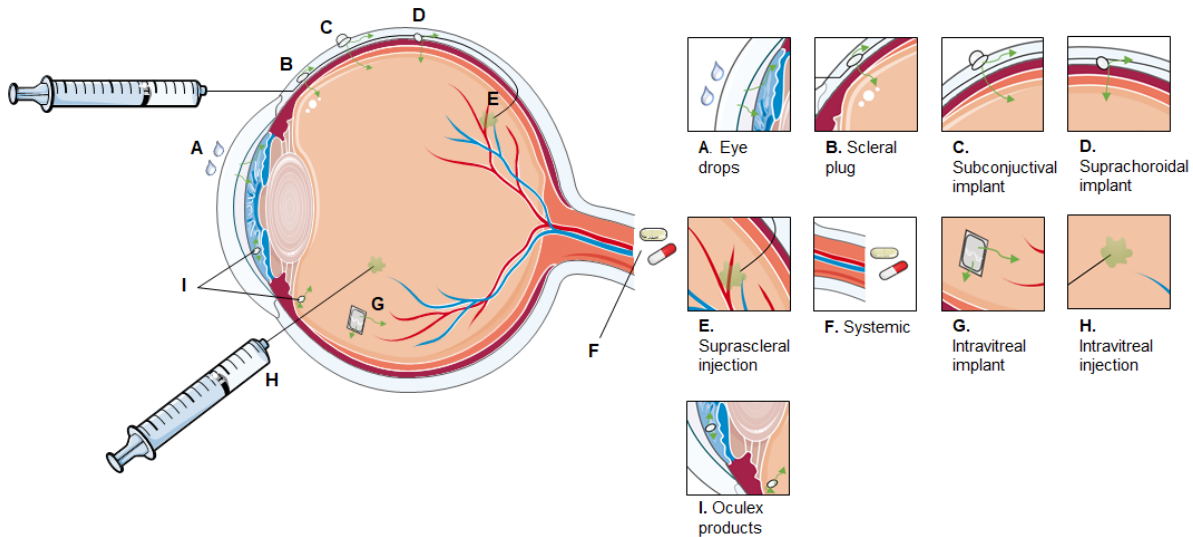
Figure 1.2 Schematic representation of ocular drug delivery systems. Adapted from [39].

Soft contact lenses (SCLs) are being regarded as a promising anterior segment drug delivery system [26]. SCLs are already implemented and well accepted, as more than 140 million people use them for corrective vision [40].

1.1.4 Contact lenses: From eye correction to drug delivery

Contact lenses are medical devices made of biocompatible polymeric materials and so have been approved by the European Medicines Agency (EMA) in Europe and by the Food and Drug Administration (FDA) in the United States of America (USA) [41]. They are used for corrective vision, through correction of the refractive error. The contact lenses are directly placed in front of the cornea (~5 µm distance), and they are supported by lids, cornea, conjunctiva and tear film [42,43]. The contact lens divides the tear film in post lens tear film (POLTF) and in pre lens tear film (PLTF) (**Figure 1.3**). The proper correction of the eye´s refractive error depends on the similarity of the back-vertex power of the contact lens/ POLTF and contact lens/PLTF systems with the ocular refraction [44].
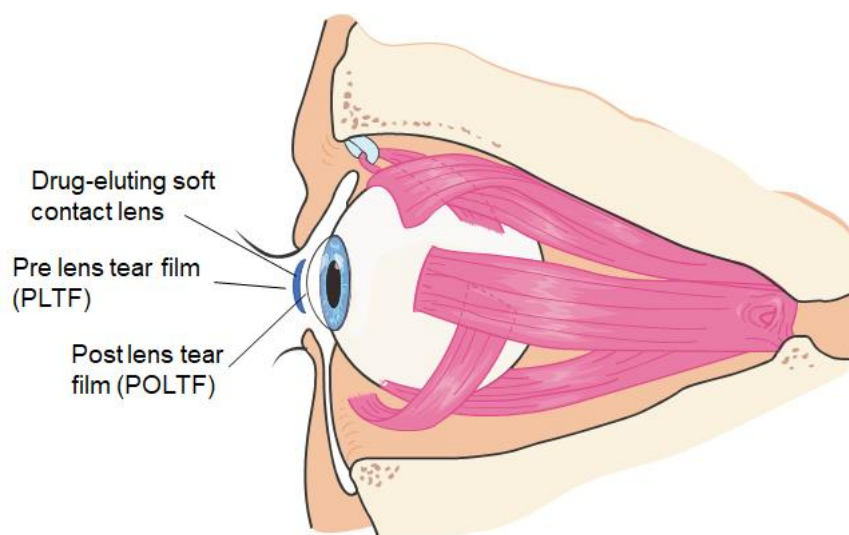
Figure 1.3 Schematic representation of a contact lens position in the human eye. Adapted from [45].

The use of contact lenses was first approached in 1888 by Adolf Eugene Fick, who introduced a glass lens in the eye, and poured a liquid between the eye and the lens. A year later, August Müller, in his work entitled "Brillengläser und Hornhautlinsen" fitted in his own eye a glass contact lens, however the extreme discomfort described by Müller precluded their use for more than half an hour, as they imply a disturbance in the normal nourishment and oxygenation of the cornea [46]. The manufacturing of contact lenses was put on hold until a dramatic change occurred in the late 1930's, when the use of polymeric materials took place. Müller and Ohring introduced the first rigid contact lenses made of poly methyl methacrylate (PMMA), in 1936. These contact lenses had the advantage of being more comfortable, lighter, durable and easier to produce than the preceding glass made contact lenses. Nevertheless, PMMA was still impermeable to oxygen, and as such, unsuitable for proper cornea oxygenation. Cellulose acetate butyrate contact lenses were then introduced in 1978 by FDA approval, due to its gas permeability, but, they were also discontinued [43]. In fact, rigid contact lenses are becoming obsolete as their reduced gas permeability and lack of comfort discourage patients [47].

The development of SCLs by Otto Wichterle in the late 1950s was regarded as a worldwide breakthrough for the clinical application of commercial hydrogel lens. Wichterle polymerized a hydroxyethyl methacrylate (HEMA) monomer with the addition of a catalyst to obtain a new polymeric material (pHEMA) with improved biocompatible properties for human body applications [44]. Further investigation of this material led to the improvement of its properties

by variation/addition of other monomers. Improved water contents, refractive indexes, ionic and O_2 permeabilities were achieved. In the 1970's Bausch&Lomb introduced the first commercial SCLs after FDA approval [48]. Unquestionable, SCLs implementation on the market was an immediate success predominantly due to their superior comfort and biocompatibility [46]. Nevertheless, continuous developments occurred, with the addition of various monomers to the SCLs mixtures. The acknowledgment that O_2 permeability of HEMA-based hydrogels was directly related to the hydrogels water content, resulted in a search for monomers that enhance hydrophilicity, namely: N-vinyl pyrrolidone (NVP), N,N-dimethyl acrylamide (DMA), glyceryl methacrylate (GMA) and methacrylic acid (MAA). However, the increase in water content undermines the hydrogel integrity and favours bacteria proliferation [43,47]. Prediction of the necessary O_2 permeability of SCLs to avoid hypoxia of the cornea [49], demonstrated that HEMA-based hydrogels, even with 90% water uptakes could never reach the necessary values for SCLs extended use [43].

Silicone-based hydrogels were introduced by Bausch&Lomb and CIBA Vision in the late 1990s, to overcome the limited O_2 permeability of conventional SCLs. Silicone-based SCLs do not rely on water uptake for O_2 permeability, instead the permeation occurs through silane groups present in the hydrogel [50]. Silicone-based SCLs are produced using siloxane macromers, namely: poly dimethylsiloxane (PDMS), tris-trimethylsiloxysilyl (TPVC) and N-tris(trimethylsiloxy)-methacryloxy-propylsilane (TRIS). Nowadays silicone-based SCLs represent more than 60% of the SCLs market in the USA [48].

In **Table 1.1** a brief summary of commercially available SCLs is presented.

11

Table 1.1 Brief summary of commercially available SCLs [51–57].

Name	USAN[a]	Manufacturer	Principal components	WU (%)[b]	Dk/L (x10^{-9} cm mlO$_2$/s ml mmHg)[c]	Modality
1 Day Acuvue	Etafilcon A	Johnson & Johnson	HEMA, MMA	58	28	Daily
1-Day Acuvue TruEye	Narafilcon A	Johnson & Johnson	mPDMS[d], DMA, HEMA, siloxane	46	118	Daily
Acuvue Oasys	Senofilcon A	Johnson & Johnson	mPDMS, DMA, HEMA, siloxane, TEGDMA[d], PVP[d]	38	147	Bi-weekly
Acuvue Vita	Senofilcon C	Johnson & Johnson	mPDMS, DMA, HEMA, siloxane, TEGDMA, PVP	41	147	Month
AirOptix Aqua	Lotrafilcon B	CIBA Vision	DMA, TRIS, siloxane	33	138	Month
Bioafinity	Comfilcon A	CooperVision	NVP, VMA[d], IBM[d]	48	160	Month
Biomedics 55	Ocufilcon D	CooperVision	HEMA	55	19.7	Daily
Focus Night & Day	Lotrafilcon A	CIBA Vision	DMA, TRIS, siloxane macromer	24	175	Month
Focus Softcolors	Vilifilcon A	CIBA Vision	HEMA, NVP, MMA	55	16	Daily
Purevision	Balafilcon A	Bausch&Lomb	NVP, TPVC, NVA[d], PBVC[d]	36	101	Month
SofLens 59	Hilafilcon B	Bausch&Lomb	HEMA, NVP	59	22	Daily

[a] USAN stands for United States Adopted Names
[b] Water uptake
[c] Oxygen transmissibility (reference to -3.00D)
[d] mPDMS: monofunctional polydimethylsiloxane, TEGDMA: Tetra-ethyleneglycol dimethacrylate, PVP: Polyvinyl pyrrolidone, VMA: N-vinyl-N-methylacetamide, IBM: Isobornyl methacrylate, NVA; N-Vinyl aminobutyric acid, PBVC: Poly(dimethysiloxy)di (silylbutanol) Bis(vinyl carbamate).

Although Wichterle discussed the possibility of using hydrogels as potential drug carriers [58], 60 years later no drug delivery contact lenses have been implemented in the market, despite promising clinical trials and proven SCLs biocompatibility and non-toxicity [43]. SCLs are still regarded as a risk factor for eye therapy, as they preclude corneal damage, discomfort and possible infections [34]. In spite of this, numerous studies have been made to revoke those pre-established statements [59–62]. The unique position of SCLs in the eye benefits drug release (See **Figure 1.3**). Drugs diffuse from the SCLs to both sides of the tear film. In the POLTF the drugs are delivered into the cornea or to the outer layers, and can subsequently reach the anterior segment. In the case of the PLTF the drugs are mainly lost by absorption into the conjunctiva or drainage [43]. Ultimately, drug residence time on the lachrymal fluid increases by a staggering 50% compared to typical eye drop therapy. The increase in drug bioavailability positively favours cornea penetration, reducing the frequency of administration and drug concentration [28,63].

Ophthalmic drugs can easily be loaded in the SCLs by simple soaking in a concentrated solution. Unfortunately, insufficient interaction and affinity occurs between the hydrogel's matrix and most drugs. As such, this simple process is usually followed by an initial burst of drug that greatly detriments the drug's therapeutic concentrations [64]. **Figure 1.4** schematically compares the ideal performance of a therapeutic SCLs with the usual ineffective soaked SCLs and with conventional eye drop therapy.
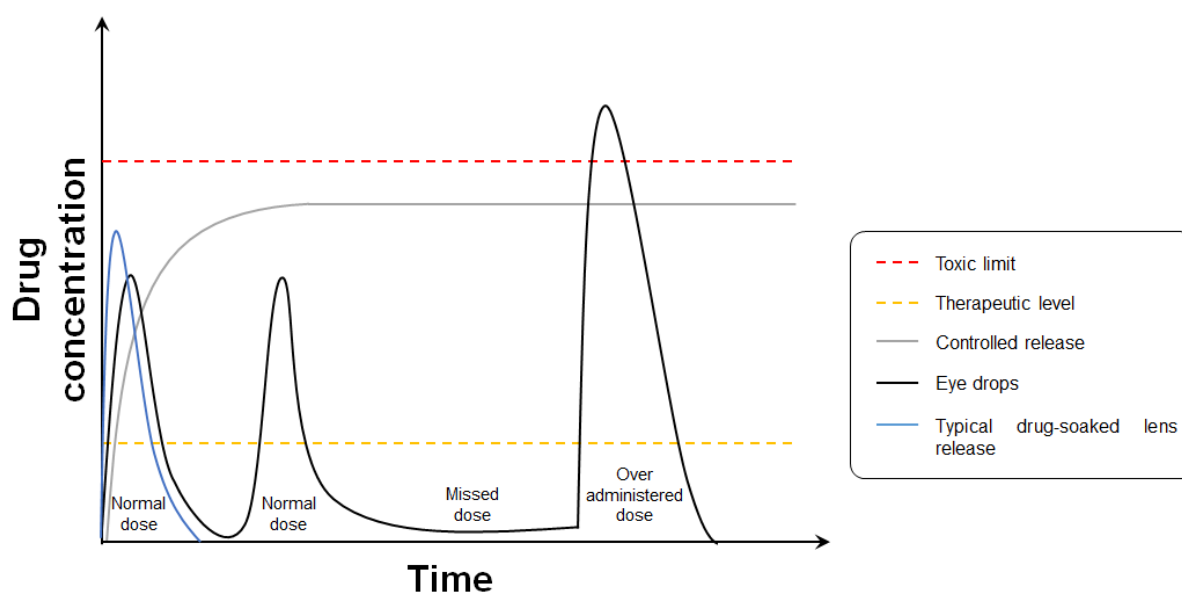
Figure 1.4 Schematic comparison between ideal therapeutic SCLs with inefficient soaked SCLs and with conventional eye drop therapy.

Several strategies have been implemented to improve the therapeutic efficacy of drug loaded SCLs, mostly focusing on the reduction of the initial burst, the increase of drug uptake and hydrogel affinity for specific ophthalmic drugs, in order to achieve a prolonged and controlled drug release [63].

1.1.4.1   Strategies for controlled drug release from SCLs

The drug loading and release behaviour from SCLs depends on the drug (e.g. molecular weight, ionizable groups, hydrophilicity) and the SCLs (e.g. composition, water content) characteristics, as well as on the loading conditions (e.g. temperature, time, concentration) [65]. Hehl e*t al.* (1999) loaded commercially available SCLs (Etafilcon A) by soaking in a tobramycin and obtained a 10 min release [66]. Tian *et al*. (2001) also soaked commercial SCLs (i.e. etalfilcon A and vasurfilcon A) and HEMA based hydrogels in ofloxacin solutions but the release time was 1 h in sink conditions [67]. Hui *et al*. (2008) studied the uptake and release of ciprofloxacin-HCl from commercially available silicone-based SCLs, achieving less than 24 h of release time [68]. Schultz *et al.* (2009) obtained a 60 – 90 min release of timolol maleate or brimonidine tartrate from commercial contact lenses (vasurfilcon A) [69]. Soluri *et al*. (2012) loaded ketotifen fumurate (anti-allergy drug) on several commercially available SCLs, however none of the SCLs led to more than 4 h of release [70]. Many other examples exist that demonstrate the inefficiency of the soaking method in several cases, ultimately proven by the absence of commercial drug delivery SCLs. Regardless, several efforts have been pursued to make drug-elution SCLs a success.

Vitamin E

The use of Vitamin E as a drug barrier was first proposed by Peng *et al.* (2010) [71]. Vitamin E is a lipophilic vitamin, with very low solubility in water. As such, it can be loaded into the SCLs by soaking in an ethanol solution, the ethanol is removed by drying the SCLs in air. Vitamin E creates aggregates inside the hydrogel matrix forcing variations of the drug molecules path, that ultimately result in a tortuous and delayed transport (**Figure 1.5**) [26]. Vitamin E shows a shorter wavelength than visible light, thus not interfering with the transparency of the SCLs [43].
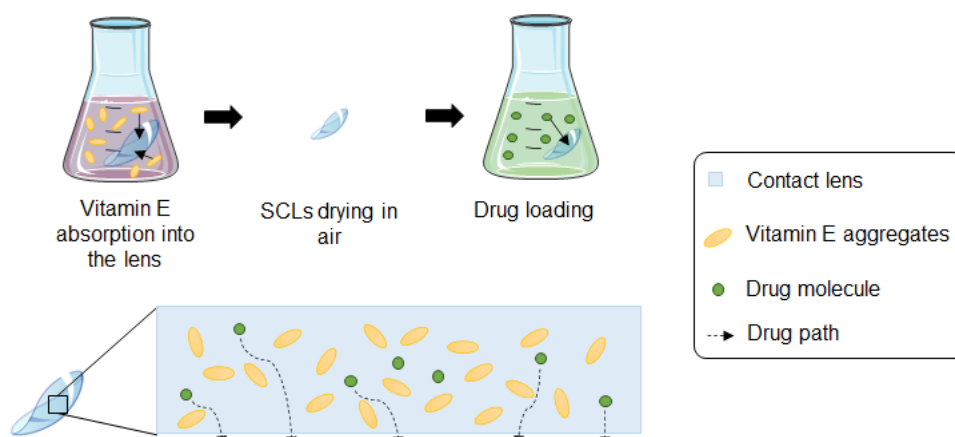
Figure 1.5 Schematic representation of Vitamin E and drug loading and Vitamin E loaded SCLs network and drug release mechanism. Adapted from [43].

Kim *et al.* (2010) extended the release of dexamethasone from silicone-based SCLs loaded with Vitamin E, to obtain a sustainable 7 – 9 days release [72]. Hsu *et al.* (2013) demonstrated an increase from 10 min to 3 h of sustainable release of cysteamine from four different silicone-based SCLs and from one HEMA-based (Etafilcon A) SCLs, due to Vitamin E incorporation [73]. Paradiso *et al.* (2016) loaded Vitamin E to increase from 2.5- to 10-fold the release time of an antibiotic (levofloxacin) and an antiseptic (chlorohexidine) drugs from silicone-based commercially available SCLs [74].

Vitamin E incorporation seems to be promising as a drug control strategy, however concerns persist in terms of decrease in O_2 and ionic permeabilities, and its resistance to typical SCLs cleaning and handling procedures [63].

Molecular Imprinting

The molecular imprinting process resides in the synthesis of novel contact lens materials to specifically target key drug molecules, for the unique purpose of increasing its uptake and ultimately controlling its release [75]. In this method the drug molecule is directly added to the monomer mixture, along with the initiator, crosslinker and functional monomers (monomers with the exclusive purpose of increasing possible interaction sites with the drug). With polymerization, tailored-active cavities are created with the size of the drug molecule, surrounded by the most suitable chemical groups (**Figure 1.6**). These memory pockets

engraved in the hydrogel matrix will efficiently recognize the drug molecule, increasing the affinity of the matrix towards the drug. This unique network arrangement results in an increase in drug uptake and can subsequently result in a more controlled release [76].
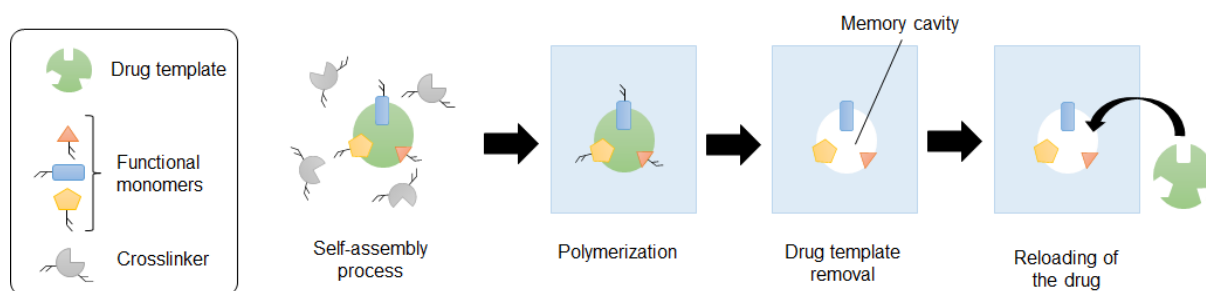
Figure 1.6 Demonstration of the molecular imprinting process. Adapted from [43].

The diffusion of the drug molecules can be affected by average mesh size, template size and drug-matrix chain interactions [77]. As such, the implementation of functional monomers is chosen according to the available binding sites of the drug molecule, without affecting the hydrogels physical properties [78]. Several functional monomers have been studied for their efficiency in the molecular imprinting method, namely, acrylic acid (AA), acrylamide (AM), MAA, methyl methacrylate (MMA) and NVP [26].

Hiratani *et al.* (2002) produced N,N-diethylacrylamide hydrogels for SCLs, using various concentrations of crosslinking agent and functional monomer (MAA) to achieve a 48 h controlled release of timolol [79]. Alvarez-Lorenzo *et al.* (2006) studied the efficiency of two different functional monomers (AA and NVP) on norfloxacin loading and release from HEMA-based hydrogels for SCLs, and found that AA resulted in a more sustainable release than NVP- [80]. Tieppo *et al.* (2012) produced HEMA-based hydrogels with AA to increase in 4- to 50-fold the release time of ketotifen fumorate, compared to non-imprinted hydrogels and to commercial eye drops (Zaditor®) [81]. Malakooti *et al.* (2015) produced polymyxin B and vancomycin imprinted AA-HEMA-based hydrogels, obtaining a sustainable 2 weeks release [82].

Molecular imprinting leads to a significant enhancement of drug loading amounts and to an increase in the drug's release time when compared to unaltered hydrogels for SCLs. The use

of this method can, however, be limited in terms of simultaneous release of drugs and its effect on basic SCLs properties [83].

Nanoparticles

SCLs can be integrated with drug nanocarriers in their matrix. These nanocarriers usually consist of nanoparticles (size < 1 µm) that entrap the drug molecules inside their polymeric structure. Both biodegradable and non-degradable polymers have been tested for the development of nanoparticles for therapeutic SCLs. Since the drug needs to diffuse from the nanoparticles first, before leaving the hydrogel and finally reaching the biological system, the drug release takes longer, thus preventing an initial burst (**Figure 1.7**). Generally, improvement of the nanoparticle's biocompatibility can be achieved by incorporating the drug nanocarriers directly in the monomer mixture previously to polymerization. The nanoparticles can also be incorporated on the SCLs matrix by simple soaking [27,29,33]. There are several concerns regarding nanotoxicity of the particles. Improvement of the nanocarriers biocompatibility can be achieved, not only by variations of their composition but also by attaching them to the hydrogel network to prevent nanoparticle migration.
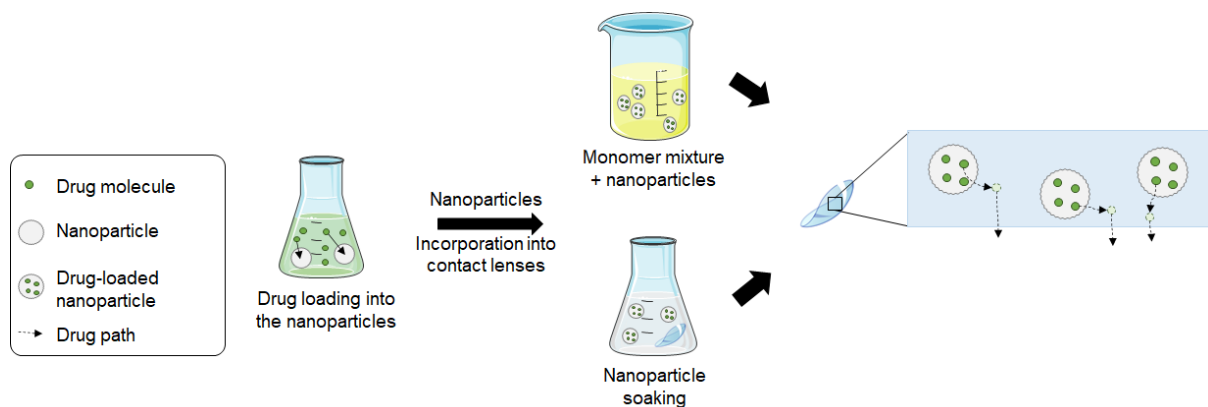
Figure 1.7 Schematic representation of nanoparticle loading and nanoparticle-laden SCLs drug release mechanism. Adapted from [43,84].

Jung *et al.* (2013) produced propoxylated glyceryl triacylate nanoparticles for the release of timolol from contact lens. The presence of the drug in the release solution was still detected

after one month, and the *in vivo* tests in Beagle dogs demonstrated the effect of the drug on the intraocular pressure [85]. Zhu *et al.* (2018) modified a pHEMA hydrogel by adding an inner layer of ethyl cellulose and Eudragit S100 nanoparticles to extend the release of diclofenac sodium salt (DCF) by pH-triggering. *In vivo* studies in rabbits using lenses made with this modified pHEMA hydrogel showed a sustainable release for 24 h [62]. Maulvi *et al.* (2019) investigated the effect of gold particles on loading and release kinetics of timolol from the contact lenses, and found through *in vivo* tests that the intraocular pressure in the eyes of the rabbits remained stable after 72 h [86].

SCLs show low uptake for hydrophobic drugs; in this case nanoparticles have been studied as a possible strategy to overcome this difficulty. Nasr *et al.* (2016) produced loteprednol etabonate loaded polycaprolactone based nanoparticles that were entrapped on a HEMA/NVP based hydrogel for contact lenses. An extended release of 12 days was obtained in *in vitro* assays [87]. Behl *et al.* (2016) used chitosan (CHI) nanoparticles loaded in HEMA-based SCLs to achieve a controlled release of dexamethasone for 22 days, increasing its bioavailability by 72% compared to typical eye drop therapy [88].

Nevertheless, these nanocarriers present several disadvantages that need to be addressed namely, in terms of their nanotoxicity, safety, and problems related to production scale-up.

Surface modification

Surface modification is generally used in commercial SCLs, with the objective of improving wettability (e.g. plasma treatment) [77,89]. The acceptance of SCLs by the users can be influenced by the interactions between the surface of the SCLs and the involving biological tissues [40]. Therefore, various studies focus on the improvement of surface properties to improve acceptance [90–92]. Additionally, future perspectives refer to the implementation of various applications through surface modification, namely addition of interactive chemical targets, stimuli-responsive drug release, bio-sensors and others [93]. Surface modification can be achieved using physical (e.g. plasma, laser) or chemical agents (e.g. chemical attack, coating). One of the most common methodologies is the application of coatings on SCLs, which can be carried out by several methods, namely, molecule adsorption/grafting [94], layer-by-layer (LbL) method [95] and immobilization of liposomes on the hydrogel matrix [96,97] (**Figure 1.8**).
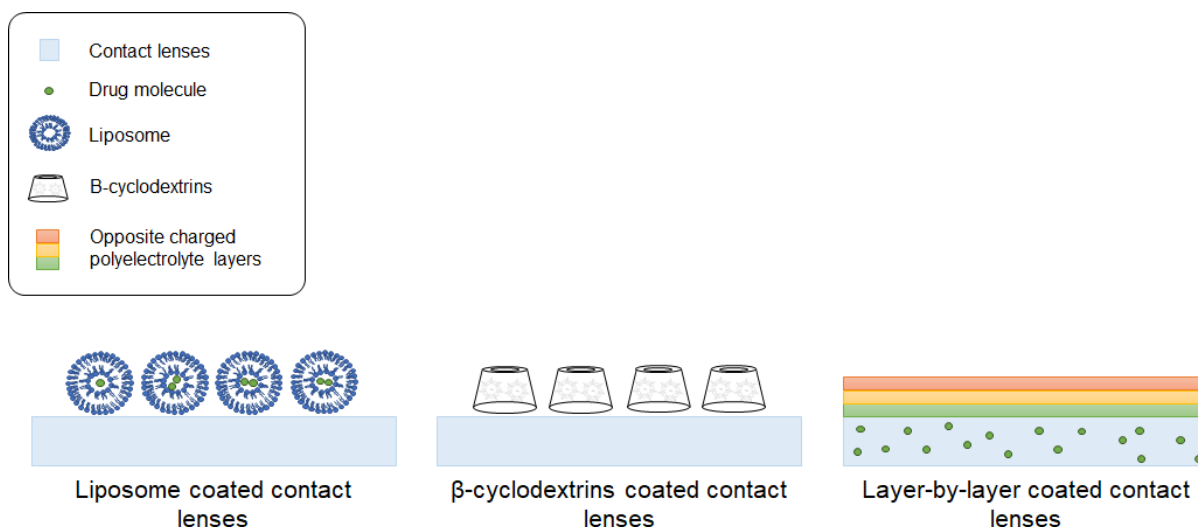
Figure 1.8 Demonstration of different surface modification methods for SCLs. Adapted from [98].

Danion *et al.* (2007) coated commercial SCLs with liposomes (n=2, 5 and 10 layers) for a sustainable 6 days release of levofloxacin [99]. Dos Santos *et al.* (2009) prepared pHEMA hydrogels for SCLs with GMA at various proportions, and grafted to the surface β-cyclodextrin, which did not make part of the structural chains but was hanging on 2-3 ether bonds through the hydroxyl groups. The β-cyclodextrin coated hydrogels were able to sustain the release of DCF in lacrimal fluid for two weeks [100].

The LbL method defined by the formation of multi-layered films by electrostatic self-assembly of polyelectrolytes is being regarded as a versatile and simple technique to provide specific target properties, and to obtain efficient therapeutic delivery devices [101]. In fact, the selection of the used polyelectrolytes can provide improved hydrophilicity [102] and antibacterial and antifouling properties [103,104]. The use of LbL coatings to control cell adhesion to biomaterials surfaces has also been described [105]. Elbert *et al*. (1999) reduced the tendency of a proteinaceous surface to the adhesion of proteins and cells, by using poly-L-lysine (PLL)/ALG multilayers [106]. HA coated intraocular lenses prevented fibroblasts adhesion and decreased the growth of bacterial films [107,108], while the addition of cross-linked HA in SCL materials reduced surface tear protein adsorption [109,110]. Croll *et al*. (2006) studied the protein adsorption on various polymeric surfaces and found that it was minimized through LbL deposition of films comprised by high molecular weight HA and CHI, ultimately reducing

foreign body adverse responses [111]. Hernandez-Montelongo *et al*. (2016) showed that HA/CHI nanofilms had antibacterial properties against *S. aureus* [103]. LbLs have also been used to build the shells of hollow capsules where solutes may be encapsulated and then released across the membrane in the presence of a concentration gradient [112,113]. In the case of LbL modified SCLs, some articles discuss the efficiency of these multi-layered coatings on drug delivery. Hu *et al*. (2014) coated a HEMA-based hydrogel for SCLs application by the LbL method, using CHI and HA as polyelectrolytes. This surface modification resulted on an improved hydrophilicity, reduced protein adsorption and increased the release time of norfloxacin (4 h) and timolol (1 h) [114]. Chen *et al*. (2015) produced a multilayer coating by the LbL method depositing polycarboxymethly-β-cyclodextrin and PLL polyelectrolytes on HEMA-based hydrogels. This multi-layered coating was loaded with orfloxacin or puerarin, and demonstrated a gradual release for 20 h. However, significant modification of the hydrogel's transparency occurred [95].

The challenge of forming coatings that do not lead to undesirable optical modifications of SCLs has driven away research on the SCLs surface modification, as great care must be taken in this type of drug control strategy [26].

Implanted drug loaded films

In this approach, multilayers of hydrogels are created by sandwiching drug loaded films between hydrogel layers. Those films are usually produced in a ring or half-ring form to avoid affecting the SCLs transparency as a clear central zone is created to allow light to pass through the pupil (**Figure 1.9**). Ciolino *et al*. (2014) produced a multilayer drug loaded poly (lactic-co-glycolic acid) films on a commercial SCL (methafilcon). *In vivo* assays showed a sustainable release for 4 weeks without hindering the biocompatibility of the lenses [115]. Maulvi *et al*. (2018) prepared two semi-circular rings individually loaded with MXF and HA, that were implanted on a separate periphery of a hydrogel for SCLs use. The release data showed proper release of MXF and HA up to 4 days, while *in vivo* assays demonstrated equivalent healing effect to that obtained with high doses of eye drop therapy [116].

These strategies can be practical from the point of view of drug-release, however since the drug loaded rings are implanted in the SCLs there are concerns regarding thickness, comfort, mechanical properties and O_2 and ionic permeabilities of the SCLs [43].
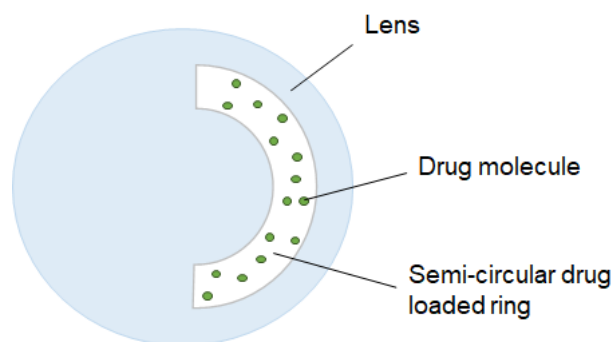
Figure 1.9 Schematic representation of a drug loaded implantable semi-circular disk in a SCLs. Adapted from [116].

Supercritical solvent impregnation

Supercritical fluid technology facilitates load/impregnation of ophthalmic drugs in SCLs. This approach relies on the fact that drugs can be dissolved in certain fluids (e.g. carbon dioxide (CO_2)) above critical temperatures and pressures, facilitating the drugs impregnation on the hydrogel's matrix. The compressed fluid mixture improves the drug's diffusion into the network by increasing the free volume. Moreover, the amount of drug loaded can be controlled by use of cosolvents and by variations in pressure and temperature. With an adequate procedure (e.g. pressurization/depressurization rates), this method does not affect negatively the physical, chemical and mechanical properties of the drugs and/or SCLs [77,117]. Costa *et al.* (2010) demonstrated the relation between the nature and concentration of the cosolvents (ethanol and water) with the impregnation capacity of the contact lenses (Balafilcon A) [118]. Yañez *et al.* (2011) assisted the molecular imprinting of flurbiprofen on SCLs (Hilafilcon B), by impregnating the drug through the supercritical fluid technique. No variations of the SCLs properties were detected, but a significant improvement of flurbiprofen loaded and subsequently released was achieved [119].

There are still security concerns about using this system in large scale for therapeutic SCLs production.

1.1.4.2 Material's properties characterized in this thesis

As medical devices SCLs must satisfy a set of requirements: they must not interfere with the user´s visual capacity; the user´s comfort has to be ensured: they cannot be toxic or injurious. Furthermore, SCLs should maintain a health ocular environment, providing a stable continuous tear film and be permeable to oxygen and ions, respectively, for cornea health and correct eye movement. In the following sections, it is given an overview about the most relevant properties of SCLs that shall be evaluated in the development of new devices and that were addressed in this work.

1.1.4.2.1 Transmittance

SCL materials must be transparent within the visible wavelength range (400-700 nm), letting the light pass through the cornea towards the retina. The velocity of light propagation depends on the interactions of the photons with the atoms of the materials, determining if the light is dispersed, absorbed or transmitted [120].

The percentage of light transmitted thought a material is given by transmittance (%), expressed according to [121]:

$$T(\%) = \left(\frac{I}{I_0}\right) \times 100 \qquad\qquad \textbf{Equation 1.1}$$

where I_0 and I represent the intensity of incident light and of the transmitted light, respectively. SCLs materials should demonstrate a transmittance over 90% [47].

1.1.4.2.2 Refractive index

The refractive index represents the ratio between the velocity of light in air and in the designated material. Ideally, SCLs materials should have a refractive index similar to that of the cornea (**Table 1.2**) [122]. Contrary to conventional SCLs, silicone-based SCLs do not

demonstrate a linear relation between refractive index and water content, due to their composition [47].

Table 1.2 Refractive index of key biological components of the eye. Adapted from [122].

Eye component	Refractive Index
Tear fluid	1.336
Cornea	1.376
Aqueous humour	1.336
Lens	1.386/1.406
Vitreous humour	1.336

1.1.4.2.3   Water uptake

Hydrogels are characterized by their capacity to swell and retain large amounts of solvent without affecting their structural integrity [123,124]. This behaviour is dependent on the presence of hydrophilic groups, pores and of the matrix crosslinking density. The swelling capacity is associated with the SCLs comfort, biofilm formation, protein adsorption, and mechanical and physical properties [125,126]. The water uptake (%) is expressed as follows [123,124]:

$$Water\ uptake\ (\%) = \frac{W_H - W_D}{W_D} \times 100 \qquad \textbf{Equation 1.2}$$

where W_H is the weight of the hydrated hydrogel and W_D is the weight of the dry hydrogel.

1.1.4.2.4   Wettability

The wettability is defined as the capacity of a fluid to spread across a material's surface, and it can be determined by the contact angle between a liquid drop and the material [127]. For SCL application it is crucial that the tear fluid is able to spread across the lens surface, maintaining its stability and uniformity. If not, optical performance can be compromised due to interference of the tear fluid on the light transmittance, and to variations of the PLTF and of POLTF, thus resulting in discomfort and dry eye sensation [126]. Surfaces with polar groups present smaller contact angles with aqueous solutions (hydrophilic surfaces), whereas surfaces with non-polar groups have higher contact angles (hydrophobic surfaces). The contact angle is the angle formed between the surface of the solid and the tangent to the liquid/vapour interface at the three-phase boundary. The equilibrium contact angle, θ, for an ideal surface relates with the three involving interfacial tensions through Young´s equation [47,128]:

$$\gamma^{LV} = \gamma^{LS} + \gamma^{SV}.\cos\theta \qquad\qquad \textbf{Equation 1.3}$$

where γ^{LV}, γ^{LS} and γ^{SV} are, respectively, the liquid/vapour, liquid/solid and solid/vapour interfacial tensions, [129].

The contact angle can be measured by the sessile drop method or by the captive bubble method. Although, the sessile method is the most commonly used method, in the case of SCLs, the captive bubble technique is more suitable as it allows the measurement of the contact angle of the materials in their hydrated state. In this case, an air bubble is formed on the bottom surface of the material that is completely immersed in a liquid. Here the contact angle is the supplementary angle of the angle α shown in **Figure 1.10**, which depicts a schematization of the captive bubble method.
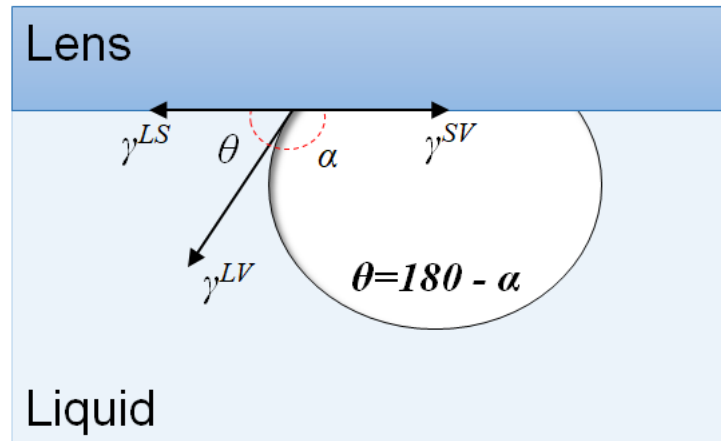
Figure 1.10 Schematic representation of the captive bubble method.

1.1.4.2.5   Ionic permeability

SCLs shall ensure the proper transport of water and ions across its network. This feature will avoid binding of the SCLs to the cornea ensuring adequate POLTF for nutrient transport, lens movement and removal of waste and debris [130,131]. The minimal required value of ionic permeability for proper lens movement in the eye is 1.065×10^{-9} cm^2/s [132]. The common methodology to determine the ionic permeability (D_{ion}) of SCLs is to use a diffusion cell (See **Figure 1.11**), where the hydrogel is placed between two chambers, a donor chamber (filled with saline solution) and a receiving chamber (with distilled and deionized (DD) water). D_{ion} can be calculated according to **Equation 1.4**, since ions pass through the hydrogel from the donor chamber to the receiving chamber, it is possible to measure the conductivity (µS/cm) of the fluid in this late chamber.

$$\frac{F.V}{A} = D_{ion} \frac{dC}{dx} \qquad \textbf{Equation 1.4}$$

where F is the rate of ion transport, V is the volume of the receiver solution, A is the cross area of the tested hydrogel and dC/dx represents the initial saline solution concentration [133]. **Figure 1.11** shows a representation of the ionic permeability apparatus used in this work.
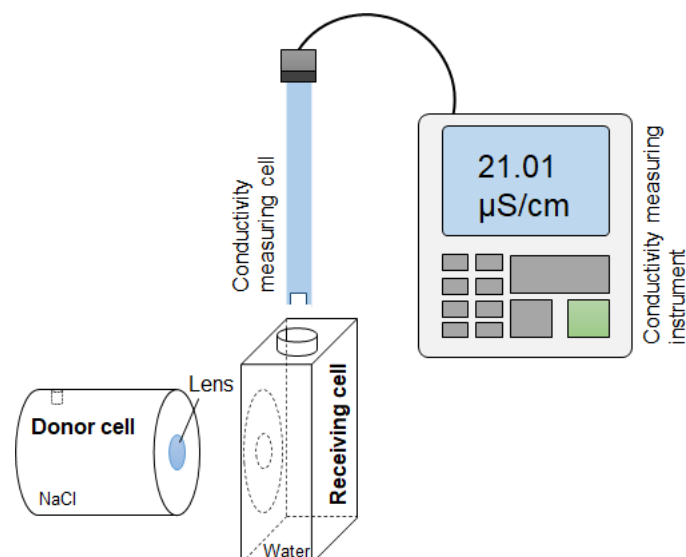
Figure 1.11 Schematic representation of the ionic permeability measurement apparatus used in this thesis.

1.1.4.2.6   Topography

Surface topography of SCLs can directly affect the user´s comfort, SCLs wettability and protein, bacteria and cell adhesion [134,135]. Baguet *et al.* (1995) correlated the tendency for biofilm formation and the increase of surface roughness [136]. Atomic force microscopy (AFM) allows high resolution observation of solid surfaces with a detailed information in real time. AFM technology relies on the interactions between a tip/probe and a material (e.g. ionic repulsion, electrostatic interactions, van der Waals forces). Such interactions are possible due to the proximity of the tip to the SCLs surface, achieved by piezoelectric devices included on the AFM instrumentation. This technique also avoids possible artefacts promoted by SCLs dehydration, as the hydrogels can be immersed in solution using a liquid cell. AFM apparatus is usually composed of four elements; (1) a cantilever, (2) a tip/probe that is directly mounted in the cantilever, (3) a piezoelectric scanner that allows a 3-dimensional movement and (4) a light source (laser) that is reflected by the back of the tip into a position sensitive photodiode detector [137,138]. The scan of the surface is usually carried out in non-contact or tapping mode. The tip movement is closely monitored by the piezoelectric element [139]. **Figure 1.12** shows a schematic of the AFM operating principle.

26
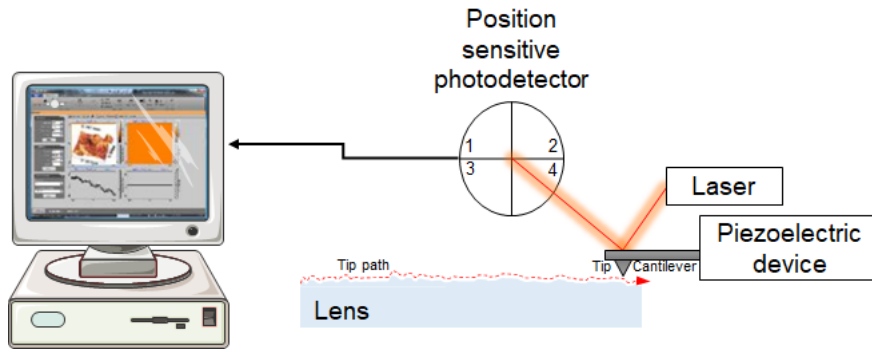
Figure 1.12 Schematic representation of the AFM operating principle. Adapted from [140].

Analysis of the AFM images leads to the value of the surface roughness at a micrometric scale. Commonly, surface roughness is characterized by the arithmetic average roughness (R_a), which is related to the variation of the height of the surface relative to a reference plane. R_a is usually calculated by integration of the surface height profile z(x) in relation to a mean line, that divides the peaks and the valleys in equal areas:

$$R_a = \frac{1}{L_g} \int_0^{L_g} |z(x) - m_L| dx \qquad \textbf{Equation 1.5}$$

where L_g is the sample profile length, and m_L is the mean line. R_a calculation is greatly influenced by the size of the scan [141,142]. Silicone-based SCLs can exhibit variations of roughness accordingly to their composition and preparation method [134].

1.1.4.2.7   Young's modulus

SCLs *in vivo* performance is directly influenced by its stiffness. SCLs in hydrated state must be flexible and soft, to ensure a good cornea fitting and to not impair the visual capacity. More, SCLs durability and handleability is also dependent on the material's mechanical properties. A decrease in water content is usually associated with an increase in hardness and brittleness of the SCLs. The tensile elastic modulus gives information on the deformation extent that one SCL can endure in elastic regime [47]. Typical Young's modulus values for SCLs range from

0.38 to 1.44 MPa. Silicone-based SCLs usually have higher Young's modulus than conventional SCLs, due to their composition [55]. Low Young's modulus can lead to higher degree of comfort due to better fitting to the cornea. The high flexibility of SCLs can induce minimal interaction with the eyelids during blinking, but it has the disadvantage of reducing the SCL lifetime. In contrast, high Young´s modulus permits better handling and extended SCL use, but it can affect comfort and ultimately lead to mechanically induce pathologies [47].

1.1.4.2.8   Interaction with lachrymal proteins

The interaction of the lachrymal proteins with SCLs can lead to undesirable side effects, such as increase in friction, loss of water content [143], biofilm formation and cell adhesion [144,145]. Protein adsorption can be measured with quartz crystal microbalance with dissipation (QCM-D). This technique relies on the piezoelectric behaviour of a quartz crystal sensor. The crystal is coated with two gold electrodes, to which is applied an electric current, that induces the oscillation of the crystal with a pre-determined frequency (resonance frequency, f) [146]. The adsorption/desorption of mass on the surface of the crystal results in fluctuations of f. Additionally, QCM-D offers information on the energy dissipation (D), that can be used to evaluate structural variations of the adsorbed mass *in situ* [146,147].

1.1.4.2.9   Optical irritation

Ocular safety assessment is crucial to prevent eye injury and visual impairment due to SCLs use, especially with the introduction of drugs. Currently, the Draize rabbit eye test represents the accepted FDA method for this type of assessment [148]. However, concerns have been reported in regard of the inhumane aspects of this test. The Hen's egg test – chorioallantoic membrane (HET-CAM) test has been referenced as a method to reduce animal testing in eye irritation analysis. This technique resides in the use of fertilized chicken eggs, where the vascular chorioallantoic membrane (CAM) is present. Usually, the designated test sample is directly placed on the CAM, and any acute effects induced are considered similar to those induced by the same test sample during the Draize rabbit test. During testing, observation of the CAM is followed to evaluate the development of irritant aspects: haemorrhage (i.e. bleeding), vascular lysis (i.e. blood vessel disintegration), and coagulation (i.e. intra- and

extravascular protein denaturation) [149,150]. Quantitative analysis of irritation potential of the tested sample is carried out by calculation of the irritation score (IS), through **Equation 1.6**:

$$IS = \left(\left(\frac{301 - T_H}{300}\right) \times 5\right) + \left(\left(\frac{301 - T_L}{300}\right) \times 7\right) + \left(\left(\frac{301 - T_C}{300}\right) \times 9\right)$$ **Equation 1.6**

where T_H, T_L and T_C represent the time in seconds when the first appearance of haemorrhage, lysis and coagulation is, respectively, observed [151,152]. The obtained IS value is classified according to the values described in **Table 1.3**. Since the HET-CAM analysis is done in 300 s, the maximum value of IS is 21.

Table 1.3 IS classification. Adapted from [152].

HET-CAM Score Range	Irritation Score
0 – 0.9	No irritation
1 – 4.9	Slight Irritation
5 – 8.9	Moderate Irritation
9 - 21	Severe Irritation

1.1.4.2.10 Cytotoxicity

Prior to *in vivo* placement, SCL materials must undergo several biocompatibility tests, namely cytotoxicity. The conjugation of these tests with complete characterization of the physical and mechanical properties of the device will permit an overall analysis of the possible biological response towards the material. Nonclinical safety tests should be carried out according to the major standards for biological evaluation of medical devices, namely the ISO (International Organization for Standardization) 10993 (Biological Evaluation of Medical Devices) [153]. In

particular, ISO 10993-5 (ISO 10993 – part 5: Tests for *in vitro* cytotoxicity) standardize the used methods and endpoints for determination of cytotoxicity. Here, a cell line is evaluated in terms of growth, replication, viability and morphology after exposure to the material or to its extract/leachate. Interestingly, the *in vitro* assays show more sensitivity than animal tests, as no biological defence mechanisms are present [153,154]. However, the direct contact can result in cell physical damage, which can lead to false related material toxicity [155]. To avoid this, the tested materials shall be placed close, but not in direct contact with the cells, simulating the POLTF. According to ISO 10993-5, a material is considered non-toxic if a cell viability of >70% is observed [154].

1.1.4.3 Sterilization

Sterilization is a crucial and mandatory step in the production of SCLs. Briefly, sterilization corresponds to any chemical or physical process that allows to eliminate/remove all living microorganisms, including viruses. Absolute sterilization cannot be proven. Instead, it is defined in terms of probability, through the sterility assurance level (SAL). SAL expresses the probability of a certain product being non-sterile after exposition to a validated sterilization process. In Europe, medical devices, namely SCLs, to be approved for commercialization need to be sterilized with a minimal SAL of 10^{-6}, in other words, the probability of not being sterile is one in a million [156,157].

Sterility can be reached by two major ways: aseptically or terminally. In aseptic production, the product is sterilized during processing, being handled in a clean room. This technique has an high risk of failing [158]. Therefore, terminal sterilization is preferred. Here, the final product within its final container or package is submitted to the sterilization treatment. Terminal sterilization eliminates the existing bioburden of the product, i.e. its inherited microbial load [159–161].

The requirements for terminally sterilization of medical devices, applicable to SCLs, are described in standard EN 556 - 1. In turn, the general criteria for tests of sterility on medical devices that must be followed when defining, validating or maintaining a sterilization process are given in ISO 11737-2:2019.

SCLs are commercialized, after terminal sterilization, in a final packaging or dispenser, containing a storage buffered solution. Several terminal sterilization methods may be used for these devices namely: steam and pressure (SP) by autoclaving, γ-irradiation, and gas sterilization (ethylene oxide) [162]. Sterilization becomes a big challenge for drug loaded SCLs, since besides keeping suitable material's properties, it is necessary ensure that the sterilization process does not impact negatively the drug release profiles nor the drug activity. SP is the most used method for SCLs sterilization, since it is cost-effective, simple and it can be used for drug loaded SCLs, in general. Contrarily, although γ-irradiation is also quite used for bare SCLs, it may lead to the chemical modification and/or degradation of the drugs [163,164], when incorporated in the hydrated devices. Ethylene oxide sterilization can potentially leave gas residues that are toxic and potentially carcinogenic [165–167]. New sterilization methods have been pursued to allow overcoming these limitations and processing thermal sensitive systems. One of those methods is high hydrostatic pressure (HHP) [168], which is often used in the food industry to improve its preservation [169], but that is still giving its first steps concerning biomedical devices. In this work SP and HHP, were used.

Steam and pressure sterilization

As referred above, SP sterilization involves the use of saturated steam under pressure in an autoclave, at a given temperature during a defined time. The efficiency of the sterilization is determined by the variations of temperature, pressure and time. During the SP process, the steam enters in contact with the product and transfers to it its stored energy (i.e. enthalpy of vaporization) through the steam condensation on the surface of the product, turning to moist. It is this moist that leads to the irreversible denaturation and coagulation of structural proteins and enzymes of the microorganisms, ultimately killing them [170,171].

High hydrostatic pressure sterilization

In HHP processing, hydrostatic pressures in the range 300-600 MPa are used to impair microorganisms present in food [172]. The increase in pressure affects the non-covalent bonds of proteins, resulting in variations in their secondary, tertiary and quaternary structures. Lipids are also affected by HHP through modifications in their structure and molecular organization [173]. Nucleic acid seems immune to pressure due to its secondary structure that is stabilized

31

by H-bonds, defined as pressure resistant. The efficiency of HHP depends on the duration of the applied pressure, the level of pressure, temperature of the assay and on the chemical environment of the product [174]. HHP has been object of study in the biomedical field, for sterilization of pharmaceutical products [175] and for inactivation of pathological microorganisms and tumour cells [174]. Rigaldie *et al*. (2003) demonstrated the inactivation and/or reduction of the number of microorganisms (i.e. *Candida albicans*), *S. aureus*, *Aspergillus niger*, *P. aeruginosa*, *Bacillus subtilis*) from contaminated drugs (insulin, heparin, and monoclonal antibodies) and from a commercial drug carrier (sphérulites®), through HHP treatments (20-500 MPa, 20-37ºC) [175]. Gollwitzer *et al*. (2009) showed complete inactivation of *S. aureus* and of *P. aeruginosa* in suspension, present in contaminated blood and adherent to metal implants by HHP (various protocols, with pressure values up to 600 MPa). Nevertheless, *Enterococcus faecium* showed tolerance until max pressure (600 MPa), and osteoarthritic infected bone protected the microorganisms against HHP [172]. Linares-Alvelais *et al*. (2018) studied the effects of HHP on the mechanical properties of 3D imprinted materials, as a method to evaluate the possibility of using HHP for sterilization of biomedical devices. HHP (600 MPa, 15 min) resulted in an enhancement of the material's mechanical properties, increasing by 30% the tensile modulus and by 26% the ultimate tensile strength, contrary to autoclaving that resulted in irreversible damage and deformation of the material's surfaces [169]. In this work the selected HHP conditions were previously tested [168].

1.1.5 Ophthalmic drugs used in this thesis

Four different ophthalmic drugs were studied in this work: two anti-inflammatories, one antibiotic and one antiseptic. The choice of the drugs was based on the need to evaluate different molecules, which are representative examples of those used in the treatment of some of the most common diseases of the anterior segment of the eye.

DCF is a non-steroidal anti-inflammatory drug (NSAID) known to suppress hyperosmolarity-induced apoptosis [176]. NSAID drugs act as inhibitors of cyclooxygenases (COX), which are active enzymes in the process of inflammation [177]. DCF is used in the control of pain and inflammation after surgery [178], corneal abrasions [179], chronic allergic conjunctivitis and seasonal allergic conjunctivitis [180]. DCF ophthalmic eye drops received FDA approval in 1998 (from Alcon, Inc.).
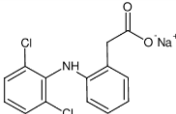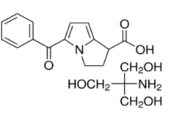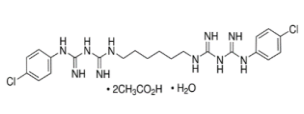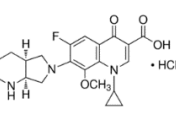
Ketorolac tromethamine (KETO) is also a NSAID drug. It is indicated for reduction of ocular pain and burning/stinging after cataract surgery [181], but also reduces the symptoms of allergies [182]. KETO ophthalmic eye drops were approved by the FDA in 2003 (Acular LS® from Allergan, Inc).

Chlorhexidine gluconate ophthalmic eye drops received approval in 2005 by the FDA (Sage Products, Inc). In this work, diacetate chlorhexidine monohydrate (CHX) will be studied, due to its low cost and availability. It is an antiseptic and antibacterial drug, with activity against yeasts and against both Gram-positive (e.g. *S. aureus*) and Gram-negative (*P. aeruginosa*) bacteria. Briefly, CHX acts on the microbial cell membrane destroying its integrity, which results in the microbial death [183].

Moxifloxacin hydrochloride (MXF) is a fourth-generation fluoroquinolone used in the treatment of keratitis, conjunctivitis, keratoconjunctivitis and bacterial endophthalmitis. It is a broad-spectrum antibiotic active against several bacteria, including *S. aureus* and *S. epidermidis* [184–186]. The action of MXF resides in the interference with the bacterial survival mechanism. MXF binds to the deoxyribonucleic acid (DNA) gyrase (topoisomerase II) and topoisomerase IV, which are two essential enzymes involved in the bacterial cell's DNA replication, translation, repair and recombination, ultimately resulting in the bacteria death [185]. MXF ophthalmic solution was approved by the FDA in 2003 (Alcon, Inc).

In **Table 1.4** the main characteristics of the four drugs used in this work are described.

Table 1.4 Characteristics of the studied ophthalmic drugs [187–189].

Drug's name	Diclofenac	Ketorolac	Chlorhexidine	Moxifloxacin
Classification	Non-steroidal anti-inflammatory	Non-steroidal anti-inflammatory	Antiseptic	Fluoroquinolone antibiotic
Molecular formula	$C_{14}H_{10}Cl_2NNaO_2$	$C_{15}H_{13}NO_3 \cdot C_4H_{11}NO_3$	$C_{22}H_{30}Cl_2N_{10} \cdot 2C_2H_4O_2 \cdot H_2O$	$C_{21}H_{25}ClFN_3O_4$
Molecular weight (g/mol)	318.13	376.4	643.57	437.89
Chemical structure				
pKa	4	3.5	10.8	6.25 9.29
Ionicity	Anionic	Anionic	Cationic	Zwitterionic
Solubility in water, 20ºC (mg/mL)	50	56.5	0.8	24

1.2 Objectives of the thesis

As stated above, SCLs are used by more than 100 million people around the world for refractive error correction. Their extended wear and biocompatibility are well established, placing them in a front road for improvement of the current inadequate ocular treatments. SCLs

demonstrated to increase drug bioavailability by 50% when compared to topical application, and can overcome current limitations namely; poor patient compliance, frequent instillations and systemic sorption. Nevertheless, the design of a therapeutic SCL requires the conjugation of different factors that may lead to an optimal system, namely: recognition of the desired application, identification of the target, eventual modification of the material´s properties, and the evaluation of the drug/material interactions. Otherwise, the likelihood of insufficient drug concentration above therapeutic values for the required time can be insufficient due to drug improper release profiles.

The aim of the present PhD thesis is to investigate new strategies, based on the use of LbL coatings and molecular imprinting, to control drug release from drug-eluting hydrogels which may be used in the production of therapeutic SCLs.

In Chapter 2, a lab-made hydrogel thereafter designated by TRIS/NVP/HEMA, was produced by crosslinking of TRIS, HEMA, NVP, with ethylene glycol dimethacrylate (EGDMA) as crosslinker. This hydrogel demonstrated adequate properties to be used in the manufacturing of SCLs [133,143], The effect of an LbL coating based on alginate (ALG) and CHI polyelectrolytes, on the release of DCF, KETO, CHX and MXF from TRIS/NVP/HEMA hydrogel and from a commercially available silicone hydrogel material for SCLs, Definitive 50, was investigated.

In Chapter 3, other LbL coatings, with various ALG, CHI, HA and PLL polyelectrolytes conjugations were tested on TRIS/NVP/HEMA hydrogel, to control the release of DCF, CHX and MXF and evaluate protein adsorption. The novelty was to use polyelectrolytes with antibacterial properties that may sustain the drug release and, simultaneously, are able to reduce the growth of bacteria responsible for the more common ocular infections.

In Chapter 4, a new LbL coating based on three ionic polysaccharides, ALG, CHI and HA was tested on TRIS/NVP/HEMA and two commercially available SCLs (Purevision and SofLens). In this new combination of polyelectrolytes, the crosslinker agent was changed from N-(3-dimethylaminopropyl)-N-ethylcarbodiimide hydrochloride (EDC) (used in chapter 3) to genipin (GE) that has several advantages, namely, is biocompatible and has very low toxicity. Furthermore, the problem of sterilizing LbL coatings based on natural based polysaccharides was tackled here for the first time.

In Chapter 5, the molecular imprinting technique was used on TRIS/NVP/HEMA to improve the release of MXF, since the studied LbL coatings were efficient only for the control of DCF release.

In Chapter 6, the LbL method and molecular imprinting strategies were combined, to control simultaneously the dual release of DCF and MXF from the TRIS/NVP/HEMA, while improving the surface properties of the material.

In Chapter 7, an overall discussion is made to integrate the main results and conclusions of chapters 2 to 6.

Finally, Chapter 8 describes the main conclusions of this thesis and future work.

1.3 References

[1]   J. V. Forrester, A.D. Dick, P.G. McMenamin, F. Roberts, E. Pearlman, Anatomy of the eye and orbit, in: Eye Basic Sci. Pract., Elsevier, 2016: pp. 1–102.

[2]   A. Lens, S.C. Nemeth, J.K. Ledford, Ocular anatomy and physiology, SLACK, 2008.

[3]   K. Rogers, The eye: The physiology of human perception, Britannica Educational Publishing, 2011.

[4]   K. Cholkar, S.R. Dasari, D. Pal, A.K. Mitra, Eye: Anatomy, physiology and barriers to drug delivery, in: Ocul. Transp. Recept. Their Role Drug Deliv., Woodhead Publishing Limited, 2013: pp. 1–36.

[5]   R.C. Tripathi, B.J. Tripathi, Anatomy of the Human Eye, Orbit, and Adnexa, in: Eye, Elsevier, 1984: pp. 1–268.

[6]   M.F. Mafee, A. Karimi, J. Shah, M. Rapoport, S.A. Ansari, Anatomy and pathology of the eye: Role of MR imaging and CT, Radiol. Clin. North Am. 44 (2006) 135–157.

[7]   R. Susanna JR, F.A. Medeiros, The optic nerve in glaucoma, Cultura Médica, 2006.

[8]   R.R. Joseph, Drug delivery to the eye: what benefits do nanocarriers offer?, Nanomedicine. 12 (2017) 683–702.

[9]   T. Ono, R. Nejima, T. Iwasaki, Y. Mori, Y. Noguchi, A. Yagi, H. Hanaki, K. Miyata, Long-term effects of cataract surgery with topical levofloxacin on ocular bacterial flora, J. Cataract Refract. Surg. 43 (2017) 1129–1134.

[10]   A. El Àmeen, S. Majzoub, G. Vandermeer, P.J. Pisella, Influence of cataract surgery on Meibomian gland dysfunction, J. Fr. Ophtalmol. 41 (2018) e173–e180.

[11]   C. Chan, Dry eye: A pratical approach, Springer, 2015.

[12]   H. Lin, S.C. Yiu, Dry eye disease: A review of diagnostic approaches and treatments, Saudi J. Opthalmology. 28 (2014) 173–181.

[13]   S. Tatlipinar, E.K. Akpek, Topical ciclosporin in the treatment of ocular surface disorders, Bras. J. Ophthalmol. 89 (2005) 1363–1367.

[14] L.D. Barber, S.C. Pflugfelder, J. Tauber, G.N. Foulks, Phase III safety evaluation of cyclosporine 0.1% ophthalmic emulsion administered twice daily to dry eye disease patients for up to 3 years, Opthalmology. 112 (2005) 1790–1794.

[15] E. Karsten, S.L. Watson, L.J.R. Foster, Diversity of Microbial Species Implicated in Keratitis: A Review, Open Ophthalmol. J. 6 (2012) 110–124.

[16] R. Kumar, D. Lloyd, Recent advances in the treatment of Acanthamoeba keratitis, Clin. Infect. Dis. 35 (2002) 434–441.

[17] B. Clarke, A. Sinha, D.N. Parmar, E. Sykakis, Advances in the diagnosis and treatment of acanthamoeba keratitis, J. Ophthalmol. 2012 (2012) 1–6.

[18] M. Elder, J.G. Dart, S. Kilvington, D.V. Seal, J. Hay, C.M.M. Kirkness, Chemotherapy for acanthamoeba keratitis, Lancet. 345 (1995) 791–793.

[19] D. Bremond-Gignac, F. Chiambaretta, S. Milazzo, A European perspective on topical ophthalmic antibiotics: current and evolving options, Ophthalmol. Eye Dis. 3 (2011) 29–43.

[20] K. Tabbara, A.M.M.A. El-Asrar, M. Khairallah, Ocular infections, Springer, 2014.

[21] J. Lorenzo-Morales, N.A. Khan, J. Walochnik, An update on Acanthamoeba keratitis: Diagnosis, pathogenesis and treatment, Parasite. 22 (2015) 1–20.

[22] A.A. Azari, N.P. Barney, Conjunctivitis: A Systematic Review of Diagnosis and Treatment, JAMA. 310 (2013) 1721–1729.

[23] H. Cronau, R.R. Kankanala, T. Mauger, Diagnosis and management of Red Eye in Primary Care, Am. Fanily Physician. 81 (2010) 137–144.

[24] K.L. Visscher, C.M.L. Hutnik, M. Thomas, Evidence-based treatment of acute infective conjunctivitis: Breaking the cycle of antibiotic prescribing, Can. Fam. Physician. 55 (2009) 1071–1075.

[25] H.P. Filipe, J. Henriques, P. Reis, P.C. Silva, M.J. Quadrado, A.P. Serro, Contact lenses as drug controlled release systems : a narrative review, Rev. Bras. Oftalmol. 75 (2016) 241–247.

[26] K.-H. Hsu, S. Gause, A. Chauhan, Review of ophthalmic drug delivery by contact

lenses, J. Drug Deliv. Sci. Technol. 24 (2014) 123–135.

[27] Y. Weng, J. Liu, S. Jin, W. Guo, X. Liang, Z. Hu, Nanotechnology-based strategies for treatment of ocular disease, Acta Pharm. Sin. B. 7 (2017) 281–291.

[28] C.-C. Peng, M.T. Burke, B.E. Carbia, C. Plummer, A. Chauhan, Extended drug delivery by contact lenses for glaucoma therapy, J. Control. Release. 162 (2012) 152–8.

[29] D.R. Janagam, L. Wu, T.L. Lowe, Nanoparticles for drug delivery to the anterior segment of the eye, Adv. Drug Deliv. Rev. 122 (2017) 31–64.

[30] J.B. Ciolino, T.R. Hoare, N.G. Iwata, A drug-eluting contact lens, Invest. Ophthalmol. Vis. Sci. 50 (2009) 3346–3352.

[31] N. Worakul, J.R. Robinson, Ocular pharmacokinetics/pharmacodynamics, Eur. J. Pharm. Biopharm. 44 (1997) 71–83.

[32] M. Labetoulle, E. Frau, C. Le Jeunne, Systemic adverse effects of topical ocular treatments, Press. Médicale. 34 (2005) 589–595.

[33] A.A. Al-Kinani, G. Calabrese, A. Vangala, D. Naughton, R.G. Alany, Nanotechnology in Ophthalmic Drug Delivery, 2012.

[34] C.J.F. Bertens, M. Gijs, F.J.H.M. van der Biggelaar, R.M.M.A. Nuijts, Topical drug delivery devices: A review, Exp. Eye Res. 168 (2018) 149–160.

[35] A.F.R. Pimenta, A. Valente, J.M.C. Pereira, H.P. Filipe, J.L.G. Mata, R. Colaço, B. Saramago, A.P. Serro, Simulation of the hydrodynamic conditions of the eye to better reproduce the drug release from hydrogel contact lenses: experiments and modeling, Drug Deliv. Transl. Res. 6 (2016) 755–762.

[36] A. Patel, K. Cholkar, V. Agrahari, A.K. Mitra, Ocular drug delivery systems: an overview, World J. Pharmacol. 2 (2013) 47–64.

[37] S.L. Law, K.J. Huang, C.H. Chiang, Acyclovir-containing liposomes for potential ocular delivery corneal penetration and absorption, J. Control. Release. 63 (2000) 135–140.

[38] R.D. Vaishaya, M. Gokulgandhi, S. Patel, M. Minocha, A.K. Mitra, Novel dexamethasone-loaded nanomicelles for the intermediate and posterior segment uveitis, AAPS PharmaSciTech. 15 (2014) 1238–1251.

[39]   B.G. Short, Safety Evaluation of Ocular Drug Delivery Formulations: Techniques and Practical Considerations, Toxicol. Pathol. 36 (2008) 46–62.

[40]   M. Vidal-Rohr, J.S. Wolffsohn, L.N. Davies, A. Cerviño, Effect of contact lens surface properties on comfort, tear stability and ocular physiology, Contact Lens Anterior Eye. 41 (2018) 117–121.

[41]   J. McKimm, K. Forrest, Professional practice for foundation doctors, SAGE Publishing, 2011.

[42]   K. Daniels, Contact lenses, SLACK Incorporated, 1999.

[43]   J. Xu, Y. Xue, G. Hu, T. Lin, J. Gou, T. Yin, H. He, Y. Zhang, X. Tang, A comprehensive review on contact lens for ophthalmic drug delivery, J. Control. Release. 281 (2018) 97–118.

[44]   A. Phillips, L. Speedwell, Contact lenses, Elsevier, 2018.

[45]   D. Gulsen, A. Chauhan, Ophthalmic drug delivery through contact lenses, Invest. Ophthalmol. Vis. Sci. 45 (2004) 2342–2347.

[46]   N. Efron, P. Morgan, C. Maldonado-Codina, N. Brennan, Contact lenses: The search for superior oxygen permeability, in: Biomater. Regen. Med. Ophthalmol., 2010: pp. 280–302.

[47]   N. Efron, C. Maldonado-Codina, Development of contact lenses from a biomaterial point of view – Materials, manufacture, and clinical application, in: Compr. Biomater., Comprehensive Biomaterials. Elsevier, 2011: pp. 517–541.

[48]   C.S.A. Musgrave, F. Fang, Contact lens materials: A materials science perspective, Materials (Basel). 261 (2019) 1–35.

[49]   D.M. Harvitt, J.A. Bonanno, Re-evaluation of the oxygen diffusion model for prediction minimum contact lens Dk/t values needed to avoid corneal apoxia, Optom. Vis. Sci. 76 (1999) 712–719.

[50]   J. Jacob, Biomaterials: Contact Lenses, in: Biomater. Sci. An Introd. to Mater. Med., Elsevier, 2013: pp. 909–917.

[51]   L. Jones, C. May, L. Nazar, T. Simpson, In vitro evaluation of the dehydration

characteristics of silicone hydrogel and conventional hydrogel contact lens materials, Contact Lens Anterior Eye. 25 (2002) 147–156.

[52] K.L. Menzies, R. Rogers, L. Jones, In vitro contact angle analysis and physical properties of blister pack solutions of daily disposable contact lenses, Eye Contact Lens. 36 (2010) 10–18.

[53] M.A. Glasier, A. Keech, H. Sheardown, L.N. Subbaraman, L. Jones, Conformational and quantitative characterization of lysozyme extracted from galyfilcon and senofilcon silicone hydrogel contact lenses, Curr. Eye Res. 33 (2008) 1–11.

[54] E. Kim, K. Ehrmann, Refractive index of soft contact lens materials measured in packaging solution and standard phosphate buffered saline and the effect on back vertex power calculation, Contact Lens Anterior Eye. 44 (2019) 1–7.

[55] E. Kim, M. Saha, K. Ehrmann, Mechanical properties of contact lens materials, Eye&Contact Lens Sci. Clin. Prat. 44 (2018) 148–156.

[56] E. Kim, R.C. Bakaraju, K. Ehrmann, Power Profiles of Commercial Multifocal Soft Contact Lenses, Optom. Vis. Sci. 94 (2017) 183–196.

[57] S. Mohammadi, L. Jones, M. Gorbet, Extended Latanoprost Release from Commercial Contact Lenses: In Vitro Studies Using Corneal Models, PLOS-ONE. 9 (2014) 1–10.

[58] O. Wichterle, D. Lim, Hydrophilic gels for biological use, Nature. 185 (1960) 117–118.

[59] A.E. Ross, L.C. Bengani, R. Tulsan, D.E. Maidana, B. Salvador-Culla, H. Kobashi, P.E. Kolovou, H. Zhai, K. Taghizadeh, L. Kuang, M. Mehta, D.G. Vavvas, D.S. Kohane, J.B. Ciolino, Topical sustained drug delivery to the retina with a drug-eluting contact lens, Biomaterials. 217 (2019) 1–13.

[60] C. Torres-Luna, N. Hu, T. Tammareddy, R. Domszy, J. Yang, N.S. Wang, A. Yang, Extended delivery of non-steroidal anti-inflammatory drugs through contact lenses loaded with Vitamin E and cationic surfactants, Contact Lens Anterior Eye. 42 (2019) 546–552.

[61] H. Ghazal, J. Ahmadouk, S. Dhanji, A. El-bushra, R. Kayyali, A. ElShaer, Patients' and prescribers' perception of contact lenses as a potential ocular drug delivery system, Contact Lens Anterior Eye. 42 (2019) 190–195.

[62]   Q. Zhu, Y. Wei, C. Li, S. Mao, Inner layer-embedded contact lenses for ion-triggered controlled drug delivery, Mater. Sci. Eng. C. 93 (2018) 36–48.

[63]   A. Hui, Contact lenses for opthalmic drug delivery, Clin. Exp. Optom. 100 (2017) 494–512.

[64]   C.J. White, A. Tieppo, M.E. Byrne, Controlled drug release from contact lenses: A comprehensive review from 1965-present, J. Drug Deliv. Sci. Technol. 21 (2011) 369–384.

[65]   C. González-Chomón, A. Concheiro, C. Alvarez-Lorenzo, Soft contact lenses for controlled ocular delivery: 50 years in the making, Ther. Deliv. 4 (2013) 1141–1161.

[66]   E.M. Hehl, R. Beck, K. Luthard, R. Guthoff, B. Drewelow, Improved penetration of aminoglycosides and fluorozuinolones into the aqueous humour of patients by means of Acuvue contact lenses, Eur. J. Clin. Pharmacol. 55 (1999) 317–323.

[67]   X. Tian, M. Iwatsu, K. Sado, A. Kanai, Studies on the uptake and release of fluoroquinolones by disposable contact lenses, CLAO J. 27 (2001) 216–220.

[68]   A. Hui, A. Boone, L. Jones, Uptake and release of ciprofloxacin-HCl from conventional and silicon hydrogel contact lens materials, Eye Contact Lens. 34 (2008) 266–271.

[69]   C.L. Schultz, T.R. Poling, J.O. Mint, A medical device/drug delivery system for treatment of glaucoma, Clin. Exp. Optom. 92 (2009) 343–348.

[70]   A. Soluri, A. Hui, L. Jones, Delivery of of ketotifen fumurate by commercial contact lens materials, Optom. Vis. Sci. 89 (2012) 1140–1149.

[71]   C. Peng, J. Kim, A. Chauhan, Extended delivery of hydrophilic drugs from silicone hydrogel contact lenses containing Vitamin E diffusion barriers, Biomaterials. 31 (2010) 4032–4047.

[72]   J. Kim, C.C. Peng, A. Chauhan, Extended release of dexamethasone from silicone-hydrogel contact lenses containing vitamin E, J. Control. Release. 148 (2010) 110–116.

[73]   K.-H. Hsu, R.C. Fentzke, A. Chauhan, Feasibility of corneal drug delivery of cysteamine using vitamin E modified silicone hydrogel contact lenses, Eur. J. Pharm. Biopharm. 85 (2013) 531–540.

[74] P. Paradiso, A.P. Serro, B. Saramago, R. Colaço, A. Chauhan, Controlled Release of Antibiotics From Vitamin E Loaded Silicone-Hydrogel Contact Lenses, J. Pharm. Sci. 105 (2016) 1164–1172.

[75] M.A. Holgado, A. Anguiano-Domingues, L. Martin-Banderas, Contact lenses as drug-delivery systems: a promising therapeutic tool, Arch. La Soc. Española Oftalmol. (English Ed. 95 (2020) 24–33.

[76] C. Alvarez-Lorenzo, F. Yañez, A. Concheiro, Ocular drug delivery from molecularly-imprinted contact lenses, J. Drug Deliv. Sci. Technol. 20 (2010) 237–248.

[77] K. Singh, A.B. Nair, A. Kumar, R. Kumria, Novel Approaches in Formulation and Drug Delivery using Contact Lenses, J. Basic Clin. Pharm. 2 (2011) 87–101.

[78] A. Sharma, J. Taniguchi, Review: Emerging strategies for antimicrobial drug delivery to the ocular surface: Implications for infectious keratitis, Ocul. Surf. 15 (2017) 670–679. https://doi.org/10.1016/j.jtos.2017.06.001.

[79] H. Hiratani, C. Alvarez-Lorenzo, Timolol uptake and release by imprinted soft contact lenses made of N,N-diethylacrylamide and methacrylic acid, J. Control. Release. 83 (2002) 223–230.

[80] C. Alvarez-Lorenzo, F. Yañez, R. Barreiro-iglesias, A. Concheiro, Imprinted soft contact lenses as norfloxacin delivery systems, J. Control. Release. 113 (2006) 236–244.

[81] A. Tieppo, C.J. White, A.C. Paine, M.L. Voyles, M.K. McBride, M.E. Byrne, Sustained in vivo release from imprinted therapeutic contact lenses, J. Control. Release. 157 (2012) 391–397.

[82] N. Malakooti, C. Alexander, C. Alvarez-Lorenzo, Imprinted contact lenses for sustained release of polymyxin B and related antimicrobial peptides, J. Pharm. Sci. 104 (2015) 3386–3394.

[83] S.A. Zaidi, Molecular imprinting: A useful approach for drug delivery, Mater. Sci. Energy Technol. 3 (2020) 72–77.

[84] G. Jha, A. Kumar, Drug delivery through soft contact lenses : An introduction, Chronicles Young Sci. 2 (2011) 98–101.

[85] H.J. Jung, M. Abou-Jaoude, B.E. Carbia, C. Plummer, A. Chauhan, Glaucoma therapy by extended release of timolol from nanoparticle loaded siliconehydrogel contact lenses, J. Control Release. 165 (2013) 82–89.

[86] F.A. Maulvi, R.J. Patil, A.R. Desai, M.R. Shukla, R.J. Vaidya, K.M. Ranch, B.A. Vyas, S.A. Shah, D.O. Shah, Effect of gold nanoparticles on timolol uptake and its release kinetics from contact lenses: In vitro and in vivo evaluation, Acta Biomater. 86 (2019) 350–362.

[87] F.H. Nasr, S. Khoee, M.M. Dehghan, S.S. Chaleshtori, A. Shafiee, Preparation and evaluation of contact lenses embedded with polycaprolactone-based nanoparticles for ocular drug delivery, Biomacromolecules. 17 (2016) 485–495.

[88] G. Behl, J. Iqbal, N.J. O´Reilly, P. McLoughlin, L. Fitzhenry, Synthesis and characterization of poly(2-hydrocyethylmethacrylate) contact lenses containing chitosan nanoparticles as an ocular delivery system for dexamethasone sodium phosphate, Pharm. Res. 33 (2016) 1638–1648.

[89] A. Grumezescu, Organic Materials as Smart Nanocarriers for Drug Delivery, 2018.

[90] C.H. Lin, H.L. Cho, Y.H. Yeh, M.C. Yang, Improvement of the surface wettability of silicone hydrogel contact lenses via layer-by-layer self-assembly technique, Colloids Surfaces B Biointerfaces. 136 (2015) 735–743.

[91] P. Dixon, A. Chauhan, Effect of the surface layer on drug release from delefilcon-A (Dailies Total1®) contact lenses, Int. J. Pharm. 529 (2017) 89–101.

[92] D. Dutta, B. Kamphuis, B. Ozcelik, H. Thissen, R. Pinarbasi, N. Kumar, M.D.P. Willcox, Development of Silicone Hydrogel Antimicrobial Contact Lenses with Mel4 Peptide Coating, Optom. Vis. Sci. 95 (2018) 937–946.

[93] P. Mehta, L. Justo, S. Walsh, M.S. Arshad, C.G. Wilson, C.K. O'Sullivan, S.M. Moghimi, I.S. Vizirianakis, K. Avgoustakis, D.G. Fatouros, Z. Ahmad, New platforms for multi-functional ocular lenses: Engineering double-sided functionalized nano-coatings, J. Drug Target. 23 (2015) 305–310.

[94] M. Korogiannaki, J. Zhang, H. Sheardown, Surface modification of model hydrogel contact lenses with hyaluronic acid via thiol-ene "click" chemistry for enhancing surface

characteristics, J. Biomater. Appl. 32 (2017) 446–462.

[95] P. Chen, X. Wang, Y. Dong, X. Hu, Development of a layer-by-layer assembled film on hydrogel for ocular drug delivery, Int. J. Polym. Sci. (2015) 1–9.

[96] P. Paradiso, R. Colaço, J.L.G. Mata, R. Krastev, B. Saramago, A.P. Serro, Drug release from liposome coated hydrogels for soft contact lenses: the blinking and temperature effect, J. Biomed. Mater. Res. B. Appl. Biomater. 105B (2017) 1799–1807.

[97] A. Danion, H. Brochu, Y. Martin, P. Vermette, Fabrication and characterization of contact lenses bearing surface-immobilized layers of intact liposomes, J. Biomed. Mater. Res. Part A. 82 (2007) 41–51.

[98] G. Guzman, S.S. Es-haghi, T. Nugay, M. Cakmak, Zero-order antibiotic release from multilayer contact lenses: Nonuniform drug and diffusivity distributions produce constant-rate drug delivery, Adv. Healthc. Mater. 6 (2016) 1–9.

[99] A. Danion, I. Arsenault, P. Vermette, Antibacterial activity of contact lenses bearing surface-immobilized layers of intact liposomes loaded with levofloxacin, J. Pharm. Sci. 96 (2007) 2350–63.

[100] J.F. dos Santos, C. Alvarez-Lorenzo, M. Silva, L. Balsa, J. Couceiro, J.J. Torres-Labandeira, A. Concheiro, Soft contact lenses functionalized with pendent cyclodextrins for controlled drug delivery, Biomaterials. 30 (2009) 1348–1355.

[101] B.S. Kim, S.W. Park, P.T. Hammond, Hydrogen-bonding layer-by-layer assembled biodegradable polymeric micelles as drug delivery vehicles from surfaces, ACS Nano. 2 (2008) 386–392.

[102] C.L. Domínguez-Delgado, I.M. Rodríguez-Cruz, E. Fuentes-Prado, J.J. Escobar-Chávez, G. Vidal-Romero, L. García-González, R.I. Puente-Lee, Drug Carrier Systems Using Chitosan for Non Parenteral Routes, in: Pharmacol. Ther., 2014: pp. 273–325.

[103] J. Hernandez-Montelongo, E.G. Lucchesib, I. Gonzalez, W.A.A. Macedo, V.F. Nascimento, A.M. Moraes, M.M. Beppu, M.A. Cotta, Hyaluronan/chitosan nanofilms assembled layer-by-layer and their antibacterial effect: A study using Staphylococcus aureus and Pseudomonas aeruginosa, Colloids Surfaces B Biointerfaces. 141 (2016) 499–506.

[104] X. Hu, X. Gong, A new route to fabricate biocompatible hydrogels with controlled drug delivery behavior, J. Colloid Interface Sci. 470 (2016) 62–70.

[105] S. Guo, X. Zhu, X.J. Loh, Controlling cell adhesion using layer-by-layer approaches for biomedical applications, Mater. Sci. Eng. 70 (2017) 1163–1175.

[106] D.L. Elbert, C.B. Herbert, J.A. Hubbell, Thin polymer layers formed by polyelectrolyte multilayer techniques on biological surfaces, Langmuir. 15 (1999) 5355–5362.

[107] C. Cassinelli, M. Morra, A. Pavesio, D. Renier, Evaluation of interfacial properties of hyaluronan coated poly(methylmethacrylate) intraocular lenses, J. Biomater. Sci. Polym. Ed. 11 (2000) 961–77.

[108] L. Drago, L. Cappelletti, E. De Vecchi, L. Pignataro, S. Torretta, R. Mattina, Antiadhesive and antibiofilm activity of hyaluronic acid against bacteria responsible for respiratory tract infections, APMIS. 10 (2014) 1013–9.

[109] M. Van Beek, L. Jones, H. Sheardown, Hyaluronic acid containing hydrogels for the reduction of protein adsorption, Biomaterials. 29 (2008) 780–789.

[110] M. Van Beek, A. Weeks, L. Jones, H. Sheardown, Immobilized hyaluronic acid containing model silicone hydrogels reduce protein adsorption, J. Biomater. Sci. Polym. Ed. 19 (2008) 1425–36.

[111] T.I. Croll, A.J. O'Connor, G.W. Stevens, J.J. Cooper-White, A blank slate? Layer-by-layer deposition of hyaluronic acid and chitosan onto various surfaces, Biomacromolecules. 7 (2006) 1610–1622.

[112] G. Berth, A. Voight, H. Dautzenberg, E. Donath, H. Möhwald, Polyelectrolyte complexes and layer-by-layer capsules from chitosan/chitosan sulfate, Biomacromolecules. 3 (2002) 579–590.

[113] J. Kang, L. Dähne, Strong response of multilayer polyelectrolyte films to cationic surfactants, Langmuir. 2011 (27AD) 4627–4634.

[114] X.H. Hu, G.J. Zhang, H.P. Tan, D. Li, X.Y. Chen, Y.S. Zhang, Synthesis and surface modification of chitosan containing hydrogel for ophthalmic drug delivery, Mater. Technol. 29 (2014) 144–151.

[115] J.B. Ciolino, C.F. Stefanescu, A.E. Ross, B. Salvador-Culla, P. Cortez, E.M. Ford, K.A. Wymbs, S.L. Sprague, D.R. Mascoop, S.S. Rudina, S.A. Trauger, F. Cade, D.S. Kohane, In vivo performance of a drug-eluting contact lens to treat glaucoma for a month, Biomaterials. 35 (2014) 432–439.

[116] F.A. Maulvi, S.S. Singjania, A.R. Desai, M.R. Shukla, A.S. Tannk, K.M. Ranch, B.A. Vyas, D.O. Shah, Contact lenses with dual drug delivery for the treatment of bacterial conjunctivitis, Int. J. Pharm. 548 (2018) 139–150.

[117] F.A. Maulvi, T.G. Soni, D.. Shah, A review on therapeutic contact lenses for ocular drug delivery, Drug Deliv. 23 (2016) 3017–3026.

[118] V.P. Costa, M.E.M. Braga, C.M.M. Duarte, C. Alvarez-Lorenzo, A. Concheiro, M.H. Gil, H.C. de Sousa, Anti-glaucoma drug loaded contact lenses prepared using supercritical solvent impregnation, J. Supercrit. Fluids. 53 (2010) 165–173.

[119] F. Yañez, L. Martikainen, M.E. Braga, Supercritical fluid-assisted preparation of imprinted contact lenses for drug delivery, Acta Biomater. 7 (2011) 1019–1030.

[120] G. Gauglitz, T. Vo-Dinh, Handbook of spectroscopy, 2003.

[121] J.E. Walsh, L. V. Koehler, D.P. Flemmin, J.P. Bergmanson, Novel method for determining hydrogel and silicone hydrogel contact lens transmission curves and their spatially specific ultraviolet radiation protection factors, Eye Contact Lens. 33 (2007) 58–64.

[122] E.S. Bennett, B.A. Weissman, Clinical Contact lens Practice, Lippincott Williams & Willkins, 2005.

[123] I. Gibas, H. Janik, Review: Synthetic polymer hydrogels for biomedical applications, Chem. Chem. Technol. 4 (2010) 297–304.

[124] K. Pal, A.K. Banthia, D.K. Majumbar, Polymer hydrogels: Characterization and biomedical applications - A mini review, Des. Monomers Polym. 12 (2009) 197–220.

[125] N. Efron, I. Tranoudis, Water properties of soft contact lens materials, Contact Lens Anterior Eye. 27 (2004) 193–208.

[126] P.C. Nicolson, J. Vogt, Soft contact lens polymers: an evolution, Biomaterials. 22 (2001)

3273–3283.

[127] J. Lemons, B. Ratner, A. Hoffman, F. Schoen, Biomaterials science: An introduction to materials in medicine, Elsevier Academic Press, 2004.

[128] Y. Yuan, T.R. Lee, Contact angle and wetting properties, in: Surf. Sci. Tech., Springer Berlin Heidelberg, 2013: pp. 3–34.

[129] A. Soleimani-Gorgani, Inkjet printing, in: Print. Polym., 2016: pp. 231–246.

[130] C.C. Peng, A. Chauhan, Ion transport in silicone hydrogel contact lenses, J. Memb. Sci. 399–400 (2012) 95–105.

[131] A.R.F. Silva, V. Compañ, J.M. González-Méijome, Reduction in ionic permeability of a silicone hydrogel contact lenses after one month of daily wear, Mater. Res. Express. 2 (2015) 1–18.

[132] R. Galante, P. Paradiso, M.G. Moutinho, A.I. Fernandes, J.L.G. Mata, A.P.A. Matos, R. Colaço, B. Saramago, A.P. Serro, About the effect of eye blinking on drug release from pHEMA-based hydrogels: An in vitro study, J. Biomater. Sci. Polym. Ed. 26 (2015) 235–251.

[133] P. Paradiso, R. Galante, L. Santos, A.P. Alves De Matos, R. Colaço, A.P. Serro, B. Saramago, Comparison of two hydrogel formulations for drug release in ophthalmic lenses, J. Biomed. Mater. Res. B. 102 (2014) 1170–1180.

[134] M. Giraldez, E. Yebra-Pimentel, Hydrogel contact lenses surface roughness and bacterial adhesion, INTECH. (2012) 95–120.

[135] H. Wang, P.K. Chu, Surface characterization of biomaterials, in: Charact. Biomater., 2013: pp. 105–174.

[136] J. Baguet, F. Sommer, V. Claudon-Eyl, T.M. Duc, Characterization of lacrymal component accumulation on worn soft contact lens surfaces by atomic force microscopy, Biomaterials. 16 (1995) 3–9.

[137] P.C. Braga, D. Ricci, Atomic Force Microscopy - Biomedical Methods and Applications, Humana Press, 2004.

[138] H.-J. Butt, B. Cappella, M. Kappl, Force measurements with the atomic force

microscope: Technique, interpretation and applications, Surf. Sci. Rep. 59 (2005) 1–152.

[139] A.M. Baró, R.G. Reifenberger, Atomic Force Microscopy in Liquid: Biological Applications, 2012.

[140] B. Bhushan, Scanning probe microscopy in Nanoscience and Nanotechnology, Springer, 2010.

[141] N. Tomczak, K.E.J. Goh, Scanning Probe Microscopy, World Scientific Publishing, 2011.

[142] P. Eaton, P. West, Atomic Force Microscopy, Oxford University Press, 2010.

[143] D. Silva, A.C. Fernandes, T.G. Nunes, R. Colaço, A.P. Serro, The effect of albumin and cholesterol on the biotribological behaviour of hydrogels for contact lenses, Acta Biomater. 26 (2015) 184–194.

[144] A.W. Lloyd, R.G.A. Faragher, M. Wassall, W. Rhys-Williams, L. Wong, J.E. Hughes, G.W. Hanlon, Assessing the in vivo cell-based ocular compatibility of contact lens materials, Contact Lens Anterior Eye. 23 (2000) 119–123.

[145] C.M. Elkins, Q.M. Qi, G.G. Fuller, Corneal cell adhesion to contact lens hydrogel materials enhanced via tear film protein deposition, PLOS-ONE. 9 (2014) 1–9.

[146] J. Teichroeb, J. Forrest, L. Jones, J. Chan, K. Dalton, Quartz crystal microbalance study of protein adsorption kinetics on poly(2-hydroxyethyl methacrylate), J. Colloid Interface Sci. 325 (2008) 157–164.

[147] F. Teng, Q. Liu, H. Zeng, In situ kinetics study of zinc sulfide activation using a quartz crystal microbalance with dissipation (QCM-D), J. Colloid Interface Sci. 368 (2012) 512–520.

[148] K.R. Wilhelmus, The Draize eye test, Surv. Ophthalmol. 45 (2001) 493–515.

[149] P. Nowak-Sliwinska, T. Segura, M.L. Iruela-Arispe, The chicken chorioallantoic membrane model in biology, medicine and bioengineering, Angiogenesis. 17 (2014) 779–804.

[150] H.T. Kiyan, B. Demirci, K.H.C. Başer, F. Demirci, The in vivo evaluation of anti-

angiogenic effects of Hypericum essential oils using the chorioallantoic membrane assay, Pharm. Biol. 52 (2014) 44–50.

[151] Current Status of In Vitro Test Methods for Identifying Mild/Moderate Ocular Irritants: The Hen's Egg Test–Chorioallantoic Membrane (HET-CAM) Test Method, 2010.

[152] H. Spielmann, S. Kalweit, M. Liebsch, I. Wirnsberger, Gerner, E. Bertram-Neis, K. Krauser, R. Kreiling, H.G. Miltenburger, W. Pape, W. Steiling, Validation project of alternatives for the Draize eye test, Toxicol. Vitr. 7 (1993) 505–510.

[153] X. Liu, D.P. Rodeheaver, J.C. White, A.M. Wright, L.M. Walker, F. Zhang, S. Shannon, A comparison of in vitro cytotoxicity assays in medical device regulatory studies, Regul. Toxicol. Pharmacol. 97 (2018) 24–32.

[154] C.S.A. (CSA), ISO 10993-5, Int. Organ. Stand. (2009) 1–34.

[155] S.C. Gad, M.G. McCord, Safety evaluation in the development of medical devices and combination products, Taylor & Francis Group, LLC, 2009.

[156] World Health Organization -The International Pharmacopoeia: 9th Edition, Accessed March 2020. (2019) https://apps.who.int/phint/en/p/about/.

[157] ISO 11607-1:2019 - Packaging for terminally sterilized medical devices - Part 1: Requirements for materials, sterile barrier systems and packaging systems, Accessed March 2020. (2019) www.iso.org/standard/70799.html.

[158] K. Bush, A.A. Gertzman, Process Development and Manufacturing of Human and Animal Acellular Dermal Matrices, in: Ski. Tissue Eng. Regen. Med., Academic press, 2016: pp. 83–108.

[159] S. Lerouge, Introduction to sterilization: definitions and challenges, in: Steriliz. Biomater. Med. Devices, Woodhead Publishing Limited, 2012: pp. 1–19.

[160] A.K.A. Silva Brun-Graeppi, C. Richard, M. Bessodes, D. Scherman, T. Narita, G. Ducouret, O.-W. Merten, The effect of sterilization methods on the thermo-gelation properties of xyloglucan hydrogels, Polym. Degrad. Stab. 95 (2010) 254–259.

[161] S.S. Block, Disinfection, sterilization and preservation, Lippincott Williams & Willkins, 2001.

[162] B. McEvoy, N.J. Rowan, Terminal sterilization of medical devices using vaporized hydrogen peroxide: a review of current methods and emerging opportunities, J. Appl. Microbiol. 127 (2019) 1403–1420.

[163] A.L.C. Topete, Effects of sterilization on drug loaded soft contact lenses, 2015.

[164] A.S.G. Oliveira, Effects of sterilization on drug loaded ophthalmic lenses materials, 2016.

[165] R. Galante, A.S. Oliveira, A. Topete, D. Ghisleni, M. Braga, T.J.A. Pinto, R. Colaço, A.P. Serro, Drug-eluting silicone hydrogel for therapeutic contact lenses: Impact of sterilization methods on the system performance, Colloids Surf B Biointerfaces. 161 (2018) 537–546.

[166] J.G. Solon, S. Killeen, Decontamination and sterilization, Surg. 33 (2015) 572–578.

[167] E. Eljarrat-Binstock, A. Bentolila, N. Kumar, H. Harei, A.J. Domb, Preparation, characterization, and sterilization of hydrogel sponges for iontophoretic drug-delivery use, Polym. Adv. Technol. 18 (2007) 720–730.

[168] A. Topete, C.A. Pinto, H. Barroso, J.A. Saraiva, I. Barahonac, B. Saramago, A.P. Serro, High hydrostatic pressure (HHP) as sterilization method for drug-loaded intraocular lenses, ACS Biomater. Sci. Eng. (2020).

[169] J.A.R. Linares-Alvelais, J.O. Figueroa-Cavazos, C. Chuck-Hernandez, H.R. Siller, C.A. Rodrigues, J.I. Martinez-Lopez, Hydrostatic high-pressure post-processing of specimens fabricated by DLP, SLA, and FDM: An alternative for the sterilization of polymer-based biomedical devices, Materials (Basel). 11 (2018) 1–12.

[170] M. Dion, W. Park, Steam sterilization principles, Pharm. Eng. 33 (2013) 1–8.

[171] B.M. Boca, E. Pretprius, R. Gochin, R. Chapoullie, Z. Apostolides, An overview of the validation approach for moist heat sterilization, Part I, Pharm. Technol. 26 (2002) 96–112.

[172] H. Gollwitzer, W. Mittelmeier, M. Brendle, P. Weber, T. Miethke, G.O. Hofmann, L. Gerdesmeyer, J. Schauwecker, P. Diehl, High hydrostatic pressure for disinfection of bone grafts and biomaterials: An experimental study, Open Ophthalmol. J. 3 (2009) 1–7.

[173] B. Lehofer, M. Golub, K. Kornmueller, M. Kriechbaum, N. Martinez, G. Nagy, J. Kohlbrecher, H. Amenitsch, J. Peters, R. Prassl, High hydrostatic pressure induces a lipid phase transition and molecular rearrangements in low-density lipoprotein nanoparticles, Part. Part. Syst. Charact. 35 (2018) 1–22.

[174] P. Diehl, J. Schauwecker, W. Mittelmeier, M. Schmitt, High hydrostatic pressure, a novel approach in orthopaedic surgical oncology to disinfect bone, tendons and cartilage, Anticancer Res. 28 (2008) 3877–3883.

[175] Y. Rigaldie, A. Largeteau, G. Lemagnen, F. Ibalot, P. Pardon, G. Demazeau, L. Grislain, Effects of high hydrostatic pressure on several sensitive therapeutic molecules and soft nanodispersed drug delivery system, Pharm. Res. 20 (2003) 2036–2040.

[176] R. Sawazaki, T. Ishihara, S. Usui, E. Hayashi, K. Tahara, T. Hoshino, A. Higuchi, S. Nakamura, K. Tsubota, T. Mizushima, Diclofenac Protects Cultured Human Corneal Epithelial Cells Against Hyperosmolarity and Ameliorates Corneal Surface Damage in a Rat Model of Dry Eye, Investig. Opthalmology Vis. Sci. 55 (2014) 2547–2556.

[177] A. Topete, A.P. Serro, B. Saramago, Dual drug delivery from intraocular lens material for prophylaxis of endophthalmitis in cataract surgery, Int. J. Pharm. 558 (2019) 43–52.

[178] E.B. Rodrigues, M.E. Farah, J.M. Bottós, F. Bom Aggio, Nonsteroidal Anti-Inflammatory Drugs in the Treatment of Retinal Diseases, Dev Ophthalmol. 55 (2016) 212–220.

[179] P.A. Szucs, A.H. Nashed, J.R. Allegra, B. Eskin, Safety and efficacy of diclofenac ophthalmic solution in the treatment of corneal abrasion, Ann. Emerg. Med. 35 (2000) 131–138.

[180] N. Dehar, A. Gupta, G. Singh, Comparative study of the ocular efficacy and safety of diclofenac sodium (0.1%) ophthalmic solution with that of ketorolac tromethamine (0.5%) ophthalmic solution in patients with acute seasonal allergic conjunctivitis, Int. J. Appl. Basic Med. Res. 2 (2012) 25–30.

[181] H.P. Sandoval, L.E. Fernández de Castro, D.T. Vroman, K.D. Solomon, A review of the use of ketorolac tromethamine 0.4% in the treatment of post-surgical infl ammation following cataract and refractive surgery, Clin. Ophthalmol. 1 (2007) 367–371.

[182] B.A. Schechter, Ketorolac tromethamine 0.4% as a treatment for allergic conjuctivitis, Expert Opin. Drug Metab. Toxicol. 4 (2008) 507–511.

[183] H.-Y. Cheung, M.M.-K. Wong, S.-H. Cheung, L.Y. Liang, Y.-W. Lam, S.-K. Chiu, Differential Actions of Chlorhexidine on the Cell Wall of Bacillus subtilis and Escherichia coli, PLOS-ONE. 7 (2012) 1–11.

[184] R.A. Kaskoos, Investigation of moxifloxacin loaded chitosan – dextran nanoparticles for topical instillation into eye: In-vitro and ex-vivo evaluation, Int. J. Pharm. Investig. 4 (2014) 164–173.

[185] D. Miller, Review of moxifloxacin hydrochloride ophthalmic solution in the treatment of bacterial eye infections, Clin Ophthalmol. 2 (2008) 77–91.

[186] C.E. Edmiston, C.J. Krepel, G.R. Seabrook, L.R. Somberg, A. Nakeeb, R.A. Cambria, J.B. Towne, In Vitro Activities of Moxifloxacin against 900 Aerobic and Anaerobic Surgical Isolates from Patients with Intra-Abdominal and Diabetic Foot Infections, Antimicrob. Agents Chemother. 48 (2004) 1012–1016.

[187] P. Djurdjevic, A. Ciric, A. Djurdjevic, M.J. Stankovc, Optimization of separation and determination of moxifloxacin and its related substances by RP-HPLC, J. Pharm. Biomed. Anal. 50 (2009) 117–126.

[188] L.F. Žilnik, A. Jazbinšek, A. Hvala, F. Vrečer, Solubility of diclofenac sodium in different solvents, Fluid Phase Equilib. 261 (2007) 140–145.

[189] Y. Xue, M. Tang, Y. Hieba, J. Fujihara, K. Takayama, H. Takatsuka, H. Takeshita, High-Performance Liquid Chromatographic Determination of Chlorhexidine in Whole Blood by Solid-Phase Extraction and Kinetics Following an Intravenous Infusion in Rats, J. Anal. Toxicol. 33 (2009) 85–95.

2 Chitosan/alginate-based multilayers to control drug delivery from SCL materials

The following results were published in the peer-reviewed article:

Diana Silva, Luis F. V. Pinto, Dimitriya Bozukova, Luis F. Santos, Ana Paula Serro, Benilde Saramago; Chitosan/alginate-based multilayers to control drug delivery from ophthalmic lens; Colloids and Surfaces B: Biointerfaces (2016) 147:81-89

Table of Contents

2.1 Introduction

In this chapter, the potential of an ALG/CHI based LbL coating produced on hydrogel materials for SCLs to act as a drug diffusion barrier, is investigated. Two different hydrogels were studied: (1) one silicone-based hydrogel, designated as TRIS/NVP/HEMA (the molecular structures of the monomers are shown in Appendix A); (2) one commercially silicone-based hydrogel under the name of Definitive 50 from Contamac Products (U.K.) (its physical properties are described in Appendix B). The natural based polyelectrolytes used to prepare the coating, ALG and CHI are biopolymers of interest for drug delivery applications, owing to their biocompatibility, non-antigenicity and non-toxicity [1–4]. ALG is an anionic polysaccharide composed of β-D-mannuronate (M block) and α-L-guluronate (G block) copolymers bound by 1,4-glucosidic linkages [5]. CHI is a cationic copolymer of β-(1-4)-linked 2-acetomido-2-deoxy-d-glucopyranase and 1-amino-2-deoxy-d-glucopyranase. Due to its physicochemical characteristics, namely permeation enhancing properties, CHI is an adequate material for drug delivery ocular devices [6]; however, it has very low mechanical integrity and enzymatically degrades, e.g. by the action of lysozyme [7]. The chemical structures and some physical properties of both polyelectrolytes are summarized in Appendix C. Two crosslinkers, $CaCl_2$ and glyoxal (GL) were added to the coating to further improve coating properties, ultimately favouring coating stability. $CaCl_2$ is known to form stronger films of ALG, improving the tensile strength and structure cohesion [8], while GL has been considered advantageous, in other studies, to improve CHI-based materials properties [9–11]. **Figure 2.1** shows schematically the crosslinking of both polyelectrolytes.

A
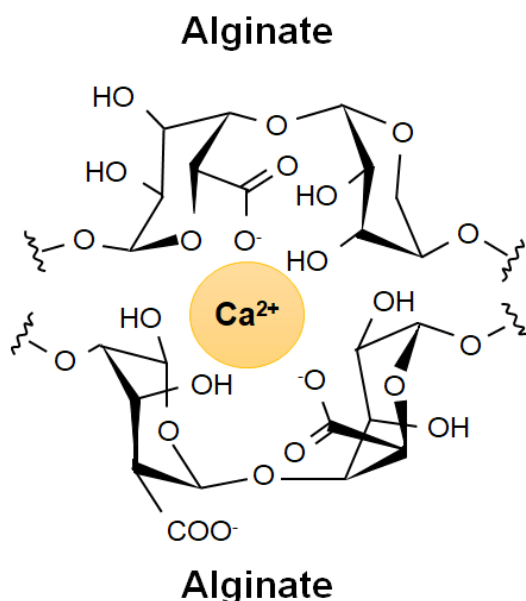
B
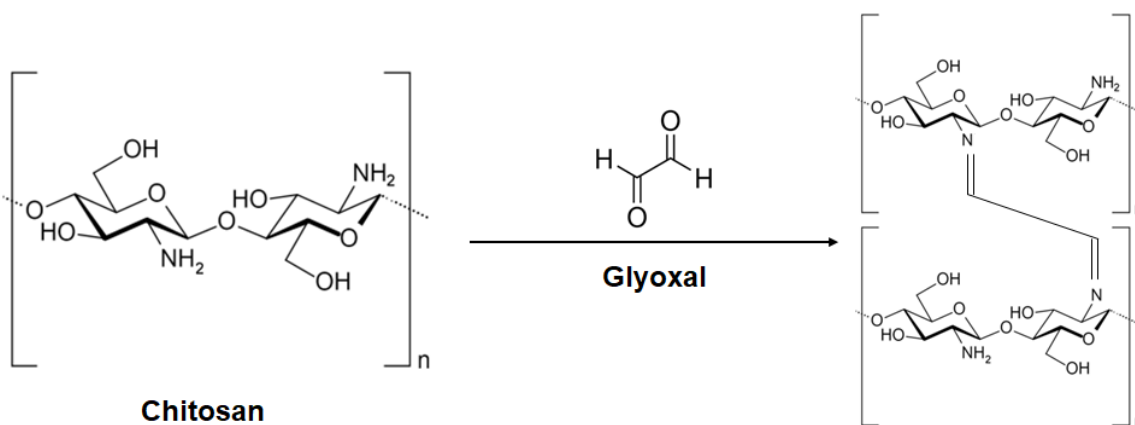
Figure 2.1 Schematic representation of the **(A)** ALG crosslinking with Ca^{2+}, and **(B)** CHI crosslinking with GL. Adapted from [8,11].

Four drugs were loaded in the LbL coated TRIS/NVP/HEMA hydrogel: two anti-inflammatories DCF and KETO, an antiseptic CHX, and the antibiotic MXF. The drug loading was carried out prior to the LbL coating, though simple soaking in individual concentrated drug solutions, and the release profiles were evaluated under sink conditions (conditions in which the volume of the release medium is at least 5 times greater than the volume present in the saturated solution). DCF was further tested in Definitive 50.

The formation of the ALG/CHI layers was followed using a QCM-D and the topography, wettability, refractive index and transmittance of the LbL coated TRIS/NVP/HEMA hydrogels was assessed. The thickness of the coatings was determined by ellipsometry.

2.2 Experimental part

2.2.1 Materials

3-Tris(trimethylsilyloxy)silylpropyl 2-methylprop-2-enoate (purity$\geq$98%, TRIS), 2-hydroxyethyl methacrylate (purity$\geq$99%, HEMA), ethylene glycol dimethacrylate (purity$\geq$98%, EGDMA), 2,2'-azobis(2-methylpropionitrile) (purity$\geq$98%, AIBN), acetic acid (purity$\geq$99.7%), alginic acid sodium salt from brown algae (average molecular weight 100,000-200,000 g/mol, 61% mannuronic acid and 39% guluronic acid, ALG), diclofenac sodium salt (purity$\geq$98.5%, DCF), ketorolac tris salt, (purity$\geq$99%, KETO), glyoxal solution 40% (w/w) in H_2O (GL), branched polyethylenimine (average molecular weight 750,000 g/mol, PEI) were provided by Sigma–Aldrich (USA). N-Vinyl pyrrolidone (purity$\geq$98%, NVP), and sodium hydroxide (purity$\geq$99%, NaOH), were obtained from Merck (Germany). Sodium chloride (purity$\geq$99%, NaCl), sulfuric acid (purity$\geq$98%, H_2SO_4), hydrogen peroxide (30% (w/v), H_2O_2), calcium chloride 2-hydrate ($CaCl_2.2H_2O$) and Chlorhexidine diacetate monohydrate (purity$\geq$ 98%, CHX) were supplied by Panreac (Germany). Moxifloxacin hydrochloride (MXF) was provided from Carbosynth (U.K.) and Hellmanex®II from Hellma GmbH (Germany). Medical grade chitosan (high deacetylation degree, >90%, average molecular weight 750,000-1,000,000 g/mol, CHI) was supplied by Altakitin (Portugal), and Definitive 50 (Contamac U.K.) was supplied by Physiol (Belgium). Polystyrene (PS) was synthesized and offered by Dra. Clara Gomes from Centro de Química Estrutural, Instituto Superior Técnico – University of Lisbon (Portugal). Lysozyme chicken egg white (pH 6.5) is from CalbioChem (U.K.). Distilled and deionised (DD, 18 MΩcm, pH 7.7) water obtained from a Millipore system was used to prepare all solutions.

2.2.2 Preparation of polymeric samples

The silicone-based hydrogel (TRIS/NVP/HEMA) was synthesized using a mixture of 0.8 M of TRIS, 3.9 M of NVP, 1.8 M of HEMA, and 30 mM of EGDMA, which was degassed by ultrasounds (5 min) and bubbling with nitrogen (10 min). Then, AIBN was added to get a concentration of 15 mM, and the solution was poured into a mould constituted by two silanized glass plates separated by a Teflon frame with 0.3 mm of thickness. The silanization process reported in [12] was followed. Polymerization was done in an oven at 60ºC for 24 h. In order to remove unreacted monomers and other impurities, the polymerized hydrogel was washed with DD water for 5 days, with total renovation two times a day. Finally, the hydrogel sheets (thickness ≈0.3 mm) were cut in disks with 9 mm of diameter. Definitive 50 samples were washed in a Soxhlet extractor with DD water, for 60 cycles, according to the recommendations of the supplier and cut in disks with an average thickness of ≈1 mm and a 6 mm diameter. All samples were dried overnight in an oven at 36ºC and stored inside closed flasks.

2.2.3 Drug loading and drug release tests

TRIS/NVP/HEMA dry samples (average weight ≈21 mg) were loaded with the drugs by individually soaking in 3 mL of drug solution with a concentration of 1 mg/mL of DCF and KETO, 2.5 mg/mL for CHX and 5 mg/mL for MXF. The loadings were done at 4ºC for 38 h in the former two cases, and 72 h in the latter cases. The drugs were dissolved in a 130 mM NaCl solution, except for CHX which was dissolved in DD water. The Definitive 50 (average weight ≈18 mg) samples were loaded with DCF using the same conditions.

The release measurements were done by soaking the samples in a 3 mL saline solution (130 mM), at 36ºC, with a 180 rpm stirring. Volumes of 200 µL were removed at schedule times to measure the drug concentration, being replaced by the same volumes of new saline solution.

The concentration of the drugs in the collected solutions was determined by measuring the absorbance with a UV-Vis spectrophotometer (Multiskan GO, Thermo Scientific) at a wavelength of 255 nm for CHX, 276 mm for DCF, 290 mm for MXF and 323 mm for KETO.

2.2.4 LbL deposition

The drug loaded hydrogels were first coated with PEI which promotes stability and homogeneity of the following layers [13,14], by soaking the hydrogels for 5 min in a PEI aqueous solution (20 mM). Meanwhile, the ALG and CHI solutions with a concentration of 10 mM each were prepared in DD water and in aqueous solution of acid acetic 1% (v/v), respectively. The pH of the ALG and CHI solutions was 6.5 and 3.0, respectively. The pH of the CHI solution was then adjusted to 5.0, with NaOH, in order to maintain its positive charge while avoiding depolymerization of CHI [15]. In some referred cases, 5% (w/w) of GL was added to the CHI solution. One double layer was achieved by dipping the hydrogel samples into ALG solution for 1 min, subsequently immersing in 1 M $CaCl_2$ solution for 3 min, and finishing with CHI solution for 1 min. Two and four double layers were also prepared, repeating the process. To protect the CHI layer from lysozyme action [7,16], a final layer of ALG (crosslinked with $CaCl_2$ was deposited). Depending on the number of double layers (n=1, 2 or 4), the coatings were designated as $((ALG-CaCl_2)/CHI)_n$. After immersion in each solution, a rinsing with DD water was done. In the case of samples produced with CHI solutions containing GL, the crosslinking of CHI was achieved by drying the samples in the oven at 45°C during 1 h, in the final stage, to form a coating designated as $(ALG-CaCl_2)/(CHI+GL)$.

In the meantime, drug loaded samples without coating (designated uncoated hydrogels) were immersed in DD water during the time of the LbL formation ($\approx$15 min) to mimic the process undergone by the coated samples. The uncoated samples prepared for comparison with those coated with $(ALG-CaCl_2)/(CHI+GL)$ were finally placed inside an oven at 45°C for 1 h. With this procedure, it was ensured that the amount of drug lost during the LbL formation, which was experimentally determined through the analysis of the respective immersion solutions, was also lost by the uncoated samples.

The prepared samples were then immediately used for the drug release tests.

2.2.5 Evaluation of the LbL coating stability

The formation of the layers was studied using a quartz crystal microbalance with dissipation (QCM-D, E4 from Q-Sense).The sensors were gold coated quartz crystals (5 MHz), which were pre-coated with a PS film by spin coating (2000 rpm, 30 s), and then coated with the

TRIS/NVP/HEMA hydrogel forming reactional mixture (described in section 2.2.2) by spin coating (5000 rpm, 30 s). The hydrogel films were thermopolymerized at 60ºC for 1 h.

The experimental baseline was obtained with the hydrogel films pre-hydrated in DD water. Normalized frequency ($\Delta f/n$) and dissipation (ΔD) changes (for the 3rd harmonic) were monitored during the process of LbL deposition. After the addition of each solution, a rinsing step was done with DD water.

The eventual degradation effect of the lysozyme on the LbL coating was studied by adding lysozyme solution after the stabilization of layers, followed by rinsing with NaCl solution. The concentration of lysozyme solution was 1.9 mg/mL to simulate that of the lacrimal fluid [17–19]. Eight independent experiments were made at 36ºC.

After each experiment, the quartz crystals were cleaned by dipping for 5 s in piranha solution: H_2SO_4/H_2O_2 7/3 v:v. Immediately afterwards, the crystals were washed in ultrasounds with a 2% (v/v) Hellmanex solution (15 min), followed by water (2 x 15 min). Then, they were rinsed with DD water, dried with a nitrogen flux and stored inside closed flasks.

2.2.6 Physical characterization of the LbL coated hydrogels

2.2.6.1   Topography

Topographic images of the surfaces of the hydrated hydrogels were obtained using an AFM (Nanosurf EasyScan 2). The analyses were done in tapping mode in a liquid cell, at room temperature. Images of 20 x 20 μm^2 were obtained with silicon probes (resonance frequency: 204-497 kHz) at a scan rate of 0.7 Hz. R_a of the surfaces was obtained for the total area of the images, using of the software WsxM 5.0 develop 8.0.

2.2.6.2   Wettability

The wettability of the hydrated hydrogels was determined by measuring the contact angles of captive air bubbles lying underneath the substrates immersed in DD water. The images of the air bubbles were obtained through a video camera (jAi CV-A50, Spain) mounted on a microscope Wild M3Z (Leica Microsystems, Germany) and analysed by running the ADSA

(Axisymmetric Drop Shape Analysis, Applied Surface Thermodynamics Research Associates, Canada) software.

2.2.6.3   Optical properties

The transmittance of the hydrated hydrogel samples was determined, in triplicate, with a UV-Vis spectrophotometer (Multiskan GO, Thermo Scientific). The wavelength interval of 400-700 nm was scanned with 1 nm intervals.

Ellipsometric functions Ψ and Δ were measured in the spectral range from 300 to 850 nm using a phase modulated spectroscopic ellipsometer (UVISEL, Horiba Jobin-Yvon), at 70º incidence angle. The thickness and refractive index of the films/hydrogels were determined through suitable modelling using DeltaPsi2 software package from Jobin-Yvon with a Cauchy dispersion function.

2.3   Results and discussion

2.3.1 Optimization of the LbL coating

The formation of the layers during the LbL deposition process was followed by QCM-D. The time course of $\Delta f/n$ and ΔD upon contact of the TRIS/NVP/HEMA hydrogel-coated quartz crystals with the polyelectrolyte solutions is shown in **Figure 2.2**.

The baseline corresponds to the coated sensors equilibrated with DD water. After injection of the PEI solution, ALG, $CaCl_2$ and CHI solutions were sequentially introduced, terminating with a second injection of ALG and $CaCl_2$. The observed frequency and dissipation shifts indicate the formation of stable layers, where the rinsing steps performed after each injection had a small effect, demonstrating that the layers remained irreversibly adsorbed on the surface. The resistance of this coating terminated with the final layer of ALG and $CaCl_2$ against lysozyme was confirmed from the observation that the injection of the protein solution did not induce any change in the frequency and dissipation of the adsorbed layers for several hours. At this point, it is important to refer that the toxicity of PEI should not be a problem because it was used as the deepest layer which remained attached to the surface. Moreover, there are

several reports in the literature about the reduction of the cytotoxicity of PEI in presence of CHI and ALG [20,21]. However, cytocompatibility testes would be necessary before *in vivo* application.
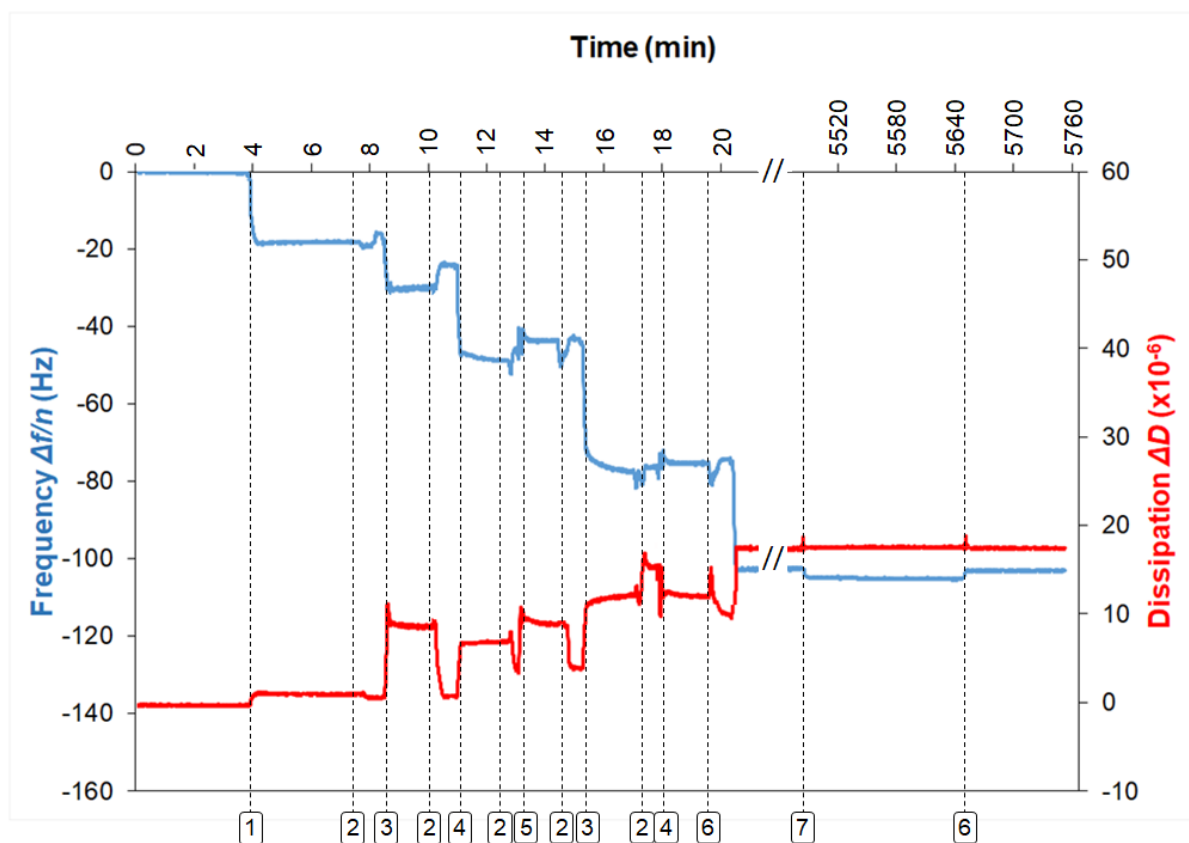
Figure 2.2 Normalized shift in the frequency, $\Delta f/n$ (blue line, left y-axis) and shift in the dissipation ΔD (red line, right y-axis) for the third harmonic of the resonant frequency of a quartz crystal sensor after being coated with a TRIS/NVP/HEMA hydrogel film, during successive additions of solutions of PEI (1), rinsing with DD water (2), ALG (3), $CaCl_2$ (4), CHI (5), rinsing with NaCl (6) and lysozyme (7) as a function of time, to form the $((ALG-CaCl_2)/CHI)_1$ coating topped with a final layer of $ALG-CaCl_2$.

In order to test the effect of the number of layers, 1, 2 and 4 $((ALG-CaCl_2)/CHI)_n$ double layers were deposited on top of the TRIS/NVP/HEMA surface always terminated by an $ALG-CaCl_2$ layer. The cumulative release profiles of DCF from TRIS/NVP/HEMA hydrogels are presented in **Figure 2.3**.
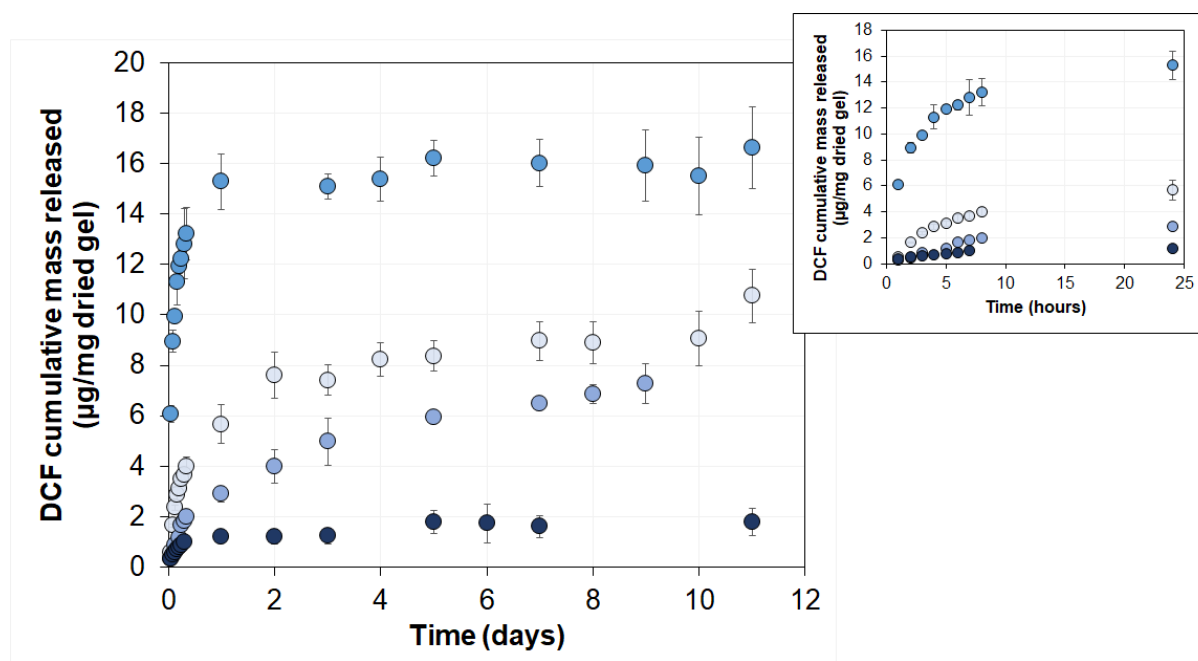
Figure 2.3 DCF cumulative release profiles from TRIS/NVP/HEMA hydrogels uncoated (⬤), and coated with $((ALG\text{-}CaCl_2)/CHI)_1$ (◯), $((ALG\text{-}CaCl_2)/CHI)_2$ (⬤), and $((ALG\text{-}CaCl_2)/CHI)_4$ (⬤), terminated by an $ALG\text{-}CaCl_2$ final layer. The insert represents the release data obtained during the first 24 h. The error bars are the ± standard deviations (n=7).

Analysis of **Figure 2.3** shows that the deposition of 1 and 2 double layers decreases the initial rate of drug release and extends the release duration, thus, significantly improving the release profile. However, 4 double layers almost hinder the release of the drug which led us to abandon this number of layers. Then, the R_a, transmittance, refractive index, coating thickness and wettability of the hydrogels with 0, 1 and 2 double layers were determined and the measured values are presented in **Table 2.1** (three first columns). The thickness of 1 double layer could not be measured apparently due to the heterogeneous nature of this coating. The contact angles on the hydrated samples with 1 double layer was not measured.

Table 2.1 Properties of uncoated and coated TRIS/NVP/HEMA hydrogels: R_a, transmittance, refractive index, coating thickness and wettability. The errors are the $\pm$ standard deviations (in all cases n=3, except the contact angles with n=10).

	Uncoated	**((ALG-CaCl$_2$)/CHI)$_1$**	**((ALG-CaCl$_2$)/CHI)$_2$**	**(ALG-CaCl$_2$)/(CHI+GL)**
R_a (nm)	20±9	26±7	16±8	33±2
Transmittance (%)	98.0±0.5	92±1	80±1	94±2
Refractive index	1.46±0.02	1.41±0.02	1.48±0.01	1.50±0.01
Coating thickness (nm)	-	-	60±3	40±1
Water contact angle (º)	35±5	-	42±2	≈0

The R_a increased after the first double layer but then decreased when the second double layer was introduced; the refractive index lowered with the first double layer, but recovered for the second one. The wettability of the hydrated sample with 2 double layers coating slightly decreased.

The AFM images showing the topography of the samples are presented in **Figure 2.4A**-**C**. The porous structure, which is typical of these hydrogels and has already been reported in a previous work [22], is clearly identified on the uncoated hydrogel. It completely disappears on the sample coated with 2 double layers. In the 1 double layer case, only a few pores are still visible.
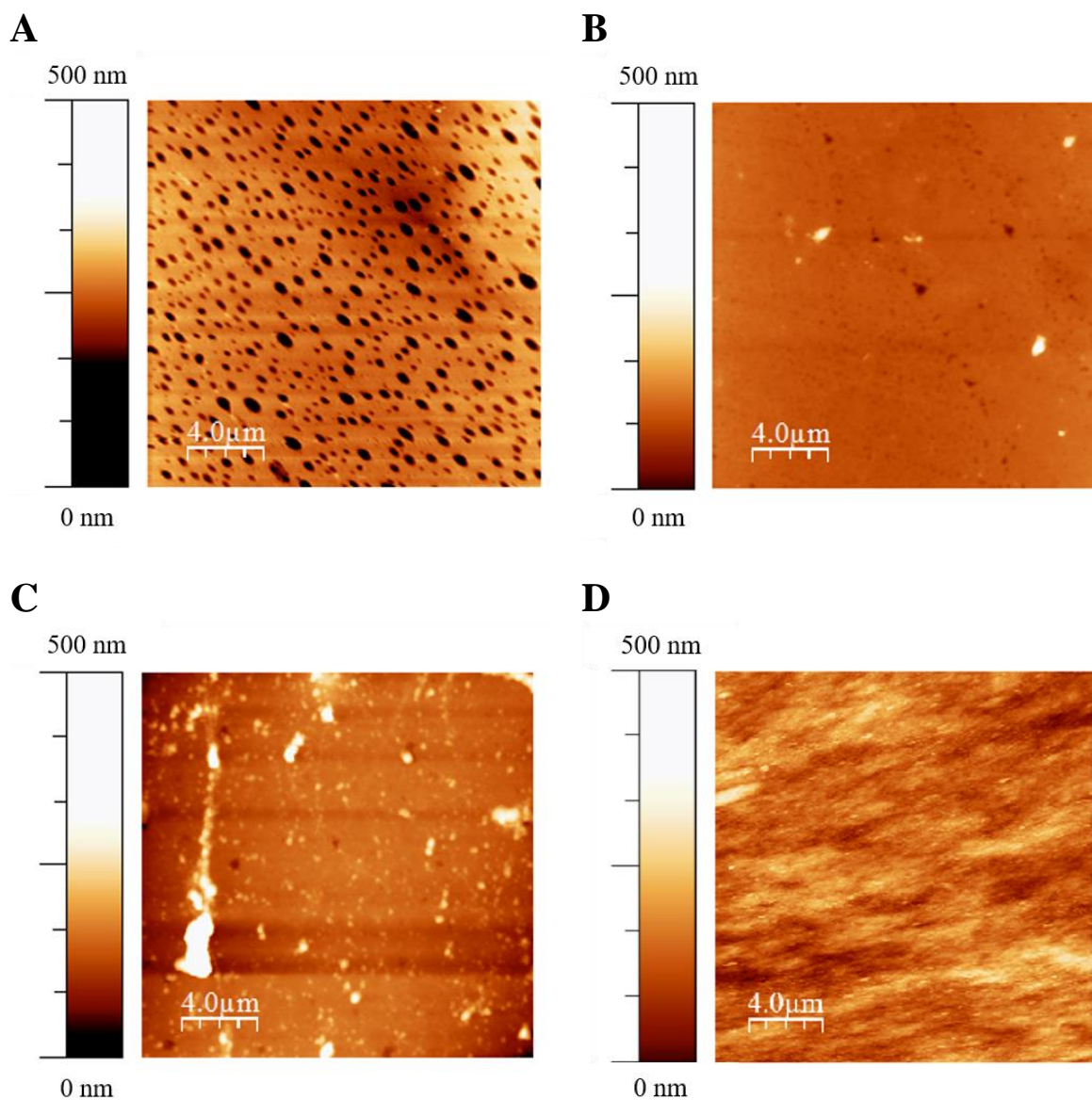
Figure 2.4 AFM images ($20 \times 20 \ \mu m^2$) of the surface of TRIS/NVP/HEMA uncoated **(A)**, coated with $((ALG\text{-}CaCl_2)/CHI)_1$ **(B)**, $((ALG\text{-}CaCl_2)/CHI)_2$ **(C)**, and coated with $(ALG\text{-}CaCl_2)/(CHI+GL)$ **(D)**.

Although 2 double layers seemed to yield a more adequate coating from the point of view of physical homogeneity and drug release control, the reduction of transmittance to 80% did not allow pursuing this route.

The attention was then focussed on the 1 double layer coating. In order to achieve a consistent uniform coating, the crosslinking agent GL, which is a small aldehyde known to be biocompatible [10], was added to the CHI solution. Since the coated sample had to be dried at

45ºC, it was not possible to follow the LbL deposition with the QCM-D. The wettability, R_a, transmittance, coating thickness and refraction index of these new coated samples were determined and are shown in **Table 2.1** (right column). This coating has very interesting properties: it is very hydrophilic; it is quite homogeneous (the ellipsometric measurements easily converged in a precise value of thickness); it ensures a transmittance value above 90% which is the minimum required for SCLs [23]; it has a small effect on the bulk refraction index of the hydrogel; it should resist to degradation against lysozyme (as demonstrated by QCM-D data, in **Figure 2.2**, for the coating without GL). The contact angle of the hydrated sample was considered to be null due to the bubble instability which derives from the rather hydrophilic nature of the surface. The AFM image, shown in **Figure 2.4D**, reveals a dense coating which completely covers the underlying hydrogel. Thus, the use of this type of LbL coating seems to be very promising for drug control release of SCLs and its effectiveness was tested in different drug/lens systems.

2.3.2 Drug release profiles of coated SCLs materials

The release profiles of DCF, KETO, CHX and MXF from TRIS/NVP/HEMA coated with 1 double layer (ALG-CaCl$_2$)/(CHI+GL) terminated with ALG-CaCl$_2$ are presented in **Figure 2.5**.

A
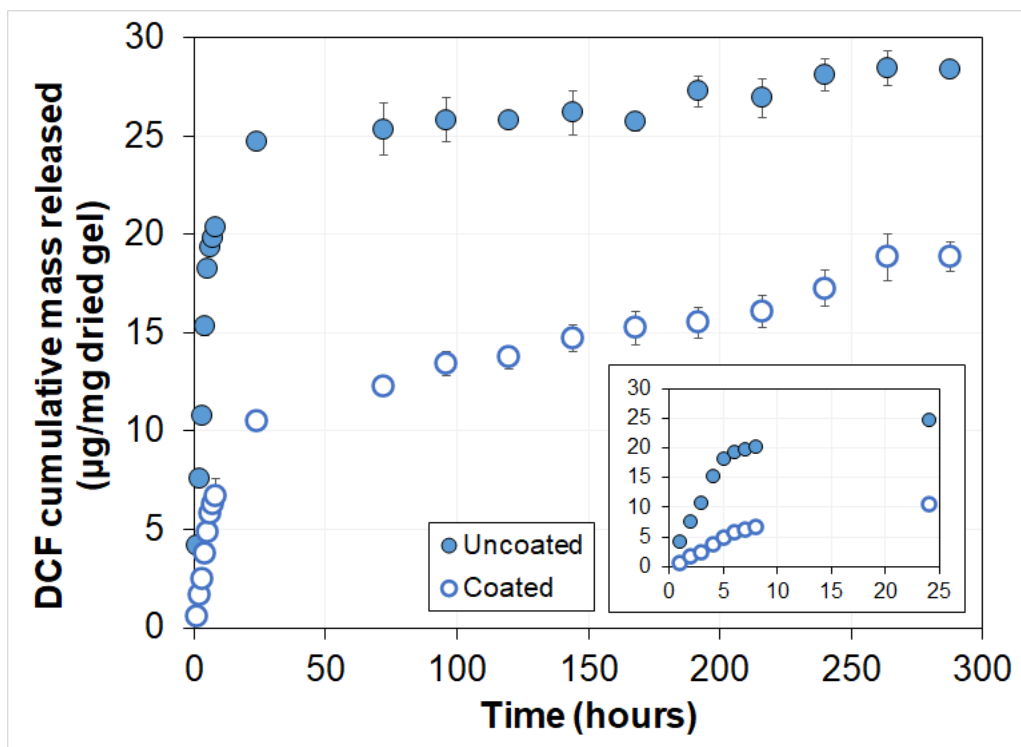
B
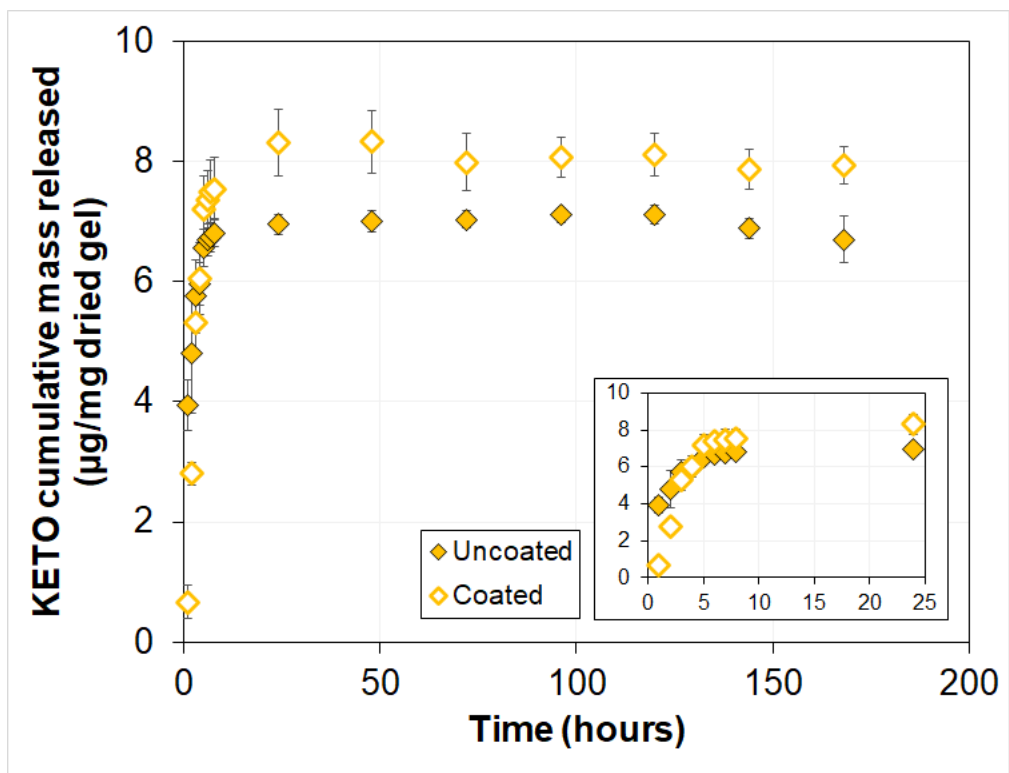
C
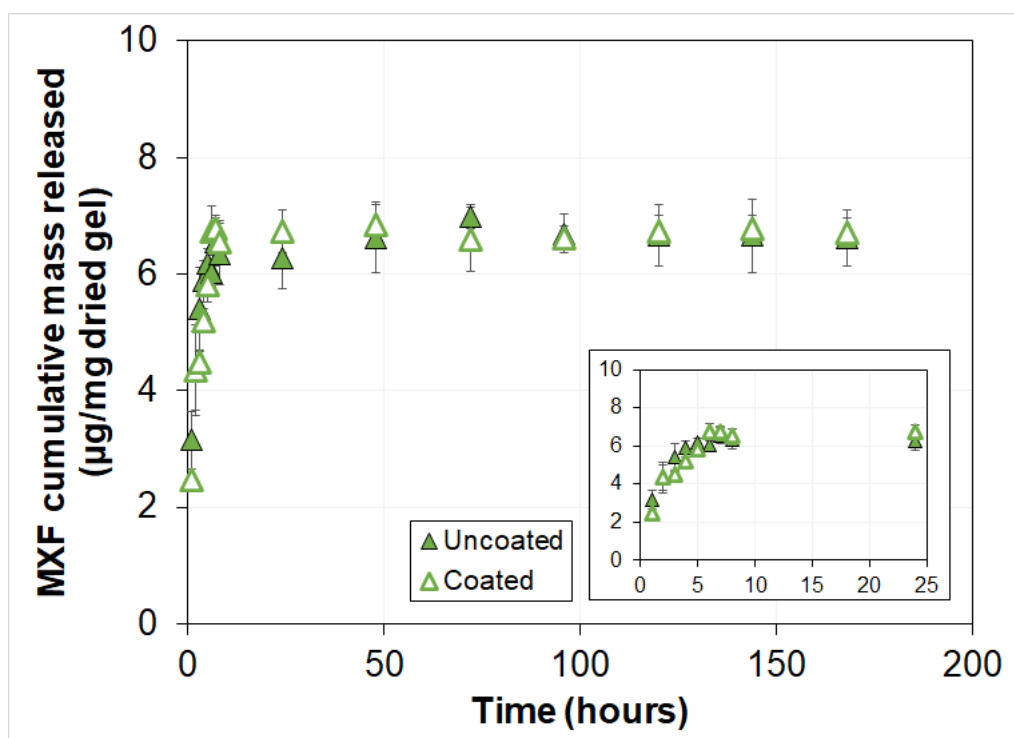
D
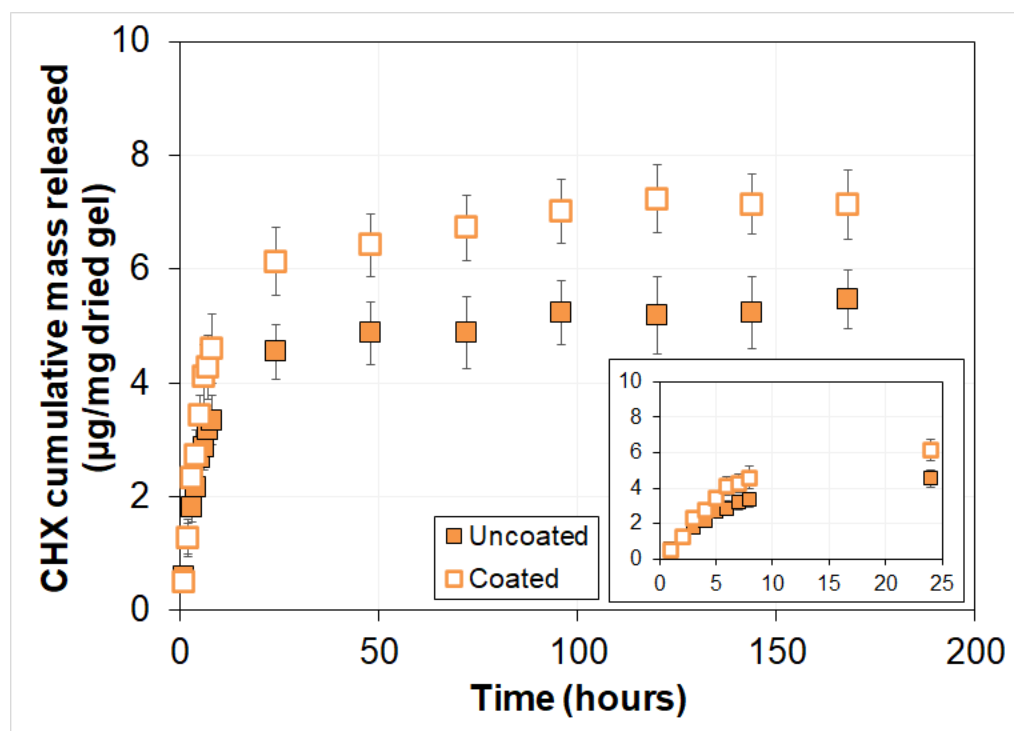
Figure 2.5 Cumulative mass release of DCF (**A**), KETO (**B**), MXF (**C**) and CHX (**D**) from TRIS/NVP/HEMA coated with 1 double layer of (ALG-CaCl$_2$)/(CHI+GL) terminated with ALG-CaCl$_2$, and from uncoated samples. The error bars are the $\pm$ standard deviations (n=7).

The inserts represent the release data obtained during the first 24 h. The uncoated hydrogels are different from those shown in **Figure 2.3** because they were dried in the oven to mimic the crosslinking of CHI with GL.

Comparison of the obtained profiles reveals that DCF stands out as leading to the most efficient release. Apparently, the uptake of DCF by the hydrogel is large and reversible yielding a cumulative mass release about three times larger than that of the other drugs. In a recent study [24], the release of DCF and CHX from TRIS/NVP/HEMA were compared in terms of drug partitioning and diffusion. Although both drugs had similar partition coefficients, CHX showed a much stronger adsorption on the polymeric matrix that DCF which was attributed to the interaction of positively charged amine groups with the acrylate groups in the HEMA monomers. MXF, being lipophilic, should adsorb on the hydrophobic sites of the chains (TRIS monomers). The difference between DCF and KETO is difficult to explain. This means that the uptake and release of DCF should be preferentially determined by the aqueous phase of the hydrogel and that bulk diffusion essentially determines the release profile.

The barrier effect of the LbL coating is clearly most effective for DCF. In the case of MXF the profile was not affected, while for KETO and CHX the released amount increased but the rate of release did not improve. DCF is the smallest molecule among the studied drugs. Taking into consideration only its size, the special efficiency in the release control demonstrated by the LbL coating is unexpected. Several authors proposed the use of CHI matrices to sustain the release of DCF from tablets or nanoparticles [25]. Sabnis *et al.* (1997) found that, in acidic media, the release of DCF from CHI matrices was slowest for CHI of high degree of deacetylation, meaning that the number of amino groups present in the polymer backbone is an important factor to control the drug release via (1) the formation of a CHI gel barrier and (2) ionic interactions between ionized amino groups and anionic DCF [26]. González-Rodríguez *et al.* (2002) prepared ALG-CHI microspheres for DCF release and claimed that drug release was controlled by the interactions between DCF and the polycation CHI, in competition with ALG [27]. However, other authors claimed that although CHI matrices efficiently entrap DCF, the ionic interaction between them is low; in other words, the complexes formed between these two molecules should have low stability [28,29]. The formation of these unstable complexes of CHI-DCF may offer an explanation for the retardation effect felt by the DCF when crossing the surface layer during the release process. There are also reports in the literature on the use

of CHI-ALG nanodispersions for ocular sustained delivery of KETO but the initial burst was not avoided [30]. In this work, the ALG/CHI based coating decreased the initial burst but did not reduce the following release rate. The increase in the amount of KETO and CHX released in the presence of the ALG/CHI coating is difficult to explain. One possibility could be a decrease in the density of the coating caused by the interaction with the drug. Abruzzo *et al.* (2013) reported a decrease in the density of ALG/CHI matrices loaded with CHX, suggesting some extension of the polymeric chains in presence of drug [31].

In view of the efficient control of the release of DCF achieved with this LbL coating on TRIS/NVP/HEMA samples, another substrate was tested. The release profiles of DCF from Definitive 50 is shown in **Figure 2.6**. Comparison with TRIS/NVP/HEMA (**Figure 2.5A**) shows that the barrier effect of the LbL coating is more striking for Definitive 50, where the initial release rate is considerably reduced and the release duration increased up to 190 h.
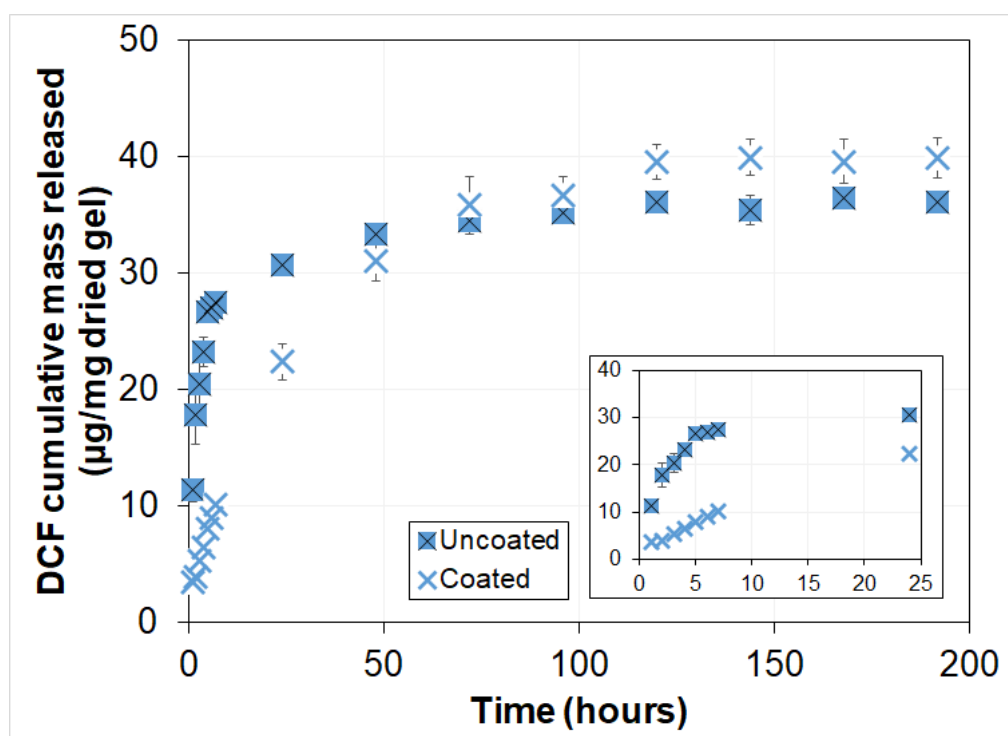
Figure 2.6 DCF cumulative release profile from Definitive 50 hydrogels coated with (ALG-CaCl$_2$)/(CHI+GL) terminated with ALG-CaCl$_2$. The inserts represent the release data obtained during the first 24 h. The error bars are the ± standard deviations (n=7).

Although further tests are needed to confirm the feasibility of using these ALG-CHI based LbL coatings on SCLs materials, namely their cytocompatibility, this study suggests that they may offer a valuable solution to control the release of DCF from different lens materials. Besides their ability to avoid the initial burst, typical of drug loaded lenses, these coatings increase dramatically the hydrophilicity of TRIS/NVP/HEMA, thus avoiding extra surface treatments usually performed to ensure high comfort to lens wearers and to minimize deposits of lipids and proteins from the tear fluid. The barrier effect of the coating seems to be independent of the size of the drug molecule, but it is strongly determined by its chemical nature. The coating was not efficient for the control of the release of the other studied drugs, even the anionic KETO.

At this time, it is not possible to give a reasonable explanation for the different behaviours. However, in view of the promising results obtained with DCF, it would be important to pursue with this investigation, looking for other types of functionalized CHI and/or crosslinking agents in order to optimize the reversible interactions between drug and coating needed to ensure a sustained release.

2.4 Conclusions

This work describes an investigation about the use of coatings obtained with the LbL deposition of ALG/CHI based layers to control the drug release from SCL materials. Optimization of the properties of the coated hydrogels taking into consideration the requirements for their application as ophthalmic lens materials was first attempted using TRIS/NVP/HEMA hydrogel and DCF. Very good results were obtained with the double layer (ALG-CaCl$_2$)/(CHI+GL) topped with a final ALG-CaCl$_2$ layer to avoid CHI degradation by tear fluid proteins. The coating is dense, homogeneous, and very hydrophilic; it does not affect the bulk refraction index, slightly reduces the light transmittance and leads to a controlled release of DCF for more than a week. Such a promising behaviour led us to investigate its performance with other drugs (KETO, MXF and CHX) and one commercial material (Definitive 50). The barrier effect of the coating revealed to be strongly affected by the characteristics of the pair hydrogel/drug: it existed for the two tested hydrogels but was more prominent for Definitive 50; surprisingly, only DCF, which is the smallest molecule, was effectively controlled. Further studies using

adequately functionalized CHI should be done to optimize the release control of each specific drug.

2.5 References

[1]   H. Lu, Z. Chen, X. Yang, L. Cen, X. Zhang, P. Gao, Layer-by-layer self-assembly of minocycline-loaded chitosan/alginate multilayer on titanium substrates to inhibit biofilm formation, J. Dent. 42 (2014) 1464–1472.

[2]   Q. Wang, Z. Dong, Y. Du, J.F.J.F. Kennedy, Controlled release of ciprofloxacin hydrochloride from chitosan/polyethylene glycol blend films, Carbohydr. Polym. 69 (2007) 336–343.

[3]   F. Ding, H. Deng, Y. Du, Q. Wang, Emerging chitin and chitosan nanofibrous materials for biomedical applications, Nanoscale. 6 (2014) 9477–9493.

[4]   Y. Yang, S. Wang, Y. Wang, X. Wang, Q. Wang, M. Chen, Advances in self-assembled chitosan nanomaterials for drug delivery, Biotechnol. Adv. 32 (2014) 1301–1316.

[5]   R. Jayakumar, K.M. Sajesh, S. Soumya, T.R. Nimal, K.P. Chennazhi, S. V. Nair, R. Jayakumar, Injectable alginate-O-carboxymethyl chitosan/nano fibrin composite hydrogels for adipose tissue engineering, Int. J. Biol. Macromol. 74 (2014) 318–326.

[6]   A. Bernkop-Schnürch, S. Dünnhaupt, Chitosan-based drug delivery systems, Eur. J. Pharm. Biopharm. 81 (2012) 463–469. https://doi.org/.

[7]   L. Wei, C. Cai, J. Lin, L. Wang, X. Zhang, Degradation controllable biomaterials constructed from lysozyme-loaded Ca-alginate microparticle/chitosan composites, Polymer (Guildf). 52 (2011) 5139–5148.

[8]   M.J. Costa, A.M. Marques, L.M. Pastrana, J.A. Teixeira, S.M. Sillankorva, M.A. Cerqueira, Physicochemical properties of alginate-based films: Effect of ionic crosslinking and mannuronic and guluronic acid ratio, Food Hydrocoll. 81 (2018) 442–448.

[9]   Q. Yang, F. Dou, B. Liang, Q. Shen, Studies of cross-linking reaction on chitosan fiber with glyoxal, Carbohydr. Polym. 59 (2005) 205–210.

[10]   L. Wang, J.P. Stegemann, Glyoxal crosslinking of cell-seeded chitosan/collagen hydrogels for bone regeneration, Acta Biomater. 7 (2011) 2410–2417.

[11]   J.A. Sirviö, M. Visanko, H. Liimatainen, Synthesis of imidazolium-crosslinked chitosan

aerogel and its prospect as a dye removing adsorbent, RSC Adv. 6 (2016) 56544–56548.

[12] R. Vasquez, R. Nogueira, M. Orfão, J. Mata, B. Saramago, Stability of triglyceride liquid films on hydrophilic and hydrophobic glasses, J. Colloid Interface Sci. 299 (2006) 274–282.

[13] C. Delajon, T. Gutberlet, R. Steitz, H. Möhwald, R. Krastev, Formation of polyelectrolyte multilayer architectures with embedded DMPC studied in situ by neutron reflectometry, Langmuir. 21 (2005) 8509–8514.

[14] J. Hernandez-Montelongo, V.F. Nascimento, D. Murillo, T.B. Taketa, P. Sahoo, A.A. Souza, M.M. Beppu, M.A. Cotta, Nanofilms of hyaluronan/chitosan assembled layer-by-layer: An antibacterial surface for Xylella fastidiosa, Carbohydr. Polym. 136 (2016) 1–11.

[15] C.K.S. Pillai, W. Paul, C.P. Sharma, Chitin and chitosan polymers: Chemistry, solubility and fiber formation, Prog. Polym. Sci. 34 (2009) 641–678.

[16] D. Mawad, C. Warren, M. Barton, D. Mahns, J. Morley, B.T.T. Pham, N.T.H. Pham, S. Kueh, A. Lauto, Lysozyme depolymerization of photo-activated chitosan adhesive films., Carbohydr. Polym. 121 (2015) 56–63.

[17] S. Jadi, M. Heynen, D. Luensmann, L. Jones, Composition of incubation solution impacts in vitro protein uptake to silicone hydrogel contact lenses, Mol. Vis. 18 (2012) 337–347.

[18] D.R. Whikehart, Proteins: Essential components of the eye, in: Biochem. Eye, Springer US, 2003: pp. 15–54.

[19] R.J. Fullard, C. Snyder, Protein levels in nonstimulated and stimulated tears of normal human subjects, Investig. Ophthalmol. Vis. Sci. 31 (1990) 1119–1126.

[20] S.-H. Min, K.-C. Park, Y.I. Yeom, Chitosan-mediated non-viral gene delivery with improved serum stability and reduced cytotoxicity, Biotechnol. Bioprocess Eng. 19 (2014) 1077–1082.

[21] S. Patnaik, A. Aggarwal, S. Nimesh, A. Goel, M. Ganguli, N. Saini, Y. Singh, K.C. Gupta, PEI-alginate nanocomposites as efficient in vitro gene transfection agents, J. Control. Release. 114 (2006) 398–409.

[22]   D. Silva, A.C. Fernandes, T.G. Nunes, R. Colaço, A.P. Serro, The effect of albumin and cholesterol on the biotribological behaviour of hydrogels for contact lenses, Acta Biomater. 26 (2015) 184–194.

[23]   N. Efron, C. Maldonado-Codina, Development of contact lenses from a biomaterial point of view – Materials, manufacture, and clinical application, in: Compr. Biomater., Comprehensive Biomaterials. Elsevier, 2011: pp. 517–541.

[24]   A.F.R. Pimenta, J. Ascenso, R. Colaço, A.P. Serro, B. Saramago, Controlled drug release from hydrogels for ophthalmic lenses: drug partitioning and diffusion, Int. J. Pharm. 515 (2016) 467–475.

[25]   S.A. Agnihotri, N.N. Mallikarjuna, T.M. Aminabhavi, Recent advances on chitosan-based micro- and nanoparticles in drug delivery, J. Control. Release. 100 (2004) 5–28.

[26]   S. Sabnis, P. Rege, L. Block, Use of chitosan in compressed tablets of diclofenac sodium: inhibition of drug release in an acidic environment, Pharm. Dev. Technol. 2 (1997) 243–255.

[27]   M.L. González-Rodríguez, M.A. Holgadoa, C. Sánchez-Lafuentea, A.M. Rabascoa, A. Finib, Alginate/chitosan particulate systems for sodium diclofenac release, Int. J. Pharm. 232 (2002) 225–234.

[28]   Y. Boonsongrit, A. Mitrevej, B. Mueller, Chitosan drug binding by ionic interaction, Eur. J. Pharm. Biopharm. 62 (2006) 267–274.

[29]   A. Bani-Jaber, D. Anani, I.I.I. Hamdan, B.A.A. Alkhalidi, Investigation of drug polymer interaction: Evaluation and characterization of diclofenac-chitosan co-precipitate, Jordan J. Pharm. Sci. 2 (2009) 140–149.

[30]   N. Morsi, D. Ghorab, H. Refai, H. Teba, Preparation and evaluation of alginate/chitosan nanodispersions for ocular delivery, Int. J. Pharm. Pharm. Sci. 7 (2015) 234–240.

[31]   A. Abruzzo, F. Bigucci, T. Cerchiara, B. Saladini, M.C. Gallucci, F. Cruciani, B. Vitali, B. Luppi, Chitosan/alginate complexes for vaginal delivery of chlorhexidine digluconate, Carbohydr. Polym. 91 (2013) 651–658.

3 Antibacterial layer-by-layer coatings to control drug release from soft contact lenses material

The following results were partially published in the peer-reviewed article:

Table of Contents

3.1 Introduction

The possibility of producing one LbL coating, using the polyelectrolytes ALG and CHI, on SCLs materials to act as a diffusion barrier for sustaining drug release was assessed in chapter 2. In the present work, other polyelectrolyte combinations were tested with a two-fold objective: to control the drug release from a silicone-based hydrogel; to ensure that its surface is kept free of bacteria. Four polyelectrolytes were chosen for these purposes: ALG, CHI, HA and PLL. ALG and CHI were selected due to their potential to form stable coatings, and according to chapter 2 to control the release of DCF. ALG films have no reported antibacterial properties but may be crosslinked with polyvalent cations to improve their water barrier properties, mechanical resistance, cohesiveness and rigidity [1]. In turn, CHI is known to have bacteriostatic or even bactericidal activities, depending on its molecular weight and deacetylation degree, as well as on the pH of the medium [2–5]. HA is a natural anionic polysaccharide with well-known lubricant and cell non-adhesive properties [6,7]. Although in literature, the antibacterial action of HA is somewhat controversial [8], there are some evidences of its bacteriostatic effect (defined as inhibition of bacterial growth) against *S. aureus* and, in a smaller extent, against *P. aeruginosa* [9,10]. PLL is a strong basic homopolypeptide with a positively charge amine group, that was initially obtained from *Stremptomcyces albulus* sp. lysinopolymerus strain 346. It is known to demonstrate antibacterial properties against Gram-positive and Gram-negative bacteria [11]. The chemical structure and some physical properties of the used polyelectrolytes can be seen in Appendix C.

EDC was selected as crosslinker due to its biocompatibility [12] and simplicity of the chemical reaction in which it binds to the polyelectrolytes, that can be achieved at room temperature [13]. The crosslinking process involves a 'zero-length' amide bond between carboxylic groups (present in ALG and HA) and primary amines (present in PLL) [14]. The EDC crosslinking process is described in **Figure 3.1**.
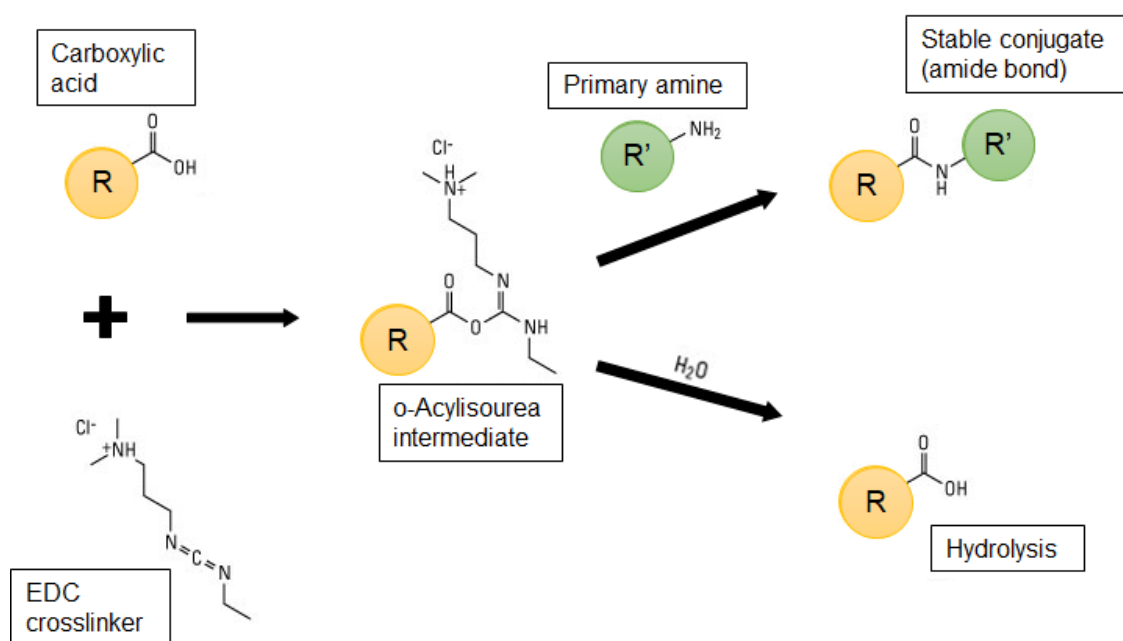
Figure 3.1 EDC reaction with formation of a o-Acylisourea intermediate, that can either in the presence of water suffer hydrolysis or in the presence of a primary amine form a stable conjugate (through an amide bond). Adapted from [15,16].

Three types of LbL coatings, involving, PLL, ALG, CHI and HA, were deposited on the surface of TRIS/NVP/HEMA hydrogel.

The performance of the above referred LbL coatings was accessed in terms of control of the release of an anti-inflammatory drug (DCF), an anti-septic drug (CHX) and an antibiotic drug (MXF), in sink conditions (**Table 1.4**, chapter 1).

The formation of the multilayers was followed using QCM-D, which was also used to check possible interactions of the coatings with two common lachrymal proteins: lysozyme and albumin. Further characterization assays were performed for the cases where the employed LbL coatings were able to control the drug delivery from the drug loaded TRIS/NVP/HEMA hydrogel, namely, topography, wettability, coating thickness, refractive index and transmittance. The antibacterial activity of the most promising coatings was also tested, using two of the bacteria responsible for common ocular infections: *S. aureus* (Gram-positive) and *P. aeruginosa* (Gram-negative) [17,18].

The potential ocular irritancy was determined using HET-CAM tests. Finally, the *in vivo* efficacy of the most promising system was predicted using a simplified mathematical model to estimate the drug concentration in the tear fluid.

3.2 Experimental part

3.2.1 Materials

3-Tris(trimethylsilyloxy)silylpropyl 2-methylprop-2-enoate (purity$\geq$98%, TRIS), 2-hydroxyethyl methacrylate (purity$\geq$99%, HEMA), ethylene glycol dimethacrylate (purity$\geq$98%, EGDMA), 2,2'-azobis(2-methylpropionitrile) (purity$\geq$98%, AIBN), acetic acid (purity$\geq$99.7%), alginic acid sodium salt from brown algae (average molecular weight 100,000-200,000 g/mol, 61% mannuronic acid and 39% guluronic acid, ALG), diclofenac sodium salt (purity$\geq$98.5%, DCF), branched polyethylenimine (average molecular weight 750,000 g/mol, PEI), N-(3-dimethylaminopropyl)-N-ethylcarbodiimide hydrochloride (purity $\geq$ 98%, EDC); and poly-(L-lysine) hydrobromide (average molecular weight 70,000–150,000 g/mol, PLL) were provided by Sigma–Aldrich (USA). N-Vinyl pyrrolidone (purity$\geq$98%, NVP), and sodium hydroxide (purity$\geq$99%, NaOH), were obtained from Merck (Germany). Sodium chloride (purity$\geq$99%, NaCl), sulfuric acid (purity$\geq$98%, H_2SO_4), hydrogen peroxide (30% (w/v), H_2O_2), and Chlorhexidine diacetate monohydrate (purity$\geq$ 98%, CHX) were supplied by Panreac (Germany). Sodium hyaluronate (average molecular weight 1000,000–2000,000 g/mol, HA) and moxifloxacin hydrochloride (MXF) was provided from Carbosynth (U.K) and Hellmanex®II from Hellma GmbH (Germany). Methanol (purity $\geq$ 99.9%, CH_3OH) was obtained from Carlo Erba. Mueller-Hinton broth (MHB) was obtained from BD Quilaban (Portugal) and Mueller-Hinton agar (MH) was from VWR (USA). Albumin bovine Fraction V standard grade (pH 7.0) was supplied by Serva. Medical grade chitosan (high deacetylation degree, >90%, average molecular weight 750,000-1,000,000 g/mol, CHI) was supplied by Altakitin (Portugal), Polystyrene (PS) was synthesized and offered by Doctor Clara Gomes from Centro de Química Estrutural, Instituto Superior Técnico – University of Lisbon (Portugal). Lysozyme chicken egg white (pH 6.5) is from CalbioChem (U.K.). Distilled and deionised (DD, 18 MΩcm, pH 7.7) water obtained from a Millipore system was used to prepare all solutions.

3.2.2 Preparation of polymeric samples

The first step of the synthesis of the cross-linked silicone-based TRIS/NVP/HEMA hydrogels was the preparation of the mixture: TRIS (0.8 M), NVP (3.9), HEMA (1.8 M), and EGDMA (30 mM). This mixture was degassed by ultrasound sonication (5min) and nitrogen bubbling (10 min) at room temperature. The initiator AIBN was added (15 mM) and the solution was homogenised by magnetic stirring. The final solution was poured into a mould formed by two silanized glass plates separated by a Teflon spacer (0.25 mm of thickness). Further details of the silanization process are described in [19].

After polymerization, at 60ºC for 24 h, the hydrogel samples were washed with DD water for 5 days, with complete solvent exchange 3 times a day, in order to remove unreacted monomers and other remaining impurities. From 13C solid state NMR spectra, the molar ratio of the three co-monomers in the TRIS/NVP/HEMA hydrogel was determined to be $1.0/3.8 \pm 0.7/2.5 \pm 0.2$. The presence of the crosslinker agent (EGDMA) was not taken into account in chain composition calculations. The hydrated hydrogel sheets (thickness 0.3 mm) were cut in disks with 10 mm of diameter (unless otherwise stated), and, finally, dried inside an oven at 40ºC overnight. The equilibrium swelling ratio of the TRIS/NVP/HEMA hydrogel was determined to decrease slightly with temperature, reaching the maximum value (65%) at 4ºC [20].

3.2.3 Drug loading and release measurements

The TRIS/NVP/HEMA dried samples (average weight ≈ 21 mg) were drug-loaded by soaking, at 4ºC, in 3 mL of drug solutions: 1 mg/mL of DCF for 38 h, 2.5 mg/mL of CHX for 72 h and 5 mg/mL of MXF for 72 h. The drugs were dissolved in saline solution (NaCl, 130 mM, pH 6.9), except CHX which was dissolved in DD water due to its low solubility in saline solution (100 µg/mL). The drug concentrations were identical to the nominal values of the pharmaceutical formulations. The choice of the drug loading conditions (temperature and time) was based on the results obtained in chapter 2.

The total amount of drug loaded was determined by methanol extraction. The drug loaded hydrogels were placed in glass vials containing 3 mL of methanol. After predetermined times, the hydrogels were removed from the vials, rinsed with DD water, blotted with absorbent paper

and placed in the same volume of fresh methanol, as before. This procedure was repeated after 2, 4, 8 and 24 h and then each 24 h until no drug was detected in the supernatant methanol. The concentration of the extracted drugs was determined by reading the absorbance of the methanol solution using the same procedure as for the drug release. Experiments with methanol extraction were done in triplicate.

Drug release experiments were carried out in the same manner as that described in section 2.2.3 of chapter 2. The release experiments were performed in sink conditions by immersion of the samples in a 3 mL saline solution (NaCl, 130 mM, pH 6.9), at 36ºC, under stirring (180 rpm). Aliquots of 200 µL were removed at schedule times to measure the drug concentration in solution, being replaced by the same volumes of fresh saline solution. Eight experiments were done for each system.

The concentration of released drugs in the collected solutions was determined using a UV-Vis spectrophotometer (Multskan GO, Thermo Scientific), at λ=255 nm for CHX, at 276 nm for DCF, and at 290 nm for MXF.

3.2.4 LbL deposition

Three types of LbL coatings were tested: ALG/PLL(EDC), HA(EDC)/CHI and HA/PLL(EDC)+Drug. EDC was used to crosslink the carboxyl groups of the polysaccharides ALG and HA and the amine groups of PLL and CHI. In the case of HA/PLL(EDC)+Drug, the objective of using EDC was to form conjugated PLL+DCF and PLL+MXF through the amine bonding between the amine groups of the polyelectrolyte and the carboxyl groups of the drugs. This procedure could not be carried out for CHX since this molecule has no carboxyl groups. In all cases, the drug loaded hydrogels were first coated with PEI by soaking the samples for 5 min in a PEI aqueous solution (20 mM). PEI is a highly positive charged polycation used to enhance the stability and uniformity of the subsequent layers [21,22]. ALG/PLL(EDC) coated hydrogels were obtained by successive dipping of the initial TRIS/NVP/HEMA hydrogel into an ALG solution (1 mg/mL), in a PLL solution (1 mg/mL), and in an EDC solution (5% w/v), for 10 min each. EDC was added after the formation of the first ALG/PLL double layer once it diffused inside the pre-formed layer (according to the QCM-D experiments described below). This experimental procedure is represented schematically in **Figure 3.2**.

The HA(EDC)/CHI coated hydrogels were obtained by successive dipping the TRIS/NVP/HEMA hydrogel into a HA solution (1 mg/mL), in an EDC solution (5% w/v), and in a CHI solution (1 mg/mL), for 10 min each. In this case, EDC had to be added directly to HA because no diffusion could be detected by addition of EDC to the double layer (as evidenced by the QCM-D tests). Finally, the HA/PLL(EDC)+Drug coated hydrogels were prepared by successive dipping the hydrogel into a HA solution (1 mg/mL), and in a solution of PLL+EDC+Drug, for 10 min each. This ternary mixture was previously prepared by adding a PLL solution (1 mg/mL), a drug solution and an EDC solution (5% w/v), in order to attain a 30/40/30 volumetric composition. The drug solutions had the same concentrations as those employed for loading the TRIS/NVP/HEMA hydrogels. After mixing, the ternary solution was kept at 4ºC for 24 h, before being used, to allow for the formation of drug conjugated layers through the establishment of covalent bonding between the carboxyl groups of DCF and of MXF and the amino groups of PLL creating an amine link [23].

All polyelectrolytes were dissolved in DD water, except for CHI which was dissolved in aqueous solution of acetic acid 1% (v/v). The pH of the solutions was adjusted to 4.5 using acetic acid or NaOH, to enable the crosslinking with EDC. At lower values of pH EDC is known to be unstable, while for higher values, its reaction rate decreases [24].

Between each immersion step, the hydrogels were rinsed with DD water- In the three cases, the dipping procedure was repeated twice to achieve two double layers which was demonstrated in chapter 2 to be the most promising approach to achieve a controlled release. After the deposition of the multilayers, the hydrogels were reloaded in the respective drug solutions for a period of time equivalent to the total immersion time in the polyelectrolyte solutions, in order to compensate the drug release that occurred during these immersions.

Drug loaded hydrogels without any coatings were also immersed in DD water (for the same period of time that was employed for the LbL formation) and then reloaded in the drug solution (to mimic as close as possible the process undergone by the coated hydrogels).

The prepared hydrogels were immediately used for the physical characterization and the drug release tests.
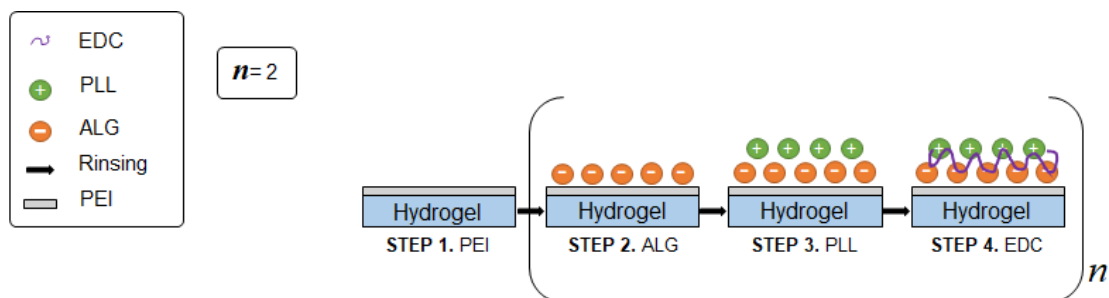
Figure 3.2 Schematic of the experimental procedure to form the ALG/PLL(EDC) coating.

3.2.5 Evaluation of the LbL formation

A quartz crystal microbalance with dissipation (QCM, E4 from Q-Sense) was used to assess the formation of the layers during the LbL deposition process. TRIS/NVP/HEMA hydrogel films were polymerized on the gold coated crystals (5 MHz), which were previously covered with a PS film, according to a previously described procedure in section 2.2.5 in chapter 2.

The experimental baseline was obtained with the TRIS/NVP/HEMA hydrogel films pre-hydrated in DD water for 5 min. The normalized frequency ($\Delta f/n$) and the dissipation (ΔD) changes for the 3rd overtone, were monitored during the entire LbL deposition process at 36°C. After the addition of each solution, a rinsing step was always performed with DD water. The stability of the films was checked by leaving the film in contact with saline NaCl solution for 48 h (results not shown). The constant values of $\Delta f/n$ and ΔD determined during this experiment confirmed that no measurable loss of polyelectrolytes occurred.

The resistance of the formed LbL coatings to the action of lysozyme (which is present in the lacrimal fluid) was checked by adding lysozyme to the top layer, followed by rinsing samples with saline NaCl solution. The interactions of the formed LbL coatings with two lachrymal proteins was tested by adding separately to the top layer a lysozyme solution (1.9 mg/mL) and a albumin solution (0.05 mg/mL) [25–30]. Eight independent experiments were done for each system.

After the experiments, the quartz crystals were cleaned by dipping for 5 s in piranha solution: H_2SO_4/H_2O_2 7/3 v:v, followed by washing in ultrasounds with a 2% (v/v) Hellmanex solution

(15 min), and in water (2 x 15 min). Finally, the crystals were rinsed with DD water, dried with nitrogen flux and stored inside closed flasks.

3.2.6 Physical characterization of the LbL coated samples

The samples coated with the most promising combination drug/LbL were characterized with respect to some of their physical properties.

Surface topography of the coated samples was assessed for the hydrated hydrogels using an AFM (Nanosurf EasyScan 2), in non-contact mode, at room temperature in a liquid cell. Images (10x10 μm^2) were obtained with Si probes (resonance frequency: 204-497 kHz) at a scan rate of 0.7 Hz. R_a of the surfaces was obtained using the WsxM 5.0 develop 8.4 software, and considering the total image area. Images of three different locations on each surface were analysed.

The thickness of the LbL coatings, was determined using an ellipsometer (UVISEL, Horiba Jobin-Yvon) in the spectral range from 300 to 750 nm at a 70º incidence angle. The thickness of the films was determined through suitable modelling using the DeltaPsi2 software package (Jobin-Yvon) with a Cauchy dispersion distribution.

The wettability of the hydrated uncoated and coated hydrogels was determined by the captive bubble method following the experimental protocol presented in chapter 2, section 2.2.6.3. A video camera (jAi CV-A50, Spain) mounted on a microscope Wild M3Z (Leica Microsystems, Germany), was used to acquire the images which were analysed with ADSA software (Axisymmetric Drop Shape Analysis, Applied Surface Thermodynamics Research Associates, Toronto, Canada).

The transmittance of the coated samples was determined with a UV-Vis spectrophotometer (Multiskan GO, Thermo Scientific). The wavelength interval of 200 to 700 nm was scanned with 1 nm intervals. The presented values are averages of three independent measurements.

The refractive index was measured using an ABBE 60 Refractometer (Bellingham+Stanley), at a wavelength of 589.3 nm (Sodium lamp) and with controlled temperature (37ºC).

The ionic permeability of the hydrated hydrogels (12 mm diameter) was measured in a Lab-made cell described in section 1.1.4.2.5, chapter 1. The experiments were done in triplicate, at 36ºC. The conductivity, in µS/cm, was measured every hour, for at least ten hours, using a conductivity meter (HI2003 edge$^{EC®}$ from HANNA instruments). The conductivity data were converted into NaCl concentrations taking into account data previously obtained from a calibration curve. D_{ion} was calculated with **Equation 1.4**, referred in chapter 1.

3.2.7 HET-CAM test

The HET-CAM test was carried according to the recommended protocol described by the Interagency Coordinating Committee on the Validation of Alternative Methods (ICCVAM). Fertilized hen´s eggs (Coren, Spain) were incubated at 37±0.5ºC with 60±3% relative humidity (RH) for 8 days. The eggs were manually rotated 180º three times a day for the duration of the incubation, on the 9th day the eggs were cut on the airspace using a rotary saw (Dremel 300, Breda). After the removal of the egg shell, the inner membrane was hydrated with a 0.9% NaCl solution for 30 min. The inner membrane was carefully removed to expose the CAM. Drug loaded and unloaded hydrogels, both with and without the most promising coating, were directly placed on the CAM, and a timer was started. The experiments were carried out in triplicate. NaCl (0.9%) and NaOH (1 M) solutions (300 µL) were used as negative and positive controls, respectively. The process was documented for a 5 min period to analyse any lysis, haemorrhaging and coagulation occurring in the CAM through calculation of the IS, using **Equation 1.6** presented in chapter 1.

3.2.8 Antibacterial assays

The antibacterial activity of the most promising coating was tested against *P. aeruginosa* (ATCC 15442) and *S. aureus* (ATCC 25923) by turbidimetry in MHB.

Briefly, strains were stocked in glycerol (20% v/v) at -80ºC. Working cultures were grown on MHA and maintained at 4ºC. Overnight cultures (16 h at 37ºC) were used to do the test. The density of the inoculum was adjusted to the turbidity of 0.5 McFarland (1.5×10^8 bacteria/mL) and 1 McFarland (3×10^8 bacteria/mL) for *P. aeruginosa* and *S. aureus*, respectively.

Coated and uncoated samples, with and without drug, were tested. Each sample was placed in a well, subsequently filled with 10 µL of bacteria suspension diluted in 500 µL of MHB. As positive control was used MHB inoculated with the respective tested microorganism, while as negative control was used only MHB. The microplates were incubated in a shaker incubator at 37ºC during 24 h.

After 24 h, a homogenized volume of 200 µL was taken from each well and placed in a 96-well plate. The optical density was measured at wavelength of 630 nm using a microplate reader (Platos R 496). All the procedures were carried out under aseptic conditions. For each assay, four measurements were carried out.

3.2.9 Statistical analysis

Statistical analysis was carried out using the R Project software v. 3.5.1. Data are presented as mean ± standard deviation. Student's t-test and one-way ANOVA test were applied to determine whether the difference of the means of two or more groups, respectively, were significant. The normality of the data was checked using Shapiro-Wilk test. The level of significance chosen was always 0.05.

3.3   Results

3.3.1 Evaluation of the LbL formation

The formation of the layers during the LbL deposition process was followed by the QCM-D, which shows the time course of $\Delta f/n$ and ΔD upon the contact of the TRIS/NVP/HEMA-coated quartz crystals with the different polyelectrolyte solutions that were employed to form the ALG/PLL(EDC) (**Figure 3.3**), HA(EDC)/CHI (**Figure 3.4**) and HA/PLL(EDC)+Drug (**Figure 3.5**) LbL coated hydrogels. **Figures 3.3** to **3.5** report the data obtained in two similar experiments which only differ in the final step where lysozyme or albumin solutions were added (**A** and **B**, in each figure, respectively), to check the effects on the coating of these two proteins which are known to be present in the tear fluid. The baseline corresponds to the hydrogel coated crystal equilibrated in DD water. In **Figure 3.3**, after the PEI injection, the

ALG, PLL and EDC solution were sequentially introduced, ending with a DCF solution which was used for reloading the hydrogels samples during the same time that the samples remained immersed in aqueous solutions for the coating process, as explained in section 3.2.5. The rinsing steps performed after each coating step led to shifts in frequency and dissipation, which indicate the removal of the loosely bound molecules. However, the layers seemed to remain stable after these rinsing steps. The addition of lysozyme (**Figure 3.3A**) and albumin (**Figure 3.3B**) led to different effects: lysozyme removed part of the upper layers as demonstrated by the significant increase in frequency; albumin adsorbed to the surface, according to the observed decrease in frequency and increase in dissipation. Similar behaviours were observed with the two other coatings (**Figure 3.4** and **3.5**), with the exception of the HA(EDC)/CHI, where the addition of albumin (**Figure 3.4B**) led to an increment in frequency which is consistent with the partial removal of the top layer instead of albumin adsorption.

In order to improve the resistance of the coatings to the action of the tear proteins, while keeping the antibacterial properties, a final layer of HA was deposited on top of the ALG/PLL(EDC) coating leading to the ALG/PLL(EDC)//HA coating. The time course of $\Delta f/n$ and ΔD during the formation of the two double layers of ALG/PLL(EDC) topped with HA, and subsequent addition of lysozyme or albumin solutions is presented in **Figure 3.6A** and **B**. The HA layer demonstrated to be resistant to the addition of lysozyme while albumin just lead to a very small frequency decrease due to its adsorption.

A
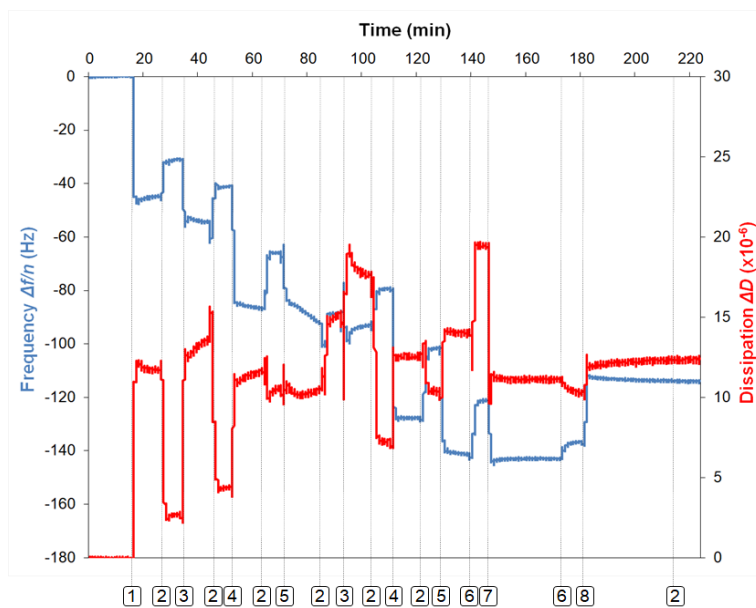
B
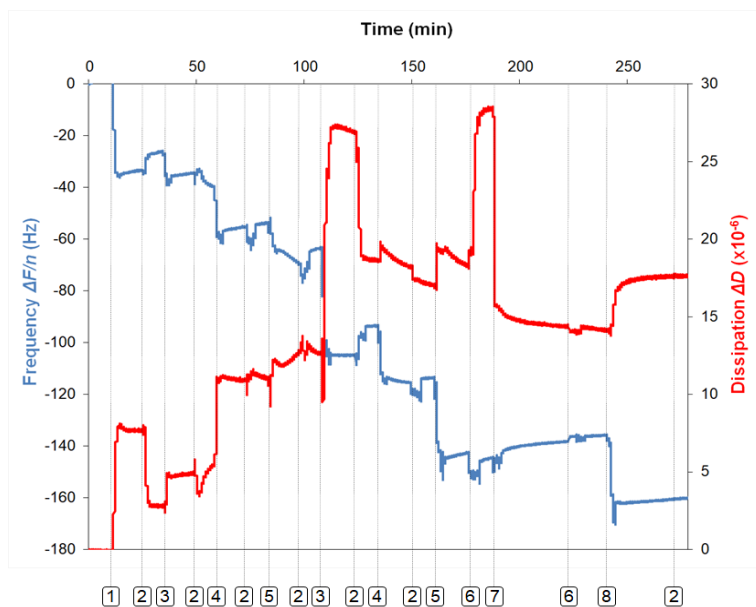
Figure 3.3 Normalized shift in the frequency, $\Delta f/n$ (blue line, left y-axis) and shift in the dissipation ΔD (red line, right y-axis) for the third harmonic of the resonant frequency of a quartz crystal sensor after being coated with a TRIS/NVP/HEMA hydrogel film, during successive additions of PEI (1), ALG (3), PLL (4) and EDC (5), as a function of time, to form two double layers of ALG/PLL(EDC) coating. The final steps correspond to the addition of DCF (7) and of the lachrymal protein solutions (8) of **(A)** lysozyme and **(B)** albumin, respectively. The successive additions are separated by rinsing with DD water (2) except after final EDC and of DCF addition where rinsing was done with NaCl (6) solution.

A
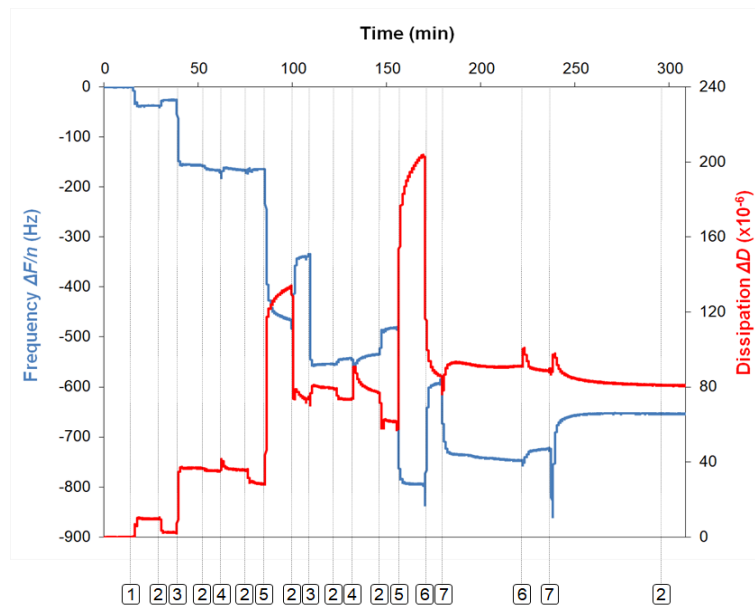
B
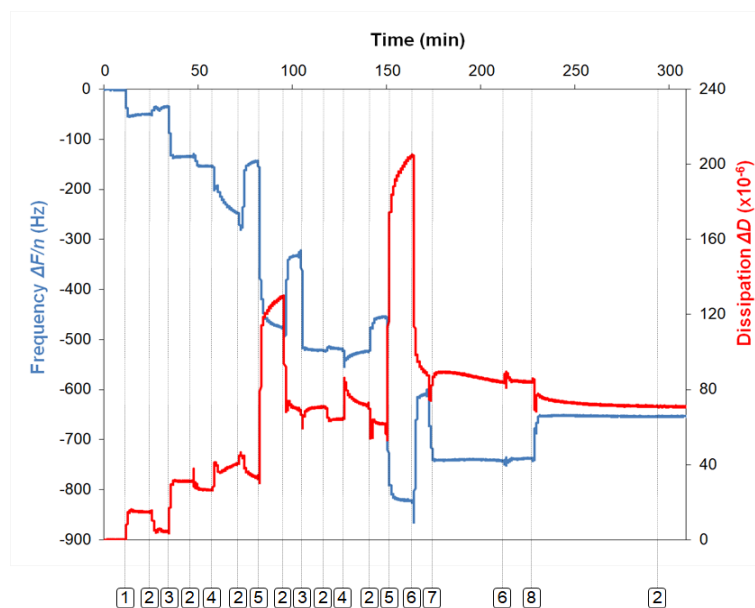
Figure 3.4 Normalized shift in the frequency, $\Delta f/n$ (blue line, left y-axis) and shift in the dissipation ΔD (red line, right y-axis) for the third harmonic of the resonant frequency of a quartz crystal sensor after being coated with a TRIS/NVP/HEMA hydrogel film, during successive additions of PEI (1), HA (3), EDC (4) and CHI (5), as a function of time, to form two double layers of HA(EDC)/CHI coating. The final steps correspond to the addition of DCF (7) and of the lachrymal protein solutions (8) of **(A)** lysozyme and **(B)** albumin, respectively. The successive additions are separated by rinsing with DD water (2) except after final EDC injection and of DCF addition where rinsing was done with NaCl (6) solution.

91

A
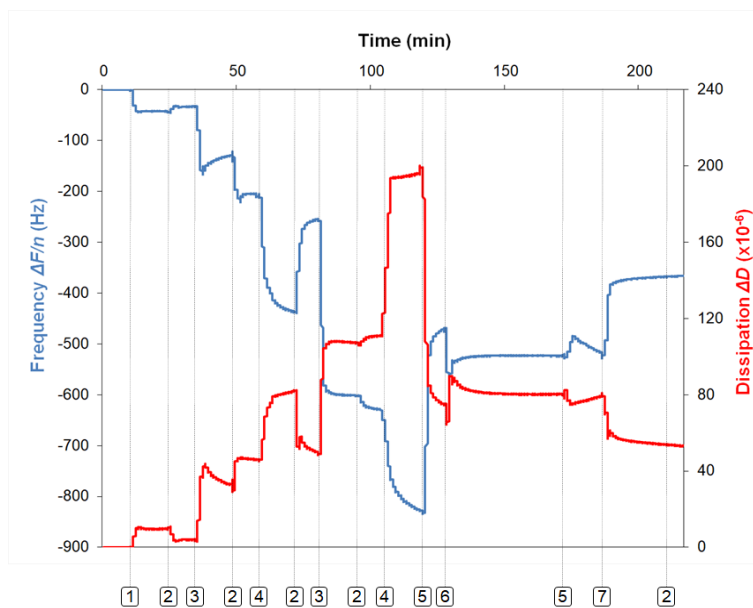
B
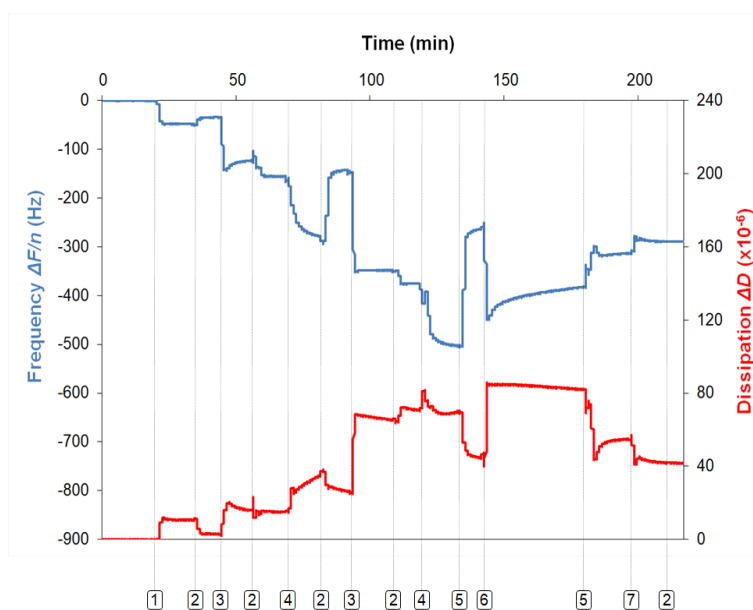
Figure 3.5 Normalized shift in the frequency, $\Delta f/n$ (blue line, left y-axis) and shift in the dissipation ΔD (red line, right y-axis) for the third harmonic of the resonant frequency of a quartz crystal sensor after being coated with a TRIS/NVP/HEMA hydrogel film, during successive additions of PEI (1), HA (3), PLL(EDC)+DCF (4), as a function of time, to form two double layers of HA/PLL(EDC)+DCF coating. The final steps correspond to the addition of DCF (6) and of the lachrymal protein solutions (7) of **(A)** lysozyme and **(B)** albumin, respectively. The successive additions are separated by rinsing with DD water (2) except after final EDC and of DCF addition where rinsing was done with 0.9% (w/v) NaCl (5) solution.

EDC (4) and CHI (5), as a function of time, to form two double layers of HA(EDC)/CHI coating.

A

B

Figure 3.6 Normalized shift in the frequency, $\Delta f/n$ (blue line, left y-axis) and shift in the dissipation ΔD (red line, right y-axis) for the third harmonic of the resonant frequency of a quartz crystal sensor after being coated with a TRIS/NVP/HEMA hydrogel film, during successive additions of PEI (1), ALG (3), PLL (4), EDC (5) and HA (6), as a function of time,

to form two double layers of ALG/PLL(EDC)//HA coating. The final steps correspond to the addition of DCF (8) and of the lachrymal protein solutions of (9) **(A)** lysozyme and **(B)** albumin, respectively. The successive additions are separated by rinsing with DD water (2) except after final EDC and of DCF addition where rinsing was done with NaCl (7) solution.

3.3.2 Drug release profiles of LbL coated ophthalmic hydrogels

The release profiles with TRIS/NVP/HEMA samples coated with two double layers of the three coatings ALG/PLL(EDC), HA(EDC)/CHI and HA/PLL(EDC)+Drug are shown in **Figure 3.7**, **3.8** and **3.9**, for DCF, MXF and CHX, respectively. In the case of DCF, the release profile obtained with the coating ALG/PLL(EDC)//HA is also included.
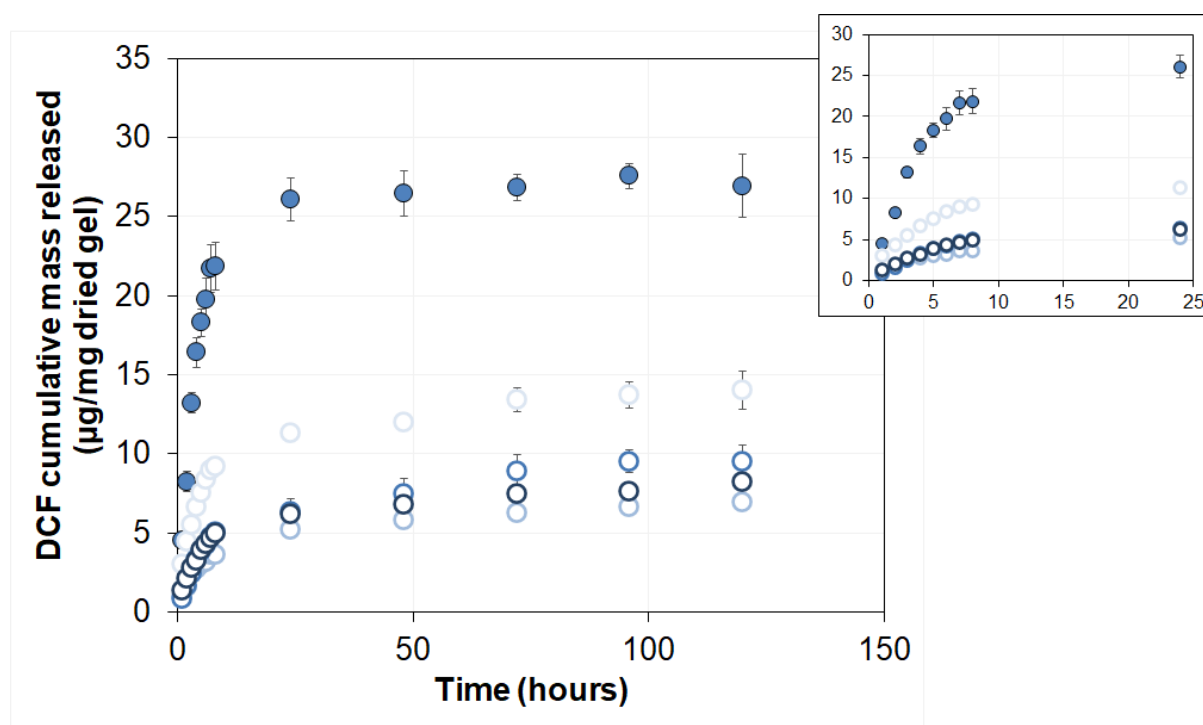
Figure 3.7 DCF release profiles from uncoated (●), ALG/PLL(EDC) (○), HA(EDC)/CHI (○) and HA/PLL(EDC)+Drug (○) coated TRIS/NVP/HEMA hydrogels. The DCF release profile obtained with ALG/PLL(EDC)//HA coated TRIS/NVP/HEMA hydrogels is also included (○). The inserts represent the first 24 h of the release data. The error bars are the ± standard deviations (n=8).
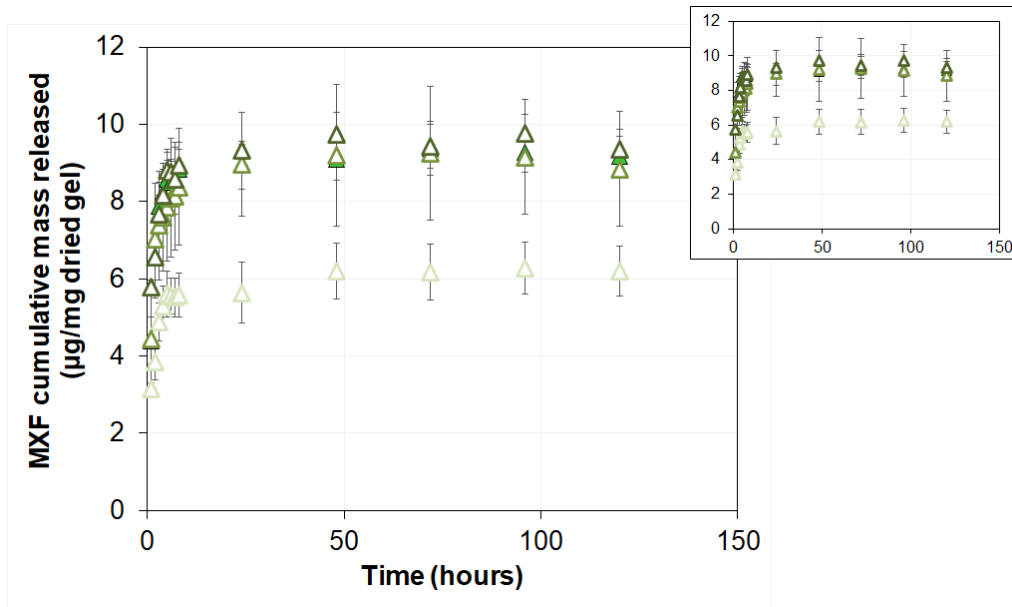
Figure 3.8 MXF release profiles from uncoated (▲), ALG/PLL(EDC) (△), HA(EDC)/CHI (△) and HA/PLL(EDC)+MXF (△) coated TRIS/NVP/HEMA hydrogels. The inserts represent the first 24 h of the release data. The error bars are the ± standard deviations (n=8).
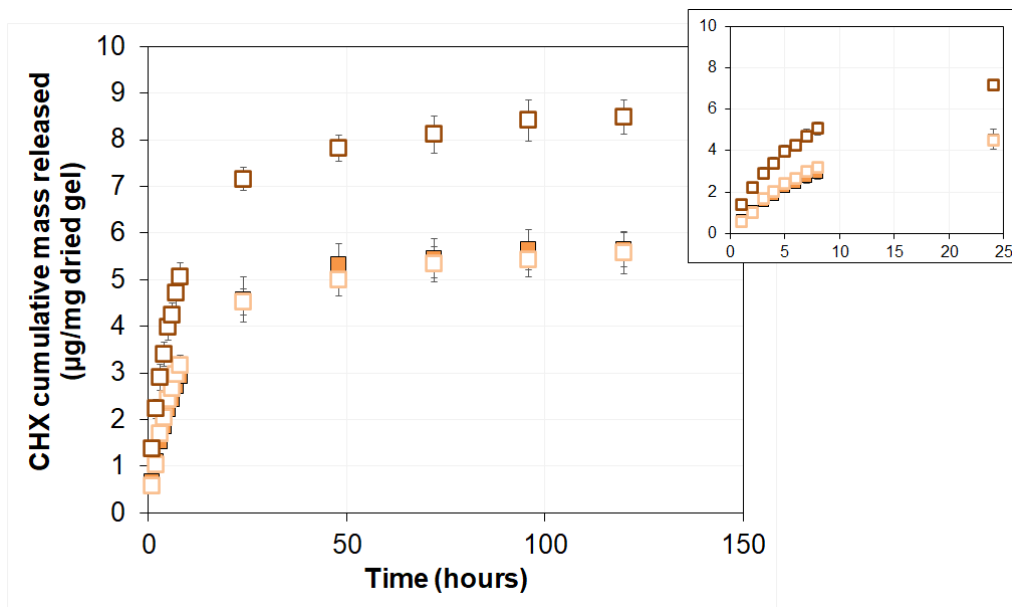
Figure 3.9 CHX release profiles from uncoated (■), ALG/PLL(EDC) (□), and HA(EDC)/CHI (□) coated TRIS/NVP/HEMA hydrogels. The inserts represent the first 24 h of the release data. The error bars are the ± standard deviations (n=8).

The results show that coatings composed of two double layers of ALG/PLL(EDC), HA(EDC)/CHI, and HA/PLL(EDC)+Drug deposited on TRIS/NVP/HEMA hydrogel samples led to the sustained release of DCF but could not control the release of MXF and CHX. Furthermore, adding a top layer of HA to the ALG/PLL(EDC) to form ALG/PLL(EDC)//HA coating decreased the amount of released DCF (p≈0) as well as the release rate, as demonstrated in **Figure 3.10**.
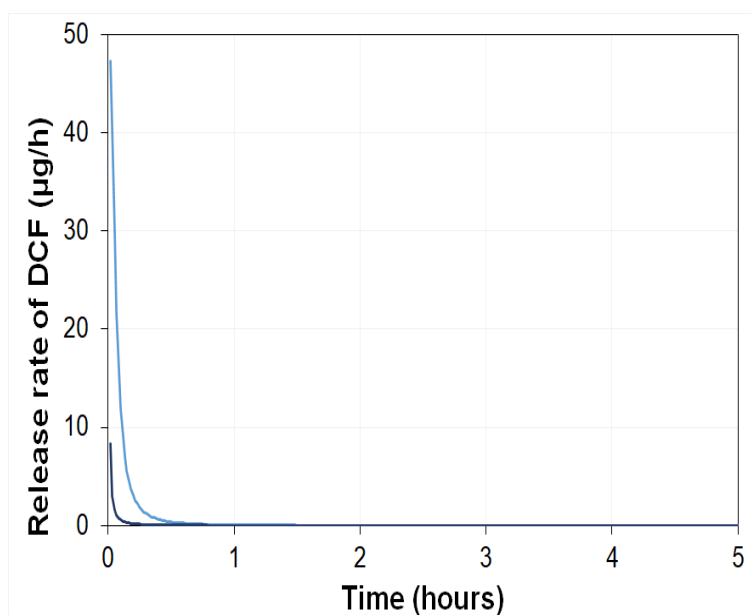
Figure 3.10 Comparison of the DCF release rates obtained with uncoated (light blue) and ALG/PLL(EDC)//HA coated (dark blue) TRIS/NVP/HEMA hydrogels.

In order to further understand the influence of the coating on the release of DCF, comparison of the amount of DCF loaded in the uncoated and the coated hydrogels (**Table 3.1**) with the amount of drug released by the corresponding hydrogels (**Figure 3.7**) was carried out. For the coating HA/PLL(EDC)+Drug, the amount of drug conjugated in the coating was determined by extracting the unloaded coated sample, and the value 3.4±0.4 µg/mg of dry gel was obtained, which represents 10% of the total amount of drug loaded.

Analysis of **Table 3.1** shows that the amount of DCF lost during the LbL deposition was not totally recovered by the reloading step. Furthermore, comparison of the amount of DCF loaded (with reloading) with the amount release demonstrates that a high percentage of drug remained

inside the polymeric matrix, varying from 48% for the uncoated hydrogel up to 84% for the HA(EDC)/CHI coated sample.

Table 3.1 Amount of DCF loaded with and without reloading, and in TRIS/NVP/HEMA hydrogels after the loading process. The errors are the ± standard deviations (n=3).

Coating	TRIS/NVP/HEMA hydrogels after LbL process	
	Amount of loaded DCF without reloading (μg/mg dried gel)	Amount of loaded DCF with reloading (μg/mg dried gel)
Uncoated	38±2	52±5
ALG/PLL(EDC)	29±2	42±6
HA(EDC)/CHI	32.7±0.7	43±2
HA/PLL(EDC)+DCF	35±3	35±4
ALG/PLL(EDC)//HA	25±4	37±10

3.3.3 Physical characterization of LbL coated ophthalmic hydrogels loaded with DCF

The LbL coated hydrogels loaded with DCF, which are the most promising systems due to the observed sustained drug release, were further characterized with respect to some of their physical properties. The wettability of the coated and uncoated samples, drug-loaded and unloaded, is compared in **Figure 3.11**. In spite of the hydrophobicity of the trimethysiloxy groups present in the TRIS monomer, the water contact angle of the uncoated

TRIS/NVP/HEMA sample is low due to the arrangement of the hydrophilic groups of HEMA and NVP in response to the polar environment [20]. The loaded drug seems to have a minor effect on the obtained contact angles (no statistical difference). However, the presence of DCF-PLL conjugate in the top layer of the HA/PLL(EDC)+DCF coating increased the contact angle ($p < 0.016$). The coating ALG/PLL(EDC) improved the wettability ($p < 0.039$), while the coating HA(EDC)/CHI had almost no effect in this property (no statistical difference). The addition of HA to ALG/PLL(EDC) to form ALG/PLL(EDC)//HA on the loaded samples led to the lowest contact angle values ($p < 0.0005$).
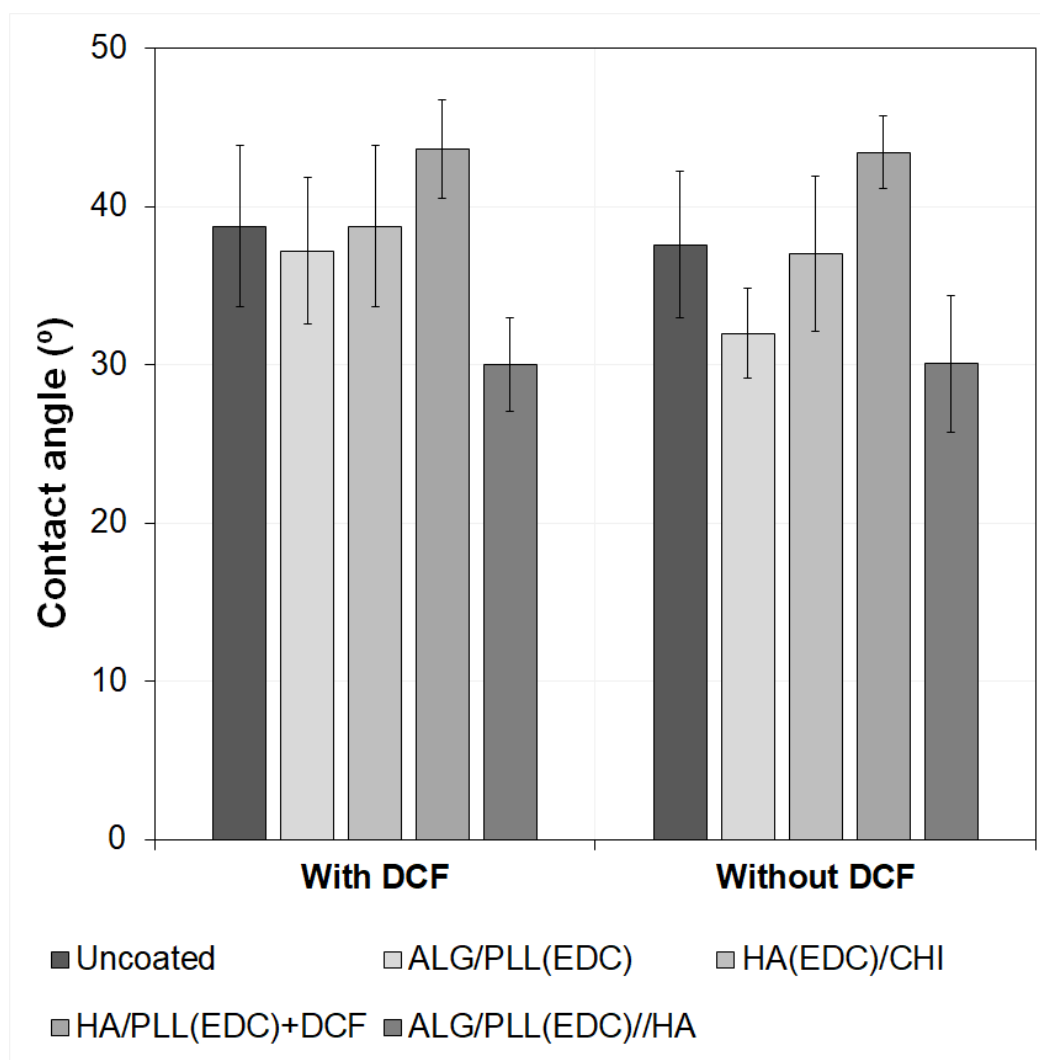
Figure 3.11 Water contact angles on the uncoated and coated hydrogels, without and with DCF. The error bars correspond to the ± standard deviations (n = 10).

The transmittance of the uncoated and coated hydrogels, in the absence and in the presence of DCF, is shown in **Figure 3.12A** and **B**, respectively.

The main differences occur in the UV (Ultraviolet light) range, where the presence of DCF in the loaded samples and even in the coating HA/PLL(EDC)+DCF of the unloaded sample reduces the transmittance to almost zero. The small peak at 276 nm in **Figure3.12A** may be attributed to DCF trapped in this trapped in this coating [31]. In the visible region, only the transmittance of the sample loaded with DCF and coated with ALG/PLL(EDC) is reduced (p = 0.00007), but remains above 90%, the minimum required for contact lenses [32].

A
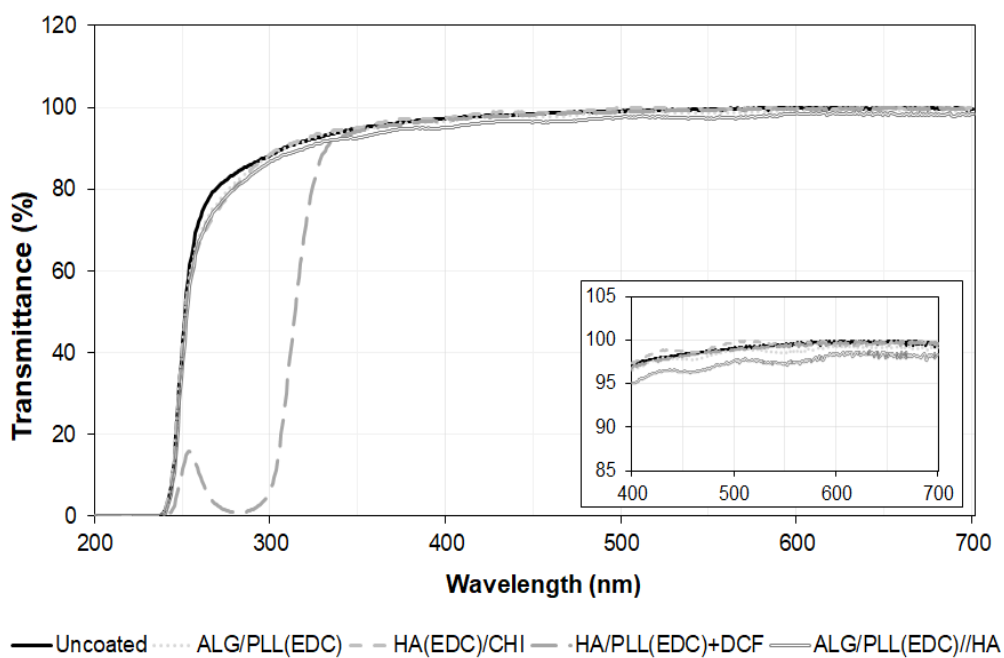
B
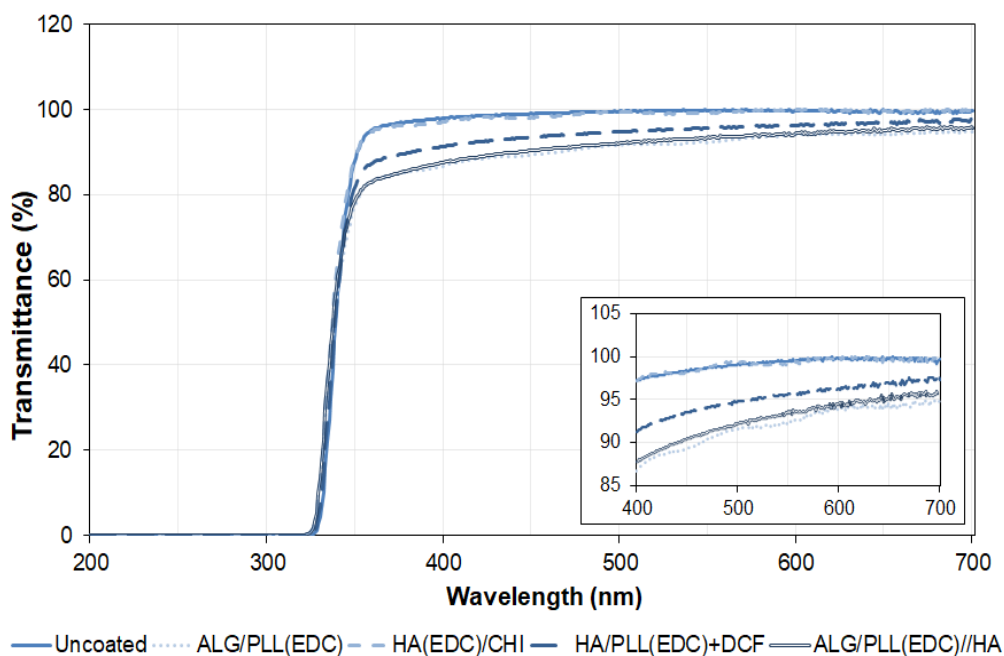
Figure 3.12 Transmittance of both uncoated and coated samples, without (**A**) and with (**B**) DCF.

The AFM images of the LbL coated hydrogels are presented in **Figure 3.13A-D**. The porous structure, which is typical of the TRIS/NVP/HEMA hydrogels [33], is hidden by the deposited coatings.

A

B

C

D
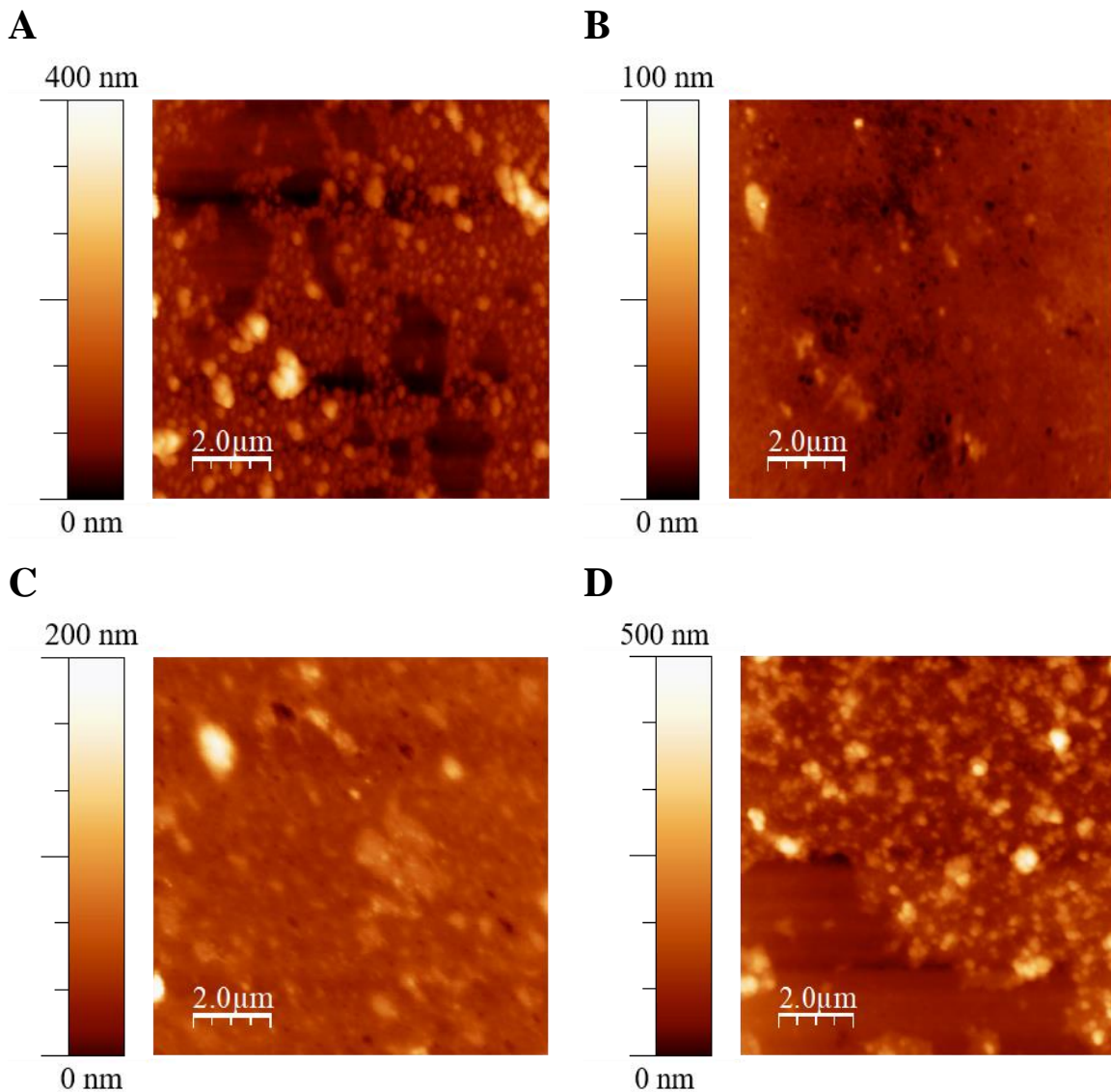
Figure 3.13 AFM images (10 x 10 μm^2) of the surface of TRIS/NVP/HEMA samples coated with ALG/PLL(EDC) **(A)**, HA(EDC)/CHI **(B)**, HA/PLL(EDC)+DCF **(C)** and ALG/PLL(EDC)//HA **(D)**.

The coatings based on ALG/PLL(EDC), with and without the top layer HA, exhibit grainy surfaces which are rougher than the underlying hydrogel surface, as demonstrated by the values of the R_a, presented in **Table 3.2**. In contrast, the HA(EDC)/CHI and the HA/PLL(EDC)+DCF coatings are more homogeneous than the former ones and even smoother than the underlying surface of TRIS/NVP/HEMA hydrogel.

Table 3.2 Properties of uncoated and coated samples loaded with DCF: R_a, coating thickness, refractive index and ionic permeability. The errors are the $\pm$ standard deviations (in all cases n=4, except for thickness n=2).

	Uncoated	ALG/PLL (EDC)	HA(EDC) /CHI	HA/PLL(EDC) +DCF	ALG/PLL (EDC)//HA
R_a (nm)	20±9	28±4	5±1	9±4	38±2
Coating thickness (nm)	-	60±9	-	90±5	69±11
Refractive index	1.417±0.002	1.411±0.003	1.418±0.001	1.419±0.002	1.417±0.002
Ionic permeability x10^{-7}(cm^2/s)	5±0.2	4±0.1	5±0.5	3±0.1	4±0.4

The thickness of the coatings, determined by ellipsometry, are also presented in **Table 3.2**. These thicknesses are of the same order of magnitude of those measured in chapter 2 for the coating (ALG-CaCl$_2$)/(CHI+GL). However, in the case of the coating HA(EDC)/CHI, it was not possible to get a reliable value for the thickness because the signal to noise ratio was always extremely low. To further study these coatings, we used the software Q-sense Dfind (Broad Fit) for viscoelastic modelling of the data obtained in QCM-D measurements. The density of

the coatings ALG/PLL(EDC), HA/PLL(EDC)+DCF and ALG/PLL(EDC)//HA was estimated to be of 1 g/cm^3, assuming the values obtained in the ellipsometric measurements for the thickness. This density is consistent with the values found for other LbL nanofilms composes of polypeptides, polysaccharides, and/or synthetic polymers [34]. In the case of the coating HA(EDC)/CHI, since the thickness was not known, we assumed the same density (1 g/cm^3) and estimated a thickness of 150 nm. This high value of the thickness, together with the irreproducible results from ellipsometry, led to the necessity to investigate further the characteristics of this coating. The thickness of one single layer HA(EDC)/CHI was successfully measured with the ellipsometer to be ≈15 nm, which should imply a double layer around 30 nm, quite different from the 150 nm value, estimated by the Q-Sense software. This value could only be reproduced if the density was increased to 5 g/cm^3 which is not realistic value. Anyway, it seems that the layers of the HA(EDC)/CHI coating have a peculiar molecular arrangement which may also be reflected in its low R_a value.

The refraction indexes of the hydrogels presented in **Table 3.2** do not show any significant effect related to the presence of the coatings.

The obtained ionic permeabilities decreased with the presence of the coatings (p = 0.048), except for HA(EDC)/CHI, but in all cases they remained quite above the required minimum value (1.067 x 10^{-9} cm^2/s) for proper contact lens movement [35].

3.3.4 HET-CAM results

Images of CAM after 5 min exposure to uncoated and ALG/PLL(EDC)//HA coated sample, loaded with DCF and unloaded, show no visual response, similarly to what was observed for the negative control behaviour (**Figure 3.14A-E**), with IS = 0. In contrast, addition of NaOH (1 M) (positive control) led to severe irritation and almost instant haemorrhage that aggravated with time (**Figure 3.14F**).
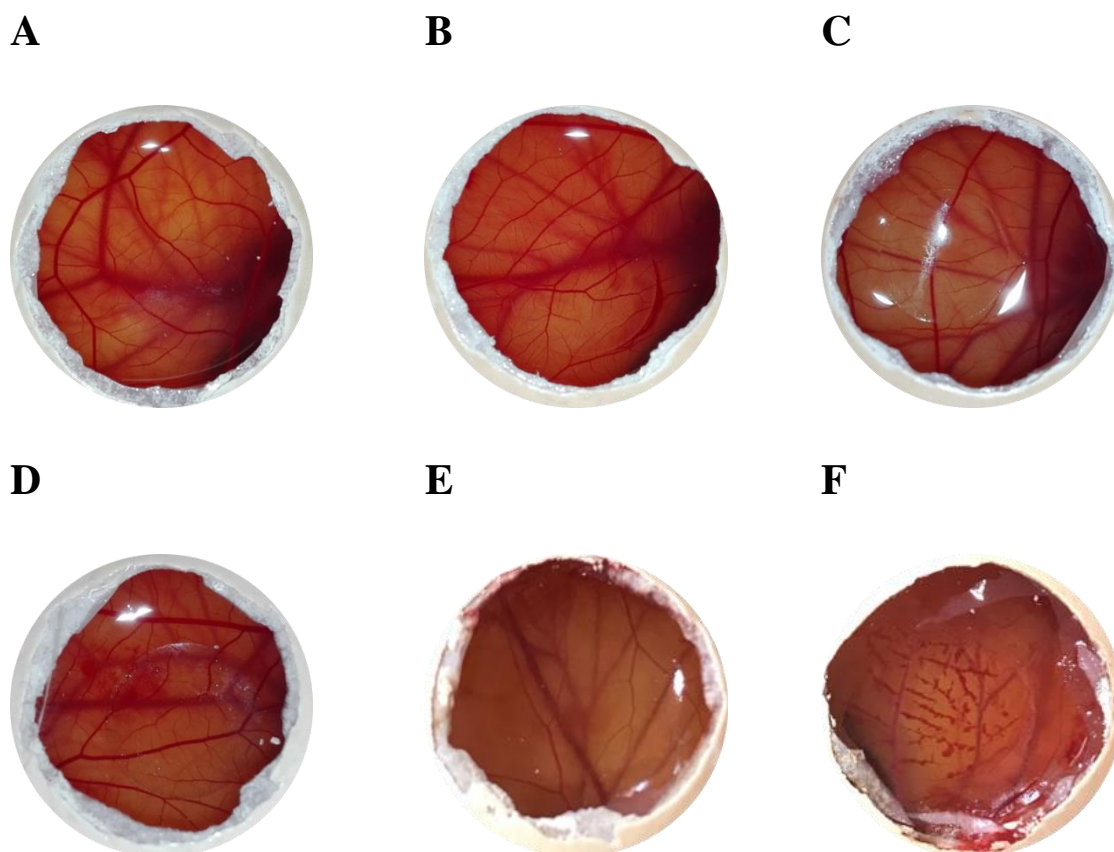
Figure 3.14 CAM images after 5 min contact with: uncoated samples loaded with DCF **(A)** and unloaded **(B)**; ALG/PLL(EDC)//HA coated samples loaded with DCF **(C)** and unloaded **(D)**; negative control **(E)** and positive control **(F)**.

3.3.5 Microbiological tests

The antibacterial activity of the coating ALG/PLL(EDC)//HA was assessed through the comparison of the behaviour of the coated and uncoated samples, loaded and unloaded with DCF. **Figure 3.15** shows the relative values for the optical densities of the incubation solutions containing *P. aeruginosa* and *S. aureus* obtained after 24 h of contact with the samples. In the case of the uncoated samples, loading with DCF almost did not affect the growth inhibition of both bacteria (no statistical difference).

Coating the unloaded samples led to an inhibition in the growth of both bacteria ($p < 0.009$), which gives evidence to the antimicrobial activity of HA (final top layer of the coating). The

association of the coating with the drug led to a slight increase of the bacterial growth inhibition ($p < 0.00003$), being more significant for *S. aureus*.
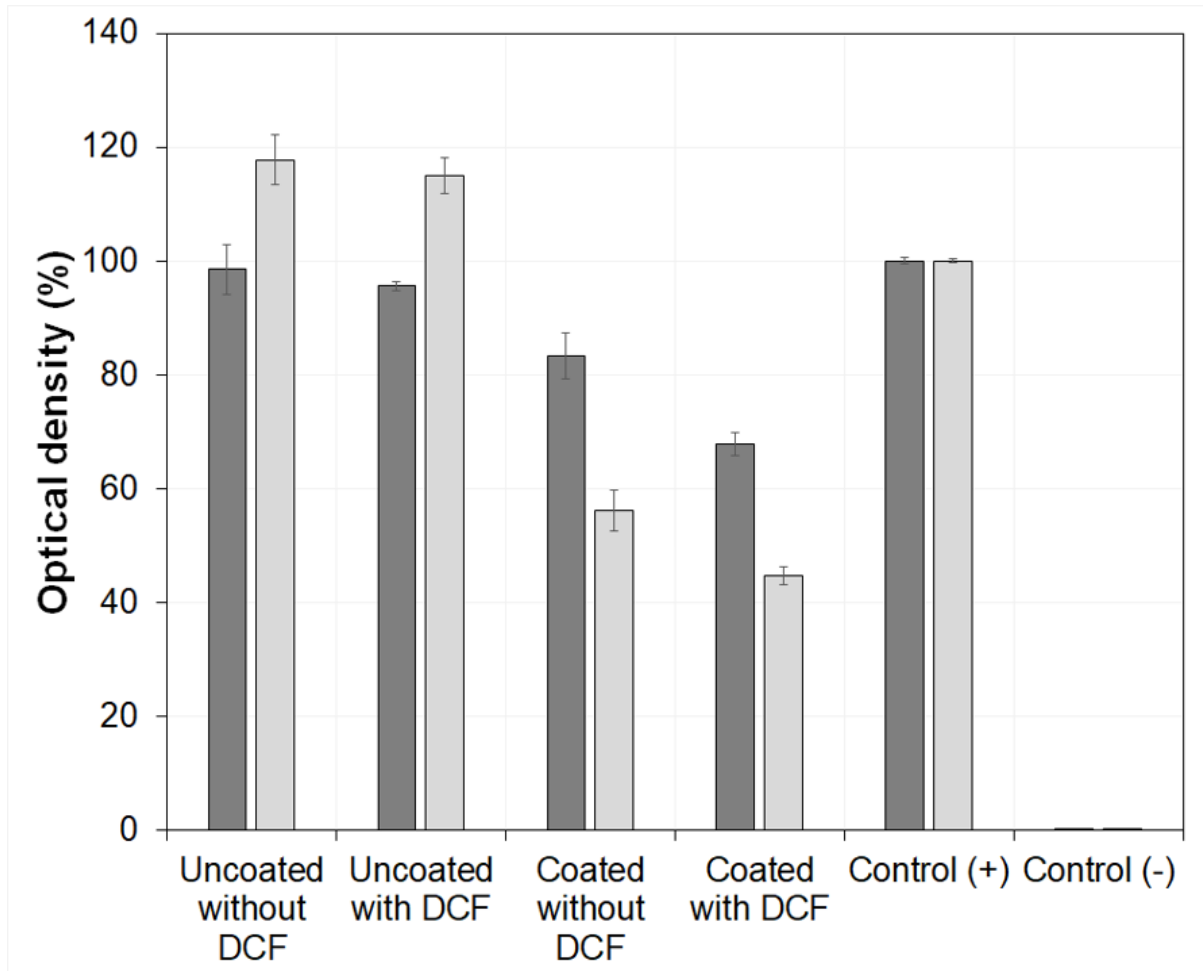
Figure 3.15 Relative values of the optical density of the incubation solutions containing *P. aeruginosa* (■) and *S. aureus* (□), after contacting with uncoated and ALG/PLL(EDC)//HA coated hydrogels, with and without DCF. The errors are the ± standard deviations (n=4).

3.4   Discussion

In the present work, LbL coatings were prepared using polyelectrolytes with antibacterial properties with the objective of combining drug release control with resistance to tear proteins and reduction of bacterial growth.

The results show that coatings composed of two double layers of ALG/PLL(EDC), HA(EDC)/CHI and HA/PLL(EDC)+Drug deposited on TRIS/NVP/HEMA hydrogel samples led to a sustained release of DCF, but could not control the release of MXF (**Figure 3.8**) and CHX (**Figure 3.9**). However, these coatings were disturbed by the presence of albumin and lysozyme, two of the most common proteins in the tear fluid, which, respectively, adsorbed and partially remove the top layers. A successful attempt to solve this problem was made through the deposition of a final layer of HA on top of the ALG/PLL(EDC) coating, giving rise to the optimized coating ALG/PLL(EDC)//HA (**Figure 3.6**) which resisted to the action of the tear proteins. The choice of ALG/PLL(EDC), among the three studied coatings, was based on the fact that this coating allowed a maximum amount of drug release (see **Figure 3.7**).

In general, the control of the drug release rates by the LbL coatings may be of steric origin and/or result from reversible interactions between the drugs and the polyelectrolytes. Among the studied drugs, DCF is the smallest molecule which means that the retardations effect felt by these molecules when crossing the surface layer during the release process was not expected to have steric origin. DCF is negatively charged at neutral pH and amphiphilic [36]. Thus, the interactions of DCF with the positively charged polyelectrolytes (PLL and CHI) may have an electrostatic nature at neutral pH. Several authors considered that in the case of CHI, besides electrostatic interactions, DCF may be physically entrapped by the CHI chains [37,38]. The interactions between PLL and DCF may result from electrostatic attractions and/or may have a hydrophobic nature. Hsu *et al.* (2014) claimed that PLL based films may be considered as moderately hydrophobic due to its reduced swelling in aqueous solutions which justifies preferential interaction with the slightly hydrophobic DCF. Furthermore, the presence of non-reacted EDC may lead to activation of the carboxylic groups of DCF favouring their reaction with the amine groups of PLL which were not involved in the reaction with the carboxylic groups of ALG. A similar interaction may exist between the carboxyl groups of DCF with the hydroxyl groups of ALG (in the presence of EDC) to form esters which will easily hydrolyse. A particular strong shielding effect is demonstrated by HA. In fact, addition of a single HA layer to the ALG/PLL(EDC) greatly reduced both the release rate and the amount of released DCF. Hydrogen bonding between the three H bond acceptors in DCF and the hydroxyl groups in HA may be responsible for this behaviour. On the other hand, Schneider *et al.* (2008) suggested a possible association of DCF with hydrophobic domains of HA [39]. These regions exist within the tridimensional structure of HA which is stabilized by hydrogen bonds. Thus,

the specific efficiency of the HA layers in the retardation of DCF release may be attributed to the formation of DCF-HA complexes.

The release rates of MXF and CHX were not reduced by the LbL coatings which may be justified by the weak interactions established with the polyelectrolytes. The carboxylic group in MXF may be involved in intramolecular H-bonding which makes it less accessible to coupling with the amine groups of PLL or the hydroxyl groups of ALG. CHX is a large molecule with two terminal Cl atoms which cannot ensure strong H-bonds with hydroxyl groups of the polyelectrolytes. Both drugs are hydrophilic ruling out the presence of hydrophobic interactions. Furthermore, the process of physical entrapment of the drug mentioned above for DCF [37] may be impossible for the larger molecules of MXF and CHX if they do not fit inside the free spaces of CHI hydrogen-bond network. The HA(EDC)/CHI coated hydrogels released a higher amount of CHX at a higher rate than the ALG/PLL(EDC) coated hydrogel and even the uncoated sample. As the molecular weights of HA and CHI are much higher than those of ALG and PLL, the chains of the former electrolytes should be less well-packed than those of the latter ones, leading to a lower density film. Thus, this film would be able to absorb a significant amount of CHX during the reloading step and to release it rapidly in the saline solution.

Some physical properties of the LbL coated hydrogels loaded with DCF which are relevant for the application of these materials in the production of SCLs were assessed.

The wettability of the samples was not significantly modified by the coatings and kept values within the range reported in the literature for commercial contact lenses [40]. The lowest contact angle was achieved through the addition of HA to the coating ALG/PLL(EDC) which results from the higher hydrophilicity of HA compared to that of PLL [41,42]. Kolansinska and Warszynski suggested that the lower contact angle of HA may be associated to the higher electric charge density of the polyanionic layer, together with the more favourable orientation of water molecules at this negatively charged layer [41].

The transmittance in the visible region and the refraction index of the samples were almost not affected by the presence of the coatings, keeping adequate values in all cases.

The topography of the samples assessed by AFM analysis varies according to the type of coating. The coatings ALG/PLL(EDC) and ALG/PLL(EDC)//HA are rougher than the

underlying surface, while HA(EDC)/CHI and HA/PLL(EDC)+DCF are smoother. Furthermore, the formed two coatings present grainy surfaces. Other authors found globular structures during deposition of the first layers of LbL assemblies involving polyelectrolyte pairs composed of at least one polypeptide or polysaccharide [43,44]. The globules were formed due to the diffusion and/or chain re-arrangement of one of the polyelectrolytes in and out of the film/air interface, which is typical of the exponential growth behaviour of that type of multilayers. However, in the presence of a crosslinking agent, this phenomenon was hindered and the globular structures were not formed [45]. Thus, the existence of grains on the surface of the ALG/PLL(EDC) and ALG/PLL(EDC)//HA coatings may result from a less efficient crosslinking process when EDC is added on top of PLL which still allows some diffusion and re-arrangement of the PLL chains. In the case of HA(EDC)/CHI the direct addition of EDC to HA enhances the crosslinking process leading to the smoothest surface. In the coating HA/PLL(EDC)+DCF, the conjugated PLL+DCF should make the diffusion/re-arrangement of PLL more difficult, thus avoiding the formation of globules.

Finally, the microbiological tests indicated that the presence of DCF in the uncoated samples reduced the growth of *S. aureus* and *P. aeruginosa* in the incubation solutions, which is in agreement with the antibacterial activity of DCF against both Gram-positive and Gram-negative species [46–49]. Coating the unloaded samples with ALG/PLL(EDC)//HA led to a similar effect. This behaviour was expected, according to the reports in literature [50], although, as referred earlier, the true antibacterial activity of HA is still a controversial issue [8]. Combining the ALG/PLL(EDC)//HA coating with DCF loading showed a synergistic effect, enhancing the bacterial growth inhibition.

Overall, the results of the release studies together with the physical characterization of the samples indicate that the coating ALG/PLL(EDC)//HA offers the best conditions to be used as a barrier to the release of DCF and, resists to the action of albumin and lysozyme. In addition, this coating increases bacterial growth inhibition and does not induce any signs of ocular irritation.

To predict the impact in the patient treatment of the DCF delivery by a contact lens made of the studied silicone-based hydrogel coated with ALG/PLL(EDC)//HA, it is necessary to estimate the drug concentration in the tear fluid using a simple mathematical model described

in [35]. According to this model, the drug concentration in the tear fluid at a given time t (in min) after lens applications may be calculated by the following equation:

$$[DRUG]_t = \frac{M_d}{V_{tear}} + (1 - r)[DRUG]_{t-1}$$

Equation 3.1

where M_d is the amount of drug delivered by a drug loaded, commercial sized lens to the lachrymal fluid during a given time interval, V_{tear} is the average tear volume in the eye $\approx 7\ \mu L$ at each instant, and r is the volume fraction of renovated fluid in each minute ≈ 0.17. The mass of the dry contact lens made of the hydrogel under study with diameter of 14 mm and thickness of 0.09 mm was 8.8 mg. As a first approximation, the tear volume is considered a homogeneous mixture although it is known that the drug in the POLTF is not perfectly mixed with the remaining fluid.

The estimated release profile for DCF from one ALG/PLL(EDC)//HA coated lens, previously loaded as described above, is presented in **Figure 3.16**, together with the ranges of the half-maximum inhibition concentrations (IC$_{50}$) values for cyclooxygenase-1 (COX-1; 0.04-0.3 µg/mL) and cyclooxygenase-2 (COX-2: 0.01-0.03 µg/mL) which are active enzymes in the presence of inflammation, involved in the catalysis of prostaglandins and thromboxanes [51].

A
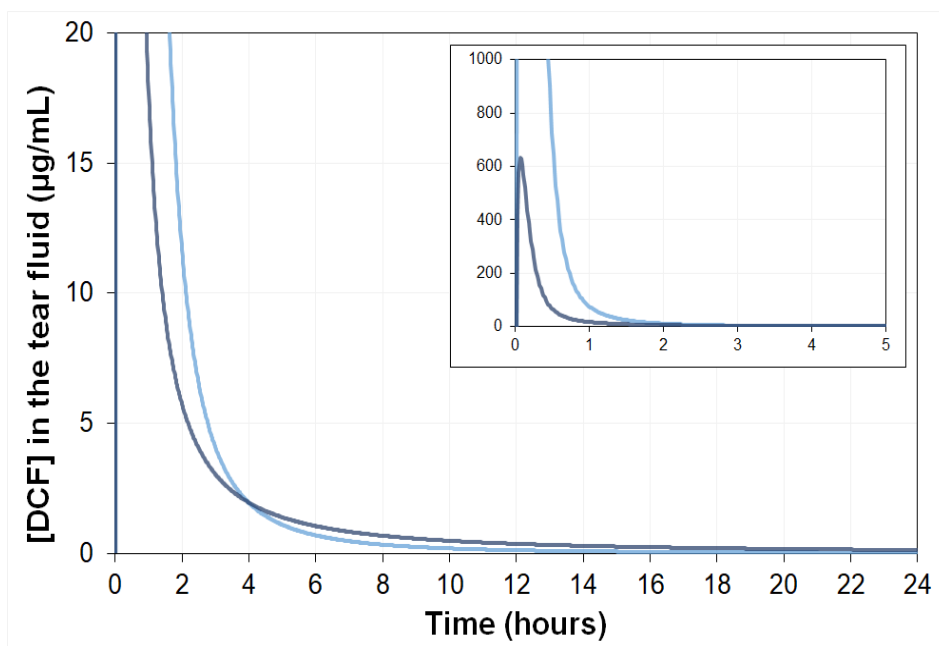
B
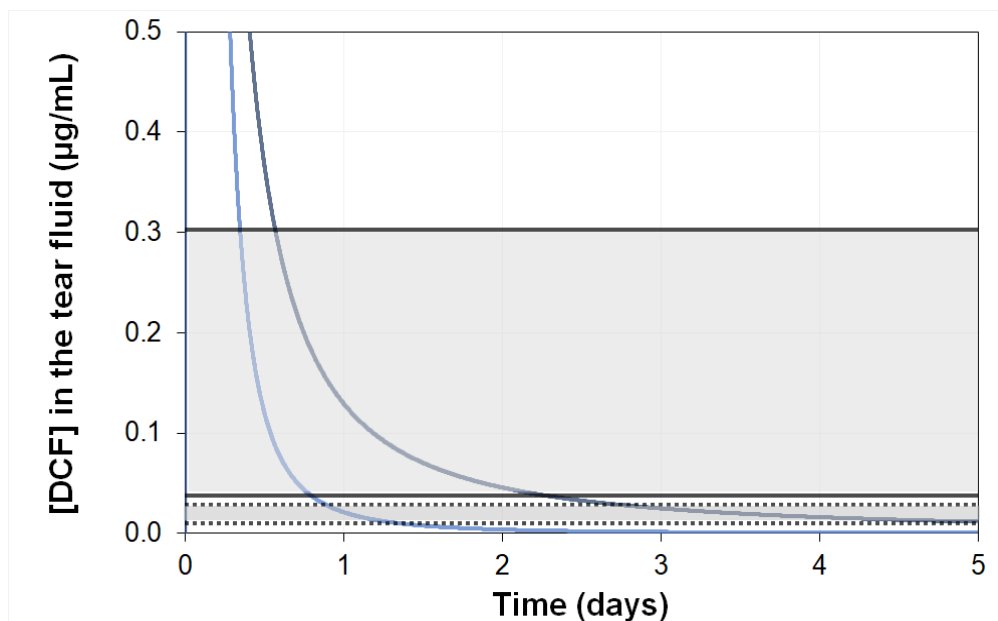
Figure 3.16 Concentration profiles of DCF in the tear fluid, estimated from the mathematical model applied to the cumulative release data for uncoated hydrogels (light blue) and ALG/PLL(EDC)//HA coated hydrogel (dark blue): **(A)** initial 24 h, where the first 5 h are shown in the insert; **(B)** 5 days. The ranges of IC_{50} for COX-1 and COX-2 are limited by the solid lines and the dotted lines, respectively.

The presence of the coating significantly decreased the initial burst release to a value of the order of the DCF concentration in commercial eye drops (1 mg/mL), while the time during which the DCF concentration in the eye remained above the lower limits of the IC_{50} values increased significantly with respect to the uncoated sample: from less than one day to more than two days for COX-1, and from a little above one day to five days for COX-2.

3.5 Conclusions

This work describes an investigation about the use of polyelectrolytes with antibacterial properties to form LbL coatings on SCLs materials with the dual purpose of controlling the release of ophthalmic drugs and reducing bacterial growth. The TRIS/NVP/HEMA hydrogel was used as the lens material and the drugs DCF, CHX and MXF were tested. Coatings composed of two double layers of ALG/PLL(EDC), HA(EDC)/CHI and HA/PLL(EDC)+Drug demonstrated to decrease the initial release rate of DCF, leading to controlled release profiles. In contrast, the release rates of MXF and CHX were not reduced by any of the employed coatings. The unique behaviour of DCF may be attributed to the establishment of molecular interactions (H-Bonds, hydrophobic or physical entrapment) between the drug molecule and the polyelectrolytes, leading to the formation of reversible complexes. The coatings are hydrophilic, do not affect the bulk refraction index, and slightly reduce light transmittance. However, they were affected by the presence of albumin and lysozyme, two of the most common proteins in the tear fluid. To overcome this problem, a final layer of HA was deposited on top of the ALG/PLL(EDC) coating. The resulting coating ALG/PLL(EDC)//HA demonstrated to be able to control the release of DCF, to resist the action of the tear proteins, to reduce the growth of *S. aureus* and *P. aeruginosa,* and to produce no ocular irritation. The concentration of DCF in the tear fluid resulting from the application of ALG/PLL(EDC)//HA coated contact lens, predicted through a simplified mathematical model, remained above the lower limits of the IC_{50} values for COX-1 and COX-2, two and five days, respectively.

3.6   References

[1]   S. Benavides, R. Villalobos-Carvajal, J.E. Reyes, Physical, mechanical and antibacterial properties of alginate film: Effect of the crosslinking degree and oregano essential oil concentration, J. Food Eng. 110 (2012) 232–239.

[2]   M.S. Benhabiles, R. Salah, H. Lounici, N. Drouich, M.F.A. Goosen, N. Mameri, Antibacterial activity of chitin, chitosan and its oligomers prepared from shrimp shell waste, Food Hydrocoll. 29 (2012) 48–56.

[3]   M. Kong, X.G. Chen, H.J. Park, Antimicrobial properties of chitosan and mode of action: A state of the art review, Int. J. Food Microbiol. 144 (2010) 51–63.

[4]   M.N. V. Ravi Kumar, R.A.A. Muzzarelli, C. Muzzarelli, H. Sashiwa, A.J. Domb, Chitosan Chemistry and Pharmaceutical Perspectives, Chem. Rev. 104 (2004) 6017–6084.

[5]   E.I. Rabea, M.E.T. Badawy, C. V. Stevens, G. Smagghe, W. Steurbaut, Chitosan as antimicrobial agent: Applications and mode of action, Biomacromolecules. 4 (2003) 1457–1465.

[6]   W.G. Pitt, R.N. Morris, M.L. Mason, M.W. Hall, Y. Luo, G.D. Prestwich, Attachment of hyaluronan to metallic surfaces, J. Biomed. Mater. Res. A. 68 (2004) 95–106.

[7]   R.A. D'Sa, P.J. Dickinson, J. Raj, B.K. Pierscionek, B.J. Meenan, Inhibition of lens epithelial cell growth via immobilisation of hyaluronic acid on atmospheric pressure plasma modified polystyrene, Soft Matter. 7 (2011) 608–617.

[8]   A. Ardizzoni, R.G. Neglia, M.C. Baschieru, C. Cermelli, M. Caratozzolo, M. Righi, B. Palmieri, E. Blasi, Influence of hyaluronic acid on bacterial and fungal species, including clinically relevant opportunistic pathogens, J. Mater. Sci. Mater. Med. 22 (2011) 2329–2338.

[9]   G.A. Carlson, J.L. Dragoo, B. Samimi, D.A. Bruckner, G.W. Bernard, M. Hedrick, P. Benhaim, Bacteriostatic properties of biomatrices against common orthopaedic pathogens, Biochem. Biophys. Res. Commun. 321 (2004) 472–478.

[10] J. Hernandez-Montelongo, E.G. Lucchesib, I. Gonzalez, W.A.A. Macedo, V.F. Nascimento, A.M. Moraes, M.M. Beppu, M.A. Cotta, Hyaluronan/chitosan nanofilms assembled layer-by-layer and their antibacterial effect: A study using Staphylococcus aureus and Pseudomonas aeruginosa, Colloids Surfaces B Biointerfaces. 141 (2016) 499–506.

[11] R. Ye, H. Xu, C. Wan, S. Peng, L. Wang, H. Xu, Z.P. Aguilar, Y. Xiong, Z. Zeng, H. Wei, Antibacterial activity and mechanism of action of e-poly-L-lysine, Biochem. Biophys. Res. Commun. 439 (2013) 148–153.

[12] N. Davidenko, J.J. Campbell, E.S. Thian, C.J. Watson, R.E. Cameron, Collagen–hyaluronic acid scaffolds for adipose tissue engineering, Acta Biomaterilia. 6 (2010) 3957–3968.

[13] J. Monreal, R. Hyde, Spheroidal and nanocrystal structures created from carbodiimide crosslinking reaction with RADA16, J. Sci. Adv. Mater. Devices. 2 (2017) 178–182.

[14] D. V. Bax, N. Davidenko, S.W. Hamaia, R.W. Farndale, S.M. Best, R.E. Cameron, Impact of UV- and carbodiimide-based crosslinking on the integrin-binding properties of collagen-based materials, Acta Biomater. 100 (2019) 280–291.

[15] C.R. Cammarata, M.E. Hughes, C.M. Ofner III, Carbodiimide induced cross-linking, ligand addition, and degradation in gelatin, Mol. Pharm. 12 (2015) 783–793.

[16] https://www.thermofisher.com, [March 2020]. (n.d.).

[17] T. Bourcier, F. Thomas, V. Borderie, C. Chaumeil, L. Laroche, Bacterial keratitis: predisposing factors, clinical and microbiological review of 300 cases, Bras. J. Ophthalmol. 87 (2003) 834–838.

[18] P. Garg, Fungal, mycobacterial, and nocardia infections and the eye: an update, Eye. 26 (2012) 245–251.

[19] R. Vasquez, R. Nogueira, M. Orfão, J. Mata, B. Saramago, Stability of triglyceride liquid films on hydrophilic and hydrophobic glasses, J. Colloid Interface Sci. 299 (2006) 274–282.

[20] P. Paradiso, R. Galante, L. Santos, A.P. Alves De Matos, R. Colaço, A.P. Serro, B.

Saramago, Comparison of two hydrogel formulations for drug release in ophthalmic lenses, J. Biomed. Mater. Res. B. 102 (2014) 1170–1180.

[21]   C. Delajon, T. Gutberlet, R. Steitz, H. Möhwald, R. Krastev, Formation of polyelectrolyte multilayer architectures with embedded DMPC studied in situ by neutron reflectometry, Langmuir. 21 (2005) 8509–8514.

[22]   J. Hernandez-Montelongo, V.F. Nascimento, D. Murillo, T.B. Taketa, P. Sahoo, A.A. Souza, M.M. Beppu, M.A. Cotta, Nanofilms of hyaluronan/chitosan assembled layer-by-layer: An antibacterial surface for Xylella fastidiosa, Carbohydr. Polym. 136 (2016) 1–11.

[23]   K. Jarquín-Yáñez, J. Arenas-Alatorre, G. Piñón-Zárate, R.M. Arellano-Olivares, M. Herrera-Enríquez, B. Hernández-Téllez, A.E. Castell-Rodríguez, Structural Effect of Different EDC Crosslinker Concentration in Gelatin-Hyaluronic Acid Scaffolds, J. Bioeng. Biomed. Sci. 6 (2016) 1–6.

[24]   M.M. Collins, C. Birkinshaw, Investigation of the swelling behavior of crosslinked hyaluronic acid films and hydrogels produced using homogeneous reactions, J. Appl. Polym. Sci. 109 (2008) 923–931.

[25]   E.R. Berman, Tears, in: Biochem. Eye, Plenum Press, New York, 1991: pp. 63–73.

[26]   A.M. Bright, B.J. Tighe, The composition and interfacial properties of tears, tear substitutes and tear models, J. Br. Contact Lens Assoc. 16 (1993) 57–66.

[27]   P.T. Janssen, O.P. van Bijsterveld, The relations between tear fluid concentrations of lysozyme, tear-specific prealbumin and lactoferrin, Exp. Eye Res. 36 (1983) 773–9.

[28]   D. Luensmann, L. Jones, Albumin adsorption to contact lens materials: A review, Contact Lens Anterior Eye. 31 (2008) 179–87.

[29]   G. Runström, A. Mann, B. Tighe, The fall and rise of tear albumin levels: A multifactorial phenomenon, Ocul. Surf. 11 (2013) 165–180.

[30]   R.N. Stuchell, J.J. Feldman, R.L. Farris, I.D. Mandel, The effect of collection technique on tear composition, Investig. Ophthalmol. Vis. Sci. 25 (1984) 374–7.

[31] M.S. Bhatia, S.R. Dhaneshwar, Simultaneous spectrophotometric determination of diclofenac sodium chlorzoxazone and paracetamol from combined dosage forms, Indian Drugs. 32 (1995) 446–450.

[32] N. Efron, C. Maldonado-Codina, Development of contact lenses from a biomaterial point of view – Materials, manufacture, and clinical application, in: Compr. Biomater., Comprehensive Biomaterials. Elsevier, 2011: pp. 517–541.

[33] D. Silva, A.C. Fernandes, T.G. Nunes, R. Colaço, A.P. Serro, The effect of albumin and cholesterol on the biotribological behaviour of hydrogels for contact lenses, Acta Biomater. 26 (2015) 184–194.

[34] C.R. Wittmer, J.A. Phelps, C.M. Lepus, W.M. Saltzman, M.J. Harding, P.R. VanTassel, Multilayer nanofilms as substrates for hepatocellular applications, Biomaterials. 29 (2008) 4082–4090.

[35] R. Galante, P. Paradiso, M.G. Moutinho, A.I. Fernandes, J.L.G. Mata, A.P.A. Matos, R. Colaço, B. Saramago, A.P. Serro, About the effect of eye blinking on drug release from pHEMA-based hydrogels: An in vitro study, J. Biomater. Sci. Polym. Ed. 26 (2015) 235–251.

[36] R. Rodriguez, C. Alvarez-Lorenzo, A. Concheiro, Cationic cellulose hydrogels: kinetics of the cross-linking process and characterization as pH-/ion-sensitive drug delivery systems., J. Control. Release. 86 (2003) 253–265.

[37] A. Bani-Jaber, D. Anani, I.I.I. Hamdan, B.A.A. Alkhalidi, Investigation of drug polymer interaction: Evaluation and characterization of diclofenac-chitosan co-precipitate, Jordan J. Pharm. Sci. 2 (2009) 140–149.

[38] Y. Boonsongrit, A. Mitrevej, B. Mueller, Chitosan drug binding by ionic interaction, Eur. J. Pharm. Biopharm. 62 (2006) 267–274.

[39] A. Schneider, C. Vodouhê, L. Richert, G. Francius, E.L. Guen, P. Schaaf, J.-C. Voegel, B. Frisch, C. Picart, Multifunctional polyelectrolyte multilayer films: Combining mechanical resistance, biodegradability, and bioactivity, Biomacromolecules. 8 (2008) 139–145.

[40] M.C. Lin, T.F. Svitova, Contact lenses wettability in vitro: Effect of surface-active

ingredients, Optom. Vis. Sci. 87 (2010) 440–447.

[41]   M. Kolasinska, P. Warszynski, The effect of nature of polyions and treatment after deposition on wetting characteristics of polyelectrolyte multilayers, Appl. Surf. Sci. 252 (2005) 759–765.

[42]   S. Yamanlar, S. Sant, T. Boudou, C. Picart, Surface functionalization of hyaluronic acid hydrogels by polyelectrolyte multilayer films, Biomaterials. 32 (2011) 5590–5599.

[43]   P. Kujawa, P. Moraille, J. Sanchez, A. Badia, F.M. Winnik, Effect of molecular weight on the exponential growth and morphology of hyaluronan/chitosan multilayers: A surface plasmon resonance spectroscopy and atomic force microscopy investigation, J. Am. Chem. Soc. 127 (2005) 9224–9234.

[44]   C. Picart, Polyelectrolyte Multilayer Films: From Physico-Chemical Properties to the Control of Cellular Processes, Curr. Med. Chem. 15 (2008) 685–697.

[45]   L. Richert, F. Boulmedais, P. Lavalle, J. Mutterer, E. Ferreux, G. Decher, P. Shaaf, J.-C. Voegel, C. Picart, Improvement of stability and cell adhesion properties of polyelectrolyte multilayer films by chemical cross-linking, Biomacromolecules. 5 (2004) 284–294.

[46]   N.K. Dutta, S. Annadurai, K. Mazumdar, S.G. Dastidar, J.E. Kristiansen, J. Molnar, M. Martins, L. Amaral, Potential management of resistant microbial infections with a novel non-antibiotic: the antiinflammatory drug diclofenac sodium, Int J Antimicrob Agents. 30 (2007) 242–9.

[47]   J.T. Riordan, J.M. Dupre, S.A. Cantore-Matyi, A. Kumar-Singh, Y. Song, S. Zaman, S. Horan, N.S. Helal, V. Nagarajan, M.O. Elasri, B.J. Wilkinson, J.E. Gustafson, Alterations in the transcriptome and antibiotic susceptibility of Staphylococcus aureus grown in the presence of diclofenac, Ann. Clin. Microbiol. Antimicrob. 10 (2011) 1–11.

[48]   A. Salem-Milani, E. Balaei-Gajan, S. Rahimi, Z. Moosaki, A. Abdollahi, P. Zakeri-Milani, M. Bolourian, Antibacterial effect of diclofenac sodium on enterococcus faecalis, J. Dent. Tehran Univ. Med. Sci. 10 (2013) 16–22.

[49]   E.F. Ahmed, R.M.A. El-Baky, A.B.F. Ahmed, N.G. Waly, G.F.M. Gad, Antibacterial

activity of some non-steroidal anti-inflammatory drugs against bacteria causing urinary tract infection, Am. J. Infect. Dis. Microbiol. 5 (2017) 66–73.

[50]   L. Drago, L. Cappelletti, E. De Vecchi, L. Pignataro, S. Torretta, R. Mattina, Antiadhesive and antibiofilm activity of hyaluronic acid against bacteria responsible for respiratory tract infections, APMIS. 10 (2014) 1013–9.

[51]   R. Reddy, S.J. Kim, Critical appraisal of ophthalmic ketorolac in treatment of pain and inflammation following cataract surgery, Clin. Ophthalmol. 5 (2011) 751–75.

4 Diclofenac sustained release from sterilised soft contact lenses materials using an optimised layer-by-layer coating

Table of Contents

4.1 Introduction

In the previous two chapters it was investigated the possibility of improving the release of ophthalmic drugs from SCLs materials through LbL coatings, which could act as drug diffusion barriers. DCF was the only drug whose release was effectively controlled by the use of natural based polyelectrolyte coatings. Chapter 3 described the ALG/PLL(EDC)//HA coating, which demonstrated additional antifouling and anti-bacterial properties, but led to a high drug retention inside the polymeric matrix, implying some drug waste. Therefore, in this chapter a new, more efficient LbL coating was sought, which could significantly improve the release of DCF, present antifouling and anti-bacterial properties and resist sterilization processes.

A combination of three ionic polysaccharides ALG, CHI and HA cross-linked with GE, were used to form one triple-layer coating (designated as ALG/CHI/HA) on a silicone-based hydrogel (TRIS/NVP/HEMA) and two commercial lenses: SofLens and Purevision from Bausch&Lomb. ALG is capable of forming stable coatings, but as there is no evidence of ALG showing antibacterial properties [1], it was used as first layer, followed by CHI, known for its antibacterial activity [2–5]. HA was used as top layer because data from chapter 3 demonstrated that, besides its inhibitory effect of the growth of *S. aureus* and *P. aeruginosa*, it has antifouling properties against lysozyme. GE is a natural product extracted from the fruits of the plant *Gardenia jasminoides Ellis* and has been considered an efficient crosslinking agent, presenting high biocompatibility and very low toxicity [6]. The chemical structures of the TRIS/NVP/HEMA monomers are shown in Appendix A. The chemical structures and some physical properties of the used polyelectrolytes are summarized in Appendix C. A brief description of both tested commercial lenses can be found in **Table 1.1** of chapter 1.

DCF release profiles were obtained under sink conditions. The ALG/CHI/HA coating was characterized with respect to the water uptake, topography, wettability, and coating thickness. The optical properties (transmittance and refractive index) and ionic permeability of the LbL coated hydrogels were evaluated. The interaction of lysozyme and albumin, two of the most abundant proteins in the lachrymal fluid, with the coating was evaluated. The characterization of the coating was done only using the TRIS/NVP/HEMA hydrogels as substrates. The use of commercial lenses was not possible in the cases where flat substrates or deposition of the material on a sensor were required (e.g. wettability and adsorption studies by QCM-D,

respectively). Moreover, the polymeric mixtures used in the manufacture of commercial lenses, which were needed to prepare adequate samples, were not available.

Two sterilization methods, SP and HPP, were tested and their effects on the ALG/CHI/HA coated TRIS/NVP/HEMA hydrogel were assessed

The potential ocular irritancy of the sterilized hydrogels was assessed using HET-CAM assay.

The antibacterial activities of the sterilized coated TRIS/NVP/HEMA hydrogels against *S. aureus* and *P. aeruginosa*, two of the most common bacteria in ocular infections [7,8], were tested, and the cytotoxicity tests were carried out using NIH/3T3 cells (mouse embryonic fibroblasts).

The efficiency of the DCF loaded hydrogels was assessed through the comparison of the release profiles with the ranges of the IC_{50} values for the enzymes COX-1 and COX-2, using a simplified mathematical model described in section 3.4 of chapter 3.

4.2 Experimental part

4.2.1 Materials

SCL materials: 2-hydroxyethyl methacrylate (purity≥99%, HEMA), 2,2'-azobis(2-methylpropionitrile) (purity≥98%, AIBN) and 3-tris(trimethylsilyloxy)silylpropyl 2-methylprop-2-enoate (purity≥98%, TRIS) were provided by Sigma-Aldrich (USA); ethylene glycol dimethacrylate (purity≥98%, EGDMA) and N-vinyl pyrrolidone (purity≥98%, NVP) were obtained from Merck (USA); contact lenses SofLens (Hilafilcon B) diopter -3.00, water content 59%, Dk/t 16 and Purevision (Balafilcon A) diopter -3.00, water content 36%, Dk/t 130 were provided by Bausch&Lomb. Drug, and reagents for drug release and loading quantification: diclofenac sodium salt (purity≥ 98.5%, DCF) from Sigma-Aldrich (USA), sodium chloride (purity≥99%, NaCl) from PanReac (Spain), and methanol (purity≥99.9%, CH_3OH) from Carlo Erba (Spain). For the coating production: alginic acid sodium salt from brown algae (average molecular weight 100,000-200,000 g/mol, 61% mannuronic acid and 39% guluronic acid, ALG), and branched poly(ethylenimine) (average molecular weight 750,000 g/mol, PEI) were provided by Sigma-Aldrich (USA); genipin (purity≥98%, GE), and

sodium hyaluronate (average molecular weight 1,000,000–2,000,000 g/mol, HA) were purchased from Carbosynth (UK); medical grade chitosan (high deacetylation degree, >90%, average molecular weight 750,000-1,000,000 g/mol, CHI) was supplied by Altakitin (Portugal). For QCM-D tests: hydrogen peroxide (30% (w/v), H_2O_2), and sulfuric acid (purity≥98%, H_2SO_4) were obtained from PanReac (Spain), Hellmanex®II from Hellma GmbH (Germany), lysozyme chicken egg white (pH 6.5) from Merck (USA),and albumin bovine Fraction V standard grade (pH 7.0) from Serva (Germany). For the HET-CAM test: sodium hydroxide, (purity≥99%, NaOH) was obtained from Merck (USA). For the cytotoxicity tests: acetic acid (purity≥99.7%), calf serum (CS), dulbecco's modified eagle's medium (DMEM), dimethyl sulfoxide (DMSO), hydrochloric acid (HCl), isopropanol, NIH/3T3 fibroblasts (93061524), and penicillin-streptomycin solution (10000U/mL penicillin, 10 mg/mL streptomycin) were provided by Sigma-Aldrich (USA); octylphenoxypolyethoxyethanol (IGEPAL®) was obtained from Merck (USA).

All solutions were prepared with distilled and deionised (DD, 18 MΩcm, pH 7.7) water, which was obtained with a Millipore system.

4.2.2   Synthesis of polymeric samples

A silicone-based hydrogel (designated as TRIS/NVP/HEMA) was prepared was previously described in section 2.2.2 of chapter 2. A solution, with the monomers TRIS (0.8 M), NVP (3.9 M), HEMA (1.8 M), and the crosslinker EGDMA (30 mM) was degassed at room temperature for 5 min with ultrasound sonication, and for 10 min with a nitrogen flux. The solution was then homogenized by magnetic stirring after the addition of the initiator AIBN (15 mM), and finally poured into a mould made of two silanized glass plates with a Teflon spacer (0.25 mm of thickness). Silanization was done according to the procedure described elsewhere [9]. The samples were obtained after thermal polymerization in oven at 60ºC for 24 h. Then, the hydrogels were washed in DD water, which was renewed three times a day, until no monomers were detected in the washing solution (five days). Finally, disks with 12 mm (unless otherwise stated) of diameter were cut from the hydrated samples.

SofLens and Purevison lenses were washed using the same conditions. All dry hydrogels were stored inside closed flasks, after drying for 72 h at 36ºC in an oven.

4.2.3 DCF loading and release measurements

The dry hydrogels were soaked in a 3 mL saline solution (130 mM NaCl, pH 6.9) containing DCF (1 mg/mL), at 4ºC for 38 h. The loading conditions were optimized in a previous work [10], and in previous chapters. The saline solution has a neutral pH to mimic the pH of human tears (pH 7). Also, human tears have very low buffer capacity [11]. Drug release from the hydrogels was studied in vials with 3 mL of the same saline solution, at 36ºC, which guarantees sink conditions (maximum DCF concentration well below the solubility of DCF in saline, which is ≥1 mg/mL). Aliquots of 200 µL were taken at schedule times to obtain the drug concentration value, and subsequently replaced with the same volume of fresh NaCl solution. The release data was studied in a cumulative manner taking into account the dilution effect of the release medium replacement. For each system, three experiments were carried out. DCF concentration was quantified at λ=276 nm using a UV-Vis spectrophotometer (Multiskan GO, Thermo Scientific).

The amount of drug loaded by TRIS/NVP/HEMA hydrogels was determined by methanol extraction. DCF loaded hydrogels were placed in 3 mL of methanol, at room temperature. At 2, 4, 8 and 24 h, and every 24 h while it was possible to measure the DCF concentration, hydrogels were rinsed with DD water, blotted with absorbent paper and replaced in fresh methanol. The concentration of DCF was determined in the same manner has previously described. Four experiments were carried out.

4.2.4 LbL deposition

First, the DCF-loaded hydrogels were soaked for 5 min in the PEI solution (10 mg/mL), to promote stability and homogeneity of the following layers [12,13]. In the meantime, ALG (1 mg/mL) and HA (2 mg/mL) solutions were prepared in DD water, while CHI was dissolved (1 mg/mL) in an aqueous solution of acetic acid 1% (v/v). The pH of CHI solution was adjusted to 5, to avoid loss of positive charge and consequent precipitation [14]; for all other polyelectrolytes and crosslinker solutions the pH was set to 7, which is more favourable for GE reaction [6], and to maintain ALG and HA negative charges [15,16]. One triple layer was achieved by sequential dipping the samples in ALG, CHI and HA solutions for 1 min each, and finishing with GE for 5 min. Between each dipping a rinsing with DD water was carried out.

The crosslinking of GE was carried out in the oven at 36ºC during 24 h, in a vial with DCF solution (1 mg/mL). A schematic representation of the experimental LbL procedure is shown in **Figure 4.1**.
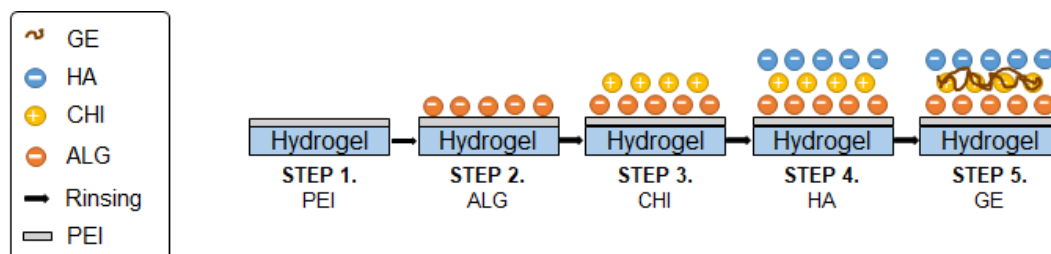
Figure 4.1 Schematic representation of the ALG/CHI/HA coating procedure.

Uncoated drug loaded hydrogels were immersed in DD water during the time spent in the LbL formation, and then put in the oven immersed in the drug solution, at 36ºC during 24 h, to emulate the LbL process. SofLens and Purevision lenses were submitted to the same surface modification. Immediately after preparation, the samples were used in the drug release assays.

4.2.5   Evaluation of the coating formation

The formation of each layer was followed in real time with a QCM-D (E4 from Q-Sense). Quartz crystals (5 MHz) were spin coated (2000 rpm, 30 s) with a PS film, followed by the deposition of the TRIS/NVP/HEMA hydrogel mixture (5000 rpm, 30 s). Polymerization was achieved at 60ºC for 1 h inside a nitrogen atmosphere. The experimental baseline was obtained for hydrogel coated quartz crystals, after pre-hydration in DD water (10 min). The normalized frequency ($\Delta f/n$) and the dissipation (ΔD) changes for the 3rd harmonic, were studied during each layer deposition at 36ºC. Two lachrymal proteins, lysozyme (1.9 mg/mL) and albumin (0.05 mg/mL) were selected to evaluate possible interactions with the coating. The proteins solutions were added after the final top layer and followed by rinsing with DD water. Four measurements were carried out for each system.

The quartz crystals were recovered after cleaning in a piranha solution (H_2SO_4/H_2O_2, 7/3 v:v), by dipping for 5 s. Followed by an intensive washing process in ultrasounds for 15 min in a 2% (v/v) Hellmanex solution and two times (x15 min) in water. The crystals were properly stored after a DD water rinsing, and a drying process achieved by nitrogen flux.

4.2.6   Characterization of the coated TRIS/NVP/HEMA hydrogels

The water uptake of the LbL coated hydrogels in DD water was evaluated. The uncoated and coated hydrogels were dried after preparation and weighted (W_D). Afterwards the hydrogels were placed in 3 mL of the DD water at 4ºC, measurements were carried out in triplicates for each system. At schedule times, the hydrogels were removed from the vials, blotted in absorbent paper and weighted, until stabilization (W_W). **Equation 1.2** (chapter 1) was used to calculate the water uptake.

The captive bubble method was used to evaluate the hydrated hydrogels' wettability. Air bubbles (3 – 4 µL) were formed underneath the substrates using a micrometer syringe with a curved needle. The images were obtained by a video camera (jAi CV-A50, Spain) mounted on a microscope Wild M3Z (Leica Microsystems, Germany), and their analysis was done with ADSA software (Axisymmetric Drop Shape Analysis, Applied Surface Thermodynamics Research Associates, Toronto, Canada). Ten experiments were carried out.

Topographic images of the uncoated and coated surfaces of the hydrated hydrogels were obtained in non-contact mode with an AFM (Nanosurf EasyScan 2), at room temperature. Silicon probes (resonance frequency: 204-497 kHz) at a scan rate of 1.2 Hz were used to obtain 10 x 10 μm^2 images. The R_a was calculated using WSxM 5.0 develop 8.4 software for the total area of the images. Three images of each sample, kept in a liquid cell, were obtained.

The transmittance of hydrated hydrogels was recorded, in triplicate, in a UV-Vis spectrophotometer (Multiskan GO, Thermo Scientific), in the 200 – 700 nm interval.

The coating thickness and the refractive index for the hydrated hydrogels were studied by ellipsometry. Ellipsometric functions Ψ and Δ were determined in a wavelength range 300 – 850 nm, at 70º incidence angle, through a phase modulated spectroscopic ellipsometer

(UVISEL, Horiba Jobin-Yvon). The modelling was done by DeltaPsi2 software package from Jobin-Yvon with a Cauchy dispersion function. Three experiments were made for each sample.

The ionic permeability of the hydrogels previously hydrated in DD water was quantified, using a Lab-made cell (see section 1.1.4.2.5 in chapter 1). Three measurements were performed. The conductivity of the acceptor solution was measured every hour for 12 h, at 36ºC, using a conductivity meter (HI2003 edge$^{EC®}$ from HANNA instruments). The conductivity data were converted into NaCl concentrations through a previously obtained a calibration curve. D_{ion} was calculated from **Equation 1.4** (chapter 1).

4.2.7 Sterilization

Two different sterilization procedures were carried out to investigate possible degradation of the coated TRIS/NVP/HEMA hydrogels. SP was carried out by placing the hydrated hydrogels, contained in closed vials with 3 mL of drug solution, inside an autoclave at 121ºC and 1 bar for 1 h.

For the HHP method, the uncoated and coated samples were placed inside special sealed bags (polyamide and polyethylene, 90-micron, 10 x 10 cm^2, Penta Iberica), with 3 mL of NaCl (130 mM) for the unloaded samples, and 3 mL of drug solution for the loaded samples. The samples were submitted to a 600 MPa pressure at 70ºC for 10 min in a High-Pressure equipment (Hiperbaric 55, Burgos, Spain). After sterilization, drug release assays were carried out in sink conditions. Four experiments were carried out for each sterilization process.

4.2.8 Antibacterial assays

Uncoated and coated TRIS/NVP/HEMA hydrogels without DCF, and coated hydrogels loaded with DCF, were sterilized by HHP and tested against *P. aeruginosa* (ATCC 15442) and *S. aureus* (ATCC 25923). Their antibacterial activity was evaluated by turbidimetry in MHB. The strains were grown for 24 h at 37ºC. The grown colonies were suspended in an 0.9% NaCl sterile solution to achieve a turbidity of 0.5 McFarland (1.5×10^8 bacteria/mL) for *P. aeruginosa*, and 1 McFarland (3×10^8 bacteria/mL) for *S. aureus*.

The hydrated hydrogels were placed individually in wells, which were filled with 10 µL of bacteria suspension diluted in 500 µL of MHB. A positive and a negative control were done, with inoculated MHB and with simple MHB, respectively. The microplates were incubated at 37ºC with stirring (100 rpm) for 24 h.

Aliquots of 200 µL from each well were placed in a 96-well plate, to measure the optical density, at 630 nm, by using a microplate reader (Platos R 496). Tests were performed under aseptic conditions. Experiments were done in quadruplicate for each system.

4.2.9 HET-CAM test

The potential ocular irritation of the uncoated and coated TRIS/NVP/HEMA hydrogels without drug, and coated hydrogels with drug was evaluated by the HET-CAM. Fertilized hen´s eggs (Sociedade Agrícola da Quinta da Freira, SA, Portugal) were placed in an egg incubator (Incubator, 56S) at 37±0.5ºC and 60±5% RH, for 8 days. After the incubation, the eggs were cut open on the airspace with a rotary saw (Dremmel 3000, Breda). The exposed inner membrane was hydrated with 0.9% NaCl solution for 30 min and then carefully removed to gain access to the CAM. The sterilized TRIS/NVP/HEMA samples were blotted with an absorbent paper and laid directly in contact with the CAM, and time was recorded. Triplicates were carried out for each system. Negative (NaCl, 0.9%) and positive (NaOH, 1 M) controls were similarly tested. The assay was recorded for 5 min to evaluate lysis, haemorrhage and coagulation, which may occur in the CAM, through calculation of the IS (**Equation 1.6**, chapter 1)

4.2.10 Cytotoxicity tests

Cytotoxicity tests were carried out according to ISO standard 10993-5 using NIH/3T3 fibroblasts. The cells were grown in T75 flasks in DMEM, supplemented with 10% CS and 1% penicillin-streptomycin solution.

The NIH/3T3 cells were placed in a 24-well-plate with a density of 1×10^5 cells/mL and cultured at 37ºC, in a humified 5% CO_2 incubator for 24 h. The HHP sterilized hydrogels (5 mm

diameter) were placed in an 8.0 µm pore polycarbonate membrane Transwell® insert (Corning® Transwell®, Sigma). The inserts were individually placed on each well, and aliquots of 0.1 mL of DMEM were added on top of all samples. A negative control (DMEM) and a positive control (DMEM with 5% DMSO) were also tested. The plates were incubated for another 24 h.

Cell viability was assessed by a colorimetric method using the MTT assay. Briefly, the inserts and culture medium were removed and 300 µL of MTT dissolved in serum-free DMEM (0.5 mg/mL) were added to each well. Incubation of the plates was carried out for another 3 h. Subsequently, formazan crystals were dissolved by adding to each well 450 µL of MTT solvent (4 mM HCL, 0.1% IGEPAL in isopropanol). The absorbance was measured at 595 nm in a microplate reader (Platos R 496). Five replicates for each system were done, and the viability results were normalized to the negative control.

4.2.11 Statistical analysis

R Project software v. 3.6.1 was used for the statistical analysis. Experimental values are given as mean ± standard deviation. Student´s t-test and one-way ANOVA test were used to check if two or more sets of data were significantly different. Shapiro-Wilk test was analysed the normality of the data. The level of significance was set to 0.05.

4.3 Results

4.3.1 Evaluation of the LbL formation

The deposition of each layer during the LbL formation on the quartz sensors coated with TRIS/NVP/HEMA hydrogel was investigated using QCM-D. The changes of $\Delta f/n$ and ΔD for the 3rd overtone obtained in two similar experiments which differ only in step 7 are shown in **Figure 4.2A** and **B**. The coated crystal equilibrated with DD water was used as the baseline. After the injection of PEI solution, ALG, CHI, HA and GE solutions were added in sequence to form the ALG/CHI/HA coating. The rinsing steps after adding each polysaccharide led to an increase in frequency and a decrease in dissipation, indicating the loss of weakly bound molecules. Nevertheless, the layers remained stable after the rinsing process. Then, the

interaction of the coating with two different lachrymal proteins, albumin and lysozyme, was assessed. Albumin was slowly and stably adsorbed to the surface, as shown by the slow frequency decrease as a function of time (**Figure 4.2A**); lysozyme had almost no effect and was removed after the rinsing step (**Figure 4.2B**).

A
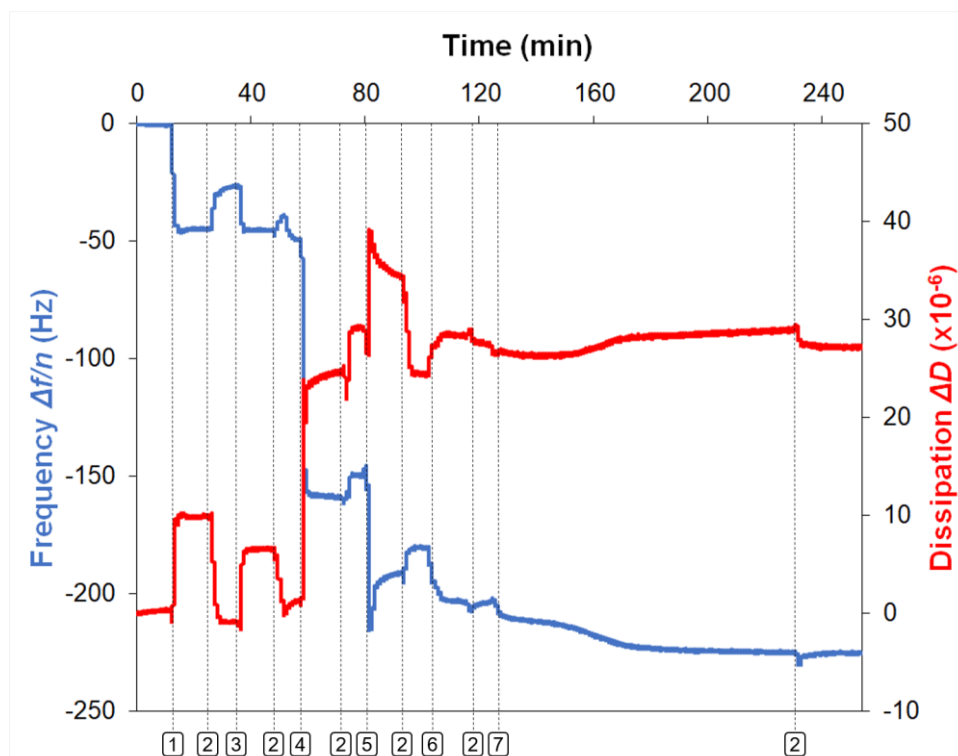
B
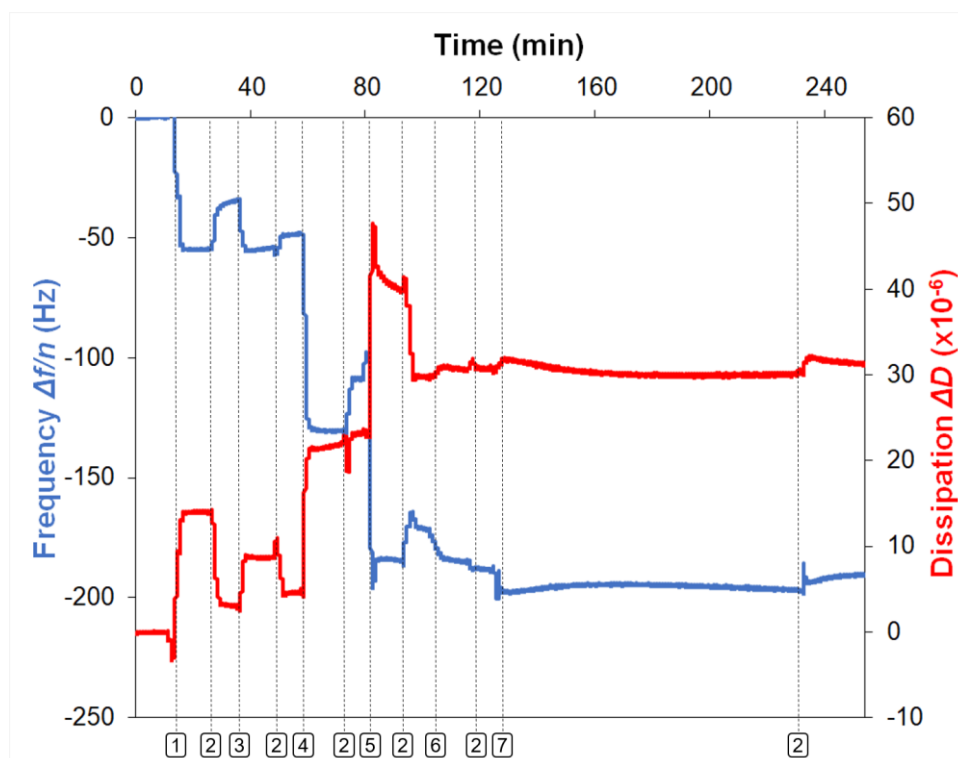
Figure 4.2 Normalized shift in the frequency, *Δf/n* (blue line, left y-axis) and shift in the dissipation *ΔD* (red line, right y-axis) for the 3rd harmonic of the resonant frequency of a quartz

crystal sensor after being coated with a TRIS/NVP/HEMA hydrogel film, during successive additions of PEI (1), ALG (3), CHI (4), HA (5) and GE (6), as a function of time, to form one double layer ALG/CHI/HA coating. The final step (7) corresponds to the addition of albumin (**A**) and lysozyme (**B**). The successive additions are separated by rinsing with DD water (2).

4.3.2 Drug loading and release

After preparation, drug loading was achieved by simple soaking the hydrogels, followed by the LbL surface modification. The efficiency of the drug loading process was evaluated by determining the amount of the drug loaded in the uncoated and coated TRIS/NVP/HEMA hydrogels. Interestingly, the presence of the coating did not affect the amount of drug loaded (p = 0.958), as the same value was obtained for the uncoated (113±5 ug/mg of dried gel) and coated samples (113±2 ug/mg of dried gel). These results were not unexpected, considering that the drug loading process took place before the deposition of the coating and that the uncoated drug loaded samples were submitted to a process that mimicked the one undergone by the coated hydrogels.

The effect of the coating on DCF release from the TRIS/NVP/HEMA hydrogels and the SofLens and Purevision lenses was assessed under sink conditions (**Figure 4.3A**-**C**). Since SofLens are daily wear SCLs, the drug release was analysed only for 24 h. The coating showed a barrier effect for the release of DCF, avoiding the initial burst demonstrated by the uncoated hydrogels.

A
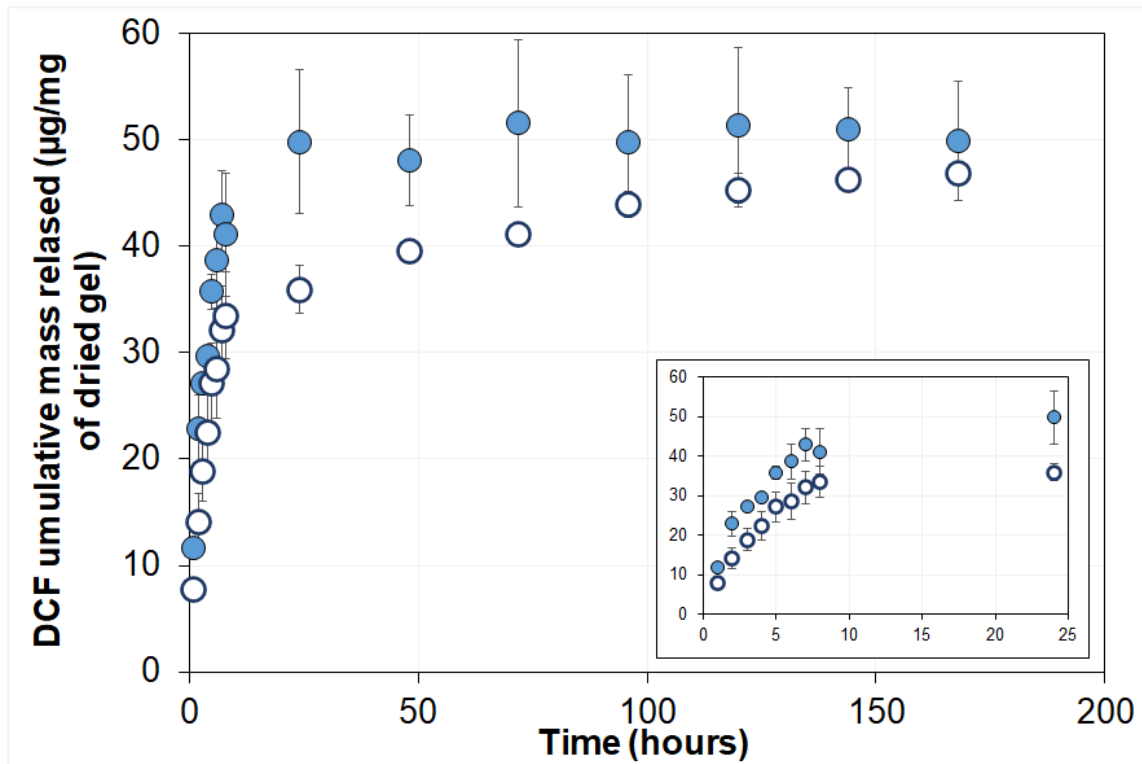
B
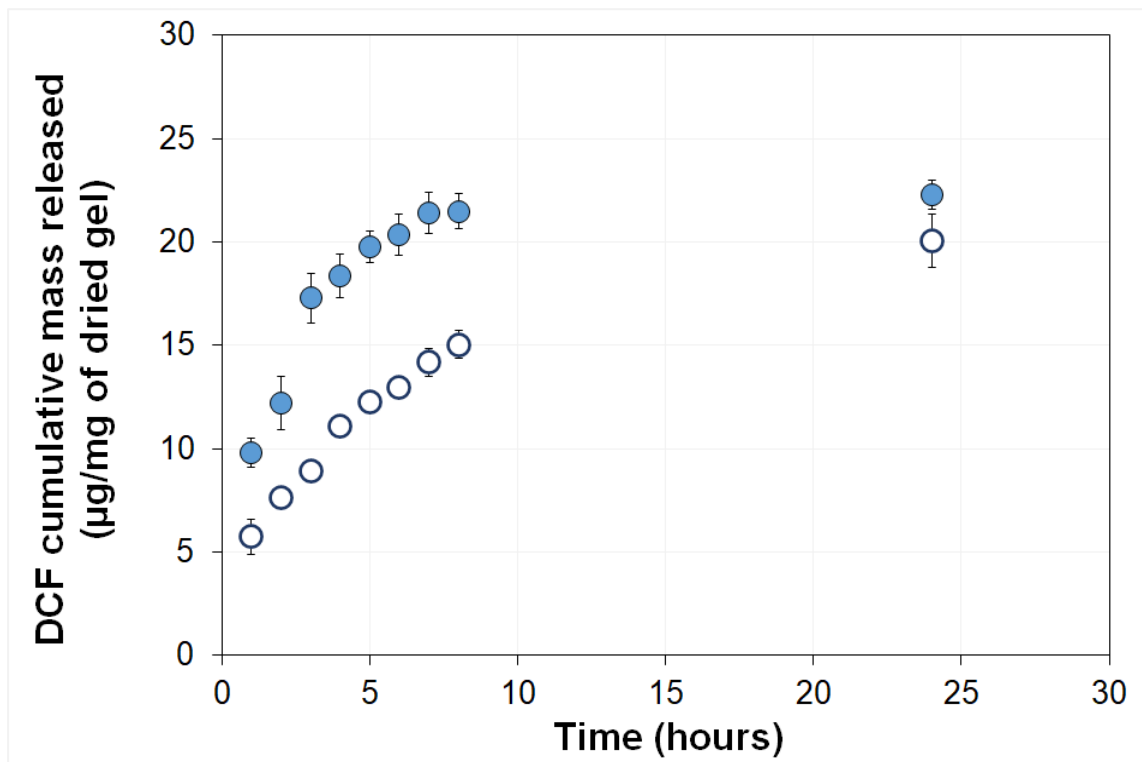
C
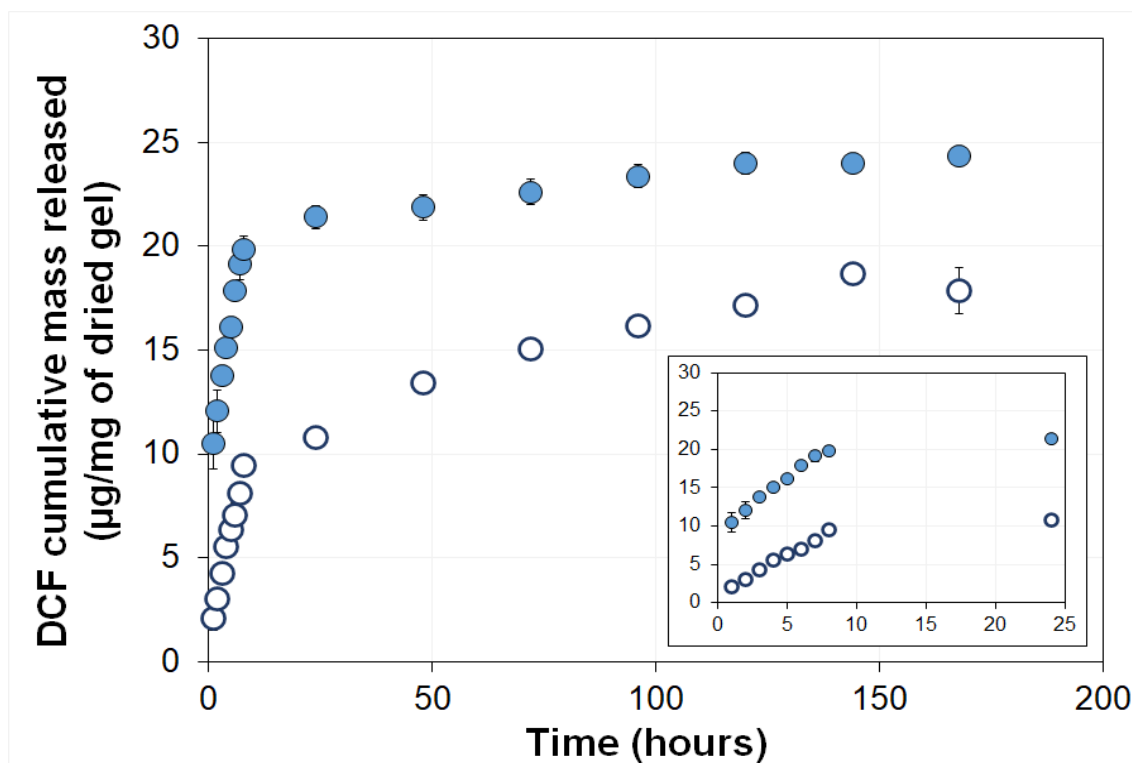
Figure 4.3 DCF release profiles from TRIS/NVP/HEMA hydrogels (**A**), SofLens (**B**) and Purevision (**C**) with (○) and without (●) ALG/CHI/HA coating. The inserts show the first 24 h of the release data. The error bars are the ± standard deviations (n=4). For daily wear SofLens the drug release was analysed only for 24 h.

The cumulative release in percentage (**Figure 4.4**) showed that the uncoated samples release >90% of the total amount of drug in the first 24 h, while coated samples achieve this plateau after 120 h.

A
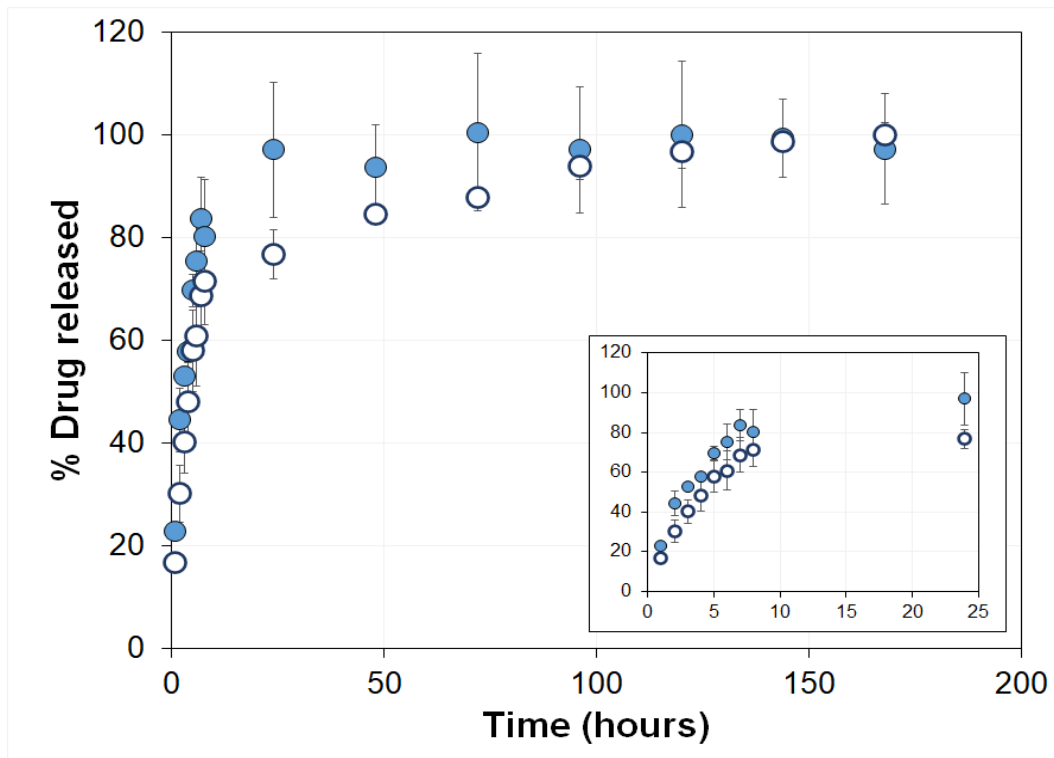
B
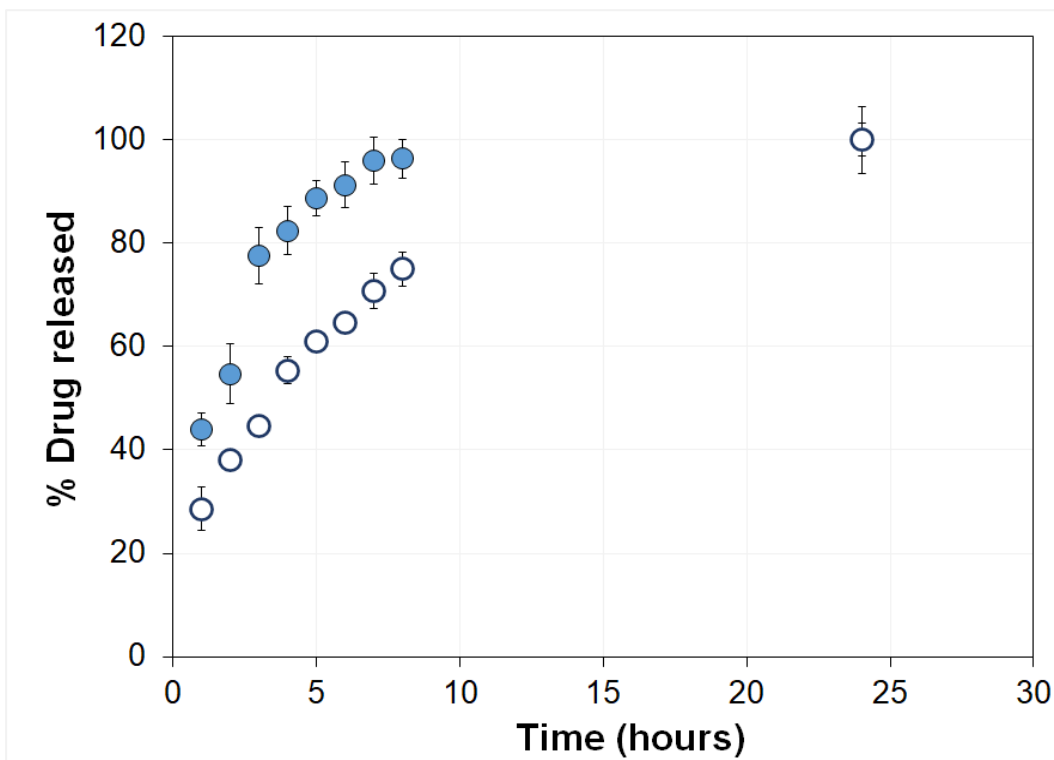
C
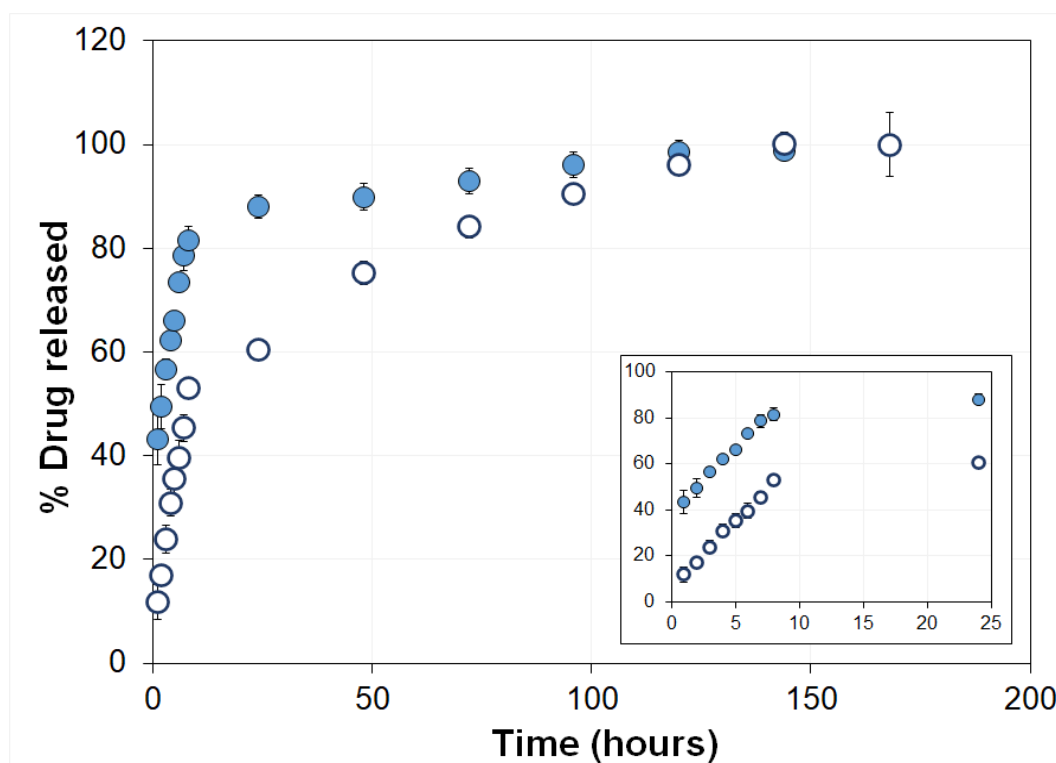
Figure 4.4 Percentage cumulative mass released vs time for DCF from TRIS/NVP/HEMA samples **(A)**, SofLens **(B)** and Purevision **(C)** with (○) and without (●) ALG/CHI/HA coating. The inserts show the first 24 h of the release data. The error bars are the ± standard deviations (n=4). For daily wear SofLens the drug release was analysed only for 24 h.

Comparison of the amounts of drug loaded with the drug released demonstrates that a high percentage of drug was kept inside the TRIS/NVP/HEMA hydrogel (55% for the uncoated and 59% for the coated samples). Although this hydrogel is thicker than the commercial lenses, it leads to a higher initial release rate which means that the diffusivity of the drug is larger and/or the drug distribution inside the polymeric matrix is not homogeneous.

4.3.3 Characterization of the coated TRIS/NVP/HEMA hydrogels loaded with DCF

Some physical properties of the LbL coated TRIS/NVP/HEMA hydrogels, which are relevant for its application in therapeutic SCLs were assessed. The water uptake of the uncoated and coated hydrogels is shown in **Table 4.1**. No significant difference was assessed for the water content (%) value with the presence of the ALG/CHI/HA coating (p =0.658). The transmittance profiles of the uncoated and coated hydrogels loaded with DCF differed in the 600 nm region (**Figure 4.5**), where a decrease (p < 0.00004) in transmittance occurred due to the blue colour of the coated samples (**Figure 4.6A** and **B**). resulting from the crosslinking of GE [17]. However, even in this region, the transmittance of the coated hydrogels was above the required value (90%) [18].
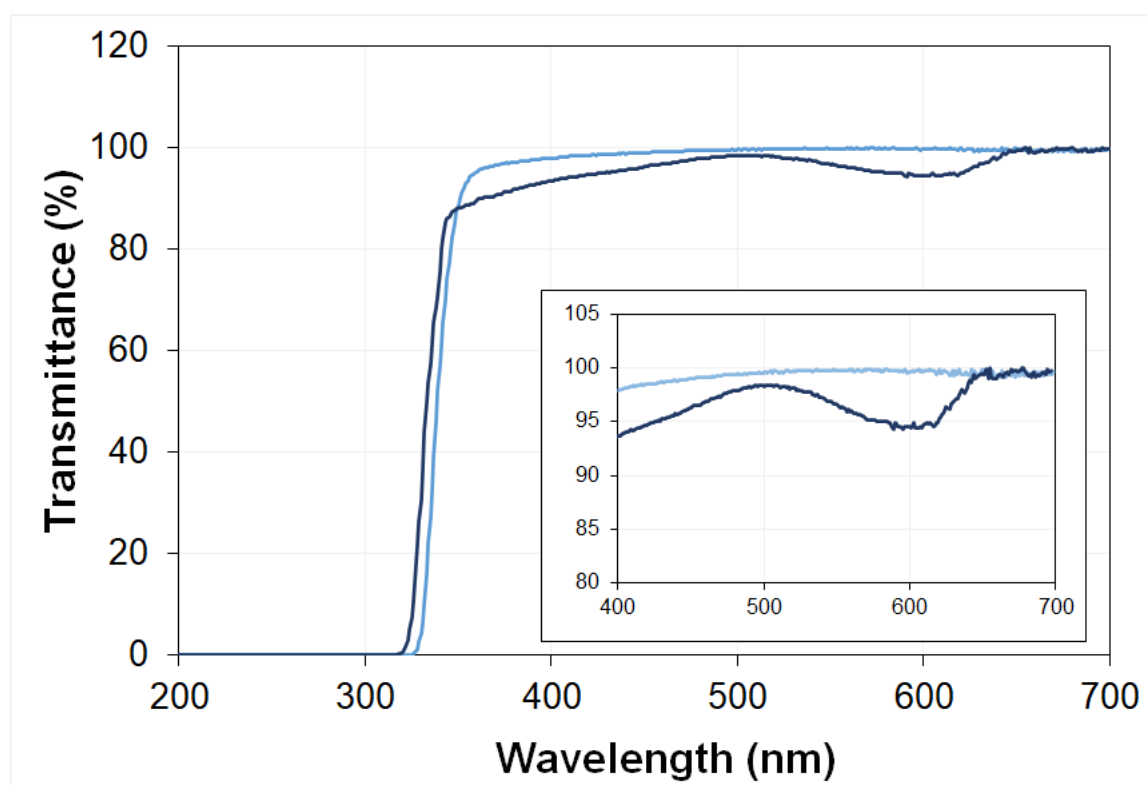
Figure 4.5 Transmittance of uncoated (——) and coated (——) TRIS/NVP/HEMA hydrogels loaded with DCF. The insert expands the spectra in the 400 to 700 nm interval.

137

A   B
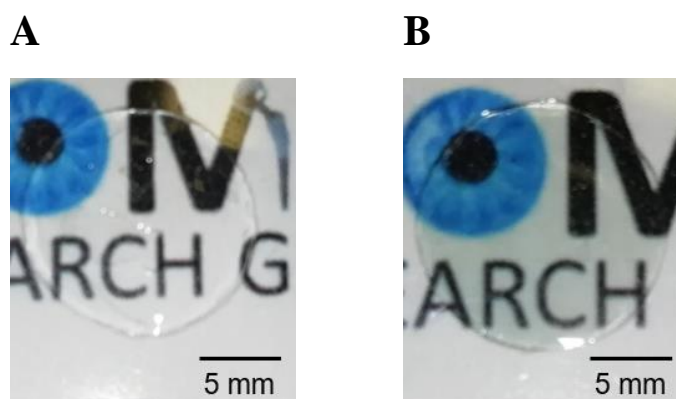
Figure 4.6 Pictures of TRIS/NVP/HEMA samples: uncoated, non-sterilized **(A)** and coated, non-sterilized **(B)**.

The AFM topographic images of the uncoated and ALG/CHI/HA coated hydrogels are shown in **Figure 4.7**. The coating, showing some scattered grainy structures, completely hided the typical porous structure of the TRIS/NVP/HEMA hydrogels. The R_a of the coated hydrogel was smaller when compared to that of the uncoated one (p = 0.045) (**Table 4.1**).

A
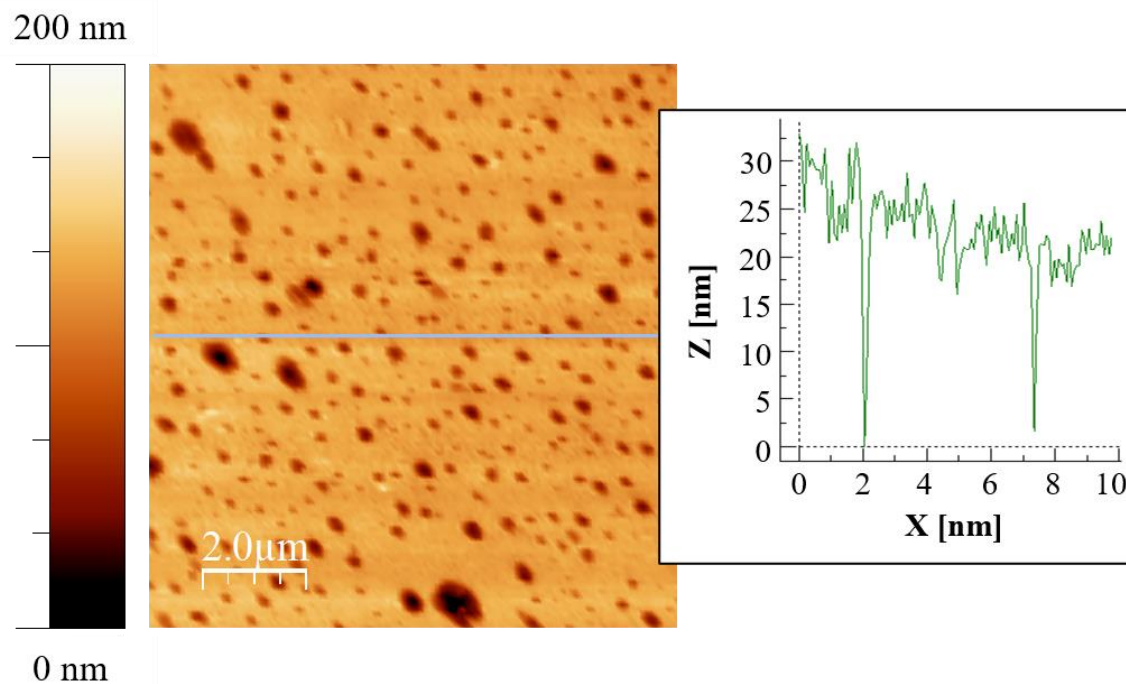
B
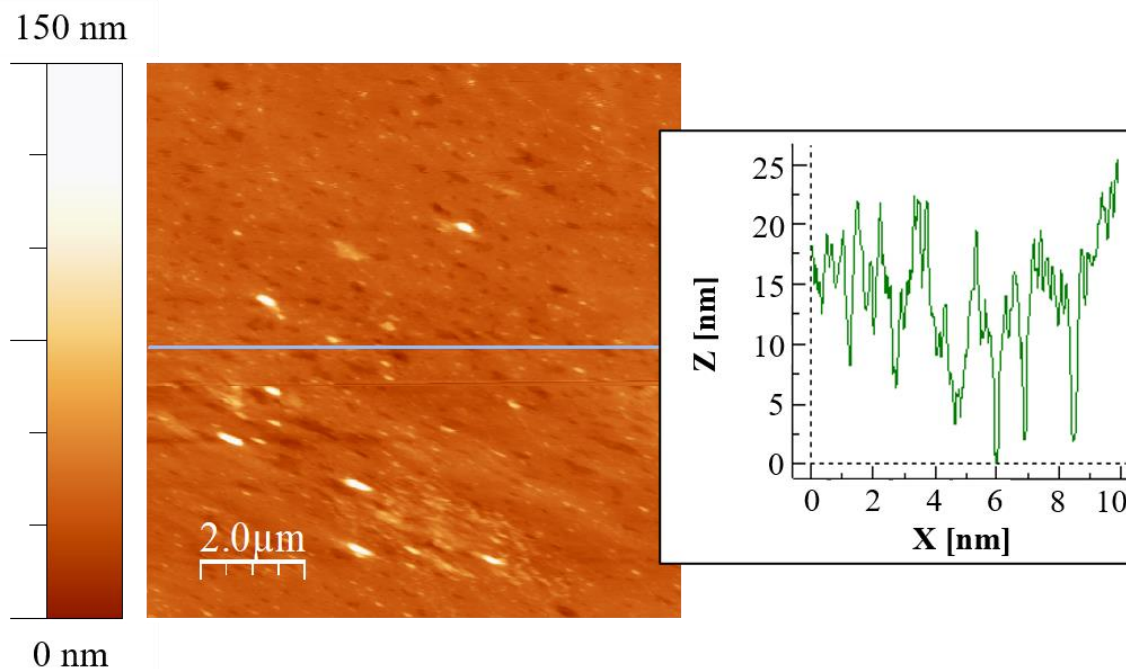
Figure 4.7 AFM images (10 x 10 µm^2) of the surface of uncoated **(A)** and coated **(B)** TRIS/NVP/HEMA hydrogels. The profiles correspond to the grey lines indicated in the images for the uncoated and coated hydrogels.

139

Table 4.1 Properties of uncoated and coated TRIS/NVP/HEMA hydrogels: water uptake, R_a, coating thickness, water contact angle, refractive index, and ionic permeability. The errors are shown as ± standard deviations (in all cases n=3, except for thickness n=5 and water contact angle n=10).

Property	Uncoated	Coated
Water uptake (%)	76±2	75±4
R_a (nm)	20±9	6±2
Coating thickness (nm)	-	71±7
Water contact angle (º)	35±5	32±3
Refractive index	1.417±0.002	1.358±0.003
Ionic permeability (cm²/s)	$5 \times 10^{-7} \pm 0.2 \times 10^{-7}$	$4 \times 10^{-7} \pm 0.5 \times 10^{-7}$

A 71±7 nm coating thickness was estimated (**Table 4.1**) from the viscoelastic modelling of the QCM-D data (Q-sense Dfind software (Broad Fit)), assuming for the film density the value 1 g/cm³, which has been found for other films of polyelectrolyte, polysaccharide, and/or synthetic polymer [19]. A 10% change in the value of the density would imply values of the thickness varying between 63 nm and 80 nm. These values agree with the thickness estimated by ellipsometry, 80±2 nm, and are comparable to those measured in chapter 2 and 3 for similar coatings. However, it was difficult to find suitable modelling for the ellipsometric data obtained with the coated TRIS/NVP/HEMA hydrogel, probably due to their high dispersion, which may be attributed to some heterogeneity in this type of hydrogels.

The wettability of the hydrogels did not reveal any alteration after the surface modification since they were already hydrophilic. Although TRIS/NVP/HEMA is slightly hydrophobic in the dry state, it becomes hydrophilic in the hydrated state, and its hydrophilic nature remained

after the deposition of the ALG/CHI/HA coating, as shown by the contact angle values in **Table 4.1**. In the presence of the coating, the refraction index decreased (p < 0.0000002) to a value within the average values for contact lenses [20], and the ionic permeability also decreased but remained well above the minimum required value (1.067×10^{-9} cm^2/s) for proper contact lens movement [21].

4.3.4 Sterilization effects

To evaluate the resistance of the coating to sterilization, uncoated and coated drug-loaded TRIS/NVP/HEMA hydrogels were submitted to SP, and HHP sterilization. After SP sterilization, the coating revealed irreversible degradation, turning black (**Figure 4.7A**). In the case of HHP sterilization, no visible degradation of the coating was observed (**Figure 4.7B**).
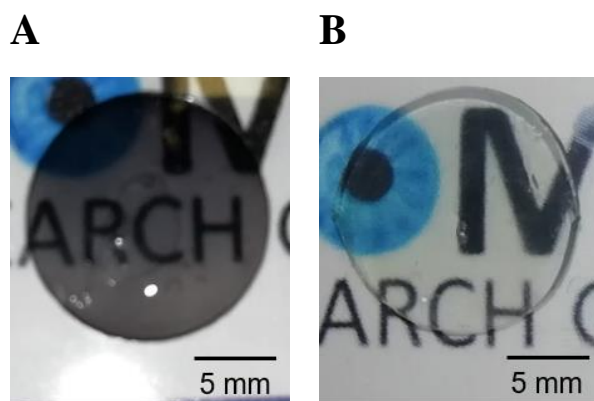
Figure 4.8 Pictures of the coated TRIS/NVP/HEMA hydrogels: after SP sterilization (**A**), and HHP sterilization (**B**).

The release profiles of the uncoated and coated hydrogels were recorded under sink conditions before and after sterilization (**Figure 4.9**). HHP sterilization did not appear to affect the hydrogel matrix, as the release profiles for the uncoated samples with and without sterilization were similar. A small decrease in the amount of the drug release occurred after HHP sterilization of the coated hydrogels (p < 0.0004), as further crosslinking of the coating could

have occurred, but the pattern of the drug release profile was maintained. In fact, increasing the pressure may facilitate the approach of the polymeric chains and favour electrostatic interactions involved in the GE crosslinking process [22]. This hypothesis was indeed confirmed by the decrease in transmittance around 600 nm from >95% to 91% after HHP sterilization (**Figure 4.10**). Nevertheless, the value remains above 90%, which is the minimum required for SCLs [18]. The refraction index of the sterilized hydrogels did not show significant differences when compared to non-sterilized samples (p = 0.239), varying from 1.358±0.03 for the samples before sterilization and 1.369±0.017 for the sterilized samples.
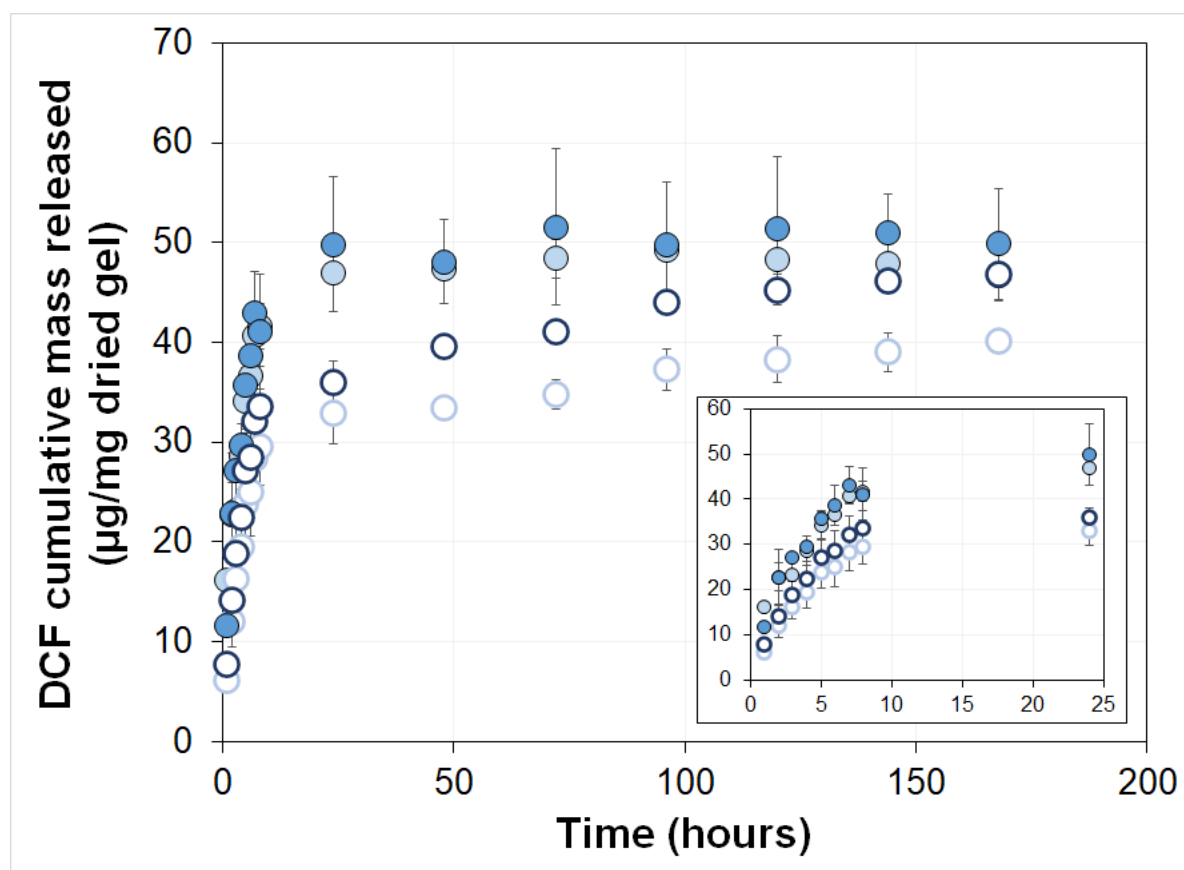
Figure 4.9 DCF release profiles from TRIS/NVP/HEMA hydrogels with (open symbols) and without (closed symbols) ALG/CHI/HA coating, before (dark symbol) and after (light symbol) HHP sterilization. The insert represents the first 24 h of the release data. The error bars are the ± standard deviations (n=4).
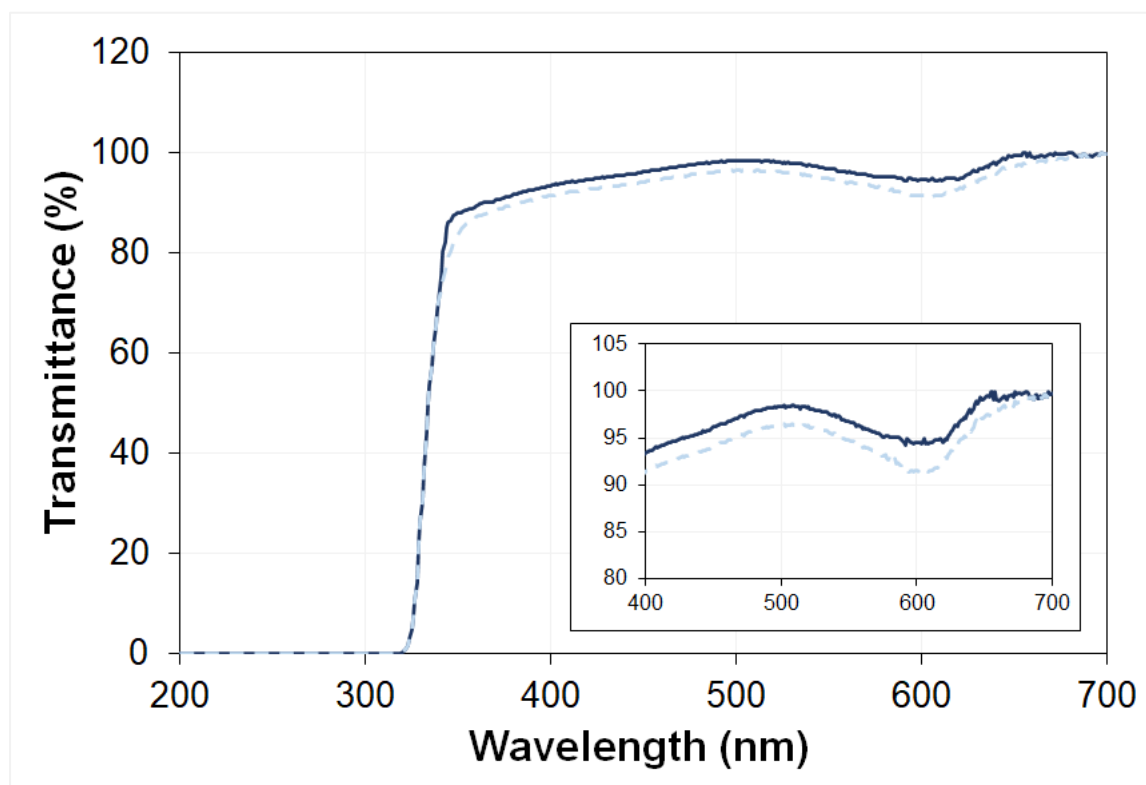
Figure 4.10 Transmittance of both coated TRIS/NVP/HEMA hydrogels loaded with DCF before (——) and after (– –) HHP sterilization. The insert represents the transmittance between 400 and 700 nm wavelength.

4.3.5 Antibacterial assays

The next step was to challenge the unloaded (uncoated and coated) and drug-loaded (coated) hydrogels against *S. aureus* and *P. aeruginosa* (**Figure 4.11**). Unloaded hydrogels without the coating did not demonstrate any capability of inhibiting the bacteria growth after 24 h incubation. The coating revealed some antibacterial activity, which must be related to the top layer of HA, as demonstrated in the chapter 3. The combination of DCF and coating was especially efficient in reducing the growth of *S. aureus* ($p < 0.000004$).
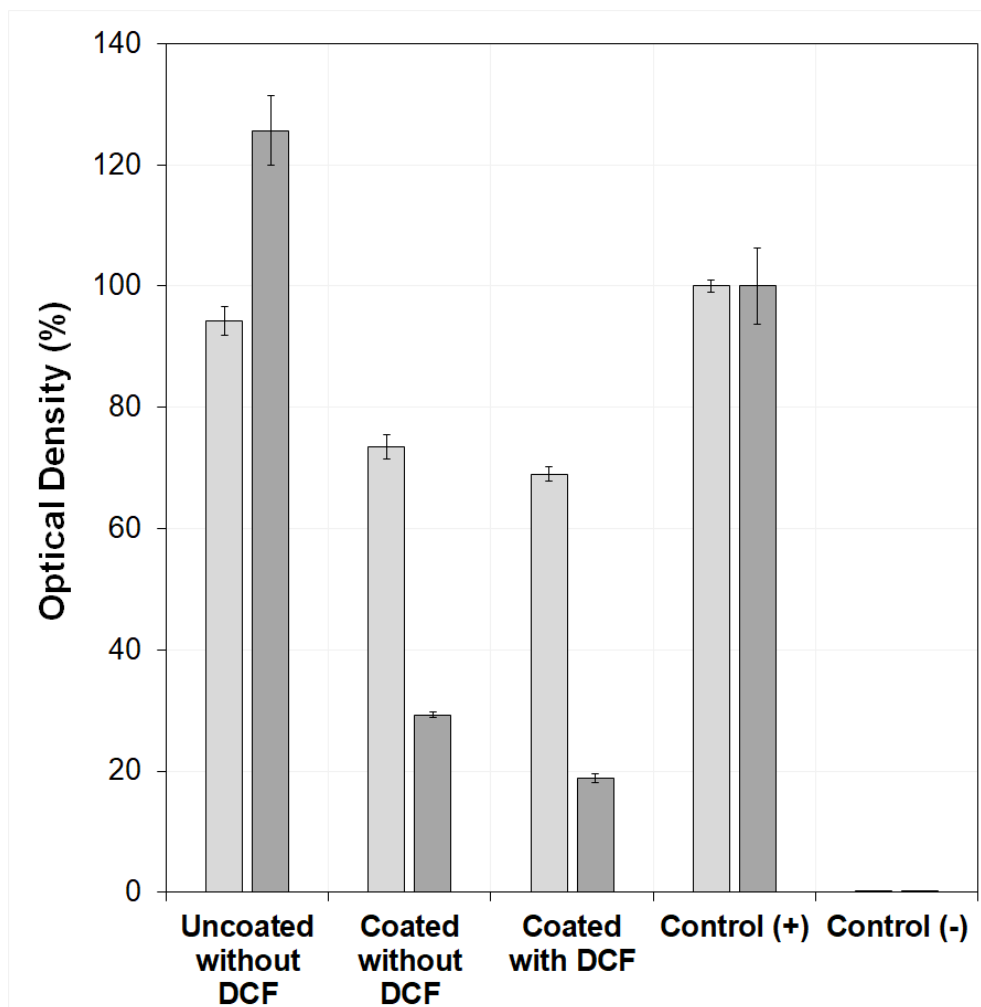
Figure 4.11 Optical density values of media containing *P. aeruginosa* (▢) or *S. aureus* (▦) after 24 h incubation with uncoated and coated TRIS/NVP/HEMA hydrogels with and without DCF. The error bars represent the ± standard deviations (n=4).

4.3.6 HET-CAM test

HHP sterilized non-loaded uncoated and coated TRIS/NVP/HEMA hydrogels, and DCF-loaded and coated hydrogels, were directly placed on the CAM for 5 min. All hydrogels behaved similarly to the negative control (NaCl, 0.9%), in opposition to the severe irritation and haemorrhage caused by the positive control (NaOH, 1 M) (**Figure 4.12**).
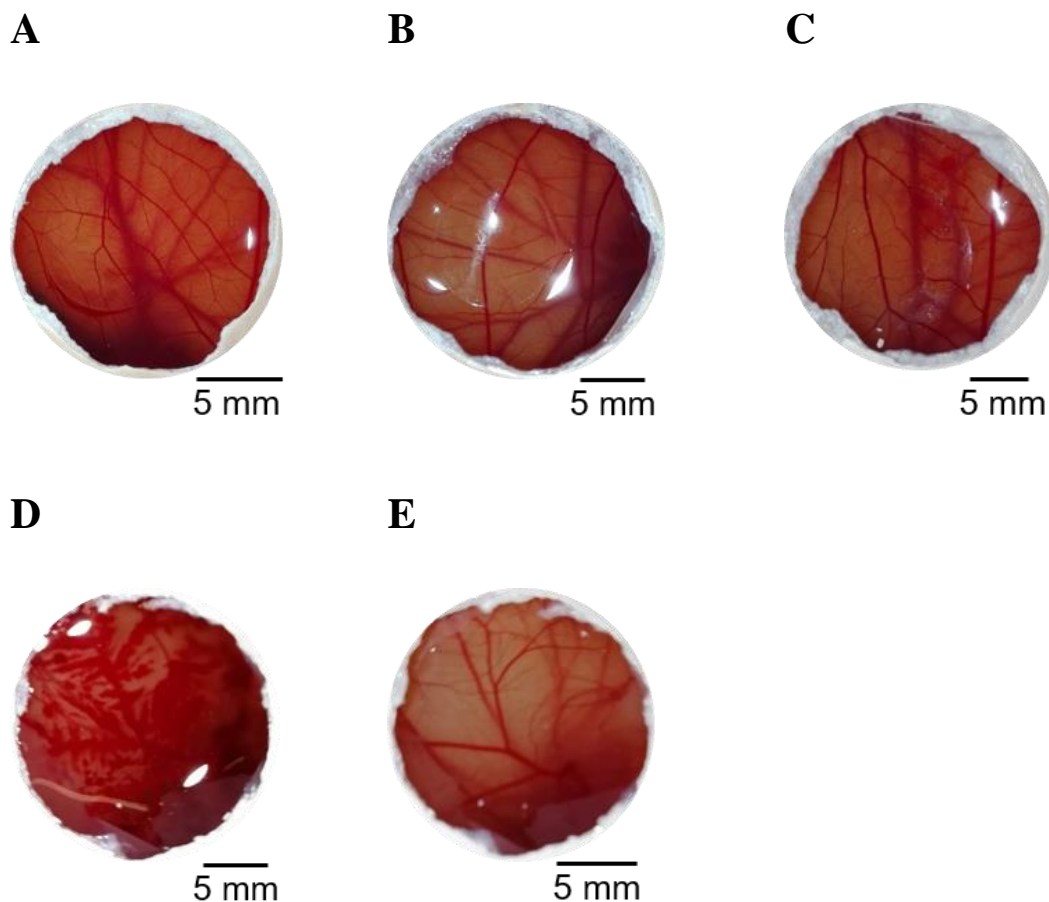
Figure 4.12 CAM images after 5 min contact with: Unloaded TRIS/NVP/HEMA hydrogels without coating **(A)** and with coating **(B)**, and loaded samples with coating **(C)**. Positive control **(D)** and negative control **(E)**.

4.3.7 Cytotoxicity tests

The MTT test was used to assess the cell viability of NIH/3T3 cells after incubation with HHP sterilized unloaded TRIS/NVP/HEMA hydrogels, with and without coating, and DCF loaded coated hydrogels. As seen in **Figure 4.13**, without DCF, both uncoated and coated samples demonstrated cell viability of ~100%. The presence of the drug resulted in a small decrease in viability (p = 0.045), but such viability level (> 80%) indicates that the hydrogel is not toxic.
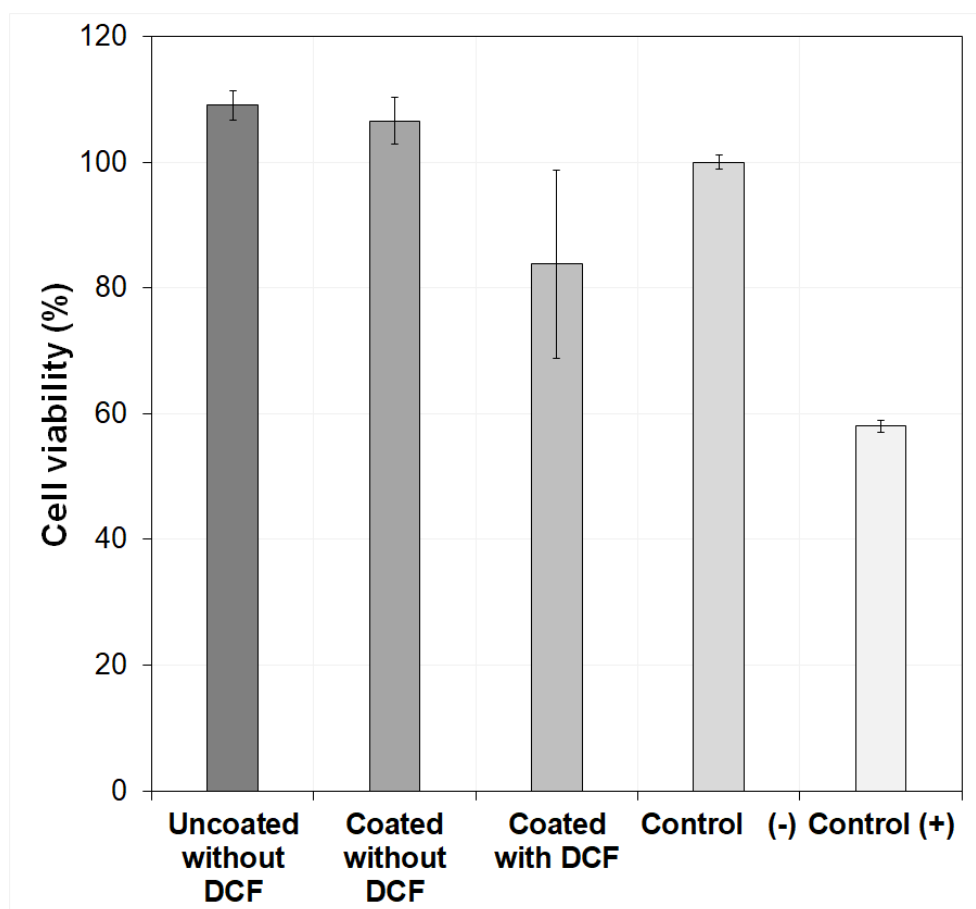
Figure 4.13 NIH/3T3 cells viability (%) determined by MTT assay, after 24 h exposure to uncoated and coated TRIS/NVP/HEMA hydrogels without and with DCF. Bars represent mean values ± standard deviations (n=5).

4.4 Discussion

In the present work, a combination of polysaccharides ALG, CHI and HA was explored with the aims of regulating drug release kinetics and keeping the antibacterial properties and tear protein resistance, while avoiding permanent drug trapping inside the hydrogel. Moreover, and mandatory from the point of view of the clinical use of SCLs as medicated medical devices, the coating should withstand sterilization protocols; an issue largely unattended. The new coating designated as ALG/CHI/HA was designed using GE as crosslinker. GE can spontaneously react with amino groups of CHI (**Figure 4.14**) and provide positively charged amino groups that would attract negatively charged carboxylic groups of ALG and HA [23]. GE is a small molecule, able to freely diffuse through HA and interact with CHI. It can also

form glycosidic bonds with the available hydroxyl groups of HA, further stabilizing the LbL coating [24].
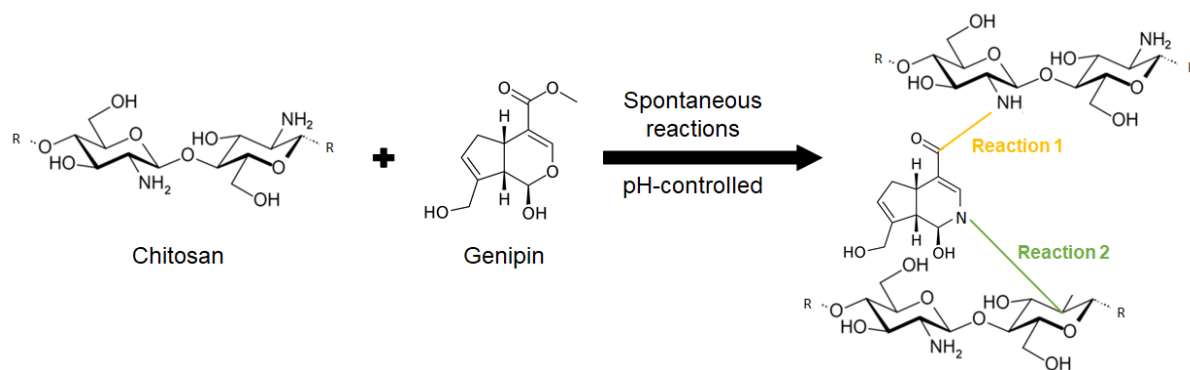
Figure 4.14 GE crosslinking reactions with CHI. Substitution of the ester group of GE by a secondary amine linkage (reaction 1) and formation of an intermediate aldehyde group on GE due to a ring-opening reaction from a nucleophilic attack by the amino groups in CHI (reaction 2) [23,25].

The coating ALG/CHI/HA was able to improve the release kinetics of DCF from the commercial lenses SofLens and Purevision as well as from the TRIS/NVP/HEMA sample. The initial burst was reduced and the release period was significantly extended. Furthermore, the coating did not compromise the optical properties and even reduced the surface roughness (see **Table 4.1**). The presence of HA, as the upper layer, minimized the interaction with lysozyme, in agreement with the results shown in chapter 3.

A simple mathematical model described in section 3.4 of chapter 3, was used to estimate the efficiency of the coated samples in contrast with the uncoated samples in terms of drug delivery in an *in vivo* simulation. Briefly, this mathematical model estimates the amount of drug delivered by the drug eluting SCLs to the lachrymal fluid (M_d), during a given time interval (Δt), through the following equation:

$$M_d = q \, m_t \, \Delta t \qquad\qquad \textbf{Equation 4.1}$$

where m_t is the dry mass of the lens and q is the drug release rate per unit mass of dry gel which may be obtained by fitting the drug release data to the Korsmeyer-Peppas equation [26]. The concentration of DCF in the tear fluid at time t (in min) was calculated using **Equation 3.1** in chapter 3. For the TRIS/NVP/HEMA hydrogel the mass of the dry gel was estimated for a 14 mm diameter and 0.09 mm thickness (8.8 mg). The tear volume was considered homogeneous, regardless the fact that the drug does not completely mix with the lachrymal fluid.

The release profiles estimated for uncoated and coated hydrogels are shown in **Figure 4.15**. The ranges of the IC$_{50}$ values for the enzymes active in the inflammatory response, COX-1 (0.04 – 0.3 µg/mL) and COX-2 (0.01-0.03 µg/mL) [27], were included to allow an evaluation of the samples efficiency in terms of DCF delivery in the tear fluid. The presence of the coating ensured drug levels were well above the lower limits of COX-1 and COX-2 for 15 days. The drug burst decreased for the coated samples, especially in the case of TRIS/NVP/HEMA hydrogel.
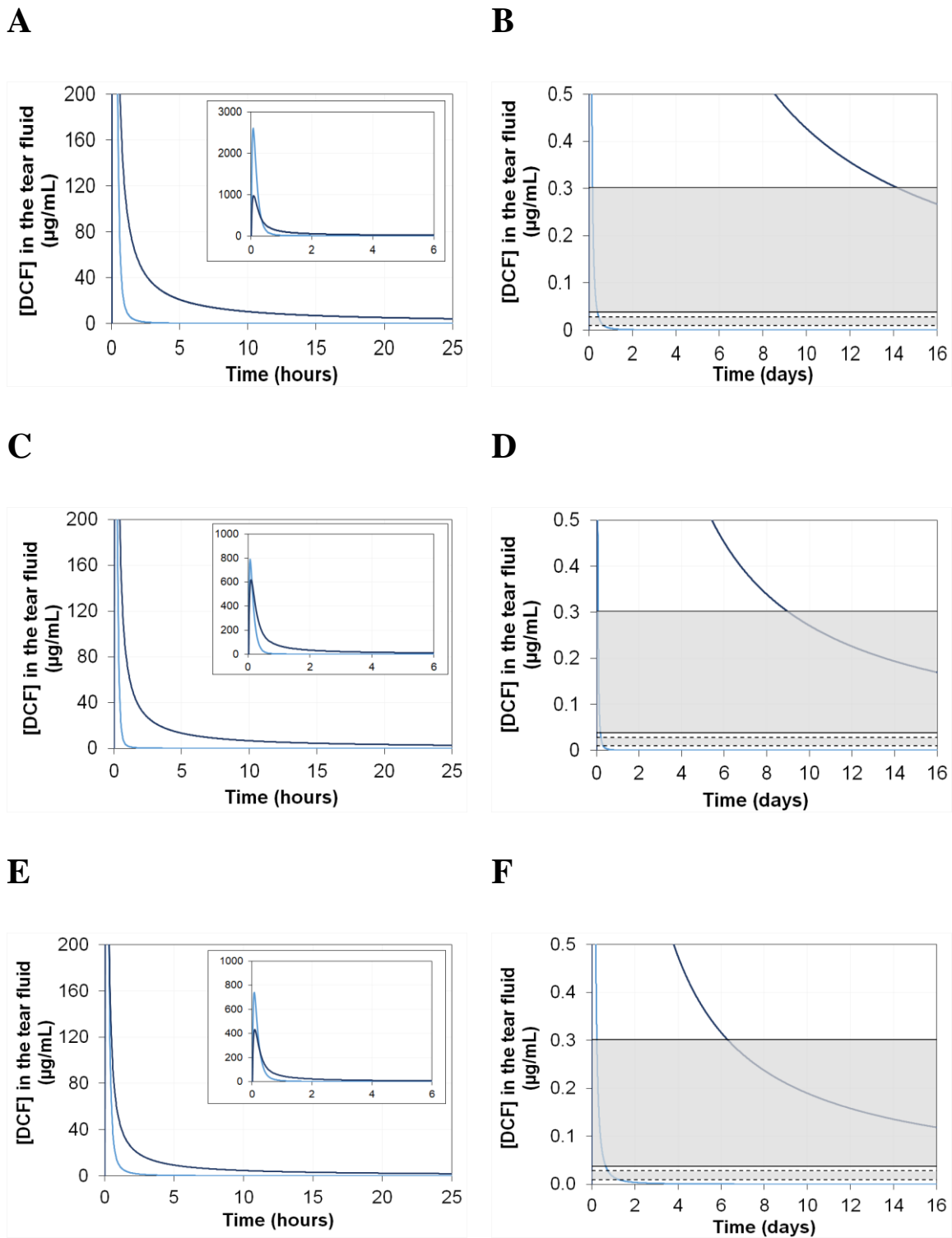
Figure 4.15 Mathematical estimation of the DCF concentration in the lachrymal fluid obtained from the cumulative release data for TRIS/NVP/HEMA hydrogels (**A** and **B**), SofLens (**C** and **D**) and Purevision (**E** and **F**) SCL coated with ALG/CHI/HA (——) compared to uncoated samples (——). **Figures 4.15A**, **C** and **E** show the first 24 h, while **Figures 4.15B**, **D** and **F** refer

to an extended period of 16 days. The shaded areas represent the ranges of IC_{50} limited by solid lines for COX-1 and dotted lines for COX-2. The inserts represent the first 6 h of release.

The polyelectrolytes chosen for the LbL coating are known to interact with DCF molecule, favouring the retardation of its diffusion and thus controlling the release rate. DCF sustained release can be attributed to physical entrapment inside the CHI matrix [28,29] and/or the three-dimensional structure of HA bonds, as well as bonding between carboxyl groups of DCF and hydroxyl groups of ALG. The specific efficiency of the HA layers for sustained release of DCF may be attributed to hydrogen bonding between the H bond acceptors in DCF and the hydroxyl groups in HA, while other authors suggested a preferential interaction of DCF with the hydrophobic domains of HA [30]. In addition, GE can also be involved in the control of DCF release through the interaction with the secondary amine of this molecule.

Regarding the scale-up for the manufacturing of coated SCLs with naturally based polyelectrolytes, stability against sterilization is critical. Commercial lenses are usually sterilized during the packaging process by SP sterilization [31]. As previously demonstrated, this method cannot be applied to natural polymers coating. Naturally obtained polyelectrolytes used in the LbL coating are known to suffer hydrolysis during the sterilization as a result of high temperature [31,32].

According to previous reports [33], HHP sterilization seems to be an alternative method to overcome the SP disadvantages. The HHP sterilization did not affect the uncoated TRIS/NVP/HEMA hydrogels but may have led to additional crosslinking of the ALG/CHI/HA coating, further improving the barrier effect for DCF. This effect was confirmed by the intensification of the blue colour of the coated hydrogels. As GE is known to crosslink CHI and other amines [23] in a spontaneous way, favouring amine/ester bonds [34] the blue coloration presented by the hydrogels is a secondary result of the oxygen radical induced polymerization of GE. Despite this colour change, which was responsible for a slight decrease in the optical transmittance, the optical properties of the sterilized samples remained within the limits adequate for their use as SCLs.

The antibacterial tests showed a complementary effect of the drug and the coating (**Figure 4.12**) that led to a substantial decrease in the growth of *S. aureus*, while for *P. aeruginosa* the

coating was less efficient. The antibacterial effect of the coating can be attributed to both the HA upper layer and crosslinker GE. The antibacterial effect of HA remains a controversial issue [35], but, in contrast, there is experimental evidence of this effect for GE. Wu *et al.* (2014) produced GE crosslinked hydrogels that fully inhibited *S. aureus* [36], and Wang *et al.* (2015) showed that GE, as a crosslinker, promoted the formation of a poly(sulfobetaine methacrylate)-CHI material with high antibacterial efficiency [37].

The coating ALG/CHI/HA did not reveal any ocular irritancy with a IS equal to 0 (according the HET-CAM test) and did not lead to any level of cytotoxicity. However, when the coated samples were loaded with DCF, a decrease in cell viability was obtained. According to several authors, DCF eye drop solution can affect the normal corneal epithelial healing [38–40] Such result may be related to several factors: 1) low concentration of Na^+; 2) the presence of preservatives; and 3) lipoxygenase blockers in high concentration [38,41,42]. The use of preservatives, can be reduced by drug delivery from SCLs, as these materials remain in contact with the eye increasing drug bioavailability [43].

In this work, the drug loading was done with DCF dissolved in NaCl aqueous solution, thus the slight decrease in cell proliferation shown by the coated hydrogel, loaded with DCF, can only be attributed to the active component. Qu *et al.* (2011) demonstrated that human corneal epithelial cells viability was of ~95% when exposed to DCF in a concentration 10 times lower than the one used in this work [44]. Therefore, and according to the ISO standard 10993-5 (2009), in which a cell viability ≥ 70% is accepted for medical devices, neither the coating nor the drug can be considered toxic.

Comparison of the performance of the ALG/CHI/HA coating with the other coatings developed in chapter 2 and 3 demonstrates that the new coating has strong advantages. Besides its anti-bacterial properties, it is more efficient in the control of drug release. When compared with ALG/PLL(EDC)//HA, it significantly reduces the amount of drug trapped inside the hydrogel from 78% in the former case to 59% in the present one. The higher amount of DCF retained inside the hydrogel coated with ALG/PLL(EDC)//HA derives from the fact that, below the layer of HA, the coating was composed by two double layers instead of one triple layer used in the new coating. In fact, the optimization of the number of layers carried out in chapter 2 led to the conclusion that two double layers was more favourable to control the DCF release, but with ALG/CHI/HA, one triple layer was enough, which may be attributed to the higher

efficiency of the crosslinking agent GE. In addition, GE was reported to be an excellent option for ophthalmic materials, due to its compatibility with both human retinal pigment epithelial cells and the anterior chamber of a rabbit eye model [45].

Overall, the ALG/CHI/HA coating seems very promising as a release control barrier for DCF from different substrates, including commercial SCLs. Although *in vivo* tests are necessary to confirm this claim, the measured properties strongly suggest the possibility of successfully using this coating to ensure the therapeutic ocular needs of the anti-inflammatory, DCF, for, at least, two weeks.

4.5   Conclusions

The layer-by-layer (LbL) coating composed of one triple layer of ALG/CHI/HA, crosslinked with GE, can endow SCLs with capability to regulate the release of the anti-inflammatory DCF, decreasing the initial burst, and to inhibit bacteria cell growth. Light transmittance, bulk refractive index, and ionic permeability remained within the range of values recommended for SCLs. The coating showed antifouling capability when exposed to lysozyme, was biocompatible, and showed antibacterial properties, more significantly in the case of *S. aureus*. To overcome the stability risks of polysaccharide coating when exposed to conventional sterilization methods, a new sterilization method based on the application of high hydrostatic pressure was successfully applied. The concentration of DCF, estimated by a simple mathematical model, may remain above the IC_{50} values for COX-1 and COX-2 over more than 15 days.

4.6 References

[1]   S. Benavides, R. Villalobos-Carvajal, J.E. Reyes, Physical, mechanical and antibacterial properties of alginate film: Effect of the crosslinking degree and oregano essential oil concentration, J. Food Eng. 110 (2012) 232–239.

[2]   M.S. Benhabiles, R. Salah, H. Lounici, N. Drouich, M.F.A. Goosen, N. Mameri, Antibacterial activity of chitin, chitosan and its oligomers prepared from shrimp shell waste, Food Hydrocoll. 29 (2012) 48–56.

[3]   M. Kong, X.G. Chen, H.J. Park, Antimicrobial properties of chitosan and mode of action: A state of the art review, Int. J. Food Microbiol. 144 (2010) 51–63.

[4]   M.N. V. Ravi Kumar, R.A.A. Muzzarelli, C. Muzzarelli, H. Sashiwa, A.J. Domb, Chitosan Chemistry and Pharmaceutical Perspectives, Chem. Rev. 104 (2004) 6017–6084.

[5]   E.I. Rabea, M.E.T. Badawy, C. V. Stevens, G. Smagghe, W. Steurbaut, Chitosan as antimicrobial agent: Applications and mode of action, Biomacromolecules. 4 (2003) 1457–1465.

[6]   B. Manickam, R. Sreedharan, M. Elumalai, 'Genipin' - The natural water soluble cross-linking agent and its importance in the modified drug delivery systems: An overview, Curr. Drug Deliv. 11 (2014) 139–145.

[7]   T. Bourcier, F. Thomas, V. Borderie, C. Chaumeil, L. Laroche, Bacterial keratitis: predisposing factors, clinical and microbiological review of 300 cases, Bras. J. Ophthalmol. 87 (2003) 834–838.

[8]   P. Garg, Fungal, mycobacterial, and nocardia infections and the eye: an update, Eye. 26 (2012) 245–251.

[9]   R. Vasquez, R. Nogueira, M. Orfão, J. Mata, B. Saramago, Stability of triglyceride liquid films on hydrophilic and hydrophobic glasses, J. Colloid Interface Sci. 299 (2006) 274–282.

[10]   P. Paradiso, R. Galante, L. Santos, A.P. Alves De Matos, R. Colaço, A.P. Serro, B. Saramago, Comparison of two hydrogel formulations for drug release in ophthalmic

lenses, J. Biomed. Mater. Res. B. 102 (2014) 1170–1180.

[11] A.K. Mitra, T.J. Mikkelson, Ophthalmic solution buffer systems. II. Effects of buffer type and concentration on the ocular absorption of pilocarpine and a method of ocular bioavailability prediction from physicochemical data, Int. J. Pharm. 37 (1987) 19–26.

[12] C. Delajon, T. Gutberlet, R. Steitz, H. Möhwald, R. Krastev, Formation of polyelectrolyte multilayer architectures with embedded DMPC studied in situ by neutron reflectometry, Langmuir. 21 (2005) 8509–8514.

[13] J. Hernandez-Montelongo, V.F. Nascimento, D. Murillo, T.B. Taketa, P. Sahoo, A.A. Souza, M.M. Beppu, M.A. Cotta, Nanofilms of hyaluronan/chitosan assembled layer-by-layer: An antibacterial surface for Xylella fastidiosa, Carbohydr. Polym. 136 (2016) 1–11.

[14] C.K.S. Pillai, W. Paul, C.P. Sharma, Chitin and chitosan polymers: Chemistry, solubility and fiber formation, Prog. Polym. Sci. 34 (2009) 641–678.

[15] A. Mero, M. Campisi, Hyaluronic acid bioconjugates for the delivery of bioactive molecules, Polymers (Basel). 6 (2014) 346–369.

[16] M. Li, T. Elder, G. Buschle-Diller, Alginate-based polysaccharide beads for cationic contaminant sorption from water, Polym. Bull. (2016) 1–15.

[17] T. Imsombut, Y. Srisuwan, P. Srihanam, Y. Baimark, Genipin-cross-linked silk fibroin microspheres prepared by the simple water-in-oil emulsion solvent diffusion method, Powder Technol. 203 (2010) 603–608.

[18] N. Efron, C. Maldonado-Codina, Development of contact lenses from a biomaterial point of view – Materials, manufacture, and clinical application, in: Compr. Biomater., Comprehensive Biomaterials. Elsevier, 2011: pp. 517–541.

[19] C.R. Wittmer, J.A. Phelps, C.M. Lepus, W.M. Saltzman, M.J. Harding, P.R. VanTassel, Multilayer nanofilms as substrates for hepatocellular applications, Biomaterials. 29 (2008) 4082–4090.

[20] P. Tankam, J. Won, C. Canavesi, I. Cox, J.P. Rolland, Optical assessment of soft contact lens edge-thickness, Optom. Vis. Sci. 93 (2017) 987–996.

[21]   R. Galante, P. Paradiso, M.G. Moutinho, A.I. Fernandes, J.L.G. Mata, A.P.A. Matos, R. Colaço, B. Saramago, A.P. Serro, About the effect of eye blinking on drug release from pHEMA-based hydrogels: An in vitro study, J. Biomater. Sci. Polym. Ed. 26 (2015) 235–251.

[22]   S. Mutsuo, K. Yamamoto, T. Furuzono, T. Limura, T. Ono, A. Kishida, Pressure-induced molecular assembly of hydrogen-bonded polymers., J. Polym. Sci. B. 46 (2008) 743–750.

[23]   R.A.A. Muzzarelli, M. El Mehtedi, C. Bottegoni, A. Aquili, A. Gigante, Genipin-Crosslinked chitosan gels and scaffolds for tissue engineering and regeneration of cartilage and bone, Mar. Drugs. 13 (2015) 7314–7338.

[24]   J. Roether, C. Oelschlaeger, N. Willenbacher, Hyaluronic acid cryogels with non-cytotoxic crosslinker genipin, Mater. Lett. 4 (2019) 100027.

[25]   M.F. Butler, Y.-F. NG, P.D.A. Pudney, Mechanism and kinetics of the crosslinking reaction between biopolymers containing primary amine groups and genipin., J. Polym. Sci. Part A Polym. Chem. 41 (2003) 3941–3953.

[26]   J. Siepmann, N.A. Peppas, Modeling of drug release from delivery systems based on hydroxypropyl methylcellulose (HPMC), Adv. Drug Deliv. Rev. 48 (2001) 139–157.

[27]   R. Reddy, S.J. Kim, Critical appraisal of ophthalmic ketorolac in treatment of pain and inflammation following cataract surgery, Clin. Ophthalmol. 5 (2011) 751–75.

[28]   A. Bani-Jaber, D. Anani, I.I.I. Hamdan, B.A.A. Alkhalidi, Investigation of drug polymer interaction: Evaluation and characterization of diclofenac-chitosan co-precipitate, Jordan J. Pharm. Sci. 2 (2009) 140–149.

[29]   Y. Boonsongrit, A. Mitrevej, B. Mueller, Chitosan drug binding by ionic interaction, Eur. J. Pharm. Biopharm. 62 (2006) 267–274.

[30]   A. Schneider, C. Vodouhê, L. Richert, G. Francius, E.L. Guen, P. Schaaf, J.-C. Voegel, B. Frisch, C. Picart, Multifunctional polyelectrolyte multilayer films: Combining mechanical resistance, biodegradability, and bioactivity, Biomacromolecules. 8 (2008) 139–145.

[31] T. Glasbey, S.D. Newman, Methods and systems for contact lens sterilization, Patent no: US 8,109,064 B2, 2012.

[32] C. Ji, J. Shi, Sterilization-free chitosan hydrogels for controlled drug release, Mater. Lett. 72 (2012) 110–112.

[33] A. Topete, C.A. Pinto, H. Barroso, J.A. Saraiva, I. Barahonac, B. Saramago, A.P. Serro, High hydrostatic pressure (HHP) as sterilization method for drug-loaded intraocular lenses, Submitted. (n.d.).

[34] S.D. Nath, C. Abueva, B. Kim, B.T. Lee, Chitosan-hyaluronic acid polyelectrolyte complex scaffold crosslinked with genipin for immobilization and controlled release of BMP-2, Carbohydr. Polym. 115 (2015) 160–169.

[35] A. Ardizzoni, R.G. Neglia, M.C. Baschieru, C. Cermelli, M. Caratozzolo, M. Righi, B. Palmieri, E. Blasi, Influence of hyaluronic acid on bacterial and fungal species, including clinically relevant opportunistic pathogens, J. Mater. Sci. Mater. Med. 22 (2011) 2329–2338.

[36] F. Wu, G.L. Meng, J. He, Y. Wu, F. Wu, Z.W. Gu, Antibiotic-loaded chitosan hydrogel with superior dual functions: Antibacterial efficacy and osteoblastic cell responses, ACS Appl. Mater. Interfaces. 6 (2014) 10005–10013.

[37] R. Wang, K.G. Neoh, E.T. Kang, Integration of antifouling and bactericidal moieties for optimizing the efficacy of antibacterial coatings, J. Colloid Interface Sci. 438 (2015) 138–148.

[38] J.S. Lee, Y.H. Kim, Y.M. Park, The toxicity of nonsteroidal anti-inflammatory eye drops against human corneal epithelial cells in vitro, J. Korean Med. Sci. 30 (2015) 1856–1864.

[39] J.-K. Chang, G.-J. Wang, S.-T. Tsai, M.-L. Ho, Nonsteroidal Anti-inflammatory drug effects on osteoblastic cell cycle, cytotoxicity, and cell death, Connect. Tissue Res. 46 (2005) 200–210.

[40] M.-L. Ho, J.-K. Chang, G.-J. Wang, Antiinflammatory drug effects on bone repair and remodeling in rabbits, Clin. Orthop. Relat. Res. 313 (1995) 270–278.

[41]   S. Iwamoto, T. Koga, T. Okuno, M. Koike, A. Murakami, A. Matsuda, T. Yokomizo, Non-steroidal anti-inflammatory drug delays corneal wound healing by reducing production of 12-hydroxyheptadecatrienoic acid, a ligand for leukotriene B4 receptor 2, Sci. Rep. 7 (2017) 1–10.

[42]   S. Andalib, A.M. Maeini, A. Garjani, N.A. Asl, A. Abdollahi, A comparative study pertaining to deleterious effects of diclofenac sodium and meloxicam on kidney tissue in rats, EXCLI J. 10 (2011) 149–154.

[43]   C.J.F. Bertens, M. Gijs, F.J.H.M. van der Biggelaar, R.M.M.A. Nuijts, Topical drug delivery devices: A review, Exp. Eye Res. 168 (2018) 149–160.

[44]   M. Qu, Y. Wang, L. Yang, Q. Zhou, Different cellular effects of four anti-inflammatory eye drops on human corneal epithelial cells: independent in active components, Mol. Vis. 17 (2011) 3147–3155.

[45]   J.-Y. Lai, Biocompatibility of Genipin and Glutaraldehyde Cross-Linked Chitosan Materials in the Anterior Chamber of the Eye, Int. J. Mol. Sci. 13 (2012) 10970–10985.

5 Molecular imprinted silicone-based hydrogels as soft contact lenses materials for extended moxifloxacin release

The following results were submitted for publishing in the peer-reviewed article:

Diana Silva, Hermínio C. de Sousa, Maria Helena Gil, Luís F. Santos, Madalena Salema Oom, Carmen Alvarez-Lorenzo, Benilde Saramago, Ana Paula Serro; Molecular imprinted silicone-based hydrogels as soft contact lenses materials for extended moxifloxacin release. European Journal of Pharmaceutical Sciences

Table of Contents

5.1 Introduction

Previously, it was demonstrated that the lab-made hydrogel TRIS/NVP/HEMA possesses very interesting physical properties, which make it suitable for SCLs [1]. Furthermore, this LbL coated hydrogel may be used as a platform to deliver ophthalmic drugs, as described in chapters 2 and 3. However, not every drug can be released in a sustained way using this strategy. In particular, the controlled release of the antibiotic MXF could not be achieved, even using the LbL coatings that were able to retard the release of DCF. These negative results led to the search of other strategies to improve the loading and sustain the release of MXF.

This chapter describes an attempt to optimise the MXF release from the hydrogel TRIS/NVP/HEMA using molecular imprinting with MXF, combined with the addition of acrylic acid (AA) to the monomer solution. The choice of AA, an unsaturated carboxylic acid (pKa=4.2) [2], was based on previous studies that show its usefulness to increase the amount of fluoroquinolones released due to its ability to interact with protonizable amino groups or with hydrogen bond acceptors [3,4]. The drug release profiles were tested in sink conditions in medium under stirring and in sink conditions in microfluidics cell. The simplified process of sink conditions in medium under stirring facilitates the comparison between systems; however, it does not simulate properly the drug release kinetics in the eye, in terms of *in vivo* small tear volume and flow rates. As such, to study the release using a lab-made microfluidic cell, capable of mimicking the hydrodynamic conditions of the eye, was used [5].

Characterization of the drug loaded samples was carried out to assess possible implications of the performed modifications on the physical properties of the hydrogel. Namely, topography, transmittance, refractive index, swelling, wettability, and ionic permeability were evaluated for the unmodified and modified hydrogels. Further biological characterization of the best hydrogel was carried out through antibacterial tests against two of the most common bacteria involved on ocular infections: the Gram-positive bacteria *S. aureus* and *S. epidermidis* [6,7]. The HET-CAM test was done to predict any potential ocular irritancy. Finally, cell viability was analysed using NIH/3T3 cells (mouse embryonic fibroblasts).

5.2   Experimental part

5.2.1   Materials

2,2'-Azobis(2-methylpropionitrile) (purity≥98%, AIBN), 2-hydroxyethyl methacrylate (purity≥99%, HEMA), 3-tris(trimethylsilyloxy)silylpropyl 2-methylprop-2-enoate (purity≥98%, TRIS), calf serum, dimethyl sulfoxide (DMSO), dulbecco's Modified Eagle's Medium, ethylene glycol dimethacrylate (purity≥98%, EGDMA), hydrochloric acid (HCl), isopropanol, NIH/3T3 fibroblasts (93061524), penicillin-streptomycin solution (10000U/mL penicillin, 10 mg/mL streptomycin), and 8.0 µm pore polycarbonate membrane Transwell® (Corning®) were provided by Sigma-Aldrich (USA). N-vinyl pyrrolidone (purity≥98%, NVP) and octylphenoxypolyethoxyethanol (IGEPAL®) were obtained from Merck (USA). Calcium chloride 2-hydrate ($CaCl_2.2H_2O$), potassium chloride (KCl), sodium bicarbonate ($NaHCO_3$), and sodium chloride (purity≥99%, NaCl) were purchased from PanReac (Spain). Moxifloxacin hydrochloride (MXF) was from Carbosynth (UK) and acrylic acid (purity≥99%, AA) from Alfa Aesar (Germany). Methanol (purity≥99.9%, CH_3OH) was provided by Carlo Erba (Spain). Mueller-Hinton agar (MH) was obtained from Oxoid microbiological products (UK). Distilled and deionised (DD) water (18 MΩcm, pH 7.7) used to prepare all solutions and for washing was obtained from a Millipore system. Simulated tear fluid (STF) with pH 7.4 was prepared mixing NaCl (6.8 g/L), $NaHCO_3$ (1.1 g/L), KCl (1.4 g/L) and $CaCl_2 \cdot 2H_2O$ (0.04 g/L) [8].

5.2.2   Preparation of silicone-based hydrogels

A silicone-based hydrogel intended to be used as a SCL and previously studied in chapter 2 to 4, was the starting material for a set of modifications in the hydrogel relative composition, which included addition of different amounts of a functional co-monomer (AA), and drug imprinting (see **Table 5.1**). Each mixture of TRIS, HEMA, NVP, EGDMA, AA and MXF was homogenised by magnetic stirring. The chemical structures of the employed co-monomers and MXF are shown in Appendix A and in **Table 1.4** of chapter 1, respectively.

Samples imprinted with MXF were obtained by adding the drug to the co-monomer's mixture. A maximum concentration of 3 mM of the drug was used due to solubility limitations. The

solution was then degassed by ultrasonic sonication (5 min) followed by nitrogen bubbling (10 min) to remove oxygen. The initiator (AIBN) was then added and solubilised before pouring the solutions into moulds consisting of two pre-silanized glass plates separated by a Teflon spacer (0.3 mm) [9].

The free-radical co-polymerization of the hydrogels was done at 60ºC during 24 h. After this period, samples were removed from the moulds and cut into disks with 10 mm of diameter (except when otherwise indicated), washed by immersion in DD water, under stirring (200 rpm) for 10 days and replacing the solvent 3 times a day, in order to simultaneously remove unreacted co-monomers and the template drug. The absence of MXF and unreacted co-monomers in the washing solutions was checked using a UV-Vis spectrophotometer (Multiskan GO, Thermo Scientific), in the range $\lambda = 200 - 700$ nm. The resulting hydrogels were then dried in an oven at 36ºC for 72 h.

Table 5.1 Composition of the co-monomer mixtures used to prepare the silicone-based hydrogels.

Hydrogel designation	TRIS (mM)	HEMA (mM)	NVP (mM)	EGDMA (mM)	AIBN (mM)	AA (mM)	MXF (mM)
TRIS	790	1780	3930	34	20	0	0
TRIS(100)	790	1780	3930	34	20	100	0
TRIS(200)	790	1780	3930	34	20	200	0
TRIS(300)	790	1780	3930	34	20	300	0
TRIS-I	790	1780	3930	34	20	0	3
TRIS(100)-I	790	1780	3930	34	20	100	3
TRIS(200)-I	790	1780	3930	34	20	200	3
TRIS(300)-I	790	1780	3930	34	20	300	3

5.2.3 Drug loading assays

Dried non-imprinted and imprinted hydrogels were immersed in a MXF solution (5 mg/mL in STF, 3 mL) at 4ºC for 72h. The total amount of drug loaded per hydrogel sample was determined through methanol extraction. Briefly, MXF-loaded hydrogels were removed from the drug solution and carefully blotted with absorbent paper, before being placed in glass vials with 3 mL of methanol. At pre-scheduled times, the hydrogels were removed from the vials, rinsed with DD water, blotted and placed in fresh methanol, until no more drug was detected. The concentration of MXF in the methanol solutions was determined by absorbance measurements, at $\lambda = 290$ nm. Experiments were carried out in quadruplicate for each system.

5.2.4 Physical characterization of the MXF-loaded hydrogels

Water uptake

The water uptake of the hydrogels in DD water, in STF and in MXF solution (5 mg/mL, in STF) was studied. Triplicates of dried hydrogels were weighted (W_D) and placed in 3 mL of the desired solution at 4ºC. At schedule times, the hydrogels were removed from the solution, carefully blotted in absorbent paper and weighted (W_H). The water uptake (%) was calculated using **Equation 1.2** (chapter 1).

Water contact angle measurements

The water contact angles of the hydrated hydrogels were measured by the captive bubble method. A video camera (jAi CV-A50, Spain) mounted on a microscope Wild M3Z (Leica Microsystems, Germany) was used to obtain images of air bubbles (3 – 4 µL) generated underneath the hydrogels. The images were analysed with ADSA software (Axisymmetric Drop Shape Analysis, Applied Surface Thermodynamics Research Associates, Toronto, Canada). Ten bubbles were analysed for each system.

Topography measurements

Topographic images (10 x 10 μm^2) of the surface of the MXF-loaded hydrogels were obtained at room temperature, in tapping mode using an AFM (Nanosurf EasyScan 2), in their hydrated state. The analysis was done with silicon probes (resonance frequency: 204 – 497 kHz), at scan rate of 1.2 Hz. The R_a of the surfaces was determined from the total image area, using the software WSxM 5.0 develop 9.1. Three images were obtained for each system.

Light transmittance assays

The transmittance of the hydrated, MXF-loaded hydrogels was determined with a UV-Vis spectrophotometer (Multiskan GO, Thermo Scientific). Measurements were carried out in triplicate for each system, in a wavelength interval 200 – 700 nm, with scanning steps of 1 nm.

Refractive index measurements

The refractive index of the hydrated, MXF-loaded hydrogels was determined in the spectral range 300 – 750 nm, using a phase modulated spectroscopic ellipsometer (UVISEL, Horiba Jobin-Yvon) at a 70º incidence angle. Triplicates of both non-imprinted and imprinted hydrogels were studied.

Mechanical behaviour

Dumbbell-shaped specimens with 2.5 mm width (overall width 5 mm) and 6 mm gauge length (total length 18 mm) of the MXF-loaded hydrogels in the hydrated state were submitted to tensile tests using a TA.XT Express Texture Analyser (Stable Micro Systems, UK). The samples were stretched with a speed of 0.3 mm/s and the trigger force was set to 0.005 N. The Young´s modulus was determined from the initial slope of the resultant stress-strain curves. Five independent measurements were carried out for each type of hydrogel.

Ionic permeability measurements

A lab-made PMMA cell previously described in section 1.1.4.2.5 in chapter 1, was used to determine the ionic permeability of the hydrogels. Samples hydrated in DD water (12 mm diameter disks) were used instead of the drug loaded ones to avoid the interference of the drug in the measurements. The hydrogels were mounted between the two chambers, and the conductivity of the acceptor solution was measured using a conductivity meter (HI2003 edge^{EC}® from HANNA instruments). Three measurements were carried out for each system, at 36ºC. The conductivity data were converted into NaCl concentrations according to data previously obtained from a calibration curve. D_{ion} was obtained from **Equation 1.4** (chapter 1).

5.2.5   Drug release assays

Release measurements under sink conditions in medium under stirring were carried out by placing the MXF-loaded hydrogels (four replicates) in vials with 3 mL of STF and kept under stirring (180 rpm) at 36ºC. At pre-established times, aliquots of the release medium (200 µL) were taken and replaced with fresh STF. Quantification of the drug in the collected aliquots was done by absorbance measurements, as referred above. The dilution effect due to the release medium replacement was taken into account when calculating the cumulative release curves.

Drug release experiments were also carried out in sink conditions using a lab-made microfluidic cell, that simulates the lachrymal fluid turnover. The microfluidic cell was produced from PMMA, with a chamber volume of 45 µL. This value is above typical tear fluid volume present in the eye (3.4 – 10.7 µL) [10], since smaller volumes led to clogging of the cell. A syringe pump was used at a pump rate of 3 µL/min to simulate the turnover rate of tears found for SCLs wearers (1.4 – 4.3 µL/min) [11]. **Figure 5.1** shows a schematic representation of the microfluidic cell, and the experimental apparatus used in the hydrodynamic release measurements.

A
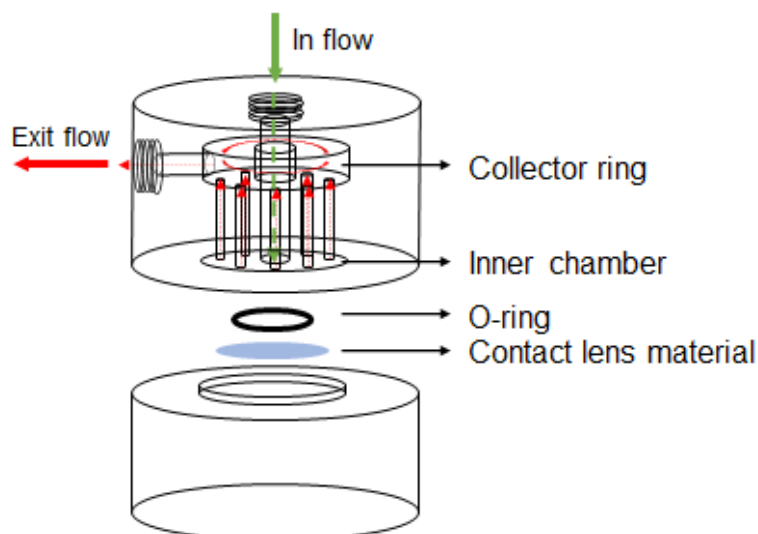
B
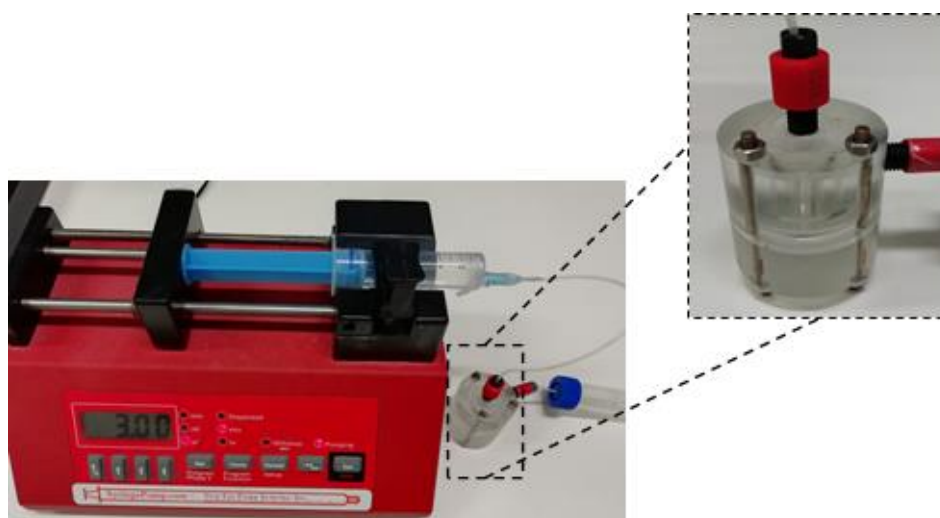
Figure 5.1 (A) Schematic representation of the microfluidic cell used. **(B)** Experimental apparatus used for the hydrodynamic release measurements.

Three independent experiments were made at 36ºC with a continuous flow (3 µL/min) of STF. The hydrogels were cut with a 12 mm diameter to better fit in the microfluidic cell. The exit solution was analysed at pre-defined times, and MXF concentration was measured by spectrophotometry, as described in section 5.2.2.

5.2.6   Sterilization of the hydrogels for biological tests

Sterilization by SP, was done prior to the HET-CAM test and the cell viability assay. This sterilization method was chosen because it was proved in previous works that it did not affect significantly the physical properties of the silicone-based hydrogel [12,13]. The hydrogel samples were placed in closed vials with 3 mL of MXF solution (5 mg/mL in STF) and autoclaved at 121ºC and 1 bar for 1 h. The hydrogels were left on the closed vials containing the drug solution, at 4ºC, until 72 h of loading was completed. To evaluate potential effects of SP on the release profile, drug release measurements were carried out under sink conditions in medium under stirring and compared to those obtained with the non-sterilized hydrogel.

5.2.7   Irritability assays

The HET-CAM assay was done to determine the potential ocular irritation effect of the hydrogel. An egg incubator (Incubator, 56S) was used to incubate fertilized hen´s eggs (Sociedade Agrícola da Quinta da Freiria, SA, Portugal) at 37±0.5ºC with 60±5% of RH. At the 9th day, the eggs were removed from the incubator and cut at the air pocked existent in the larger end using a rotary saw (Dremmel 3000, Breda). The inner membrane was hydrated with 0.9% NaCl solution for 30 min and removed carefully to expose the CAM. The sterilized hydrogel sample (previously loaded with MXF) was placed directly on the CAM for 5 min. The appearing of lysis, haemorrhage and coagulation was evaluated by calculating the IS, through **Equation 1.6**, chapter 1. The assay was carried out in triplicate. A negative and a positive control were made by adding 300 µL of NaCl (0.9%) and NaOH (1 M) on the CAM, respectively.

5.2.8   Cytotoxicity tests

Cytotoxicity of loaded hydrogels was evaluated by using NIH/3T3 fibroblasts, according to ISO standard 10993-5. DMEM supplemented with 10% CS and 1% penicillin-streptomycin solution was used to grow the cells in T75 flasks. For the cytotoxicity assay, the cells (1×10^5 cells/well) were transferred into a 24 well-plate and incubated in humified atmosphere with 5%

CO_2 at 37ºC, for 24 h. Hydrogel disks with 6 mm diameter were placed in the bottom surface of the polycarbonate membrane Transwell®. The Transwell® inserts were placed in the wells containing the cell culture, and 0.1 mL volume of DMEM was poured on top of the hydrogels. Two controls were made by adding 0.1 mL of DMEM to an empty Transwell® (negative control) and 0.1 mL of DMEM with 350 µL of DMSO to another Transwell® (positive control). Subsequently, the plates were again placed in the incubator for 24 h. The cells were visualized using an inverted light microscope (Axiovert® 25, ZEISS Microscopy – Jena, Germany) and micrographs of the adherent cells were taken.

The viability of the cells was studied by MTT assay. For that, 300 µL of MTT (0.5 mg/mL in serum-free DMEM) were added to each well and incubated for 3 h. Dissolution of formazan was achieved by adding 450 µL of MTT solvent (4 mM HCl, 0.1% IGEPAL in isopropanol). Absorbance was read at 595 nm in a microplate reader (Platos R 496). Five replicates were carried out.

5.2.9   Microbiological tests

The antibacterial activity against *S. aureus* (ATCC 25923) and *S. epidermidis* (CECT 231) was studied through agar diffusion tests, using samples of the solution collected from the microfluidic cell, and by direct contact, using the MXF loaded disks. The bacteria strains were grown by incubation for 24 h at 37ºC. An optical density of 1 McFarland (3×10^8 bacteria/mL) was achieved by suspending the grown strains in 0.9% NaCl sterile solution. MH was sterilized in an autoclave at 121ºC for 20 min, and subsequently stabilized at 50ºC in a water bath. Sterile square plates (120 x 120 mm^2) were filled with 50 mL of MH and 350 µL of bacterial suspension, and left to solidify. Antimicrobial susceptibility test disks (Oxoid) were directly placed in the plates, and 15 µL of the solutions collected from the microfluidic cells at pre-established times were added on top of the disks. For the direct contact test, sterilized hydrated samples were blotted with absorbent paper and directly placed on the agar. A negative control (test disk with 15 µL of STF) was also placed in each plate. The agar plates were incubated at 37ºC for 24 h. The produced inhibition halos were measured with an electronic calliper. All experiments were carried out in triplicate for each bacteria species.

5.2.10 Statistical analysis

R Project v. 3.6.1 software was used for the statistical analysis of the data. All data was shown as mean ± standard deviations. Student´s t-test and one-way ANOVA test were applied to calculate if two or more sets of data were significantly different. Shapiro-Wilk test was used to verify the normality of the data. The level of significance was set to 0.05.

5.3 Results

5.3.1 Physical characterization of the hydrogels

The physical properties of the produced hydrogels are summarized in **Table 5.2**.

Table 5.2 Properties of the produced hydrogels: water uptake, water contact angle, R_a, refraction index, Young's modulus, and ionic permeability. The errors are the ± standard deviations (in all cases n=3, except for Young's modulus and water contact angle where n=5 and n=10, respectively).

		TRIS	TRIS-I	TRIS (100)	TRIS (100)-I	TRIS (200)	TRIS (200)-I	TRIS (300)	TRIS (300)-I
Water uptake (%)	DD water	78±1	85±8	128±2	128±4	131±1	135±3	135±9	128±3
	STF	84±4	119±1	121±1	122±5	133±10	125±3	150±8	139±11
	MXF	130±10	135±8	147±7	195±8	199±8	224±12	253±17	262±14
Water contact angle (º)		37±1	35±4	35±4	32±3	31±5	29±4	32±5	30±2
R_a (nm)		11.2±2.5	5.1±1.6	3.9±1.4	3.1±1.4	2.3±0.4	2.2±04	2.0±0.5	1.7±0.4
Refraction index		1.359±0.008	1.361±0.011	1.360±0.005	1.361±0.008	1.365±0.003	1.369±0.013	1.357±0.005	1.357±0.005
Young's modulus (MPa)		1.09±0.04	0.91±0.02	0.92±0.07	0.78±0.03	0.74±0.02	0.72±0.02	0.59±0.02	0.52±0.02
Ionic permeability x10^{-7} (cm^2/s)		5±0.2	8±0.1	9±0.2	5±0.4	4±0.1	3±0.4	20±1	10±1

The water uptake depended on the medium composition. Water uptake in MXF solution was significantly higher than in DD water ($p<0.0001$) or in STF ($p<0.0001$), for all hydrogels. The

water uptake increased with the amount of AA added. No tendency can be identified when assessing the effect of drug imprinting.

All hydrogels present similar wettability, but slightly lower water contact angles were observed for the imprinted samples with higher concentrations of AA, specially, TRIS(200)-I and TRIS(300)-I.

The topography images of the surface of the hydrogels are depicted in **Figure 5.2** and the R_a values are given in **Table 5.2**. The molecular imprinting process and the addition of the functional monomer seems to reduce the size and number of pores. TRIS(300)-I was the hydrogel with the smoothest surface (lowest R_a).
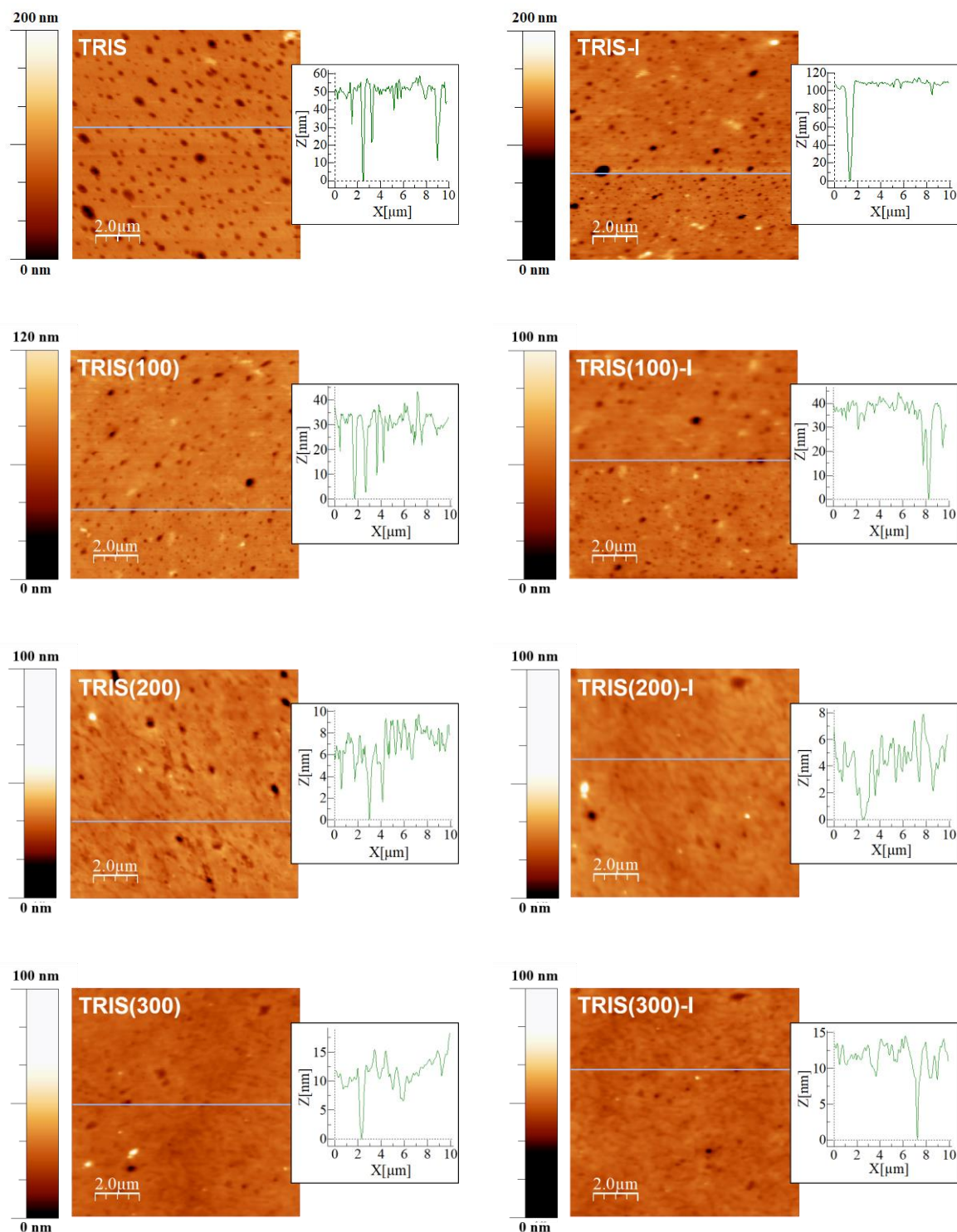
Figure 5.2 AFM images (10 x 10 µm^2) of the surface of non-imprinted (left) and imprinted hydrogels (right). The inserts correspond to the profiles of the grey lines indicated in the AFM images.

Concerning the optical properties, the light transmittance decreased slightly with the addition of the AA monomer (**Figure 5.3**), but the values were above 90% transmittance in the visible range. The refractive index (**Table 5.2**) kept approximately the same value for all hydrogels (p=0.589).
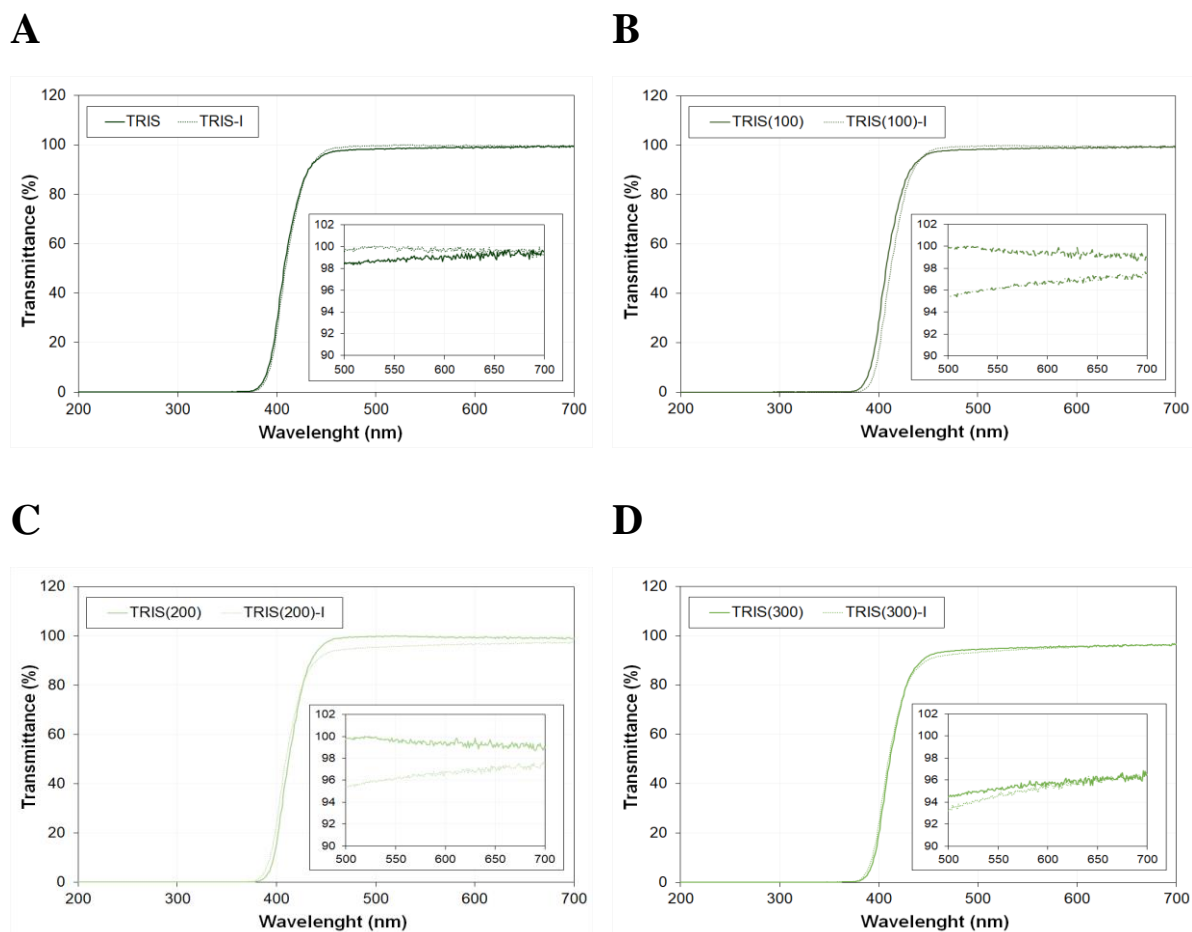
Figure 5.3 Light transmittance of non-imprinted and imprinted hydrogels, without AA (**A**), with 100 mM of AA (**B**), with 200 mM of AA (**C**), and with 300 mM of AA (**D**). The insert represents the wavelength between 500 and 700 nm.

The mechanical behaviour of the hydrogels varied with the addition of the functional monomer AA and the drug imprinting, the Young's modulus decreased, more significantly in the former case. The ionic permeability values are of the same order of magnitude for the different

hydrogels, being higher for the materials with the largest content of AA (TRIS(300) and TRIS(300)-I)

5.3.2   Drug loading and release

MXF-loaded amounts were determined for all synthesised/processed non-imprinted and imprinted samples (**Table 5.3**). It can be observed that MXF-loaded amounts increased with the increase in AA relative compositions. Moreover, all imprinted samples loaded higher amount of MXF than the corresponding non-imprinted samples, being the highest percentual increment observed for TRIS.

Table 5.3 MXF-loaded amounts, increment in MXF loading, and percentage of released after 120 hours under sink conditions in medium under stirring. The errors are the ± standard deviations (n=4).

Hydrogel code	Amount of MXF loaded (µg/mg of dried gel)	Increment in loading (%)	Drug released (%)
TRIS	9.8±0.5	-	72
TRIS-I	17.1±0.2	75	70
TRIS(100)	21.7±1.6	-	76
TRIS(100)-I	33.9±0.3	56	68
TRIS(200)	36.3±1.8	-	80
TRIS(200)-I	49.2±1.1	36	70
TRIS(300)	44.1±1.9	-	75
TRIS(300)-I	64.9±0.4	47	69

Results on the kinetics of MXF release, in sink conditions in medium under stirring, are shown in **Figure 5.4**.
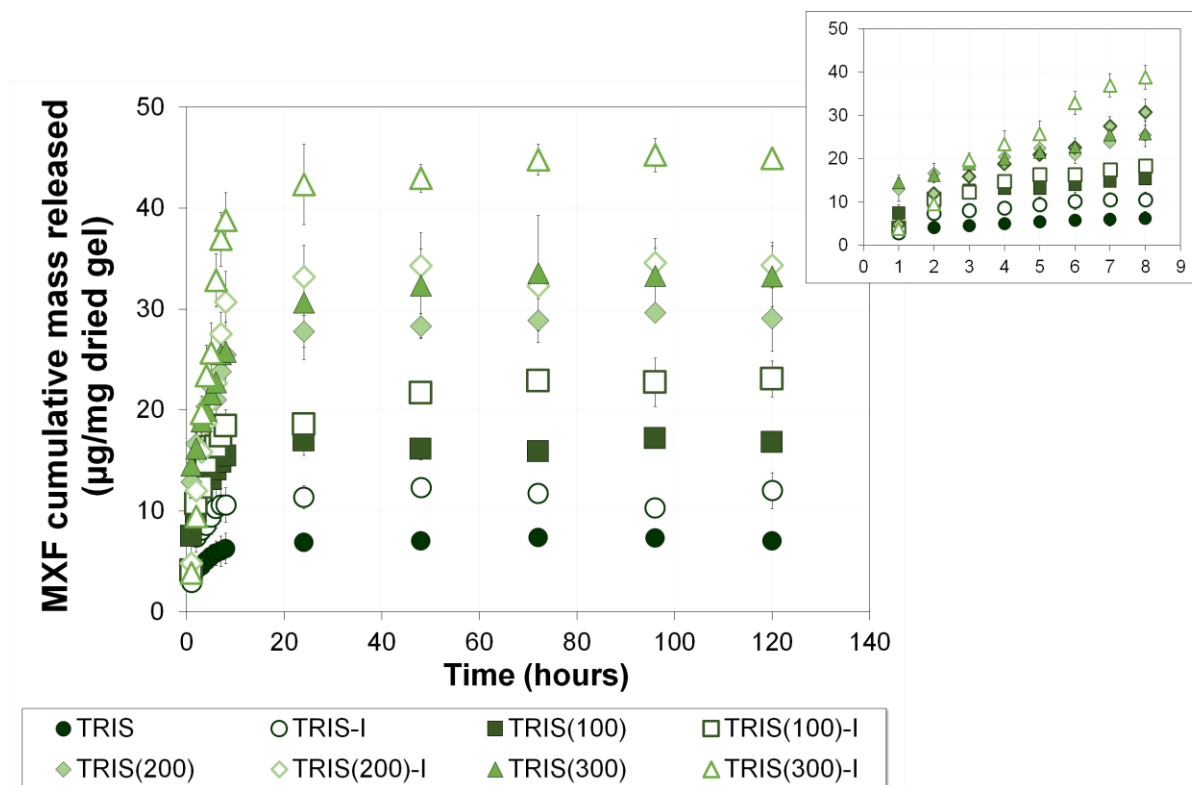
Figure 5.4 MXF release profiles from non-imprinted (solid symbols) and drug imprinted (open symbols) silicone-based hydrogels with and without AA monomer. The insert shows the first 8 h of the release data. The error bars are the ± standard deviations (n=4).

The imprinting of the drug and the addition of the AA functional monomer had a synergistic effect, increasing the amount of MXF released from the samples. The percentage of MXF released relative to the amount of MXF loaded (**Figure 5.5**), clearly evidenced that the initial burst was lower for imprinted hydrogels. Also, AA composed hydrogels released the drug more slowly than their non-imprinted counterparts. A significant percentage of drug remained inside the hydrogels, after 120 h in the release medium, such percentages ranges from 20% to 32%.

A
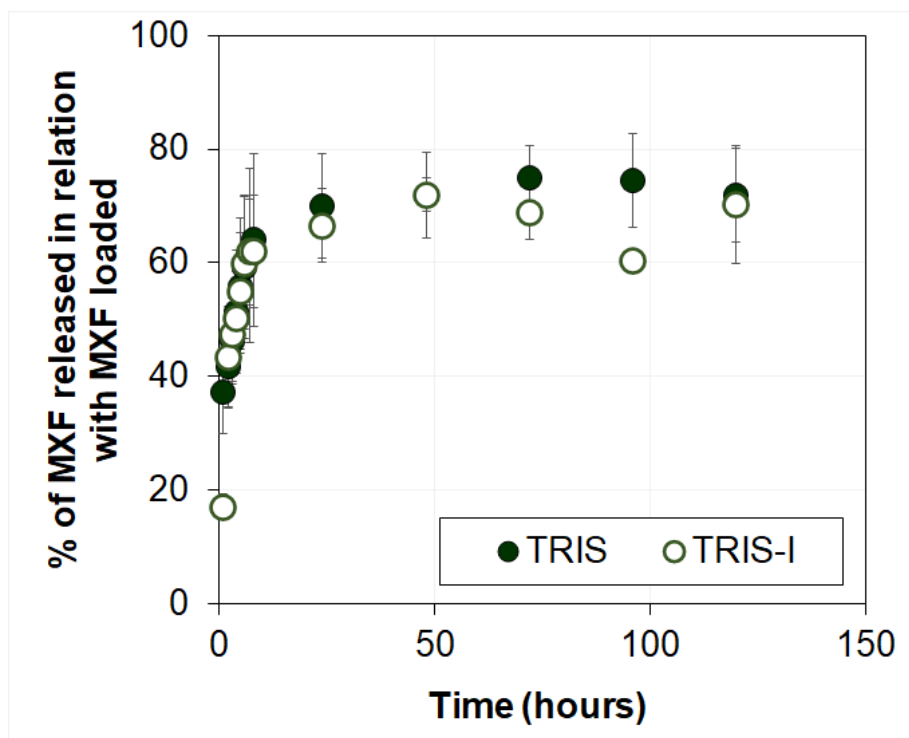
B
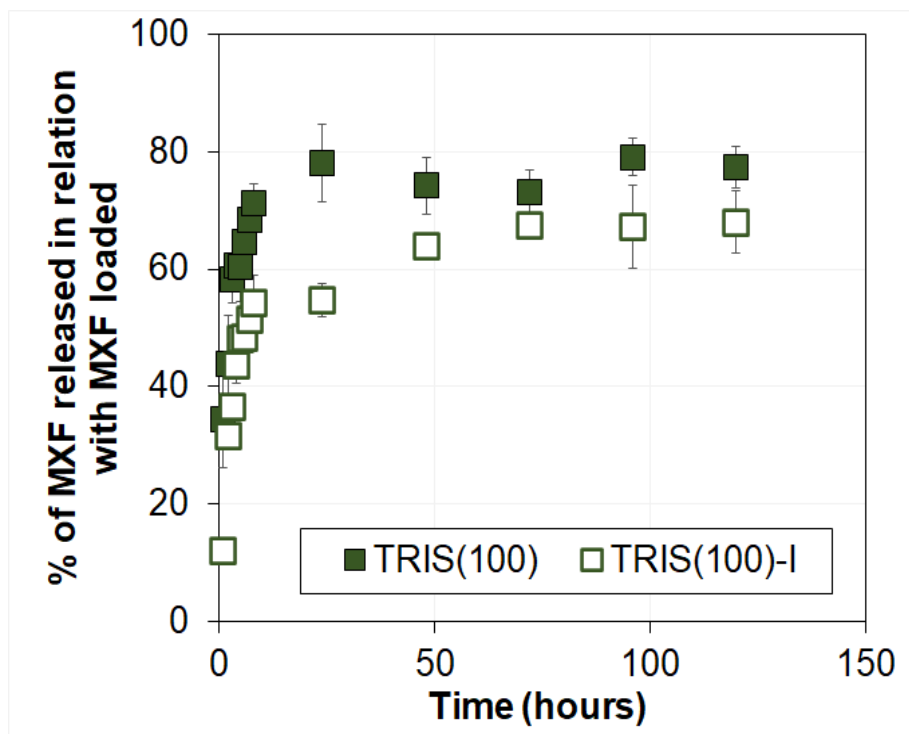
C
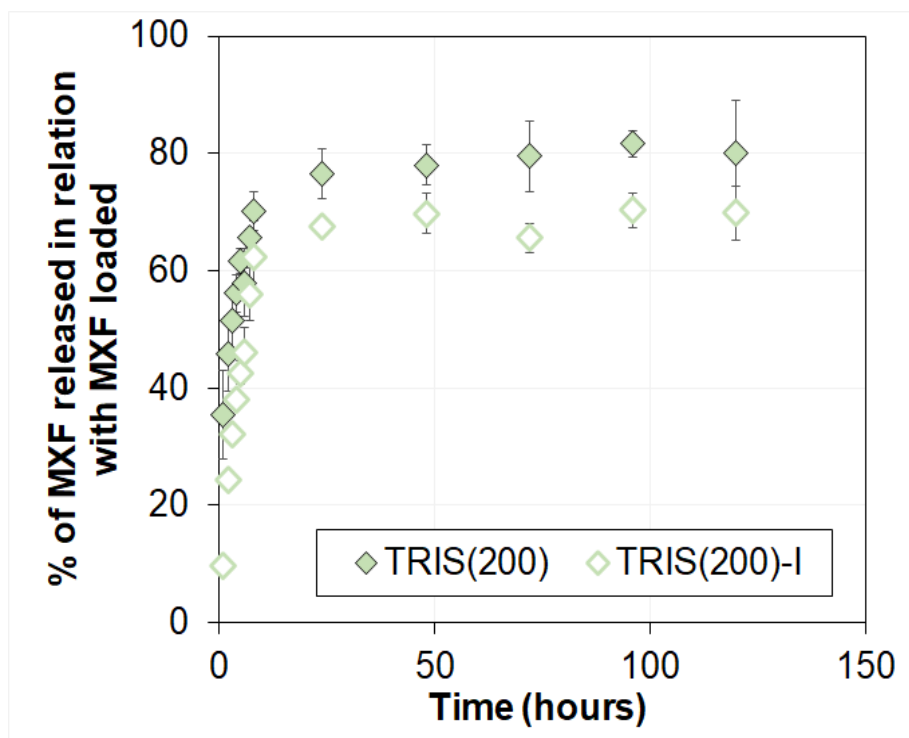
D
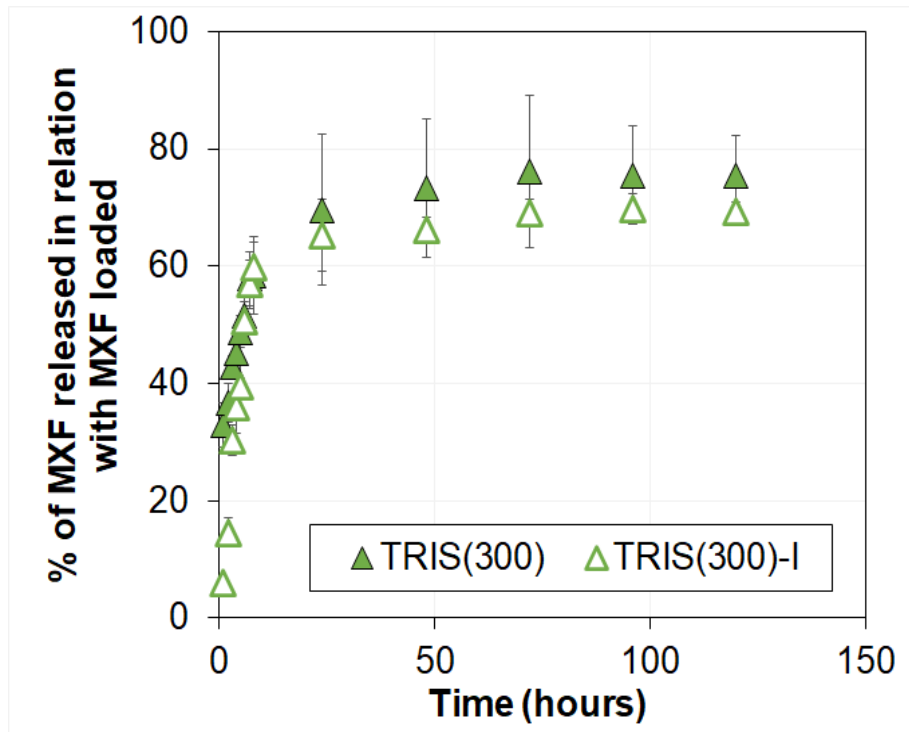
Figure 5.5 Percentage of MXF released in reference to the amount of MXF loaded, for the non-imprinted and imprinted hydrogels with (**A**) no AA, (**B**) 100 mM of AA, (**C**) 200 mM of AA, and (**D**) 300 mM of AA. The error bars are standard deviations (n=4).

In order to have an insight into the mechanism of drug release, the release data of the base hydrogel (TRIS), and of the hydrogels with the larger amount of drug loaded (TRIS(300) and TRIS(300)-I) were fitted to the Korsmeyer-Peppas equation [14]:

$$\frac{M_t}{M_\infty} = kt^n$$ **Equation 5.1**

where M_t and M_∞ are, respectively, the mass released at time t and as time approaches infinity, n is the diffusional exponent and k is a pseudokinetic constant [14]. The parameters of the fittings of the release profiles for the hydrogels, up to 60% of the total release, are shown in **Table 5.4**. The diffusional exponent values for the non-imprinted hydrogels are <0.5, regardless of the presence or absence of the AA monomer, which indicates a Fickian diffusion. On the other hand for the TRIS(300)-I n>0.5, showing a non-Fickian (anomalous) transport resultant from the overlapping of Fickian and swelling controlled processes [15]. Additionally, TRIS(300)-I demonstrates a decrease in the kinetic constant, when compared to TRIS and TRIS(300), which can be an indicative of a higher affinity of MXF with the imprinted hydrogel.

Table 5.4. Parameters n and k, and respective correlation coefficients, R^2, of drug release data fitting to **Equation 5.1**, for TRIS, TRIS(300) and TRIS(300)-I.

	TRIS	TRIS(300)	TRIS(300)-I
n	0.165	0.243	0.990
k	0.517	0.427	0.125
R^2	0.999	0.998	0.965

The effects of SP sterilization were tested on the TRIS(300)-I hydrogel, through the comparison of the MXF release patterns before and after sterilization (**Figure 5.6**). The release profiles did not show significant modifications.
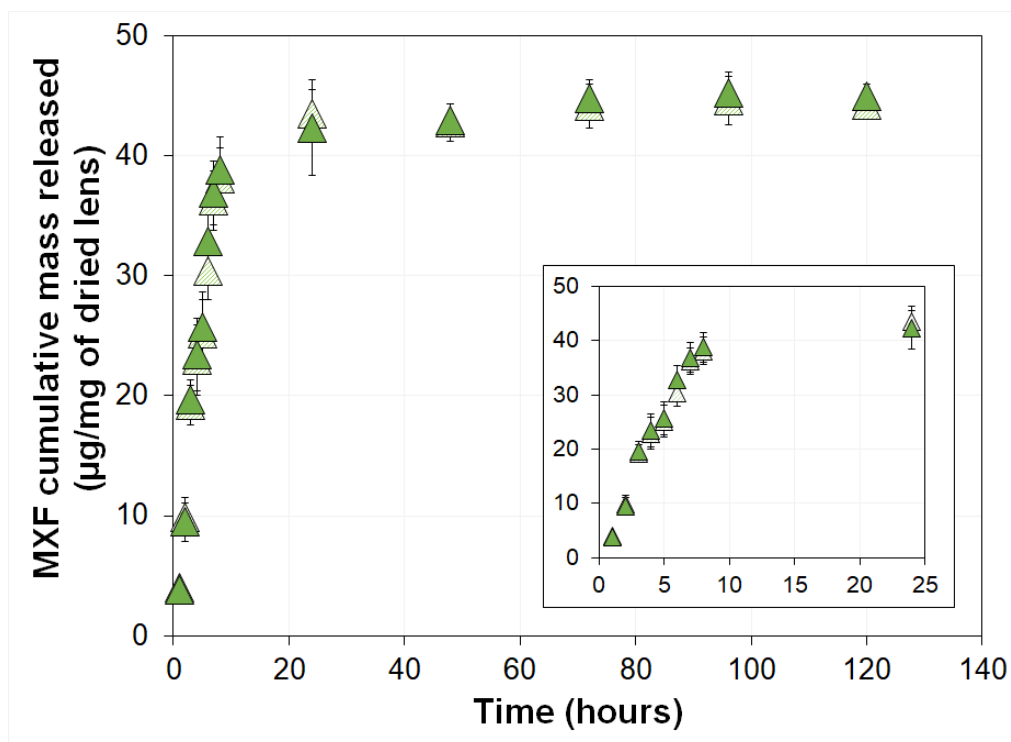
Figure 5.6 MXF release profiles from TRIS(300)-I hydrogel before (▲) and after (△) SP sterilization. The insert represents the first 24 h of release. The error bars are the ± standard deviations (n=4).

To gain an insight on how the release may occur *in vivo*, the release profiles of the hydrogels with the largest amount of AA (TRIS(300) and TRIS(300)-I) were recorded in hydrodynamic conditions, using a lab-made microfluidic cell (**Figure 5.7**). The cumulative release profiles in medium under stirring (**Figure 5.4**) and in microfluidics cell (**Figure 5.7A**), were clearly different; the release kinetics was slower for both studied hydrogels in the later conditions. TRIS(300)-I had less initial burst of MXF, but the total amount released was higher compared to that released from TRIS(300) (**Figure 5.7A**). The MXF concentration profile the exit point of the microfluidic cell and the MICs for *S. aureus* (0.008 – 0.064 µg/mL) and *S. epidermidis* (0.016 – 2 µg/mL) [7], are compared in **Figure 5.7B**. TRIS(300)-I showed a more sustained release and ensured MXF concentrations above the MICs values for 13 days, while TRIS(300) only led to higher values for 10 days.

A
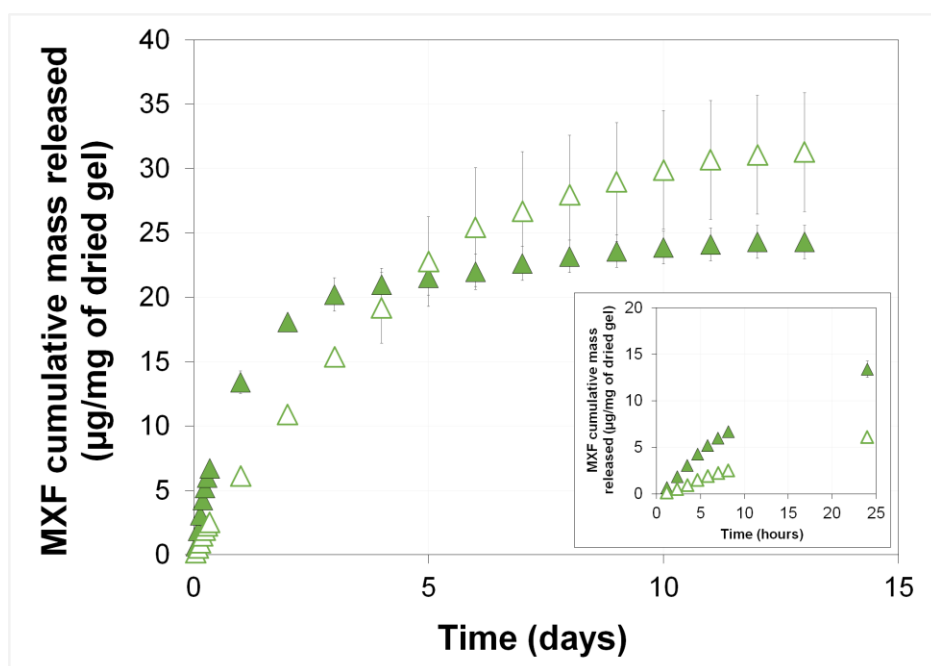
B
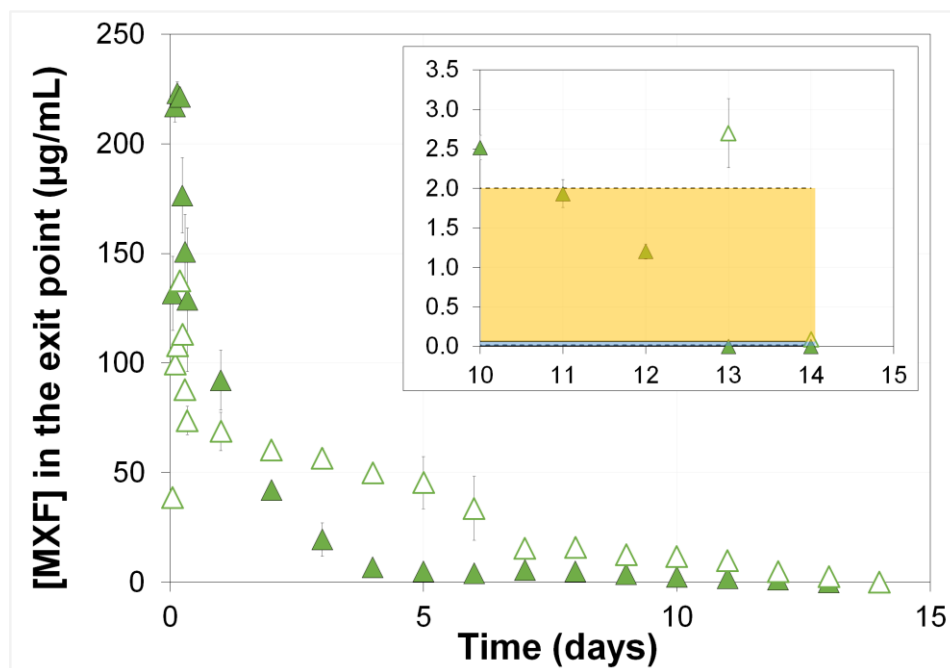
Figure 5.7 (A) MXF cumulative mass released in hydrodynamic conditions from TRIS(300) (▲) and TRIS(300)-I (△). The insert represents the first 24 h of the release data. **(B)** Concentration profile of MXF released at the exit point from the microfluidic cell for

TRIS(300) (▲) and TRIS(300)-I (△). The insert shows the last 4 days of release with the range of the MICs for *S. aureus* (blue area) and *S. epidermidis* (yellow area). The error bars are the ± standard deviations (n=3).

5.3.3 Irritation score

Sterilized TRIS(300)-I samples loaded with MXF were submitted to HET-CAM tests to predict the potential effect of the materials to induce lysis, haemorrhage or coagulation. As seen in **Figure 5.8**, the effect of TRIS(300)-I loaded samples is similar to that observed for the negative control (NaCl 0.9%), as such, the IS was equal to 0.

A   **B**   **C**
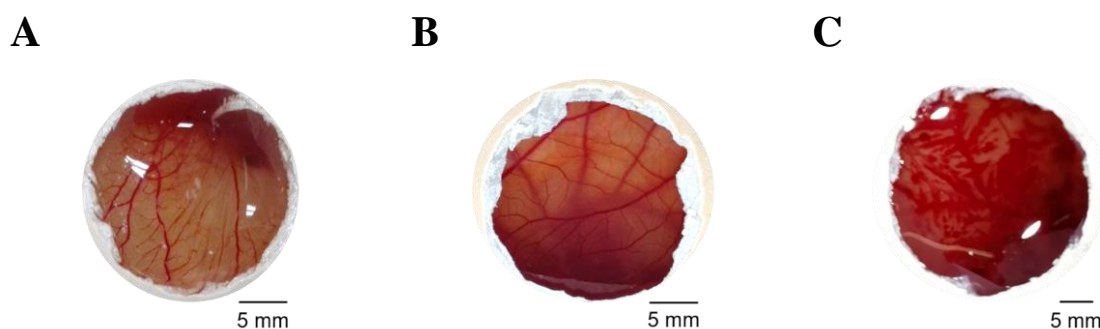
Figure 5.8 CAM images after 5 min of exposure to TRIS(300)-I loaded with MXF **(A)**. Negative control **(B)** and positive control **(C)**.

5.3.4 Cytotoxicity

The viability of NIH/3T3 cells after exposure to sterilized TRIS(300)-I hydrogels loaded with MXF is shown in **Figure 5.9**. Compared to the negative control, a decrease in the cell viability was observed for the MXF-loaded hydrogel, which still remains above 75%.

A
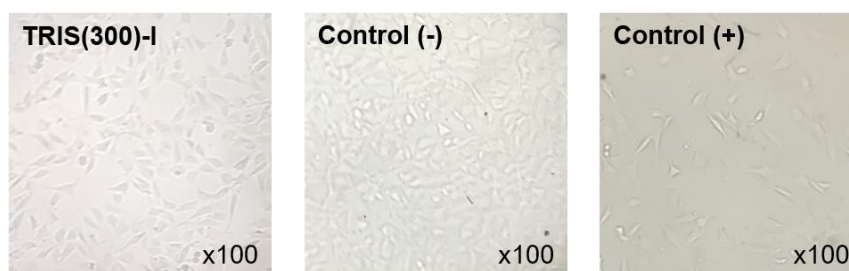
B
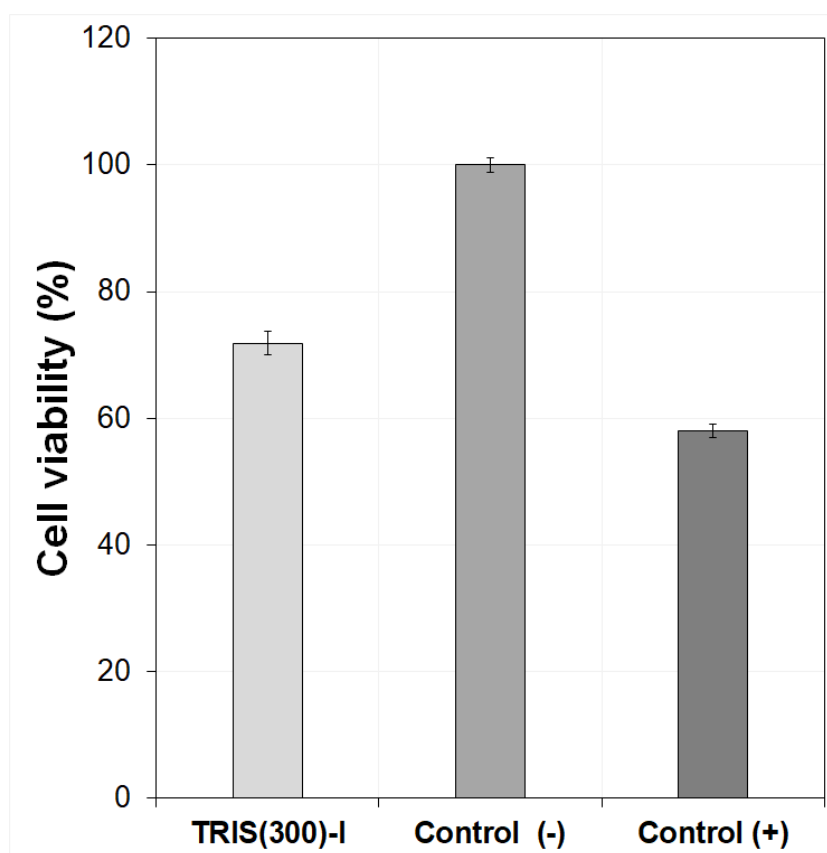
Figure 5.9 (A) Micrographs of the cells immediately before the MTT assay, **(B)** NIH/3T3 cells viability (%) determined by MTT assay, after 24 h exposure to MXF-loaded TRIS(300)-I samples. The errors are the ± standard deviations (n=5).

5.3.5   Microbiological tests

The antibacterial action of the MXF released from TRIS(300)-I loaded hydrogels against *S. aureus* and *S. epidermidis* was studied through direct contact tests with the hydrogels, and agar

diffusion tests of the supernatant solutions collected from the release tests carried out in the microfluidic cell. The results are presented in **Figure 5.10**. The inhibition halos obtained from direct contact for *S. aureus* (67±4 mm), and *S. epidermidis* (59±6 mm) were similar. For the MXF solutions collected after 10 days of release in microfluidics cell, smaller inhibition halos for both bacterial strains were attained (14±1 mm and 18±3 mm for *S. aureus* and *S. epidermidis*, respectively).
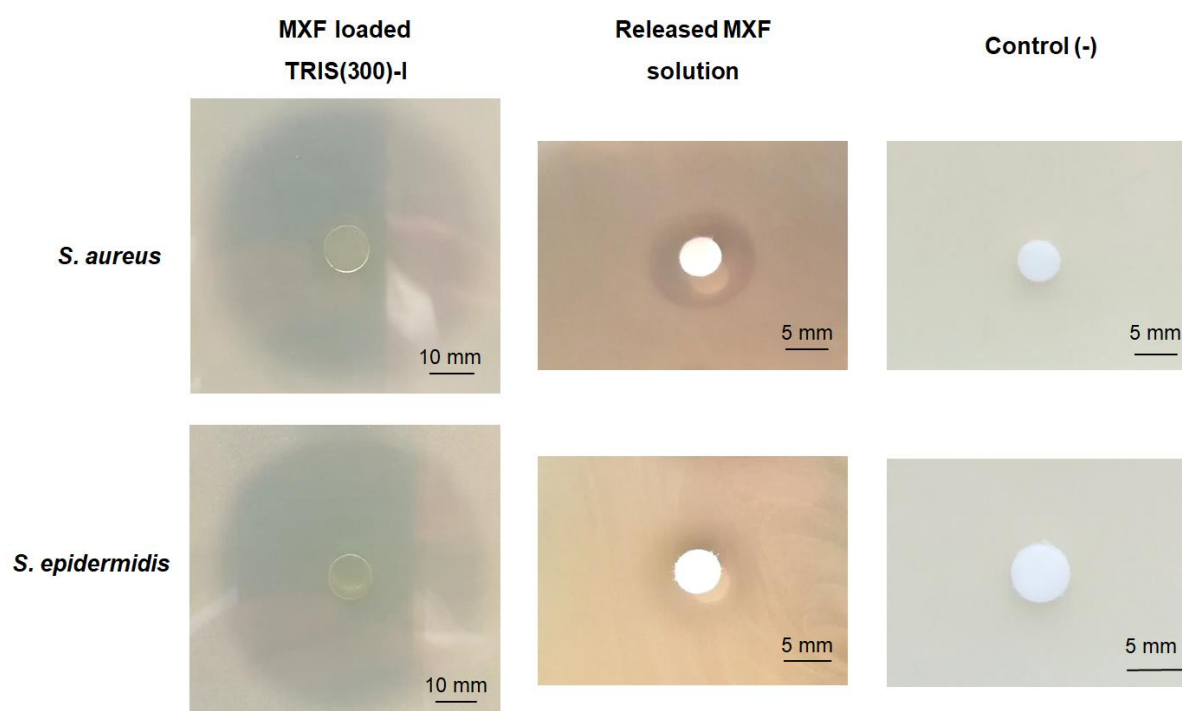
Figure 5.10 Inhibition halos after 24 h exposure to the MXF loaded TRIS(300)-I hydrogels and, to the collected MXF solution after 10 days of release in microfluidic cell for *S. aureus* and *S. epidermidis*. Negative controls (sterile STF) are also shown.

5.4 Discussion

The physical properties of the hydrogels were barely affected by the incorporation of AA and/or imprinting of the drug, except regarding water uptake. The water uptake of the hydrogels increased significantly due to the presence of the functional monomer. Sohail *et al.* (2014) verified that the equilibrium water uptake coefficients were substantially affected by the addition of increasing amounts of AA, as more carboxylic groups were available. At

physiological pH, electrostatic repulsions increase the distance between chains, leading to expansion of the hydrogel´s matrix [16]. The differences in pH among the three soaking solutions are small and do not explain the different water uptake results. The significant increase in water uptake obtained with MXF solution, could be due to the adsorption of MXF on the SCL backbone through hydrophobic interactions, which leads to the charging of the polymer chains. Thus, up taking water to swell and separate the polymer chains would attenuate the ionic repulsions of these chains. Globally, the water uptake values of the hydrogels are between ≈80 and 260%, falling within the typical values of SCLs [17].

The water contact angle decreased slightly for hydrogels with higher amount of AA, while the drug imprinting did not cause any modification. AA it is known for its hydrophilic properties, increasing not only the water absorbance [18] but also the wettability of the surface.

AFM topographic images (**Figure 5.2**) showed a decrease on the R_a values for the modified hydrogels, when compared to the original TRIS, which presents a porous surface, as presented in the previous chapters. Nevertheless, all hydrogels have a R_a within the typical values of commercial SCLs [19].

The Young's modulus of the hydrated hydrogels decreased with the addition of AA: this monomer promoted a reduced elasticity to the hydrogels, improving their softness. A reduction of the Young's modulus of more than 40% occurred for the TRIS(300) and TRIS(300)-I samples when comparing to TRIS. Faturechi *et al*. (2015) produced a gelatin/polyAA hydrogel with different ratios of polyAA, and found that an increase of polyAA led to the deterioration of the mechanical properties. In the present study, the values obtained for this parameter are within the range found for commercial SCLs (0.38 – 1.44 MPa) [20]. The incorporation of higher concentrations of AA was discarded, as mechanical properties could be reduced beyond the desirable values for SCLs [21].

The optical properties (refractive index and transmittance) were almost not affected by the modification of the hydrogels. TRIS(300)-I showed the lowest value of transmittance, which remained above the minimum necessary for SCLs (90%) [22].

The ionic permeability slightly varies among the various hydrogels, but it was in all cases above the minimum required (1.067 x 10^{-9} cm^2/s) to ensure proper SCL movement [23].

Molecular imprinting with the addition of the functional monomer AA, has been described as an efficient method to control the drug release from SCLs [24]. AA is an hydrophilic monomer [3,4,25] which can be easily polymerized by free radical polymerization through its CH_2 double bond, leaving an available carboxylic group. At physiological pH (pH=7.4), AA can electrostatically interact with oppositely charged molecules, or form H-bonds to interact with hydrogen bond acceptors [26,27]. Different relative compositions of AA were tested in order to identify the amount of functional monomer that provides the most adequate number of recognition points for the target molecule (MXF) [24].

Both the addition of the functional monomer and MXF imprinting resulted in a significant increase of the amount of drug loaded: TRIS(300)-I contained almost six times more drug than TRIS hydrogel. Additionally, the total amount of drug released in sink conditions in medium under stirring was also greater for imprinted hydrogels containing AA.

Overall, the drug loading and release results indicated that the imprinted cavities have high affinity for the drug. MXF at the normal pH of the lachrymal fluid (pH=7.2) is predominantly on its zwitterionic form (pKa1=6.25 and pKa2=9.29, see **Table 1.4**). With the carboxylic moiety at C-3 position ionized and the basic moiety at C-7 position protonated [28], MXF can form reversible electrostatic interactions with negatively charged AA [3]. Moreover, hydrogen bonds may be established between MXF and the available non-protonated amino and hydroxyl groups in TRIS and HEMA, respectively (see Appendix A). Additionally, interactions between the electrophilic carbonyl groups of TRIS and HEMA may occur with the electronegative fluorine atom of MXF [29]. The increase of the water uptake with the amount of AA in the hydrogels also contributes to explain the higher amounts of drug loaded and posteriorly released.

The hydrogels that afforded the maximum drug loading and release (TRIS(300) and TRIS(300)-I), were assayed in a microfluidic cell (**Figure 5.7**). Similarly to what was observed by Pimenta *et al*. (2016), the drug release period increased significantly using the microfluidic cell, which can be attributed to differences in the driving forces for the drug release compared to the that in medium under stirring [5]. The MXF concentration in the medium under stirring is much lower than its solubility in STF ($\geq$5 mg/mL); therefore, the gradient of concentration between the drug loaded hydrogel and the supernatant is high. When using the microfluidic cell, the significantly smaller volume of the release medium (45 µL instead of 3 mL), and its

flow originate a lower gradient of drug concentration, which explains the more sustained release. Comparison of the drug release profiles obtained with TRIS(300) and TRIS(300)-I, in microfluidics cell, (**Figure 5.7B**) shows that, only in the latter case, the lower drug burst led to a MXF concentration inferior to the toxicity limit (> 150 µg/mL) [7].

The molecular imprinting strategy increased the duration of the drug release, leading to concentrations above the MICs for 13 days. As typical MXF eye drops treatments lasts five days to seven days [30,31], it is expected that TRIS(300)-I loaded with MXF may provide an adequate release to treat ocular infections. However, it must be stressed that the obtained results are still preliminary, since factors as the lachrymal fluid composition, the real volume of liquid contacting the lens (typically 7 – 12 µL [32]), blinking among others, were not considered.

Analysis of the physical properties and the drug release profiles let to the choosing of TRIS(300)-I as the best performing material, and further tests were conducted to characterize its biological behaviour.

HET-CAM tests revealed that the hydrogel TRIS(300)-I loaded with MXF did not lead to eye irritation. Cytotoxicity tests revealed that it is not toxic, according to the ISO standard 10993-5 (2009) that states a cell viability of 70% as the limit above which the biomaterials may be used for medical devices.

The antibacterial efficacy of the released MXF was confirmed by the presence of inhibition halos after direct contact between the drug loaded TRIS(300)-I hydrogels, and the drug release solutions with the two studied bacteria (*S. aureus* and *S. epidermidis*). Other authors demonstrated that the MXF released from intraocular lens material modified through plasma grafting with HEMA was active against *S. aureus* and *S. epidermidis* [33].

5.5 Conclusions

In this work, the molecular imprinting technology using AA as functional monomer has been demonstrated to be a feasible and easy approach to improve MXF loading and release from a silicone-based hydrogel, without compromising the necessary physical properties for SCLs use. The resulting hydrogels were hydrophilic, with high transmittance, increased ionic permeability, low surface roughness and adequate stiffness. The MXF-imprinted hydrogel with

300 mM of AA (TRIS(300)-I) was able to load the highest amount of MXF through reversible bonding, which allowed a controlled release of the drug and ensured concentrations above the MICs values of *S. aureus* and *S. epidermidis*, for 13 days. Furthermore, the referred hydrogel was not toxic and did not cause ocular irritation. Overall, TRIS(300)-I hydrogels loaded with MXF exhibit prolonged release of the antibiotic and present adequate physical properties to be used in therapeutic SCLs. Although this material was positively assessed concerning the *in vitro* biological behaviour, further pre-clinic and clinic tests need to be carried out to confirm the efficacy of these SCLs to deal with ocular infections.

5.6 References

[1] P. Paradiso, R. Galante, L. Santos, A.P. Alves De Matos, R. Colaço, A.P. Serro, B. Saramago, Comparison of two hydrogel formulations for drug release in ophthalmic lenses, J. Biomed. Mater. Res. B. 102 (2014) 1170–1180.

[2] R.A. Scott, N.A. Peppas, Kinetic study of acrylic acid solution polymerization, AIChE J. 43 (1997) 135–144.

[3] C. Alvarez-Lorenzo, F. Yañez, R. Barreiro-iglesias, A. Concheiro, Imprinted soft contact lenses as norfloxacin delivery systems, J. Control. Release. 113 (2006) 236–244.

[4] A. Hui, H. Sheardown, L. Jones, Acetic and acrylic acid molecular imprinted model silicone hydrogel materials for ciprofloxacin-HCl delivery, Materials (Basel). 5 (2012) 85–107.

[5] A.F.R. Pimenta, A. Valente, J.M.C. Pereira, H.P. Filipe, J.L.G. Mata, R. Colaço, B. Saramago, A.P. Serro, Simulation of the hydrodynamic conditions of the eye to better reproduce the drug release from hydrogel contact lenses: experiments and modeling, Drug Deliv. Transl. Res. 6 (2016) 755–762.

[6] P. Garg, Fungal, mycobacterial, and nocardia infections and the eye: an update, Eye. 26 (2012) 245–251.

[7] A. Topete, A.P. Serro, B. Saramago, Dual drug delivery from intraocular lens material for prophylaxis of endophthalmitis in cataract surgery, Int. J. Pharm. 558 (2019) 43–52.

[8] F. Alvarez-Rivera, A. Concheiro, C. Alvarez-Lorenzo, Epalrestat-loaded silicone hydrogels as contact lenses to address diabetic-eye complications, Eur. J. Pharm. Biopharm. 122 (2018) 126–136.

[9] R. Vasquez, R. Nogueira, M. Orfão, J. Mata, B. Saramago, Stability of triglyceride liquid films on hydrophilic and hydrophobic glasses, J. Colloid Interface Sci. 299 (2006) 274–282.

[10] S.M. Lam, L. Tong, X. Duan, A. Petznick, M.R. Wenk, G. Shui, Extensive characterization of human tear fluid collected using different techniques unravels the

presence of novel lipid amphiphiles, J. Lipid Res. 55 (2014) 289–298.

[11]   G. Lamberti, I. Galdi, A.A. Barba, Controlled release from hydrogel-based solid matrices. A model accounting for water up-take, swelling and erosion, Int. J. Pharm. 407 (2011) 78–86.

[12]   R. Galante, D. Ghisleni, P. Paradiso, V.D. Alves, T.J.A. Pinto, R. Colaço, A.P. Paula, Sterilization of silicone-based hydrogels for biomedical application using ozone gas : Comparison with conventional techniques, Mater. Sci. Eng. C. 78 (2017) 389–397.

[13]   R. Galante, A.S. Oliveira, A. Topete, D. Ghisleni, M. Braga, T.J.A. Pinto, R. Colaço, A.P. Serro, Drug-eluting silicone hydrogel for therapeutic contact lenses: Impact of sterilization methods on the system performance, Colloids Surf B Biointerfaces. 161 (2018) 537–546.

[14]   P.L. Ritger, N.A. Peppas, A simple equation for description of solute release I. Fickian and non-Fickian release from non-Swellable devices in the form of slabs, spheres, cylinders or discs, J. Control. Release. 5 (1987) 23–36.

[15]   P.L. Ritger, N.A. Peppas, A simple equation for descrption of solute release II. Fickian and anomalous release from swellable devices, J. Control. Release. 5 (1987) 37–42.

[16]   K. Sohail, I.U. Khan, Y. Shahzad, T. Hussain, N.M. Ranjha, pH-sensitive polyvinylpyrrolidone-acrylic acid hydrogels : Impact of material parameters on swelling and drug release, Brazilian J. Pharm. Sci. 50 (2014) 173–183.

[17]   C.S.A. Musgrave, F. Fang, Contact lens materials: A materials science perspective, Materials (Basel). 261 (2019) 1–35.

[18]   F. Zhang, F. Meng, J. Lubach, J. Koleng, N.A. Watson, Properties and mechanisms of drug release from matrix tablets containing poly (ethylene oxide) and poly (acrylic acid) as release retardants, Eur. J. Pharm. Biopharm. 105 (2016) 97–105.

[19]   M. Giraldez, E. Yebra-Pimentel, Hydrogel contact lenses surface roughness and bacterial adhesion, INTECH. (2012) 95–120.

[20]   E. Kim, M. Saha, K. Ehrmann, Mechanical properties of contact lens materials, Eye&Contact Lens Sci. Clin. Prat. 44 (2018) 148–156.

[21] T.S. Bhamra, B.J. Tighe, Contact lens and anterior eye mechanical properties of contact lenses : The contribution of measurement techniques and clinical feedback to 50 years of materials development, Contact Lens Anterior Eye. 40 (2017) 70–81.

[22] N. Efron, C. Maldonado-Codina, Development of contact lenses from a biomaterial point of view – Materials, manufacture, and clinical application, in: Compr. Biomater., Comprehensive Biomaterials. Elsevier, 2011: pp. 517–541.

[23] R. Galante, P. Paradiso, M.G. Moutinho, A.I. Fernandes, J.L.G. Mata, A.P.A. Matos, R. Colaço, B. Saramago, A.P. Serro, About the effect of eye blinking on drug release from pHEMA-based hydrogels: An in vitro study, J. Biomater. Sci. Polym. Ed. 26 (2015) 235–251.

[24] C. Alvarez-Lorenzo, F. Yañez, A. Concheiro, Ocular drug delivery from molecularly-imprinted contact lenses, J. Drug Deliv. Sci. Technol. 20 (2010) 237–248.

[25] F. Tasselli, L. Donato, E. Drioli, Evaluation of molecularly imprinted membranes based on different acrylic copolymers, J. Memb. Sci. 320 (2008) 167–172.

[26] I. Lacik, S. Beuermann, M. Buback, PLP-SEC study into the free-radical propagation rate coefficients of partially and fully ionized acrylic acid in aqueous solution, Macromol. Chem. Phys. 205 (2004) 1080–1087.

[27] J. Lützenkirchen, J.V. Male, F. Leermakers, S. Sjöberg, Comparison of various models to describe the charge−pH dependence of poly(acrylic acid), J. Chem. Eng. Data. 56 (2011) 1602–1612.

[28] P. Pawar, R. Katara, S. Mishra, D.K. Majumdar, Topical ocular delivery of fluoroquinolones, Expert Opin Drug Deliv. 10 (2013) 691–711.

[29] F. Yañez, L. Martikainen, M.E. Braga, Supercritical fluid-assisted preparation of imprinted contact lenses for drug delivery, Acta Biomater. 7 (2011) 1019–1030.

[30] D. Miller, Review of moxifloxacin hydrochloride ophthalmic solution in the treatment of bacterial eye infections, Clin Ophthalmol. 2 (2008) 77–91.

[31] R.J. Hamilton, Tarascon pocket pharmacopoeia, Jones and Bartlett Publishers, Inc, 2019.

[32]   H.P. Filipe, J. Henriques, P. Reis, P.C. Silva, M.J. Quadrado, A.P. Serro, Contact lenses as drug controlled release systems : a narrative review, Rev. Bras. Oftalmol. 75 (2016) 241–247.

[33]   A.P. Vieira, A.F.R. Pimenta, D. Silva, M.H. Gil, P. Alves, P. Coimbra, J.L.G. Mata, D. Bozukova, T.R. Correia, I.J. Correia, A.P. Serro, A.J. Guiomar, Surface modification of an intraocular lens material by plasma-assisted grafting with 2-hydroxyethyl methacrylate (HEMA), for controlled release of moxifloxacin, Eur. J. Pharm. Biopharm. 120 (2017) 52–62.

6 Imprinted hydrogels with LbL coating for dual drug release from soft contact lenses materials

The following results were submitted for publishing in the peer-reviewed article:

Diana Silva, Hermínio C. de Sousa, Maria Helena Gil, Luís F. Santos, Renata A. Amaral, Jorge A. Saraiva, Madalena Salema Oom, Carmen Alvarez-Lorenzo, Ana Paula Serro, Benilde Saramago Imprinted hydrogels with LbL coating for dual drug release from soft contact lenses materials. Acta Biomaterialia

Table of Contents

6.1 Introduction

In the previous chapters, several LbL coatings were successfully used to control the release of DCF from SCLs materials. However, this approach demonstrated to be inefficient to achieve a sustained release of MXF (chapter 2 and 3). Differently, MXF release could be controlled when molecular imprinting technology was applied (chapter 5). In the present chapter both strategies (LbL coating and imprinting) were simultaneously addressed to control the release of two drugs that are commonly co-administered through eye drops to address a variety of ophthalmological disorders.

Several studies investigated the dual drug release from SCLs based systems. Rad *et al*. (2015) tested the efficacy of vitamin E loading as diffusion barrier to control the release of ciprofloxacin and betamethasone and concluded that depending on the amount of vitamin E incorporated, it was possible to retard significantly the release of both drugs [1]. Malakooti *et al*. (2015) used molecular imprinting method to develop HEMA based hydrogels for the release of polymyxin B and vancomycin. They found that the imprinting effect was only exhibited with polymyxin B: the imprinted hydrogels loaded higher amounts of this drug and led to more sustained release profiles, comparatively with non-functionalized and non-imprinted hydrogels [2]. Korogiannaki *et al*. (2015) found that the release of HA favourably enhanced the release kinetics of timolol maleate due to electrostatic interactions [3]. White *et al*. (2016) used the molecular imprinting process to control the release of multi drugs from silicone-based hydrogel contact lenses [4]. These strategies led to an improvement in drug release kinetics. However, further analysis of the literature did not allow to find any studies where different strategies have been used simultaneously to target two different ophthalmic drugs and at the same time to improve the surface properties of the hydrogels.

In this work a MXF imprinted silicone-based hydrogel was prepared according to the procedure described in chapter 5. The tested drugs were DCF and MXF (**Table 1.4** in chapter 1 shows the chemical structures and some physical properties of these drugs). The release was studied in sink in medium under stirring and in sink conditions using a lab-made microfluidic cell described in section 5.2.4, chapter 5. A LbL coating based on ALG, PLL and HA, designated as ALG/PLL(EDC)//HA, which was previously described in chapter 3, was used to control the DCF release. These biopolymers demonstrate the capability of forming stable coatings with antibacterial properties [5]. Although in literature there is some controversy about HA

antibacterial properties [6], association of HA with the antibacterial PLL resulted in the reduced growth of *S. aureus* and *P. aeruginosa*. On the other hand, HA is known to prevent cell adhesion and reduce protein adsorption [7–9], which was verified for lysozyme in chapter 3. Antifouling properties are quite relevant to prevent bacterial biofilms formation on SCLs surfaces [10]. Additionally, protein adsorption enhances corneal epithelium cell adhesion, which ultimately can affect cornea health and decrease patients' comfort [11]. The chemical structures and some physical properties of the polyelectrolytes used in this work are summarized in Appendix C.

Improvement of the release profile of MXF was attempted by molecular imprinting of this drug coupled to the modification of the polymeric matrix by introduction of the functional monomer AA, which may interact specifically with MXF through ionic interactions or hydrogen bonds [12,13].

Sterilization of the SCLs is a mandatory step to ensure its safe use. In this work, it is particularly challenging because the natural polyelectrolytes of the coating and/or the drugs may not resist the conventional sterilization methods commonly used for SCLs (SP, and γ-radiation). Thus, an alternative sterilization process that relies on HHP and that was previously validated for another LbL coating (chapter 4), was tested.

Physical properties of the hydrogels were studied, namely, topography, optical properties (transmittance and refractive index), wettability, ionic permeability and stiffness. Protein-coating interactions were analysed. Possible ocular irritancy was studied by the HET-CAM test. Antimicrobial tests were carried out against two of the most common bacteria involved in ocular infections *S. epidermidis* and *S. aureus* [14,15]. Finally, cell viability and cell adhesion were analysed using mouse embryonic fibroblastic cells (NIH/3T3)

6.2   Experimental part

6.2.1   Materials

2,2'-Azobis(2-methylpropionitrile) (purity≥98%, AIBN), 2-hydroxyethyl methacrylate (purity≥99%, HEMA), 3-tris(trimethylsilyloxy)silylpropyl 2-methylprop-2-enoate (purity≥98%, TRIS), acetic acid (purity≥99.7%), alginic acid sodium salt from brown algae

(average molecular weight 100,000-200,000 g/mol, 61% mannuronic acid and 39% guluronic acid, ALG), branched polyethylenimine (weight-average molecular weight 750,000 g/mol, PEI), calf serum (CS), diclofenac sodium salt (purity≥ 98.5%, DCF), dimethyl sulfoxide (DMSO), dulbecco's Modified Eagle's Medium (DMEM), ethylene glycol dimethacrylate (purity≥98%, EGDMA), hydrochloric acid (HCl), isopropanol, *N*-(3-dimethylaminopropyl)-*N*'-ethylcarbodiimide hydrochloride (purity≥98%, EDC), NIH/3T3 fibroblasts (93061524), poly-L-lysine hydrobromide (average molecular weight 70,000–150,000 g/mol, PLL), penicillin-streptomycin solution (10000U/mL penicillin, 10 mg/mL streptomycin) and phosphate buffer solution (pH 7.4, PBS) were provided by Sigma-Aldrich (USA). Lysozyme chicken egg white (pH 6.5), *N*-vinyl pyrrolidone (purity≥98%, NVP), sodium hydroxide (purity≥99%, NaOH) and octylphenoxypolyethoxyethanol (IGEPAL®) were obtained from Merck (USA). Sodium chloride (purity≥99%, NaCl) was purchased from PanReac (Spain). Moxifloxacin hydrochloride (MXF) and sodium hyaluronate (average molecular weight 1000,000–2000,000 g/mol, HA) were purchased from Carbosynth (UK). Methanol (purity≥99.9%, CH₃OH) was obtained from Carlo Erba (Spain). Acrylic acid (purity≥99%, AA) was purchased from Alfa Aesar (Germany). Mueller-Hinton agar (MH) was obtained from Oxoid microbiological products (UK). Albumin bovine Fraction V standard grade (pH 7.0) was supplied by Serva (Germany). Distilled and deionised (DD) water (18 MΩcm, pH 7.7), obtained from a Millipore water purifying system, was used to prepare all solutions.

6.2.2 Hydrogels preparation

MXF molecularly imprinted silicone-based hydrogels (designated as TRIS(300)-I) were prepared as described in section 5.2.2 in chapter 5. First, a monomer mixture of TRIS (0.8 M), HEMA (1.8 M), NVP (3.9 M) and AA (0.3 M) was homogenized with the crosslinker EGDMA (0.03 M) and MXF (0.003 M) using magnetic stirring. After degassing the solution by ultrasonic sonication (5 min) and nitrogen bubbling (10 min), the initiator AIBN (0.02 M) was added and completely homogenized. The solution was poured in pre-made moulds (Teflon separator, 0.3 mm) [16] and heated at 60 ℃ for 24 h. For comparison purposes, a silicone-based hydrogel without the AA monomer and without molecular imprinting (designed as TRIS) was produced in the same conditions as TRIS(300)-I. The hydrogels were removed from the moulds, cut in disks (12 mm diameter, unless stated otherwise), and submitted to washing in

DD water (10 days, medium change three times a day, 200 rpm stirring) to remove un-reacted monomers and MXF template molecules. Washed hydrogels were dried for 72 h at 36ºC and stored.

6.2.3 Methods for drug loading and drug release

A dual solution was prepared by mixing equal volumes of DCF and MXF solutions in PBS, followed by homogenisation through 2 h of magnetic stirring (100 rpm) at 50ºC, to obtain final concentrations of 0.5625 mg/mL and 1.1125 mg/mL, respectively for DCF and MXF. The produced hydrogels in the dry state were loaded by soaking on 3 mL of the dual solution for 72 h at room temperature. The conditions (drugs concentrations, time and temperature) were selected according to the criteria described in previous chapters and previous work [14], which took into account the solubility of the drugs, the hydrogel uptake, and the drug concentrations adequate for the therapeutic purposes.

The release experiments were done under sink conditions in medium under stirring through the immersion of the loaded hydrogels, after being removed from the loading solution and blotted, on vials with 3 mL of PBS at 36ºC with 180 rpm stirring. At selected times, aliquots of 200 µL were collected. To obtain the concentrations of DCF and MXF, a UV-Vis spectrophotometer (Multiskan GO, Thermo Scientific) was used, and the entire spectra (200 – 700 nm) of the collected solutions were compared to the spectra of each drug. The concentration of each drug was obtained through the deconvolution procedure described by Kim and Chauhan [17]. The measurements were done in quadruplicate.

For the most promising system, a lab-made microfluidic cell previously described in section 5.1 in chapter 5, was used to study the drug release under hydrodynamic conditions, which simulate better the *in vivo* eye conditions. The measurements were done in triplicate at 36ºC with a continuous flow (3 µL/min) of PBS. The out-flow solution was collected and analysed at selected times using the same method described above.

The amounts of drugs loaded in the hydrogel were determined with a methanol extraction. For this purpose, the drug-loaded hydrogels were placed in glass vials filled with 3 mL of methanol. The hydrogels were carefully removed from the vials at pre-established times, rinsed with DD water, and placed in other vials with fresh methanol. The procedure was repeated until no drug

could be detected in the methanol. Four experiments were carried out for each drug-loaded hydrogel.

6.2.4 LbL deposition

The LbL coating ALG/PLL(EDC)//HA was deposited on the hydrogels according to the procedure described in section 3.2.4 in chapter 3, and schematically depicted in **Figure 6.1**. A primary layer of PEI was formed by soaking the loaded hydrogels on a PEI solution (10 mg/mL) for 5 min, to allow the stabilization of the following layers. After that, two double layers of ALG and PLL were deposited by 10 min soaking on 1 mg/mL solution of each polyelectrolyte. After each PLL deposition, the hydrogels were dipped for 10 min in an EDC (5% wt) solution for crosslinking. A final top layer of HA (1 mg/mL) was formed to protect the preceding layers against enzymatic action of lachrymal proteins. The pH of the polyelectrolyte solutions was set at 7, by addition of NaOH or acetic acid, to enhance EDC crosslinking. Between each dipping, the samples were rinsed with DD water. After the LbL procedure, the coated hydrogels (designed as TRIS(300)-I-LbL) were placed on fresh dual drug loading solution to compensate the loss of drug during the immersions, for an equivalent time to that of the LbL procedure.
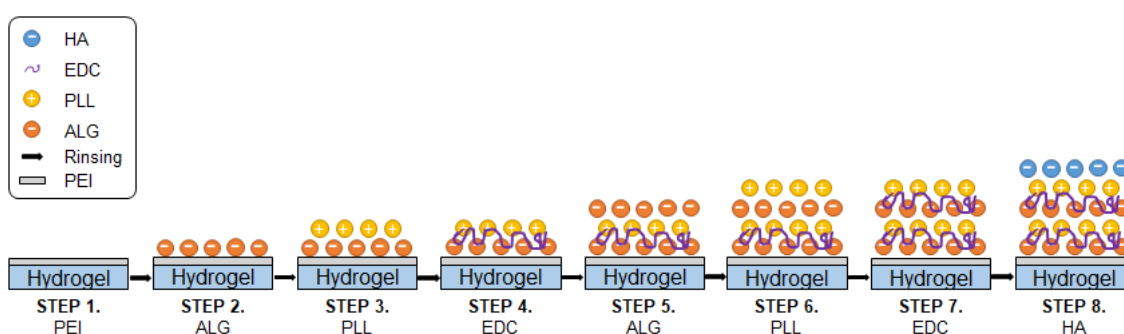
Figure 6.1 Schematic representation of the ALG/PLL(EDC)//HA coating procedure.

Uncoated hydrogels were placed in DD water for the same time as the LbL procedure, and reloaded with the drugs to simulate the process undergone by the coated hydrogels.

Additionally, for comparison purposes, non-imprinted hydrogels were also coated (designed as TRIS-LbL). All hydrogels were used immediately after preparation for release measurements and physical characterization. Images of the produced hydrogels can be found in **Figure 6.2**.
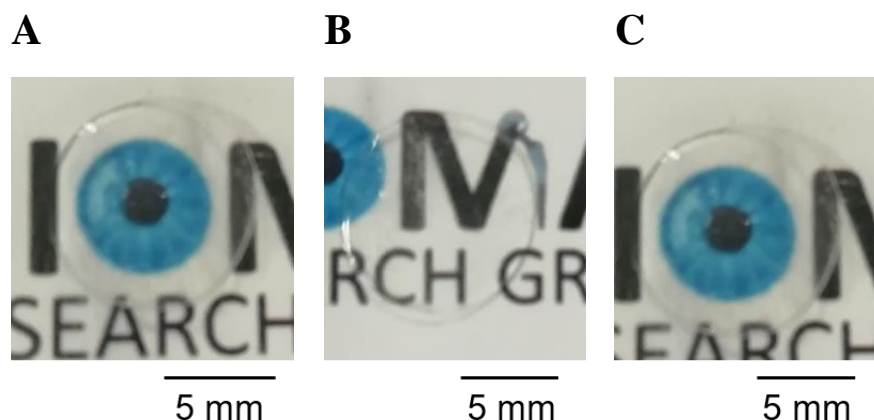
Figure 6.2 Pictures of the produced hydrogels: not sterilized TRIS **(A)**, TRIS(300)-I **(B)** and TRIS(300)-I-LbL **(C)**.

6.2.5 Evaluation of the LbL formation

The formation of the LbL coating was followed using a quartz crystal microbalance with dissipation (QCM-D, E4 from Q-Sense). Quartz crystals (5 MHz) with gold electrodes were pre-coated with a thin layer of polystyrene (PS) by spin coating (2000 rpm, 30 s), followed by the monomer mixture used for the formation of TRIS(300)-I hydrogel (5000 rpm, 30 s) and thermal polymerization at 60ºC for 1 h. The baseline was obtained by pre-hydrating the crystals coated with TRIS(300)-I in DD water for 10 min. Variations of frequency ($\Delta f/n$) and dissipation (ΔD) for the 3rd harmonic upon addition of each polyelectrolyte solution were monitored. Rinsing with DD water was carried out between each addition. The interaction of the LbL coatings with lachrymal proteins was studied through the injection of aqueous solutions of albumin (0.05 mg/mL) and lysozyme (1.9 mg/mL). Four independent measurements were done for each analysis.

6.2.6 Physical characterization of the hydrogels

The hydrogels were characterized with respect to some of the most important physical properties for SCLs application. The characterization was made for the drug-loaded samples except in the case of wettability and ionic permeability where drug release during the measurements would interfere with the results.

The water uptake of the hydrogels in DD water was studied. The dry hydrogels were weighted (W_D) and placed in 3 mL of the DD water at room temperature. At pre-selected times, the hydrogels were removed from the solution, carefully blotted in absorbent paper and weighted (W_W). Three measurements were made. The water uptake (%) was calculated by using **Equation 1.2** (chapter 1).

The wettability was studied by the captive bubble method. A video camera (jAi CV-A50, Spain) mounted on a microscope Wild M3Z (Leica Microsystems, Germany) was used to acquired pictures of the air bubbles produced underneath the hydrogels immersed in DD water. The images were analysed using the ADSA software (Axisymmetric Drop Shape Analysis, Applied Surface Thermodynamics Research Associates, Toronto, Canada). Ten bubbles were produced.

The refractive index was measured, at a 70º incidence angle, using a phase modulated spectroscopic ellipsometer (UVISEL, Horiba Jobin-Yvon) in the range 300-750 nm. The measurements were done in triplicate.

The transmittance was measured with a UV-Vis spectrophotometer (Multisckan GO, Thermo Scientific). Scanning was carried out in the wavelength range (200 – 700 nm) with of 1 nm intervals. At least three measurements were performed.

The ionic permeability was measured in a Lab-made cell described in section 1.1.4.2.5 in chapter 1. Experiments were done in triplicate at 36ºC. The conductivity was measured at each 30 min for 12 h, using a conductivity meter (HI2003 edge$^{EC®}$ from HANNA instruments), and converted into NaCl concentrations according to data previously obtained from a calibration curve. **Equation 1.4** in chapter 1 was used to obtain the D_{ion}.

The Young's modulus was determined from the initial slope of the tensile stress-strain curves obtained with a TA.XT Express Texture Analyser (Stable Micro Systems, UK) using the

software Exponent. The test speed was 0.3 mm/s and the trigger force was 0.005 N. Dumbbell-shaped samples with 2.5 mm width (overall width 5 mm) and 6 mm gauge length (total length 18 mm) of the drug-loaded hydrogels in the hydrated state were used. Five measurements were done.

An AFM (Nanosurf EasyScan 2) was used to obtain topographic images of the surfaces, at room temperature. The analysis was performed in non-contact mode, using silicon probes (resonance frequency: 204 – 497 kHz) and a scanning rate of 1 Hz. WSxM 5.0 develop 9.1 software was used to obtain the R_a for images of total area 10 x 10 μm^2. Three images were obtained.

6.2.7 Sterilization

TRIS(300)-I-LbL hydrogels were placed inside special sealed bags (polyamide and polyethylene, 90-micron, 10 x 10 cm^2, Penta Iberica), with 3 mL of PBS or dual drug solution in PBS, for the unloaded or the DCF+MXF loaded hydrogels, respectively. The sterilization procedure, was done using a high pressure equipment (Hiperbaric 55, Burgos, Spain) at 600 MPa and 70ºC for 10 min.

6.2.8 Antibacterial assays

The antibacterial activity of the sterilized DCF+MXF loaded TRIS(300)-I and TRIS(300)-I-LbL hydrogels was tested against *S. aureus* (ATCC 25923) and *S. epidermidis* (CECT 231) by direct contact. The strains were grown at 37ºC for 24 h. The grown strains were suspended on sterile 0.9% NaCl solutions to achieve an optical density of 1 McFarland (3×10^8 bacteria/mL). MH growing medium was sterilized by autoclaving at 121ºC, 1 bar for 20 min, and maintained in its liquid state at 50ºC in a water bath. Then, 50 mL of the medium was carefully homogenized with 350 µL of each bacterial suspension and poured on sterile square plates (120 x 120 mm^2) to solidify. The hydrogels (with 10 mm diameter) were removed from the sterile sealed bags, blotted with sterile absorbent paper, and finally placed on the petri dishes. A negative control (antimicrobial test disk with 15 µL of sterilized PBS) was added to all plates.

The plates were incubated for 24 h at 37ºC. The obtained inhibition halos were measured with an electronic calliper. Triplicates were done for each bacteria strain.

6.2.9 HET-CAM test

Sterilized unloaded and DCF+MXF loaded TRIS(300)-I-LbL hydrogels were tested for possible ocular irritancy through the HET-CAM test. Fertilized hen's eggs (Sociedade Agrícola da Quinta da Freiria, SA, Portugal) were placed inside an egg incubator (Incubator, 56S) at 37 ± 1ºC with 60 ± 4% RH for 8 days. The eggs were cut open on the air space on the 9th day, using a rotary saw (Dremmel 3000, Breda) to expose the inner membrane. A solution of NaCl (0.9%) was poured on the inner membrane to hydrate, and the eggs were further incubated for 30 min. The hydrated inner membrane was carefully removed with the help of tweezers, to give access to the CAM. The hydrogels were directly placed on top of the CAM for 5 min. After the assay, lysis, haemorrhage and coagulation were evaluated, and the IS was calculated according to **Equation 1.6** in chapter 1. The measurements were done in triplicate. Positive (NaOH, 1 M) and negative (NaCl, 0.9%) controls were also tested.

6.2.10 Cell viability

Cell viability of NIH/3T3 fibroblasts was assessed after exposure to unloaded and DCF+MXF loaded sterilized hydrogels, according to ISO standard 10993-5, using porous Transwell® inserts (8.0 µm pore polycarbonate membrane Corning® Transwell®, Sigma). After cultured in DMEM medium, supplemented with 2 mM L-glutamine, 10% CS and 1% Penicillin-Streptomycin, cells were seeded at a density of $1x10^5$ cells/well on a 24 well-plate and incubated for 24 h at 37ºC with a humified 5% CO_2 atmosphere. After 24 h, the culture medium was replaced by fresh DMEM medium, the inserts containing the sterilized hydrogels were placed on each well and 0.1 mL of DMEM was poured on top of each hydrogel. Positive (DMEM with 7.5% DMSO) and negative (only DMEM) controls were also prepared. Cells were incubated for an additional 24 h under the same conditions. The MTT assay was used to quantify cell viability. For that, each Transwell® and the medium were removed and 300 µL of MTT (0.5 mg/mL in serum-free DMEM) was directly poured over the cells followed by 3 h

incubation. The formazan crystals were dissolved in 450 µL of MTT solvent (4 mM HCl, 0.1% IGEPAL in isopropanol). The absorbance was read at 595 nm in a microplate reader (Platos R 496). Quintuplicates were carried out for each system.

6.2.11 Cell adhesion

To evaluate any possible effect of the coating on cell adhesion, unloaded and DCF+MXF loaded sterilized TRIS(300)-I and TRIS(300)-I-LbL hydrogels were tested using NIH/3T3 fibroblasts. First, the cells were grown on DMEM for 24 h in an incubator at 37ºC with a humified 5% CO_2 atmosphere. The sterilized hydrogels were removed from the sealed bags, blotted with sterilized absorbent paper and placed on the bottom of a well in a 24 well-plate. A drop (25 µL) of the cell suspension ($2x10^4$ cells) was carefully spotted on the middle of the hydrogel surface. For the negative control the cell drop was directly placed on the middle of an empty well. After incubation for 1 h to promote adhesion, 600 µL of DMEM were added on the lateral side to avoid touching the hydrogel and the cells and the plate was incubated for 24 h under the same conditions. The surface of the hydrogels was visualized under an inverted light microscope (Axiovert® 25, ZEISS Microscopy – Jena, Germany). The hydrogels were washed with PBS, placed in new wells and MTT assay was carried out to quantitative evaluate cell adhesion to the surface. Five measurements were made for each system.

6.2.12 Statistical analysis

Statistical analysis was carried out using R Project v. 3.6.1 software and presented as mean standard deviations. Shapiro-Wilk test was used to verify the normality of the data. For parametric data, One-way ANOVA test and Student's t-test were used to calculate if two or more sets of data were significantly different. For non- parametric paired Willcon was used. The level of significance was set to 0.05.

6.3 Results

6.3.1 Evaluation of LbL formation

Formation of the LbL coating was confirmed by QCM-D, by monitoring the changes of $\Delta f/n$ and ΔD for the 3$^{\text{rd}}$ harmonic after addition of each polyelectrolyte solution to the TRIS(300)-I coated quartz crystals (**Figure 6.3A** and **B**). The rinsing steps induced an increase in frequency and a decrease in dissipation as loosely bond molecules were removed, but nevertheless, the formed layers remained stable. Interestingly, the coating performed differently against two relevant ocular proteins, lysozyme and albumin. The addition of the lachrymal proteins to the top layer of HA (step 7) induced two different behaviours: lysozyme was scarcely adsorbed and completely removed after the final rinsing (**Figure 6.3A**), while albumin adsorbed significantly and remained adsorbed after the rising (**Figure 6.3B**).

A
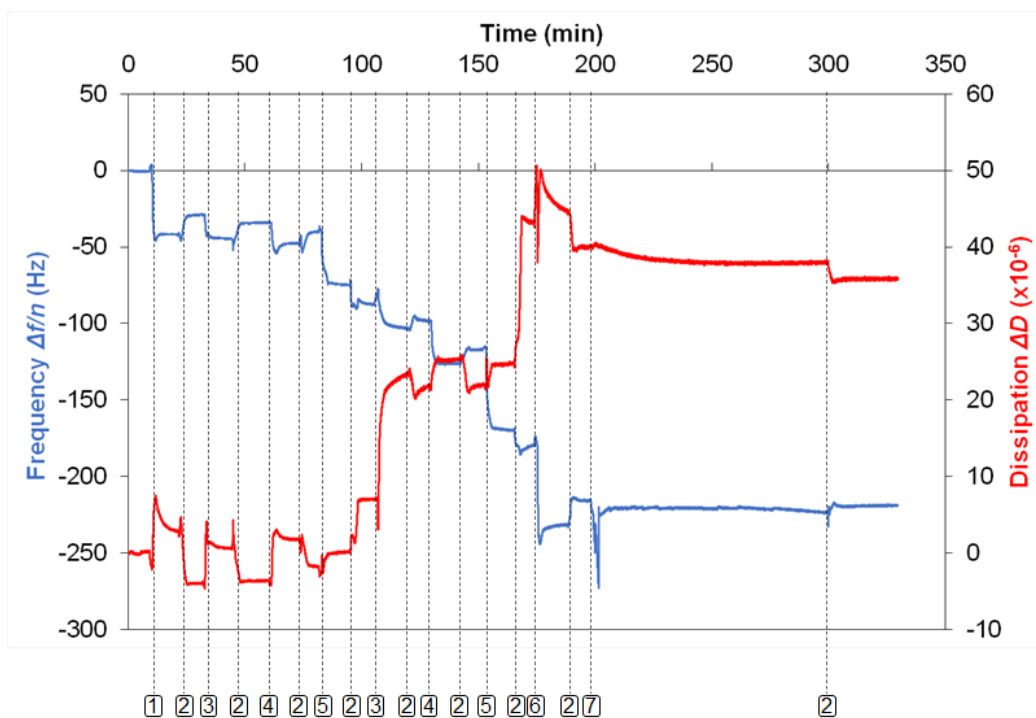
B
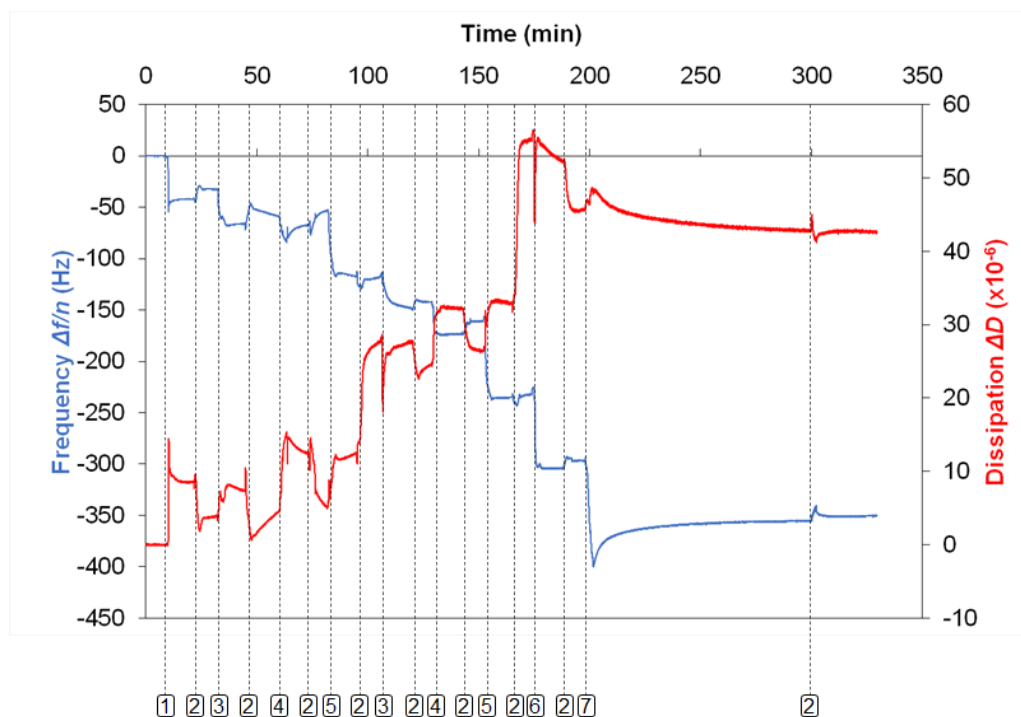
Figure 6.3 Normalized shift in the frequency *Δf/n* (blue line, left y-axis) and shift in dissipation *ΔD* (red line, right y-axis) for the 3rd harmonic of the resonant frequency of a quartz crystal

sensor after coated with TRIS(300)-I hydrogel film, during successive additions of solutions of PEI (1), ALG (3), PLL (4), EDC (5) and HA (6) as a function of time, to form two double layers of ALG/PLL with a top layer of HA (ALG/PLL(EDC)//HA). The final step (7) corresponds to the addition of lysozyme **(A)** and albumin **(B)**. A rinsing step (2) was carried out between each injection.

6.3.2 Drug loading and release

The amounts of drugs loaded inside the four different hydrogels (uncoated and coated, non-imprinted and imprinted hydrogels) are summarized in **Table 6.1**. The imprinting process associated with the addition of the functional monomer led to an increase in the MXF uptake, but decreased the amount of DCF loaded. The presence of the coating did not interfere with the amount of DCF loaded in the imprinted (p=0.547) and non-imprinted hydrogels (p=0.101). The same conclusion was found for MXF loaded in the imprinted (p=0.865) and non-imprinted hydrogels (p=0.865).

Table 6.1 DCF and MXF loaded by uncoated non-imprinted (TRIS), coated non-imprinted (TRIS-LbL), uncoated MXF-imprinted (TRIS(300)-I) and coated MXF-imprinted hydrogels (TRIS(300)-I-LbL). The errors are the ± standard deviations (n=4).

Hydrogel designation	Drug loaded (µg/mg of dried gel)	
	DCF	MXF
TRIS	54±3	8.6±0.9
TRIS-LbL	57±2	9±1
TRIS(300)-I	35±3	45±2
TRIS(300)-I-LbL	36±2	44±3

For comparative purposes the DCF+MXF release profiles were evaluated for all hydrogels in medium under stirring. As expected from the data of **Table 6.1**, the amount of DCF released from the TRIS(300)-I decreased compared to TRIS (**Figure 6.4A**). The release of DCF from the uncoated hydrogels (TRIS and TRIS(300)-I) revealed an initial burst, which was considerably attenuated in the presence of the coating (TRIS-LbL and TRIS(300)-I-LbL). Similar release profiles were obtained for both imprinted and non-imprinted coated hydrogels.

The release of MXF from TRIS and TRIS-LbL (**Figure 6.4B**) was similar: the drug was quickly released, achieving >85% of the total drug released after 7 h. This behaviour is in agreement with our previous findings about the inefficiency of this type of LbL coatings to retard the release of MXF (see chapter 3). Differently, the imprinting process led to a significant increase in the amount of MXF released (since the loading was also higher) and a more sustained release was achieved. For example, in the case of TRIS(300)-I-LbL only 23% of the total amount of MXF was released in the first 1 h.

A
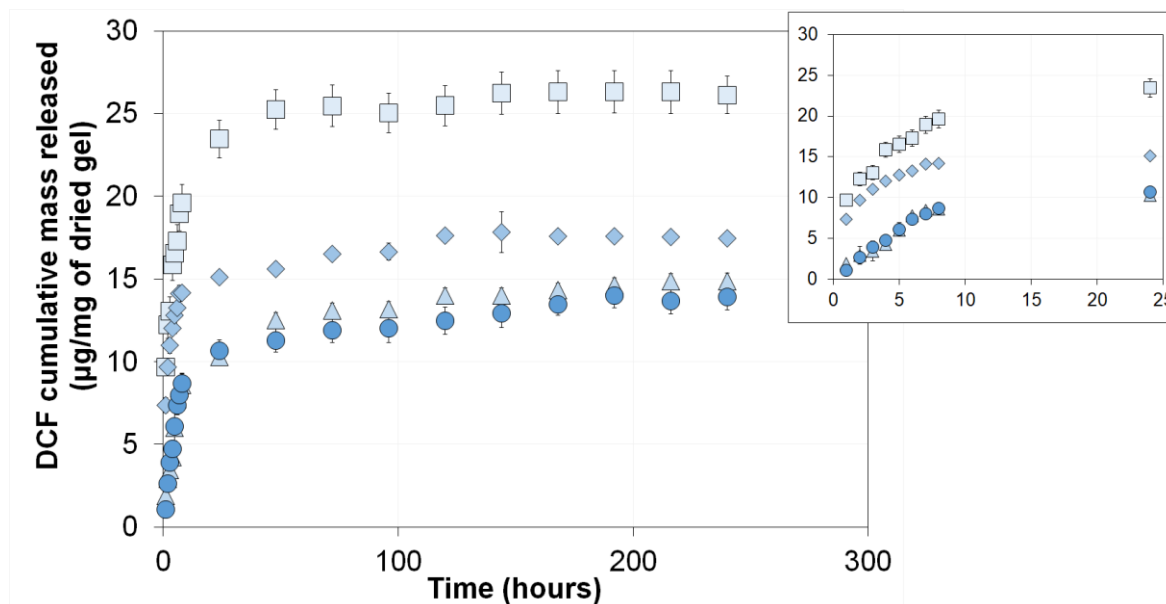
B
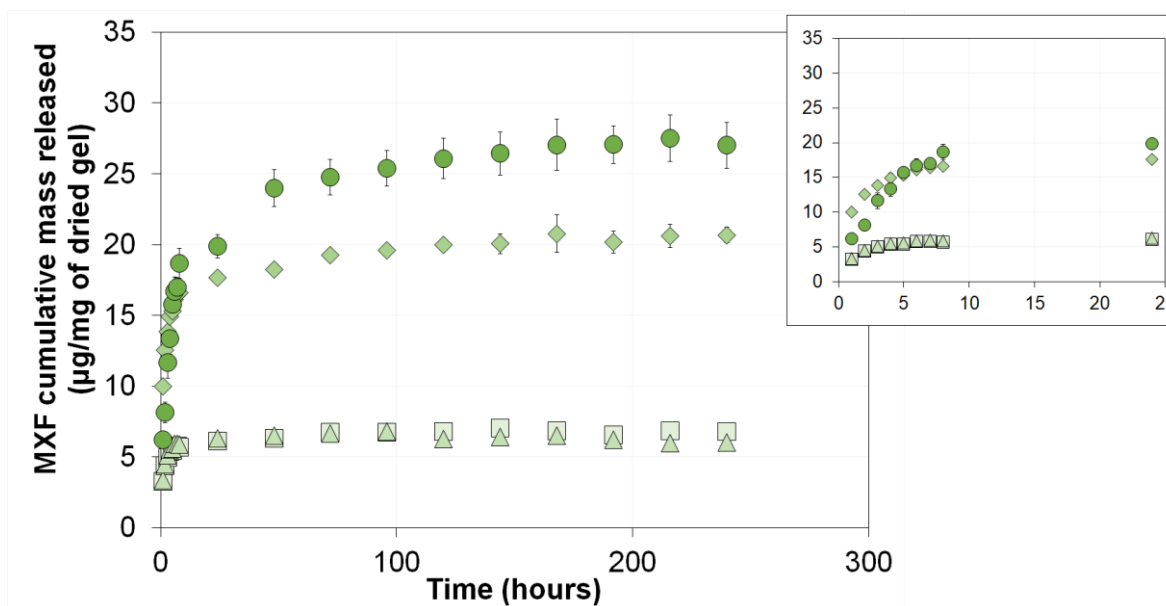
Figure 6.4 DCF (**A**) and MXF (**B**) release profiles from TRIS (■), TRIS-LbL (▲), TRIS(300)-I (♦) and TRIS(300)-I-LbL (●) samples. The inserts represent the first 24 h of the release data. The error bars represent the ± standard deviations (n=4).

The above results show that TRIS(300)-I-LbL is the most adequate platform for the simultaneous delivery of DCF and MXF, and therefore the dual drug release was also assessed under hydrodynamic conditions using the microfluidic cell. The release profiles obtained as

concentration vs time are presented in **Figure 6.5** together with the IC_{50} range of values found in literature for COX-1 (0.04 – 0.3 µg/mL) and COX-2 (0.01 – 0.03 µg/mL), which are active enzymes in the process of inflammation, and the MICs for *S. aureus* (0.008 – 0.064 µg/mL) and *S. epidermidis* (0.016 – 2 µg/mL) [14,18]. The concentrations of the released DCF and MXF stayed above the IC_{50} and the MICs values, for 9 and 10 days, respectively.

A
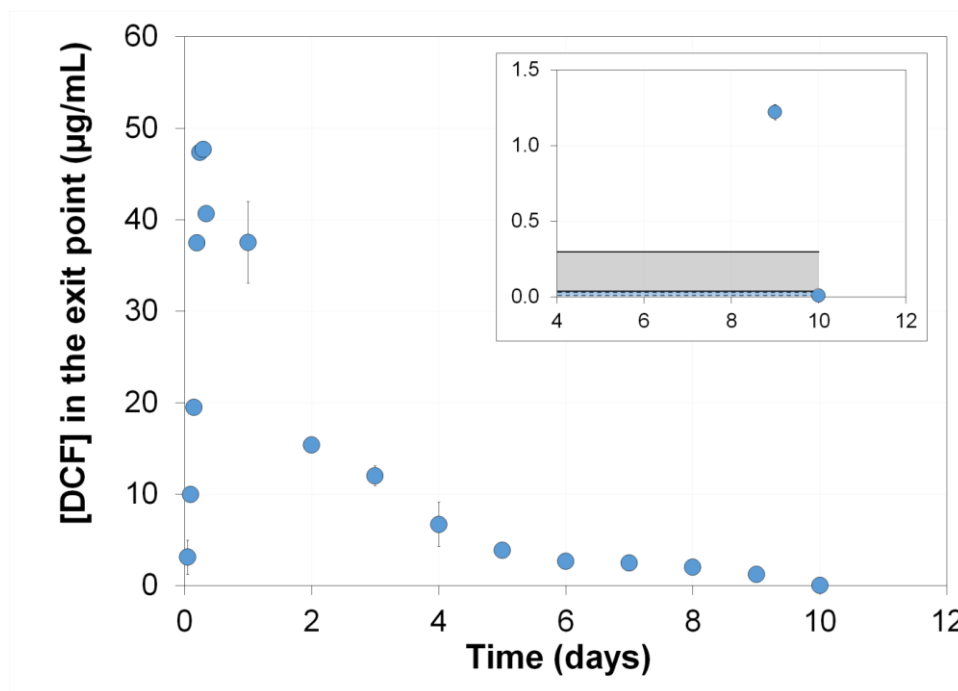
B
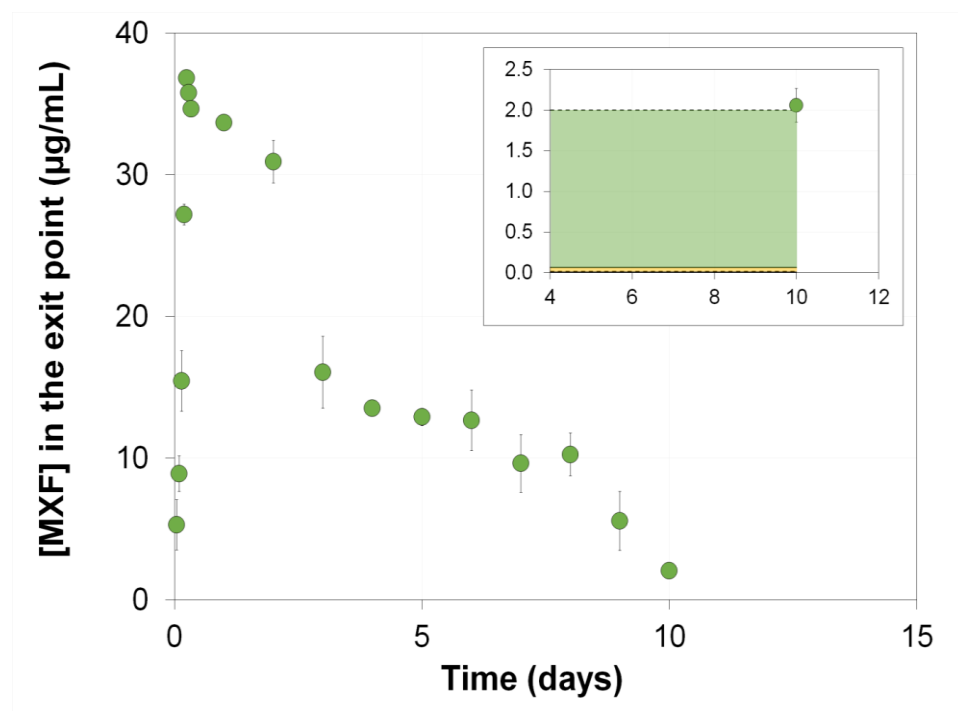
Figure 6.5 Concentration profile of DCF **(A)** and MXF **(B)** released from TRIS(300)-I-LbL at the exit point of the microfluidic cell compared to the range of IC_{50} for COX-1 (grey area) and COX-2 (blue area), and the MICs for *S. aureus* (yellow area) and *S. epidermidis* (green area) [14,18]. The error bars represent the ± standard deviations (n=3).

6.3.3 Physical characterization

The results of the measurements of the physical properties that are critical for SCLs application are summarized in **Table 6.2** for TRIS, TRIS(300)-I and TRIS(300)-I-LbL.

The water uptake was significantly higher for the imprinted hydrogels (TRIS(300)-I and TRIS(300)-I-LbL) when compared to TRIS (p <0.0001). The effect of the LbL coating on the water uptake is negligible (p=0.568).

The water contact angle decreased after the imprinting process for TRIS(300)-I (p<0.0001) and for TRIS(300)-I-LbL (p<0.0001). The coating did not affect the refraction index (p=0.478). The transmittance remained above 90% in all cases. The ionic permeability of the coated hydrogels decreased when compared to TRIS(300)-I (p=0.016). The values of the Young's modulus of TRIS(300)-I and TRIS(300)-I-LbL were close (p=0.813), but lower than those obtained for TRIS (p=0.0002). The R_a of TRIS(300)-I-LbL increased significantly when compared to TRIS(300)-I (p=0.019) and slightly, with respect to TRIS (p=0.012). The R_a of TRIS(300)-I-LbL increased significantly when compared to TRIS(300)-I (p=0.019) and slightly, with respect to TRIS (p=0.012). The pores on the surface of TRIS (**Figure 6.6A**) decreased on the smooth surface of TRIS(300)-I (**Figure 6.6B**), and were mostly hidden by the coating (**Figure 6.6C**), which exhibited a grainy surface.

A
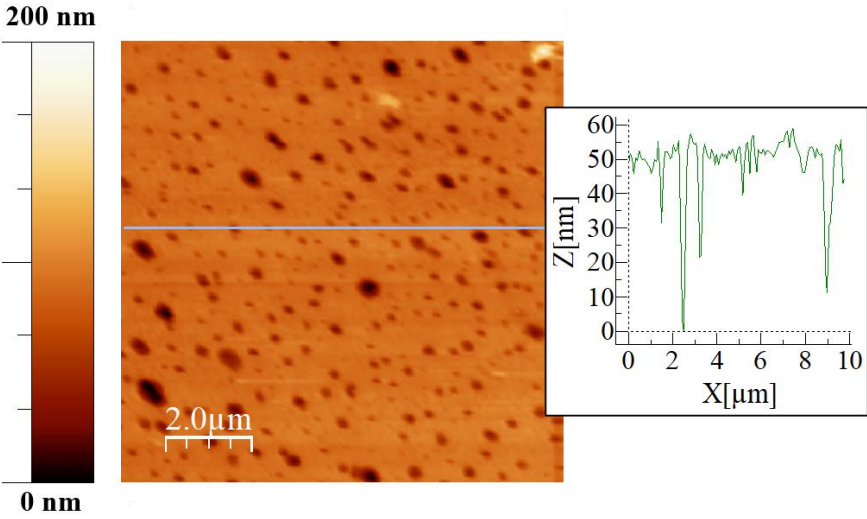
B
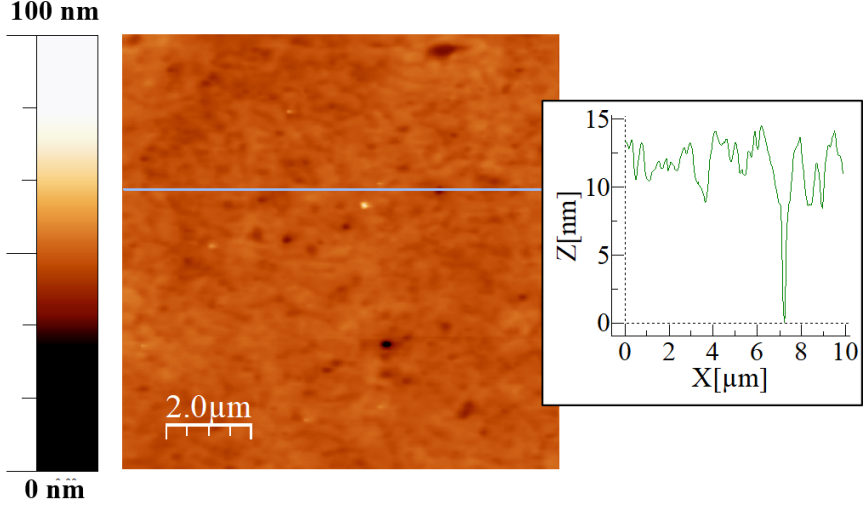
C
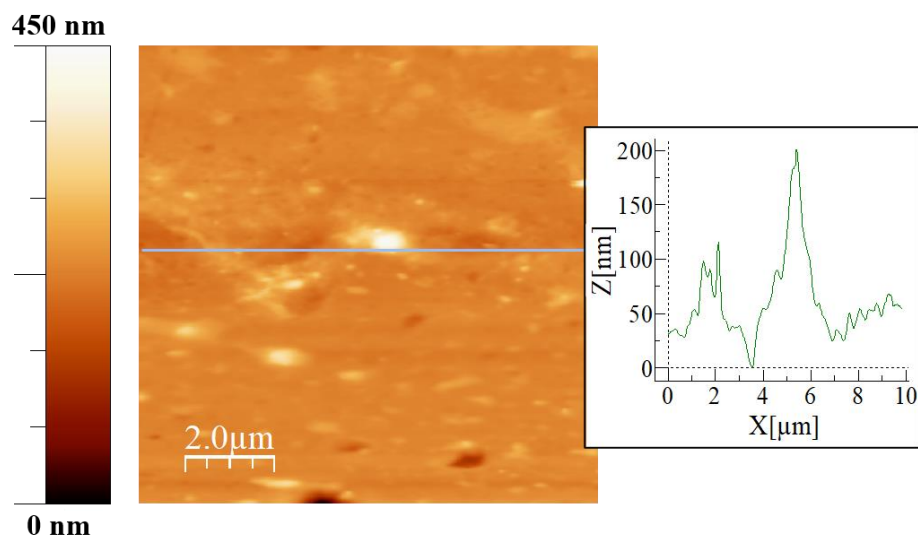
Figure 6.6 AFM images (10 x 10 µm^2) of the surface of TRIS **(A)**, TRIS(300)-I **(B)**, and TRIS(300)-I-LbL **(C)** along with the corresponding section analysis for each of them.

The thickness of the coating was assessed by fitting the QCM-D data with a viscoelastic modelling (Broad Fit), assuming the value 1 g/cm^3 for the density of the coating, according to obtained data in chapter 3.

Table 6.2 Properties of TRIS, TRIS(300)-I and TRIS(300)-I-LbL: water uptake, water contact angle, refraction index, transmittance, ionic permeability, Young's modulus, R_a and coating thickness. The errors are the ± standard deviations (in all cases n=3, except for Young's modulus (n=5) and water contact angle (n=10)).

	TRIS	TRIS(300)-I	TRIS(300)-I-LbL
Water uptake (%)	74±4	122±5	119±2
Water contact angle (º)	37±1[a]	30±2[a]	31.6±0.2
Refractive index	1.36±0.01[a]	1.36±0.01[a]	1.38±0.02
Transmittance (%)	98.8±0.5[a]	94.6±1.2[a]	96.2±0.8
Ionic permeability (cm²/s)	$5 \times 10^{-7} \pm 0.2 \times 10^{-7}$[a]	$1 \times 10^{-6} \pm 1 \times 10^{-7}$[a]	$7.4 \times 10^{-7} \pm 3.2 \times 10^{-7}$
Young's modulus (MPa)	1.09±0.04[a]	0.52±0.02[a]	0.054±0.09
R_a (nm)	11.2±2.5[a]	1.7±0.4[a]	14.5±3.1
Coating thickness (nm)	-	-	100±12

[a] From section 5.3.1 in chapter 5.

6.3.4 Sterilization effects

The effect of HHP sterilization on the optical properties and drug release behaviour of the TRIS(300)-I-LbL hydrogels was assessed to infer about any eventual degradation of the

samples and, in particular, of the coating. Visual observation of the samples before (**Figure 6.2C**) and after (**Figure 6.7**) being sterilized did not reveal any differences

5 mm
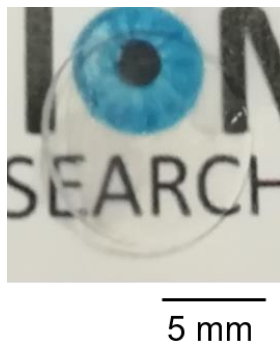
Figure 6.7 Picture of the TRIS(300)-I-LbL hydrogel after HHP sterilization.

The release profiles of the drugs obtained in medium under stirring do not present significant differences relatively to those obtained with non-sterilized hydrogels (**Figure 6.8A** and **B**).

A
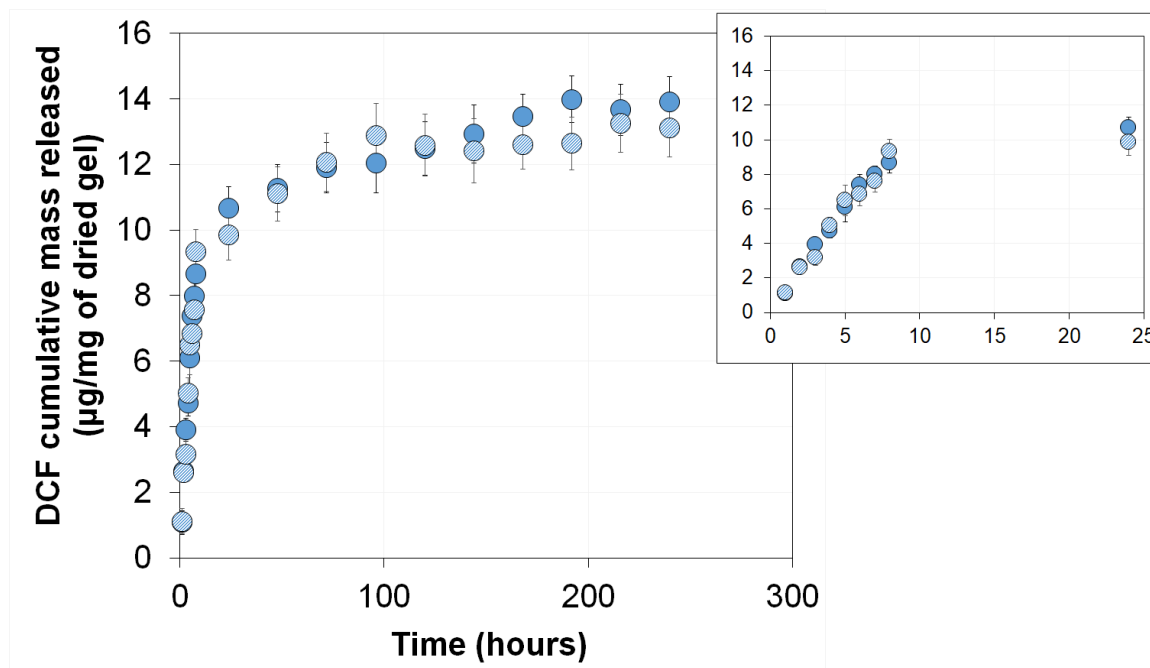
B
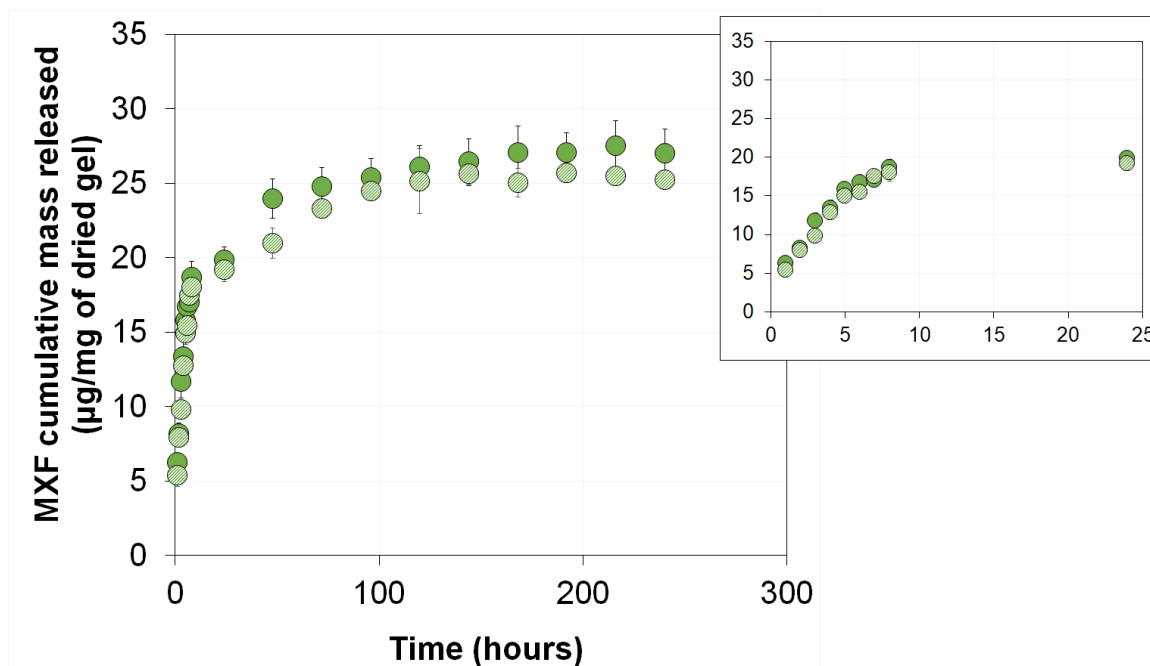
Figure 6.8 DCF **(A)** and MXF **(B)** release profiles for TRIS(300)-I-LbL before (●) and after HHP (◉) sterilization. The inserts represent the release for the first 24 h. The error bars are the ± standard deviations (n=4).

The transmittance decreased with the HHP process (**Figure 6.9**), although the obtained values were still above the required minimum of 90% [19]. The refractive index was not affected (p=0.25), varying from 1.38±0.02 for the samples before sterilization and 1.37±0.02 for the sterilized samples.
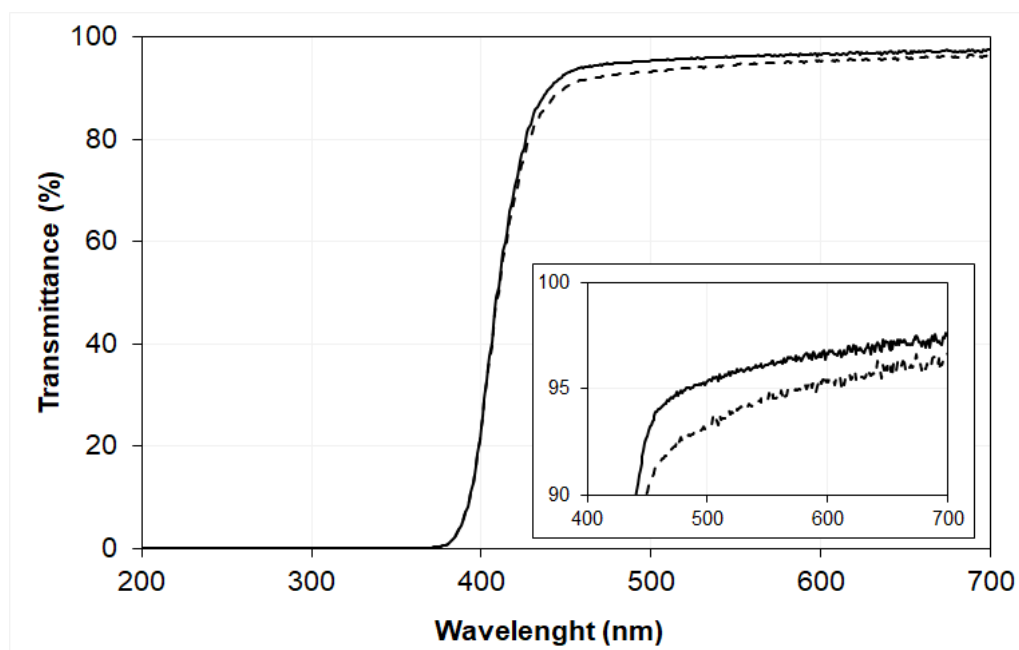
Figure 6.9 Transmittance of DCF+MXF loaded TRIS(300)-I-LbL hydrogels non-sterilized (full line) and HHP (dotted line). The insert represents the wavelength between 400 and 700 nm.

6.3.5 Antibacterial assays

The effectiveness of the antibiotic MXF against *S. aureus* and *S. epidermidis* was confirmed by the formation of inhibition halos from the direct contact with DCF+MXF loaded uncoated (TRIS(300)-I) and coated (TRIS(300)-I-LbL) hydrogels, after being sterilized (**Figure 6.10**). The growth inhibition zones for both bacteria were slightly larger for the TRIS(300)-I-LbL hydrogels (p=0.0005) than for its uncoated counterpart (p=0.059). For both hydrogels MXF was more effective against *S. aureus* than against *S. epidermidis* (p=0.031 for TRIS(300)-I, p=0.078 for TRIS(300)-I-LbL).
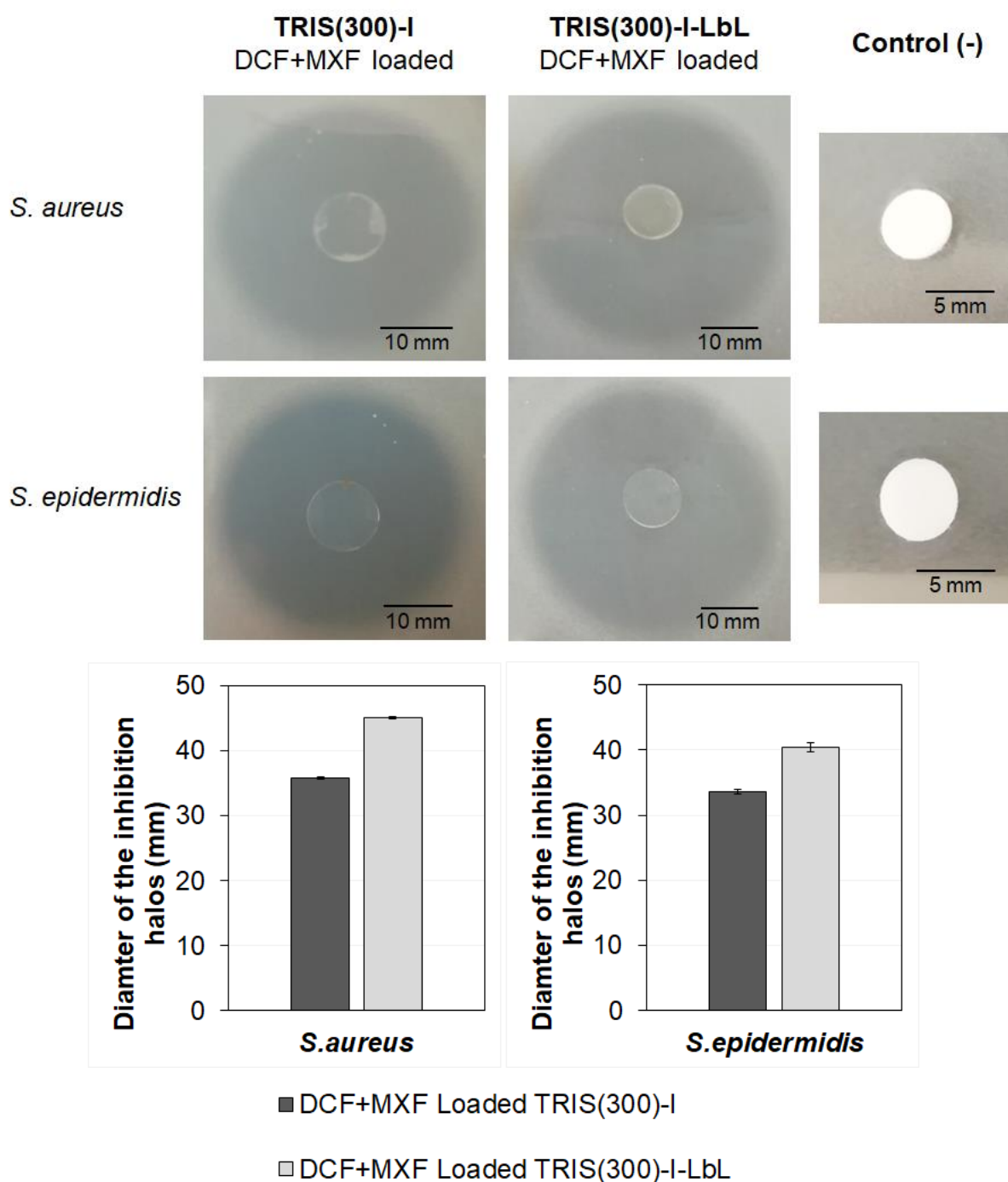
Figure 6.10 Inhibition halos after 24 h of direct contact with DCF+MXF loaded TRIS(300)-I and TRIS(300)-I-LbL hydrogels against *S. aureus* and *S. epidermidis*. Negative controls (sterile PBS) are also shown. Diameter of the obtained inhibition halos. The error bars are the ± standard deviations (n=3).

6.3.6 HET-CAM tests

All sterilized unloaded and drug loaded TRIS(300)-I-LbL hydrogels successfully passed the HET-CAM test and thus can be considered as non-irritant in contact with the ocular surface, as no lysis, haemorrhage or coagulation was detected on the chorioallantoic membrane after 5 min of direct contact with the samples. **Figure 6.11** shows that both hydrogels had outcomes similar to the negative control (NaCl 0.9%), with IS equal to 0.
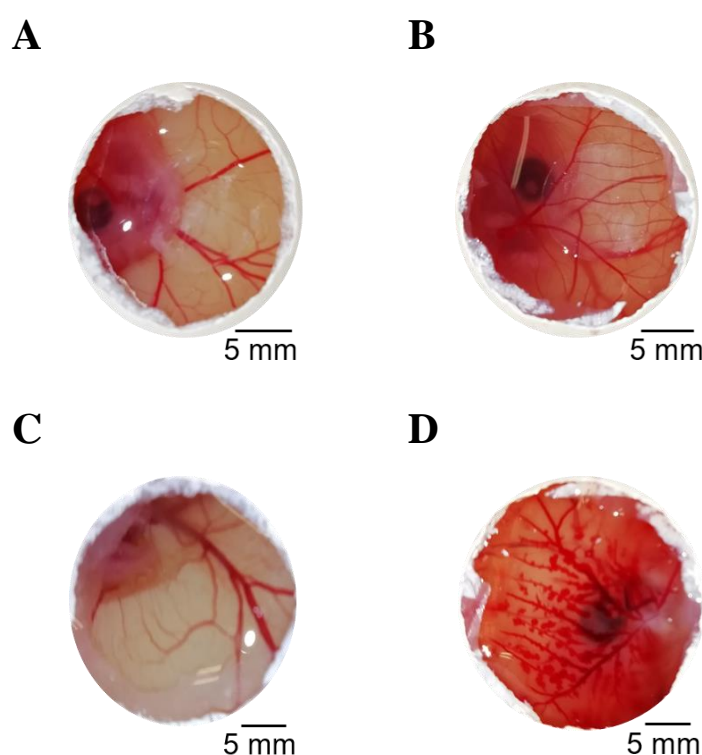
Figure 6.11 Fertilized hen's CAM images after 5 min of exposure to TRIS(300)-I-LbL unloaded **(A)** and loaded with DCF+MXF **(B)**, after HHP sterilization. Negative control (NaCl, 0.9%) **(C)** and positive control (NaOH, 1 M) **(D)** are also shown.

6.3.7 Cytotoxicity tests

The biocompatibility of the hydrogels was evaluated in NIH/3T3 cells using a Transwell® insert to mimic the separation between the hydrogels and the ocular tissue (i.e. cornea) by the post lens tear fluid. The insert containing the hydrogel was kept close but about a millimeter off the

bottom of the well preventing the mechanical disturbance of the cell layer. The porosity of the insert membrane allows the diffusion of leachable chemicals towards the cell layer. Unloaded LbL coated hydrogel was not toxic to fibroblastic cells, as shown by ~100% viability after exposure, but the presence of DCF+MXF induced a decrease of ~24% on cell viability (76.2±0.7%) (**Figure 6.12**).
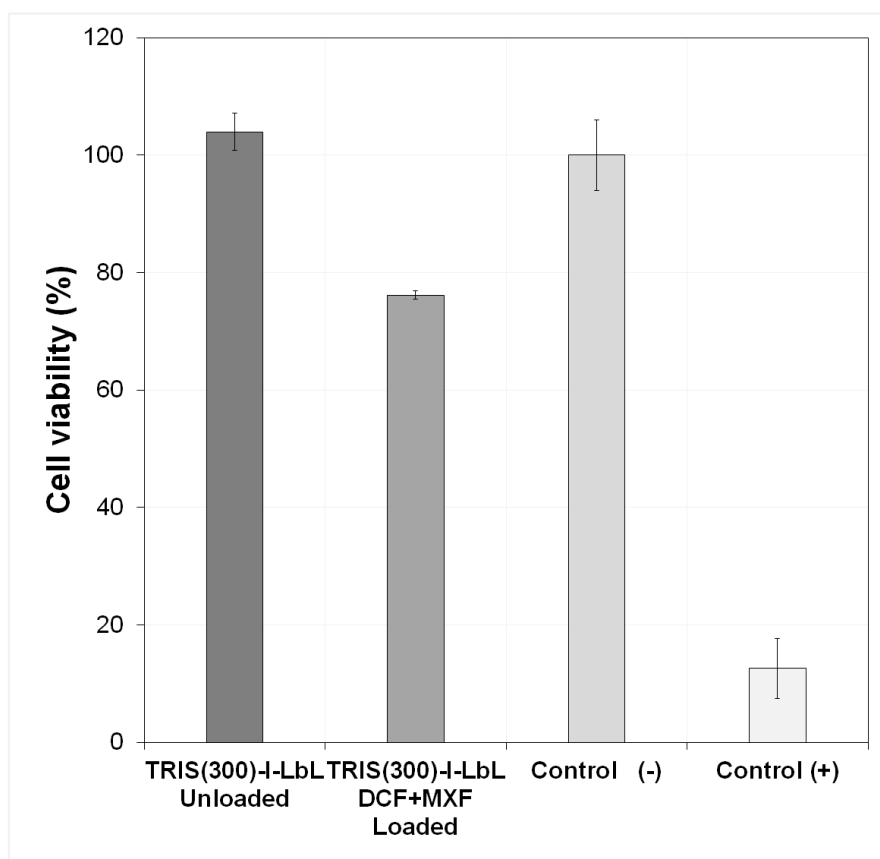
Figure 6.12 NIH/3T3 cells viability (%) determined by MTT assay, after 24 h exposure to unloaded and DCF+MXF loaded TRIS(300)-I-LbL hydrogels after HHP sterilization. Bars represent mean values ± standard deviations (n=5).

6.3.8 Cell adhesion

The possible undesirable cell adherence to the lenses was evaluated *in vitro* with NIH/3T3 fibroblasts on both coated and non-coated hydrogels. After 24 h culture on close contact, we observed that the cells were not fully seeded onto the LbL coated surface, remaining mainly on

a round shape. On the contrary, cells completely adhered and proliferated on the surface of unloaded and DCF+MXF loaded TRIS(300)-I, with their typical spindle-like morphology (**Figure 6.13A**). To quantify adherence, lenses were first rinsed with PBS to remove non-adherent cells, followed by the MTT assay. Accordingly, to what was observed before, viable cells were detected only on the uncoated hydrogel, albeit in a small number (**Figure 6.13B**). As expected after the toxicity assays, the presence of the drugs resulted in a decrease in absorbance (p=0.007). Altogether, these results indicate that the coating turned the hydrogel less prone to cell adhesion.

A
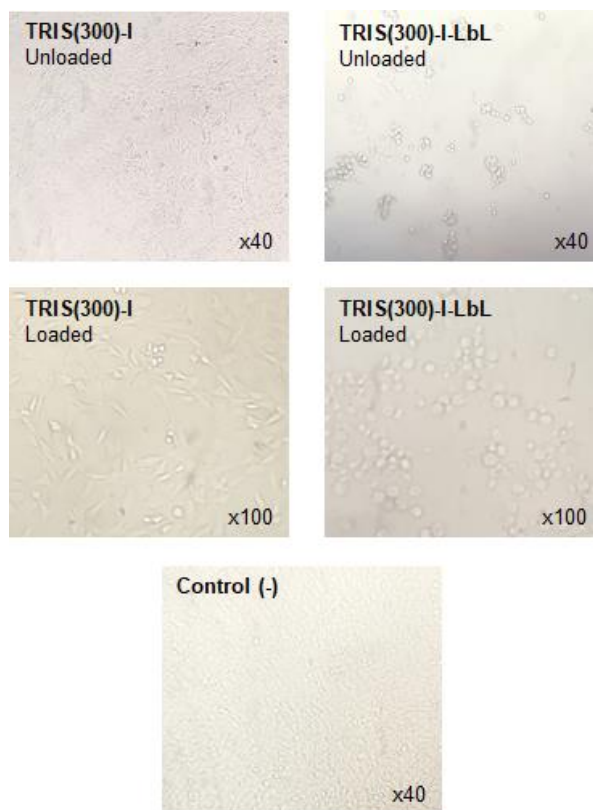
B
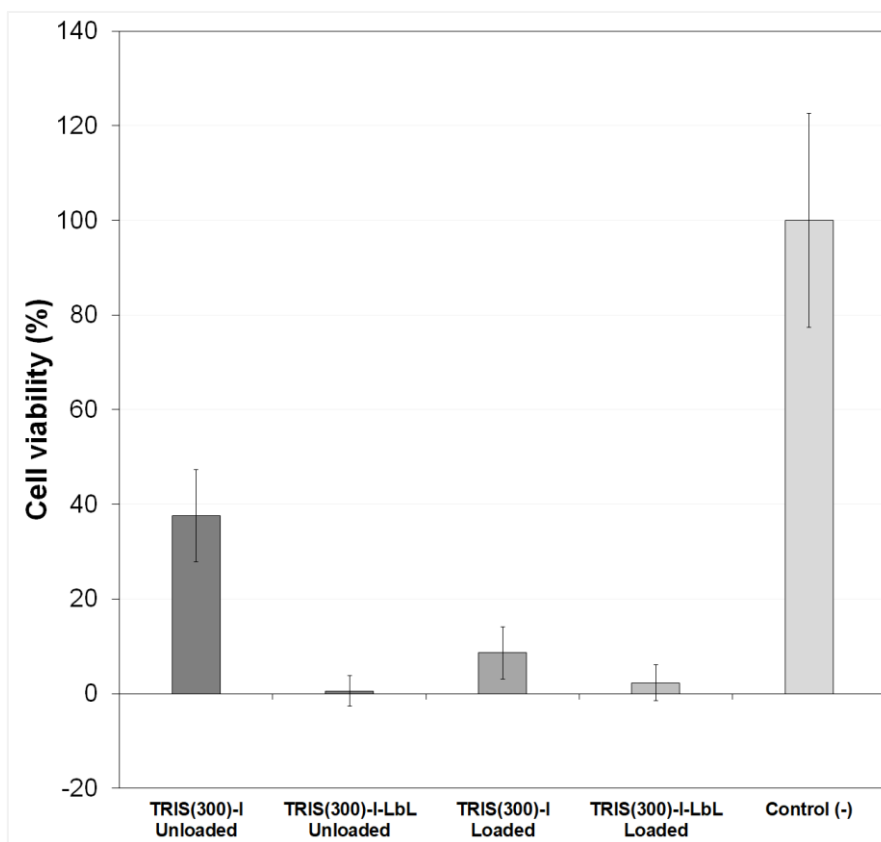
Figure 6.13 (A) Micrographs of cell attachment on top of hydrogels surfaces or the well after 24 h incubation and immediately before PBS rinsing. **(B)** NIH/3T3 cells viability (%) determined by MTT assay, after PBS rinsing. Bars represent mean values ± standard deviations (n=5).

6.4 Discussion

The treatment of most ocular infections and the associated inflammation implies the combination of anti-inflammatory agents with antibiotic drugs. As such, sustained dual drug release from SCLs is an important objective to be pursued. In previous chapters, several strategies to overcome unsuitable single drug release from silicone-based hydrogels for SCLs were carried out. However, the best solution to control the release of one drug may not work for a different drug. This was the situation previously reported for TRIS hydrogels (chapter 3),

where LbL coating successfully controlled the release of DCF, but was inefficient towards the MXF release, which was later optimized with molecular imprinting (chapter 5). In the present work, combination of both strategies was attempted to sustain the simultaneous release of DCF and MXF from TRIS hydrogels.

Separately, the controlled release of DCF by the ALG/PLL(EDC)//HA coating was attributed to the formation of reversible bonds between the drug and the polyelectrolytes. At physiological pH, electrostatic interactions between the negatively charged DCF and the positively charged PLL may occur [20,21]. Hydrophobic interactions could also arise between PLL or HA with DCF, which has been described as an amphiphilic drug [15]. Furthermore, unreacted EDC may be involved in the control of the DCF release through the activation of the carboxylic groups in the drug molecule that can react with free amine groups of ALG [22]. In the case of MXF, besides the existence of the molecular scale cavities in the hydrogel matrix, reversible electrostatic interactions with negatively charged AA greatly improve drug loading/release concentration and kinetics. AA is also known to form H-bonds with hydrogen bond acceptors [23].

The results of the combination of imprinting and coating on drug loading and release are not straightforward. The DCF uptake in the imprinted hydrogel, TRIS(300)-I, decreased significantly (~40%) when compared to the non-imprinted hydrogel, TRIS (**Table 6.1**), which leads to the consequent reduction of DCF release (**Figure 6.4A**). This effect may be attributed to the electrostatic repulsion between AA and DCF, or simply derives from the rearrangement of the hydrogel matrix due to the formation of MXF specific cavities. It is foreseeable that DCF molecules do not fit well into the MXF imprinted domains due to the different molecular architecture of these two drugs (as indicated in **Table 1.4** in chapter 1). The LbL coating of both TRIS and TRIS(300)-I hydrogels led to similar DCF release profiles, greatly decreasing the initial burst.

The presence of the coating on the imprinted hydrogel (TRIS(300)-I-LbL) resulted in a small change of the MXF release kinetics when compared to the uncoated TRIS(300)-I (**Figure 6.4B**), but did not affect the amount of drug loaded (**Table 6.1**). This specific coating was never previously assessed for MXF release, but a similar coating (ALG/PLL(EDC) without HA top layer) did not induce any control in the release of MXF (section 3.3.2 in chapter 3). Therefore,

one can assume that the observed reduction of the initial burst of MXF may be due to the interaction of the hydroxyl groups in HA with H bond acceptors in MXF.

The drug release profiles obtained with the microfluidic cell are more useful to approach the *in vivo* behaviour than those obtained under sink conditions in medium under stirring, which are still widely used for a preliminary screening of the capability of the hydrogels to sustain drug release. Disregarding the release device used, the amounts of released were below the known toxic levels for DCF (>100 µg/mL) and MXF (>150 µg/mL) (**Figures 6.5A** and **B**) [14]. The usual therapy of ocular infections with eye drops involves the application of four drops a day for DCF (duration of treatment depends on the patient) [24–27], and three drops a day for MXF (4 to 7 days) [28,29]. Thus, the periods of nine and ten days for which the DCF and MXF released concentrations were, respectively, above the minimum therapeutic values suggest that DCF+MXF loaded TRIS(300)-I-LbL hydrogels can provide suitable dual release for treatment of ocular infections.

Comparison of the amounts of drugs loaded and released revealed that nearly 50% of DCF and MXF loaded remained trapped inside the hydrogel's matrix after several days in the release medium. It is interesting to notice that, although the LbL coating did not modify the amount of MXF loaded, the amount of MXF released from the imprinted hydrogels increased in the presence of the LbL coating (**Figure 6.4B**), which may be due to the diffusion of drug towards the outer layers of the hydrogels during the LbL coating.

Combination of imprinting and coating only caused minor detrimental effects on some physical properties of the hydrogel, namely, ionic permeability, stiffness, and roughness, but all values remained within the range of typical values for SCL materials. In fact, the decrease seen in the water contact is due to the presence of the highly hydrophilic AA monomer [12]. The transmittance was above that necessary for SCLs use [19], and the ionic permeability was above the minimum required for SCLs (1.067×10^{-9} cm^2/s) [30]. The Young's modulus values were in agreement with other works in literature, that claimed that the addition of AA decreases the Young's modulus of hydrogels [23]. However, the stiffness of both imprinted hydrogels remains within the report values for SCLs [31], and the R_a values were compatible with SCLs requirements [32]. Finally, the estimated thickness of the LbL coating was consistent with values found for similar LbL coatings [33].

Sterilization of the LbL coated, imprinted hydrogels with HHP was successfully applied since no degradation of the samples was detected. The drug release profiles remained almost equal, meaning that the matrix structure and the coating did not suffered significant changes. The slight decrease in the transmittance observed has no practical consequences in the optical performance of the material. It should be stressed that this sterilization method seems to be the unique possibility to sterilize LbL coatings based on natural polyelectrolytes. A similar LbL coating was irreversibly damaged after sterilization with SP (autoclave) (chapter 4).

The obtained inhibition halos were significantly increased for TRIS(300)-I-LbL hydrogels when compared to TRIS(300)-I. This result can be related to the increase in the amount of MXF released from the coated hydrogel, but also, to some extent, to the antibacterial properties of the coating (chapter 3).

The unloaded TRIS(300)-I-LbL hydrogels demonstrated to be safe. The DCF+MXF loaded TRIS(300)-I-LbL hydrogels, although not eye irritant, induced a decrease of ~24% of cell viability, when compared to the unloaded ones. Several authors described a toxicity effect of DCF and MXF, decreasing cell proliferation and viability [34,35]. Bezwada *et al*. (2007) showed that MXF (1 mg/mL) was toxic for corneal keratocytes and endothelial cells, regardless of time exposure [36]. Kim *et al*. (2007) evaluated the exposure of human corneal epithelial cells to levofloxacin and MXF, and observed that MXF showed higher toxicity than levofloxacin [37]. Lee *et al*. (2015) discussed the *in vitro* toxicity of nonsteroidal anti-inflammatory eye drops to human corneal epithelial cells, and found that DCF presented the highest cytotoxicity after 12 h and 24 h of exposure, among the different tested drugs [38]. Abdelkader *et al*. (2018) reported extremely low corneal epithelial cell viability (21%) related to DCF solution (0.1% w/v) application [39]. It must be concluded that the DCF+MXF loaded TRIS(300)-I-LbL hydrogels are less toxic than the correspondent eye drops, and are suitable for medical device application according to the ISO standard 10993-5 (2009), which establishes a minimum of cell viability >70%.

The cell antifouling effect of the LbL coating was clearly demonstrated in **Figure 6.13**, which shows practically no adherence of cells to the surfaces of the unloaded and the DCF+MXF loaded TRIS(300)-I-LbL hydrogels. This is a very interesting characteristic of the coatings as cell adhesion may harmfully lead to cornea erosion [40]. **Figure 6.13A** also shows that the number of cells that are adherent to the surface of the uncoated samples is smaller for the drug

loaded hydrogel. Such reduction and consequent decrease in cell viability could be caused by the toxicity of both drugs. The non-adhesive effect of the ALG/PLL(EDC)//HA coating ultimately implied that, after rinsing and transfer of the hydrogels to a clean well, almost no cells were dragged and the cell viability was close to zero (**Figure 6.13B**). Several authors stated that the anti-adhesion behaviour of natural based LbL coatings, like the one in this study, could be linked to cell-polyelectrolyte interactions [41–43]. Khademhosseini *et al*. (2004) demonstrated the ability of HA coated glass surfaces to resist protein adsorption and cell adherence [44]. Muzzio *et al*. (2016) prepared multilayer coatings using a polycation as the outermost layer and found that natural based coatings of HA and ALG with a top layer of PLL led to the reduction of the cell adhesion areas [45]. In another study, Muzzio *et al*. (2017) attributed the anti-adhesive behaviour of CHI/HA coatings towards certain types of cells, to the hydrophilic nature and low roughness of these coatings [46].

Overall, the promising results reported in this work strongly suggest the possibility of applying TRIS(300)-I-LbL hydrogels as therapeutic drug carriers for ocular treatments in the near future. The imprinting and coating processes improved the anti-fouling properties of the SCL material, and ensured a controlled release of antibiotic and anti-inflammatory drugs for an extended period of time. Further *in vivo* assays are needed to confirm the biological performance of DCF+MXF loaded TRIS(300)-I-LbL hydrogels.

6.5   Conclusions

A combined application of molecular imprinting and LbL coating on a silicone-based hydrogel enabled the simultaneous sustained release of DCF and MXF for an extended period of time. The molecular imprinting technique with the addition of AA monomer produced specific memory cavities that increase MXF uptake and controlled its release. The ALG/PLL(EDC) coating with a top layer of HA decreased the initial burst of DCF and MXF release, improved the release kinetics and led to antifouling properties. The formation of reversible bonds between the functional monomer, the polyelectrolytes and the drugs can justify the observed behaviour. Neither ocular irritation nor cytotoxicity were detected for the DCF+MXF loaded TRIS(300)-I-LbL hydrogels. Additionally, the hydrogels were also able to withstand the HHP sterilization conditions. The antibacterial effect of MXF released from the sterilized samples

against *S. aureus* and *S. epidermidis* was confirmed by the antimicrobial tests. The release profiles obtained under hydrodynamic conditions demonstrated that DCF concentration remained above the lower limits of the IC_{50} values for 9 days and MXF concentration remained above the MIC of *S. aureus* and *S. epidermidis* for more than 10 days.

6.6 References

[1] M.S. Rad, S.A. Mohajeri, Simultaneously load and extended release of betamethasone and ciprofloxacin from Vitamin E-loaded silicone-based soft contact lenses, Curr. Eye Res. 3683 (2016) 1–7.

[2] N. Malakooti, C. Alexander, C. Alvarez-Lorenzo, Imprinted contact lenses for sustained release of polymyxin B and related antimicrobial peptides, J. Pharm. Sci. 104 (2015) 3386–3394.

[3] M. Korogiannaki, G. Guidi, L. Jones, Timolol maleate release from hyaluronic acid-containing model silicone hydrogel contact lens materials, J. Biomater. Appl. 30 (2015) 361–376.

[4] C.J. White, S.A. DiPasquale, M.E. Bryne, Controlled release of multiple therapeutics from silicone hydrogel contact lenses, Optom. Vis. Sci. 93 (2016) 377–386.

[5] R. Ye, H. Xu, C. Wan, S. Peng, L. Wang, H. Xu, Z.P. Aguilar, Y. Xiong, Z. Zeng, H. Wei, Antibacterial activity and mechanism of action of e-poly-L-lysine, Biochem. Biophys. Res. Commun. 439 (2013) 148–153.

[6] A. Ardizzoni, R.G. Neglia, M.C. Baschieru, C. Cermelli, M. Caratozzolo, M. Righi, B. Palmieri, E. Blasi, Influence of hyaluronic acid on bacterial and fungal species, including clinically relevant opportunistic pathogens, J. Mater. Sci. Mater. Med. 22 (2011) 2329–2338.

[7] C. Cassinelli, M. Morra, A. Pavesio, D. Renier, Evaluation of interfacial properties of hyaluronan coated poly(methylmethacrylate) intraocular lenses, J. Biomater. Sci. Polym. Ed. 11 (2000) 961–77.

[8] M. Van Beek, A. Weeks, L. Jones, H. Sheardown, Immobilized hyaluronic acid containing model silicone hydrogels reduce protein adsorption, J. Biomater. Sci. Polym. Ed. 19 (2008) 1425–36.

[9] M. Van Beek, L. Jones, H. Sheardown, Hyaluronic acid containing hydrogels for the reduction of protein adsorption, Biomaterials. 29 (2008) 780–789.

[10]   A.W. Lloyd, R.G.A. Faragher, M. Wassall, W. Rhys-Williams, L. Wong, J.E. Hughes, G.W. Hanlon, Assessing the in vivo cell-based ocular compatibility of contact lens materials, Contact Lens Anterior Eye. 23 (2000) 119–123.

[11]   C.M. Elkins, Q.M. Qi, G.G. Fuller, Corneal cell adhesion to contact lens hydrogel materials enhanced via tear film protein deposition, PLOS-ONE. 9 (2014) 1–9.

[12]   C. Alvarez-Lorenzo, F. Yañez, A. Concheiro, Ocular drug delivery from molecularly-imprinted contact lenses, J. Drug Deliv. Sci. Technol. 20 (2010) 237–248.

[13]   R.A. Scott, N.A. Peppas, Kinetic study of acrylic acid solution polymerization, AIChE J. 43 (1997) 135–144.

[14]   A. Topete, A.P. Serro, B. Saramago, Dual drug delivery from intraocular lens material for prophylaxis of endophthalmitis in cataract surgery, Int. J. Pharm. 558 (2019) 43–52.

[15]   R. Rodriguez, C. Alvarez-Lorenzo, A. Concheiro, Cationic cellulose hydrogels: kinetics of the cross-linking process and characterization as pH-/ion-sensitive drug delivery systems., J. Control. Release. 86 (2003) 253–265.

[16]   R. Vasquez, R. Nogueira, M. Orfão, J. Mata, B. Saramago, Stability of triglyceride liquid films on hydrophilic and hydrophobic glasses, J. Colloid Interface Sci. 299 (2006) 274–282.

[17]   J. Kim, A. Chauhan, Dexamethasone transport and ocular delivery from poly (hydroxyethyl methacrylate) gels, Int. J. Pharm. 353 (2008) 205–222.

[18]   R. Reddy, S.J. Kim, Critical appraisal of ophthalmic ketorolac in treatment of pain and inflammation following cataract surgery, Clin. Ophthalmol. 5 (2011) 751–75.

[19]   N. Efron, C. Maldonado-Codina, Development of contact lenses from a biomaterial point of view – Materials, manufacture, and clinical application, in: Compr. Biomater., Comprehensive Biomaterials. Elsevier, 2011: pp. 517–541.

[20]   B.B. Hsu, M.-H. Park, S.R. Hagerman, P.T. Hammond, Multimonth controlled small molecule release from biodegradable thin films, Proc. Natl. Acad. Sci. U.S.A. 111 (2014) 12175–12180.

[21] Y. Boonsongrit, A. Mitrevej, B. Mueller, Chitosan drug binding by ionic interaction, Eur. J. Pharm. Biopharm. 62 (2006) 267–274.

[22] M.M. Collins, C. Birkinshaw, Investigation of the swelling behavior of crosslinked hyaluronic acid films and hydrogels produced using homogeneous reactions, J. Appl. Polym. Sci. 109 (2008) 923–931.

[23] C. Alvarez-Lorenzo, F. Yañez, R. Barreiro-iglesias, A. Concheiro, Imprinted soft contact lenses as norfloxacin delivery systems, J. Control. Release. 113 (2006) 236–244.

[24] N. Dehar, A. Gupta, G. Singh, Comparative study of the ocular effi cacy and safety of diclofenac sodium (0.1 %) ophthalmic solution with that of ketorolac tromethamine (0.5 %) ophthalmic solution in patients with acute seasonal allergic conjunctivitis, Int. J. Appl. Basic Med. Res. 2 (2012) 25–30.

[25] J. Shimazaki, H. Fujishima, Y. Yagi, Effects of diclofenac eye drops on corneal epithelial structure and dunction after small , incision, Opthalmology. 103 (1995) 50–57.

[26] A. Kawahara, T. Utsunomiya, Y. Kato, Y. Takayanagi, Comparison of effect of nepafenac and diclofenac ophthalmic solutions on cornea , tear film , and ocular surface after cataract surgery : the results of a randomized trial, Clin. Opthalmology. 10 (2016) 385–391.

[27] Z. Butt, M.G. Fsadni, P.S. Raj, Diclofenac-Gentamicin Combination Eye Drops Compared with Corticosteroid-Antibiotic Combination Eye Drops after Cataract Surgery, Clin. Drug Invest. 15 (1998) 229–234.

[28] D. Miller, Review of moxifloxacin hydrochloride ophthalmic solution in the treatment of bacterial eye infections, Clin Ophthalmol. 2 (2008) 77–91.

[29] A. Sheikh, B. Hurwitz, Topical antibiotics for acute bacterial conjunctivitis: A systematic review, Br. J. Gen. Pract. 51 (2001) 473–477.

[30] R. Galante, P. Paradiso, M.G. Moutinho, A.I. Fernandes, J.L.G. Mata, A.P.A. Matos, R. Colaço, B. Saramago, A.P. Serro, About the effect of eye blinking on drug release from pHEMA-based hydrogels: An in vitro study, J. Biomater. Sci. Polym. Ed. 26 (2015) 235–251.

[31] E. Kim, M. Saha, K. Ehrmann, Mechanical properties of contact lens materials, Eye&Contact Lens Sci. Clin. Prat. 44 (2018) 148–156.

[32] D. Silva, A.C. Fernandes, T.G. Nunes, R. Colaço, A.P. Serro, The effect of albumin and cholesterol on the biotribological behaviour of hydrogels for contact lenses, Acta Biomater. 26 (2015) 184–194.

[33] C.R. Wittmer, J.A. Phelps, C.M. Lepus, W.M. Saltzman, M.J. Harding, P.R. VanTassel, Multilayer nanofilms as substrates for hepatocellular applications, Biomaterials. 29 (2008) 4082–4090.

[34] J.-K. Chang, G.-J. Wang, S.-T. Tsai, M.-L. Ho, Nonsteroidal Anti-inflammatory drug effects on osteoblastic cell cycle, cytotoxicity, and cell death, Connect. Tissue Res. 46 (2005) 200–210.

[35] T.-H. Tsai, W. Chen, F.-R. Hu, Comparison of fluoroquinolones: cytotoxicity on human corneal epithelial cells, Eye. 24 (2010) 909–917.

[36] P. Bezwada, L.A. Clark, S. Schneider, Intrinsic cytotoxic effects of fluoroquinolones on human corneal keratocytes and endothelial cells, Curr. Med. Reseach Opin. 24 (2008) 419–424.

[37] S.-Y. Kim, J.-A. Lim, J.-S. Choi, E.-C. Choi, C.-K. Joo, Comparison of antibiotic effect and corneal epithelial toxicity of levofloxacin and moxifloxacin in vitro, Cornea. 26 (2007) 720–725.

[38] J.S. Lee, Y.H. Kim, Y.M. Park, The toxicity of nonsteroidal anti-inflammatory eye drops against human corneal epithelial cells in vitro, J. Korean Med. Sci. 30 (2015) 1856–1864.

[39] H. Abdelkader, Z. Fathalla, H. Moharram, T.F.S. Ali, B. Pierscionek, Cyclodextrin enhances corneal tolerability and reduces ocular toxicity caused by diclofenac, Oxid. Med. Cell. Longev. 2018 (2018) 1–13.

[40] M. Markoulli, E. Papas, N. Cole, B. Holden, Corneal erosions in contact lens wear, Contact Lens Anterior Eye. 35 (2012) 2–8.

[41] E. Lih, S. Heang, Y. Ki, J. Ho, D. Keun, Polymers for cell/tissue anti-adhesion, Prog.

Polym. Sci. 44 (2015) 28–61.

[42] X. Xu, L. Wang, S. Guo, L. Lei, T. Tang, Applied surface science surface chemical study on the covalent attachment of hydroxypropyltrimethyl ammonium chloride chitosan to titanium surfaces, Appl. Surf. Sci. 257 (2011) 10520–10528.

[43] S. Yamanlar, S. Sant, T. Boudou, C. Picart, Surface functionalization of hyaluronic acid hydrogels by polyelectrolyte multilayer films, Biomaterials. 32 (2011) 5590–5599.

[44] A. Khademhosseini, K.Y. Suh, J.M. Yang, G. Eng, J. Yeh, S. Levenberg, R. Langer, Layer-by-layer deposition of hyaluronic acid and poly- l -lysine for, Biomaterials. 25 (2004) 3583–3592.

[45] N.E. Muzzio, M.A. Pasquale, D. Gregurec, E. Diamanti, M. Kosutic, O. Azzaroni, S.E. Moya, Polyelectrolytes multilayers to modulate cell adhesion: A study of the influence of film composition and polyelectrolyte interdigitation on the adhesion of the A549 cell line, Macromol. Biocience. 16 (2016) 482–495.

[46] N.E. Muzzio, M.A. Pasquale, S.E. Moya, O. Azzaroni, Tailored polyelectrolyte thin film multilayers to modulate cell adhesion, Biointerphases. 12 (2017) 04E403 1-12.

7 General discussion

Table of Contents

7.1 General discussion

As discussed in chapter 1 ocular drug delivery to the anterior segment of the eye is a challenging task due to the physiological mechanisms of the eye and the low permeability of the cornea [1]. As such in this thesis an investigation of drug-eluting SCLs materials was carried out, to improve the drugs bioavailability.

Several strategies to control drug release from SCL materials were developed. Almost all tests were done with a lab-made hydrogel based on silicone (TRIS/NVP/HEMA), which demonstrated adequate properties to be used in long wear SCLs [2,3]. The advantage of using a lab-made material was the possibility of producing samples with different shapes, which could be used in a variety of experiments.

Among the different possibilities to modify the samples, special emphasis was given to the use of LbL coatings. Surface modification through the LbL method can favourably improve the SCLs material's surface, depending on the used polyelectrolyte's properties. Moreover, by varying the compounds involved in the multilayer formation and the assembly conditions, a variety of coatings with different characteristics may be produced [4]. As such, in this work several coatings were produced and optimized to achieve proper drug control release.

In chapter 2 one coating based on the combination of ALG and CHI was tested to control the release of four different drugs (DCF, KETO, CHX and MXF). Two SCL materials were tested: TRIS/NVP/HEMA, and the commercial material Definitive 50.

Initially, TRIS/NVP/HEMA was coated with an ALG/CHI multilayer, using $CaCl_2$ and GL as crosslinkers to improve coating stability. The designated (ALG-$CaCl_2$)/(CHI+GL) coating with an ALG-$CaCl_2$ top layer, surprisingly showed a barrier effect clearly more effective for the release of the smallest molecule, DCF (**Figure 2.5A**). This may be related with the formation of unstable DCF-CHI complexes that retard the release of the drug [5]. In the case of KETO and MXF (**Figure 2.5B** and **C**), the profile was not much affected, while for CHX (**Figure 2.5D**) the released amount increased but the release kinetics did not improve. The interactions between ALG and CHX can be responsible for the increase in CHX released amount. Interestingly, this coating was able to retain its features in a different hydrogel, Definitive 50, also leading to an effective control of the release of DCF.

Considering the successful improvement of the DCF release kinetics in chapter 2 by application of an ALG/CHI coating, further investigation of the LbL method was carried out to add other functionalities to the coating. Other polyelectrolytes with antibacterial and antifouling properties and different assembly conditions were tested, with the objective of improving both the drug´s release kinetics and the surface properties. In chapter 3, three coatings were studied, involving the combination of ALG, CHI, HA and PLL, and using EDC as biocompatible crosslinker. These coatings consisted in two double layers of ALG/PLL(EDC), HA(EDC)/CHI or HA/PLL(EDC)+Drug. Three different drugs were incorporated in the hydrogel by soaking: DCF, MXF and CHX. However, only DCF presented favourably release kinetics, as a result from the reversible bonding between the carboxylic groups of DCF and the amine groups of PLL or CHI through the activating action of EDC. Both MXF and CHX release profiles from the coated hydrogels exhibit an initial burst similar to that shown by their correspondent uncoated counterparts. Although characterization of all three coatings demonstrated suitable physical properties for SCLs use, the most interesting coating was ALG/PLL(EDC) because it demonstrated the best DCF release kinetics of all. One disadvantage of these coatings was their low resistance to the tear proteins. Both albumin and lysozyme were found to adsorb or degrade the upper layer of the coatings (**Figure 3.3** to **3.5**). This problem was not unexpected, since lysozyme is known to actively degrade CHI, through hydrolysis of the biopolymers linkages, especially for CHI with higher levels of deacetylation, which is our case [6]. In the case of PLL, there is some controversy in the literature, as some authors report its enzymatic degradation by several proteins [4,7], while other authors used it to protect previous layers from lysozyme [8].

To overcome this problem, we chose the best coating and added a top layer of HA, due to its antifouling properties [9,10], to obtain a new coating: ALG/PLL(EDC)//HA. This new HA top layer not only protected the preceding layers from degradation, but also completely prevented the adsorption of lysozyme.

The ALG/PLL(EDC)//HA coating demonstrated suitable physical properties for SCLs use, and inhibited *S. aureus* and *P. aeruginosa* growth, while controlling the release of DCF. However, the barrier effect concerning the drug release was reinforced with the single addition of a HA top layer, resulting in a significant decrease of the amount of DCF released.

The results presented in chapters 2 and 3 were subject of further optimization, considering the number of layers and their sequence, to improve the release characteristics of DCF, while

retaining antibacterial and antifouling properties. This optimization resulted in the development of a new triple layer coating designated as ALG/CHI/HA (Chapter 4). This new coating was applied on three different hydrogels (i.e. TRIS/NVP/HEMA and two commercial SCLs: SofLens and Purevision). The idea was to verify any possible modifications of its barrier effect due to substrate interference. Interestingly, the release kinetics of DCF was greatly improved with the ALG/CHI/HA coating for all three hydrogels. The application of a simple mathematical model allow to infer that the concentration of DCF in the lachrymal fluid remained above IC_{50} values for COX-1 and COX-2 for more than 15 days (**Figure 4.15**), which represented a 13 day increase when compared to that estimated for ALG/PLL(EDC)//HA coating (**Figure 3.16**). The LbL coating process of ALG/CHI/HA did not require reloading in DCF solution, as the amount of drug lost during the coating process was negligible, in contrast with the situation found for the previously studied ALG/PLL(DC)//HA coating.

The coating ALG/CHI/HA was stabilized with the crosslinker agent GE. This natural crosslinker was selected in detriment of EDC and GL, which are synthetic crosslinker agents described as biocompatible but with an higher risk of cytotoxicity than natural-based reagents [11]. The antibacterial properties against *P. aeruginosa* of the ALG/CHI/HA coating (**Figure 4.11**) were similar to those of the ALG/PLL(EDC)//HA coating (**Figure 3.15**). However, the new coating was significantly more efficient for *S. aureus*, demonstrating ~20% of optical density decrease, when compared to the ALG/PLL(EDC)//HA coating. Such behaviour can be related, not only to the HA top layer, present in both coatings, but also to the use of GE, known to promote antibacterial properties when applied in this type of surface modifications [12].

Additionally, chapter 4 tackled the problem of sterilization, which is a crucial step in SCLs manufacturing. It is well established that SCLs are commercialized in blisters sterilized through methods like SP and γ-radiation. However, great concerns arise relatively to the implementation of such processes in drug-loaded and/or LbL coated hydrogels. In fact, DCF in wet conditions is degraded by γ-radiation [13,14], while the ALG/CHI/HA coating demonstrated irreversible damage after being subjected to SP sterilization. The solution for this problem was found with HHP sterilization. This process has been poorly explored for biomaterials sterilization. However, it was studied in detail in our research group to determine the conditions needed to sterilize hydrogels for ophthalmic lenses, namely intraocular lenses [15]. HHP appeared to offer a positive and safe solution, because not only ALG/CHI/HA

withstood the sterilization process and maintained its optical properties, but also demonstrated the barrier effect leading to a sustained release of DCF and ensured sterility

In chapters 2 and 3, the studied LbL coatings were inefficient in controlling the MXF release. The inefficiency of those coatings is related to the lack of interactions between the polyelectrolytes with the zwitterionic MXF molecule, while the size of the molecule could prevent its entrapment in the CHI matrices. Therefore, an alternative method was implemented in order to increase the amount of drug loaded and obtain a sustained release of MXF from the hydrogels. This method is described in chapter 5 and involves molecular imprinting of MXF coupled with the addition of a functional monomer AA, at various ratios. Both modifications were applied to TRIS/NVP/HEMA, and resulted in a significant increase in the amount of drug loaded and released. Interestingly, the imprinted hydrogels demonstrated a significant decrease of the initial burst when compared to their non-imprinted counterparts (**Figure 5.4**). The presence of specific cavities in the hydrogel matrix hampered the drug release in the first hours, ultimately improving the release kinetics. Optimization of the produced hydrogels, demonstrated that TRIS(300)-I hydrogel retained the best physical characteristics, while increasing the amount of MXF loaded by 6.5-fold and the released by 6-fold, when compared to the TRIS/NVP/HEMA hydrogel.

In this chapter, the drug release was also evaluated in hydrodynamic conditions, to approximate the release to the *in vivo* conditions (**Figure 5.7**). As described in [16], the release rate is greatly affected by the release conditions, and the release in hydrodynamic conditions is much slower than in sink conditions in medium under stirring. Comparison of the release profiles obtained with TRIS/NVP/HEMA and TRIS(300)-I showed that the MXF concentration released by the latter hydrogel remained above the MICs for *S. aureus* and *S. epidermidis* for two more days than in the former case.

The positive results described in chapter 5 paved way to tackle the problem of dual release. The treatment of most ocular infections implies the conjugation of an anti-inflammatory and an antibiotic drug. As such, dual release from SCLs has been subject of several studies. As different drugs have different interactions with the polymeric matrix, the use of one strategy to improve the release of both drugs release can be an unsuccessful endeavour. Chapter 6 describes how the conjugation of surface modification and molecular imprinting on the same system resulted in a sustained release of DCF and MXF (**Figure 6.4**). The TRIS(300)-I hydrogel was coated with ALG/PLL(EDC)//HA (designated as TRIS(300)-I-LbL in chapter 6).

This coating was selected in detriment of the more efficient ALG/CHI/HA due to the fact that in contrast with the observed resistance of the ALG/CHI/HA coated TRIS/NVP/HEMA hydrogel to HHP sterilization, the ALG/CHI/HA coated TRIS(300)-I-LbL hydrogel became dark blue after HHP sterilization due, probably, to an excessive crosslinking of the coating. This colouring decreased the transmittance of the samples to values <70%.

A significant difference between the DCF release from TRIS/NVP/HEMA (**Figure 3.7**) and TRIS(300)-I-LbL (**Figure 6.4A**), both coated with ALG/PLL(EDC)//HA, was observed. The coating on TRIS(300)-I-LbL was still able to sustain the release of DCF, avoiding the initial burst of drug, but the amount of drug release was not reduced. Although, the concentration of DCF in the loading solution was reduced (due to solubility issues) the amount of drug loaded was similar for coated TRIS(300)-I-LbL and for coated TRIS/NVP/HEMA. Thus, the amount of drug loaded was not the cause for the release differences. Instead, possible influence of the release conditions could induce the variation in DCF release. Furthermore, as previously described, the barrier effect of a specific coating is not independent of the type of substrate.

In the case of MXF, the release profile obtained with the uncoated TRIS(300)-I hydrogel double loaded (**Figure 6.4B**), demonstrated a similar kinetics to that observed for the same hydrogel single loaded (**Figure 5.4**), but the amount of MXF released was smaller than in the latter case. The reduction in the amount of drug release should be related to the decrease in the amount of MXF loaded, considering that the MXF concentration in the DCF+MXF loading solution was smaller than in the MXF loading solution due to solubility issues. Although the LbL coatings were not efficient in the control of MXF, the presence of the coating ALG/PLL(EDC)//HA on the TRIS(300)-I-LbL sample, resulted in a modification of MXF release kinetics. Indeed, a more sustainable release was observed, as possible interactions with the HA top layer, through the formation of H-bonds with the MXF molecule, could influence and retard its release.

Overall, the results shown in chapters 2 to 6 demonstrated a promising possibility of implementing such coated and/or imprinted hydrogels as therapeutic drug carriers for ocular treatments. The results obtained in each chapter raised questions, which were addressed in the following chapter aiming at the optimization and future implementation of efficient therapeutic SCLs.

7.2 References

[1]   F.A. Maulvi, T.G. Soni, D.. Shah, A review on therapeutic contact lenses for ocular drug delivery, Drug Deliv. 23 (2016) 3017–3026.

[2]   D. Silva, A.C. Fernandes, T.G. Nunes, R. Colaço, A.P. Serro, The effect of albumin and cholesterol on the biotribological behaviour of hydrogels for contact lenses, Acta Biomater. 26 (2015) 184–194.

[3]   P. Paradiso, R. Galante, L. Santos, A.P. Alves De Matos, R. Colaço, A.P. Serro, B. Saramago, Comparison of two hydrogel formulations for drug release in ophthalmic lenses, J. Biomed. Mater. Res. B. 102 (2014) 1170–1180.

[4]   M. Westwood, D. Roberts, R. Parker, Enzymatic degradation of poly-L-lysine-polygalacturonic acid multilayers, Carbohydr. Polym. 84 (2011) 960–969.

[5]   Y. Boonsongrit, A. Mitrevej, B. Mueller, Chitosan drug binding by ionic interaction, Eur. J. Pharm. Biopharm. 62 (2006) 267–274.

[6]   V. Guarino, T. Caputo, R. Altobelli, L. Ambrosio, Degradation properties and metabolic activity of alginate and chitosan polyelectrolytes for drug delivery and tissue engineering applications, AIMS Mater. Sci. 2 (2015) 497–502.

[7]   K. Ren, J. Ji, J. Shen, Construction and enzymatic degradation of multilayered poly-L-lysine/DNA films, Biomaterials. 27 (2006) 1152–1159.

[8]   P. Calvo, J.L. Vila-Jato, M.J. Alonso, Effect of lysozyme on the stability of polyester nanocapsules and nanoparticles: stabilization approaches, Biomaterials. 18 (1997) 1305–1310.

[9]   W.G. Pitt, R.N. Morris, M.L. Mason, M.W. Hall, Y. Luo, G.D. Prestwich, Attachment of hyaluronan to metallic surfaces, J. Biomed. Mater. Res. A. 68 (2004) 95–106.

[10]   R.A. D'Sa, P.J. Dickinson, J. Raj, B.K. Pierscionek, B.J. Meenan, Inhibition of lens epithelial cell growth via immobilisation of hyaluronic acid on atmospheric pressure plasma modified polystyrene, Soft Matter. 7 (2011) 608–617.

[11]   H. Chen, W. Ouyang, C. Martoni, S. Prakash, Genipin cross-linked polymeric alginate-chitosan microcapsules for oral delivery: In-vitro analysis, Int. J. Polym. Sci. (2009) 1–

16.

[12] R. Wang, K.G. Neoh, E.T. Kang, Integration of antifouling and bactericidal moieties for optimizing the efficacy of antibacterial coatings, J. Colloid Interface Sci. 438 (2015) 138–148.

[13] A.L.C. Topete, Effects of sterilization on drug loaded soft contact lenses, 2015.

[14] A.S.G. Oliveira, Effects of sterilization on drug loaded ophthalmic lenses materials, 2016.

[15] A. Topete, C.A. Pinto, H. Barroso, J.A. Saraiva, I. Barahonac, B. Saramago, A.P. Serro, High hydrostatic pressure (HHP) as sterilization method for drug-loaded intraocular lenses, Submitted. (n.d.).

[16] A.F.R. Pimenta, A. Valente, J.M.C. Pereira, H.P. Filipe, J.L.G. Mata, R. Colaço, B. Saramago, A.P. Serro, Simulation of the hydrodynamic conditions of the eye to better reproduce the drug release from hydrogel contact lenses: experiments and modeling, Drug Deliv. Transl. Res. 6 (2016) 755–762.

8 Conclusions and Future work

Table of Contents

8.1 Conclusions

The aim of this thesis was to investigate new strategies based on LbL coatings and molecular imprinting, to control the drug release from drug-eluting hydrogels, which may be used in the production of therapeutic SCLs. An extensive study of the systems' properties was done as it is fundamental to ensure several key characteristics for their approval as SCL materials. The general conclusion is that it is possible to produce systems with potential to be implemented as extended ophthalmic drug delivery SCLs with antibacterial and antifouling properties. A right combination of polyelectrolytes of the LbL coating and/or functional monomers for the hydrogel modification is needed for each drug. The specific conclusions of each chapter are summarised in the following paragraphs.

In chapter 2 it was demonstrated that it is possible to sustain the release of DCF from TRIS/NVP/HEMA hydrogel for more than one week, through the use of the (ALG-CaCl$_2$)/(CHI+GL) coating topped with a final ALG/CaCl$_2$ layer to avoid CHI degradation by lysozyme. The wettability, the bulk refraction index, and the light transmittance of the substrate were almost not affected by the presence of the coating. However, the control of the release of KETO, CHX and MXF could not be achieved. The deposition of this coating on a different silicone-based material revealed a less efficient barrier effect, demonstrating that the characteristics of the combination hydrogel/drug/coating greatly affect the release results.

Chapter 3 describes an investigation about the use of polyelectrolytes with antibacterial properties to form LbL coatings on TRIS/NVP/HEMA hydrogel with the dual purpose of controlling the release of ophthalmic drugs, and reducing bacterial growth. Coatings composed of two double layers of ALG/PLL(EDC), HA(EDC)/CHI and HA/PLL(EDC)+Drug led to a decrease of the initial burst of DCF, leading to controlled release profiles, but they could not control the release of MXF and CHX. The coatings were hydrophilic and kept the optical properties of the systems within adequate values, but they were affected by the presence of albumin and lysozyme in the release medium. To overcome this problem, a final layer of HA was deposited on top of the ALG/PLL(EDC) coating. The resulting coating ALG/PLL(EDC)//HA demonstrated to be able to control the release of DCF, to resist the action of the tear proteins, to reduce the growth of *S. aureus* and *P. aeruginosa*, and to prevent ocular irritation. However, the percentage of released drug was low, i.e. the coating led to a significant retention of drug inside the polymeric matrix. The concentration of DCF in the tear fluid,

predicted through a simplified mathematical model, shall remain above the lower limits of the IC_{50} values for COX-1 and COX-2, two and five days, respectively.

In chapter 4 a new combination of electrolytes was tested with the objective of increasing the period of efficient drug release. A LbL coating composed of one triple layer of ALG/CHI/HA, crosslinked with GE, decreased the initial burst of DCF and led to a controlled release, while inhibiting *S. aureus* and *P. aeruginosa* growth. Light transmittance, bulk refractive index, and ionic permeability remained within the range of values recommended for SCLs. The coating was biocompatible, showed antifouling properties and did not lead to irritancy. It was successfully sterilized by a new sterilization method based on the application of HHP. The concentration of released DCF, estimated by the mathematical model referred above, remained above the IC_{50} values for COX-1 and COX-2 for at least 15 days.

Chapter 5 describes an attempt to control the release of the antibiotic MXF from the TRIS/NVP/HEMA hydrogel modified by molecular imprinting together with the addition of the functional monomer AA. The resulting hydrogels were hydrophilic, with high transmittance, increased ionic permeability, low surface roughness and adequate stiffness. The hydrogel with 300 mM of AA and imprinted drug (TRIS(300)-I) was able to load the highest amount of MXF through reversible bonding, which allowed a controlled release of the drug and ensured concentrations above the MIC values for *S. aureus* and *S. epidermidis*, for 13 days. Furthermore, the referred hydrogel was not toxic and did not cause ocular irritation.

In chapter 6, a combined approach of molecular imprinting and LbL coating on the TRIS/NVP/HEMA hydrogel was attempted to enable the simultaneous controlled release of DCF and MXF, for an extended period of time. The MXF molecular imprinting with the addition of AA monomer led to increased MXF uptake and controlled its release. The ALG/PLL(EDC)//HA coating decreased the initial burst of DCF and MXF release, improved the release kinetics and led to antifouling properties. Neither ocular irritation nor cytotoxicity were detected for the DCF+MXF loaded TRIS(300)-I-LbL hydrogels. Additionally, the hydrogels were also able to withstand the HHP sterilization conditions. The antibacterial effect of MXF released from the sterilized samples against *S. aureus* and *S. epidermidis* was confirmed by antimicrobial tests. The release profiles obtained under hydrodynamic conditions that simulate those found in the eye, demonstrated that DCF concentration remained above the IC_{50} values for 9 days and MXF concentration remained above the MICs of *S. aureus* and *S. epidermidis* for more than 10 days.

8.2 Future work

This work has provided some insights on the possibilities for the development of therapeutic SCLs, as substitutes of conventional commercially available ocular treatments. Nonetheless, several investigation paths can be pursued to continue this research work. Such work could include:

Coating adhesion to the substate

The study of LbL coatings, which demonstrated favourable surface properties in addition to a sustained release of DCF, should be complemented with the analysis of the adhesion forces between the coating and the hydrogels. Knowledge of the adhesion strength of the coating is needed to evaluate its capability of resisting user's manipulation and manufacturing processes.

AFM could be used for this analysis, through the use of the AFM tip as a scratching tool. Additionally, the coatings should be dyed for observation purposes.

Structural information of modified imprinted SCL materials

Structural information of modified imprinted samples through the use of nuclear magnetic resonance (NMR) should be obtained, to better understand the molecular dynamics and to have quantitative information about the atomic ratios of the different compounds involved.

Evaluation of the coating-drug interactions

In this thesis, the interactions between the polyelectrolytes of the coatings and the drugs were discussed based on their molecular structures. However, the infrared (IR) spectroscopy technique, should be used to further evaluated the coating-drug interactions. Analysis of the differences between the absorption peaks in the IR spectra for the drug-coating system, and the individual spectra of the drug and of the coatings could improve the understanding of the occurring interactions.
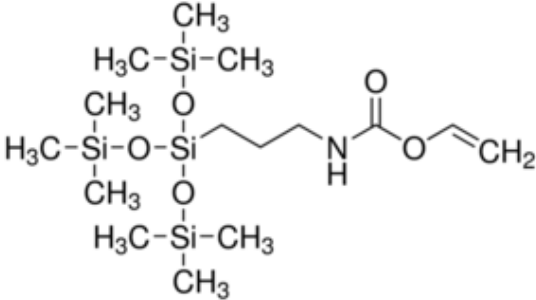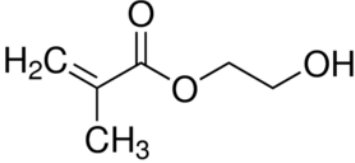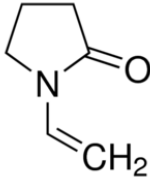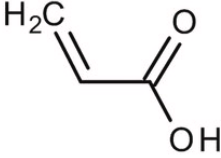
Oxygen permeability

The oxygen permeability is a key property for the acceptance of materials for SCLs, in particular, the extended-wear versions. Since cornea is not vascularized, the main path for the oxygen to reach the cells is through diffusion from the atmosphere. Thus, it is crucial that the SCLs materials have high values of oxygen permeability. However, there are great incongruities in terms of oxygen permeability values and their units in the literature. It would be extremely useful to have a compilation of measurement techniques and standardized data that would allow for significant comparisons. A systematic analysis of the dependence of the oxygen permeability on the nature of the functional monomers used in the SCL material would contribute for an efficient investigation of new SCL materials.

In vivo analysis of the drug-eluting SCLs application

The complexity of the human eye can only be tackled through *in vivo* analysis. Such tests could help in further developing and optimizing LbL coated imprinted SCLs. Ethical issues are a minor concern, since tests of SCLs do not imply invasive procedures for the animals.

Appendix A

Chemical structures of the monomers used.

Monomer	Chemical structure
3-Tris(trimethylsiloxy)silyl propyl methacrylate (TRIS)	
2-Hydroxyethyl methacrylate (HEMA)	
N-Vinyl pyrrolidone (NVP)	
Acrylic acid (AA)	

Appendix B

Characteristics of the commercial silicone-based SCLs material Definitive 50 [1].
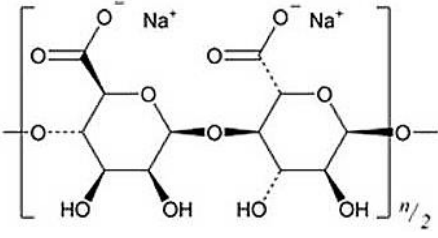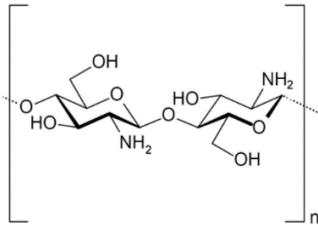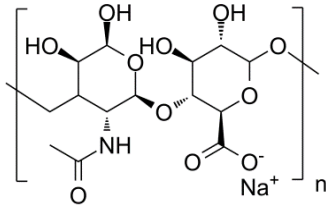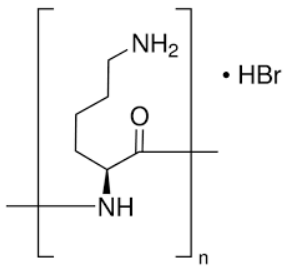
Property	Definitive 50
Classification	Soft Contact Lens
Principal components	Silicon hydrogel materials
Dk/t $(x10^{-9}$ cm mlO_2/s ml mmHg) (35ºC)	62.5
Swell factor (20ºC)	1.29
Water content by weight % (20ºC)	50
Refractive index (20ºC)	1.406
Light transmission % (380-780 nm)	97.5
Young's modulus (MPa)	0.6

References

[1] https://www.contamac.com/ [March 2020]

Appendix C

Characteristics of the studied polyelectrolytes.

	Molecular structure	Molecular weight (g/mol)	pKa	Ionicity
Alginate (ALG)		100 000 – 200 00	3.4 – 3.7[a]	Anionic
Chitosan (CHI)		750 – 1000	6.5[b]	Cationic
Hyaluronate (HA)		1 000 000 – 2 000 000	3-4[c]	Anionic
Poly-L-lysine (PLL)		70 000 – 150 000	9.4[d]	Cationic

[a] From [1]

[b] From [2]

[c] From [3]

[d] From [4]

References

[1]   J.-J. Chuang, Y.-Y. Huang, S.-H. Lo, T.-F. Hsu, W.-Y. Huang, S.-L. Huang, Y.-S. Lin, Effects of pH on the Shape of Alginate Particles and Its Release Behavior, Int. J. Polym. Sci. 1 (2017) 1–9.

[2]   J. Hernandez-Montelongo, E.G. Lucchesib, I. Gonzalez, W.A.A. Macedo, V.F. Nascimento, A.M. Moraes, M.M. Beppu, M.A. Cotta, Hyaluronan/chitosan nanofilms assembled layer-by-layer and their antibacterial effect: A study using Staphylococcus aureus and Pseudomonas aeruginosa, Colloids Surfaces B Biointerfaces. 141 (2016) 499–506.

[3]   A. Mero, M. Campisi, Hyaluronic acid bioconjugates for the delivery of bioactive molecules, Polymers (Basel). 6 (2014) 346–369.

[4]   J. Zhou, B. Wang, W. Tong, E. Maltseva, G. Zhang, R. Krastev, C. Gao, H. Möhwald, J. Shen, Influence of assembling pH on the stability of poly(l-glutamic acid) and poly(l-lysine) multilayers against urea treatment, Colloids Surfaces B Biointerfaces. 62 (2008) 250–257.